Transport and degradation of urban biocides from facades to groundwater

Tobias Junginger

Ecole Doctoral des Sciences de la Terre et de l'Environnement (ED 413)
Institut Terre et Environnement de Strasbourg (ITES)
UMR 7063/ ENGEES/ CNRS

Thèse présentée par :

Tobias Junginger

Soutenue le : **20 janvier 2023**

Pour obtenir le grade de : Docteur de l'Université de Strasbourg

Discipline Sciences de la Terre et de l'Univers

Spécialité Géochimie

Transport and degradation of urban biocides from facades to groundwater

THÈSE dirigée par :

M. IMFELD Gwenaël	Directeur de recherche, CNRS, France
M. PAYRAUDEAU Sylvain	Professeur, ENGEES, France

RAPPORTEURS :

M. BURKHARDT Michael	Professeur, Fachhochschule Ostschweiz, Suisse
M. Moilleron Régis	Professeur, Université Paris-Est Créteil, France

AUTRES MEMBRES DU JURY :

Mme. PASSEPORT Elodie	Professeure, Université de Toronto, Canada
Mme. BOLLMANN Ulla E.	PhD., Commission géologique du Danemark et du Groenland, Danemark

Invités :

M. LANGE Jens	Professeur, Université de Fribourg-en-Brisgau, Allemagne

Abstract

Urban biocides are used in facade materials like paint and render to prevent growth of algae and fungi. Biocides are released with wind driven rain and contaminate surface water, soil and groundwater with potential ecotoxicological effects to the ecosystem. The general goal of this thesis is to improve the understanding of reactive transport of urban biocides from their sources (i.e., construction materials/facades) to receiving compartments (i.e., surface water, soil, and groundwater). The overall approach of the thesis relies on concentration measurements of biocides and transformation products, compound-specific isotope analysis and reactive transport modelling, from the laboratory (e.g., single experiment in microcosms) to the district scale (transport, retention and reaction co-occurring). We first examined the degradation pathways and the mechanisms of the biocide terbutryn during photodegradation, abiotic hydrolysis and biodegradation under controlled laboratory conditions, using multi-element compound specific isotope analysis and transformation product measurements. We further developed a framework to use compound-specific isotope analysis for urban biocides under environmental conditions, discussing its potential and limitations. By using an integrative approach, from laboratory microcosm experiments to field scale experiments for short-term (e.g., days to months) to long-term assessments (e.g., years), we showed that solar irradiation and the volume of facade runoff are the main hydroclimatic variables causing the release of transformation products of terbutryn from facades and provide estimates of the contribution of TPs in facade leachate over several years. Additionally, we evaluated the reactive transport of urban biocides through typical urban surfaces, showing that permeable pavements and gravel drainage are potential 'hot spots' for biocide entry towards groundwater. In contrast, vegetated surfaces acted largely as a sink with high biocide retention potential. On the district scale, we provided estimates of biocide fluxes under sustainable stormwater management practice. The results indicate high infiltration of biocides close to building facades, while only small proportions of biocides reach the stormwater retention facilities resulting in risk of deterioration of groundwater quality. Altogether, this thesis underscores environmental risks associated with the release of urban biocides and their transformation products but also discusses alternative approaches with biocide-free materials, thus paving the way towards a biocide-free city.

Acknowledgments

This thesis was conducted in the frame of the European Regional Development Fund (ERDF), support measure INTERREG V in the Upper Rhine as part of the NAVEBGO project (sustainable reduction of biocide inputs to groundwater in the Upper Rhine region).

First, I would like to thank my supervisors Gwenaël Imfeld and Sylvain Payraudeau for their great support throughout these intense last three years. Thank you for the discussions, exchanges, feedback and advises regarding my thesis and all other topics that crossed my path!

I would also like to thank the jury members for accepting the evaluation of this thesis: Michael Burkhardt, Régis Moilleron, Elodie Passeport, Ulla Bollmann and Jens Lange.

A special thanks goes to the whole NAVEBGO team. The discussions during the meetings were a huge inspiration for my thesis and helped me advance, while the exchanges after the meetings resulted in great friendship. Thank you for the collaborations, Felicia, Guillaume, Jens, Lena, Maurice, Marcus, Olli, Klaus, Alexander, Johannes, Frank, Mirco and many others directly and indirectly involved in the project. Further, I acknowledge Jörg Sigmund for providing materials and helpful comments for the facade leaching experiment. The Eurométropole Strasbourg (EMS) and especially Maxime Pomies, Michaël-Camine and Yan Dubrowski, provided help in choosing the field site and with provided data. The City of Schiltigheim allowed us to install our experimental setups for several months. I would also like to acknowledge the FreWaB-PLUS and COMLEAM team for providing feedback, discussions, and fruitful reflections on our modeling.

Throughout my thesis, I had support in lab- and field work or through discussions in our work group. Thank you, Benoît, Eric, Jérémy, Delphine, Roch, Anna, Jean-Baptiste, Mathilde, Morgane, Lara, Jérôme, Quentin and Guillaume. I would also like to mention Laura for her intensive work with me on the last chapter, giving feedback and implementing new results in the model.

I am very grateful for the colleagues that I met in and around the lab, helping with scientific and non-scientific problems and cheering me up. Thank you, Lulu, for the fantastic muffins (legendary!), Tetyana, for the IRMS lessons, Adrien, for the discussions, Sara, for always being available for coffee breaks, Dani, for the strong support in pushing the

Committee4PhD, Felix, for the endless reservoir of chocolate, Lou, for the great support in really everything, Oscar, for being such a positive mind, Clarissa, you paved the way in Tübingen, David, Frank, Imane, Emma, Mouna, Jesi, Céline, Nicolas, P.O., and all the other wonderful people I met for sticking around with me! It was a pleasure to spend the last three years with all of you! Throughout the three years, I had a fantastic colocation. Thank you, Pauline, Bea, Seb, and Raph. You were such a great support! Tire ta baguette!

Even though not directly involved in the thesis work, I had support from many more people that helped me go through theses three years through discussions, friendship, patience and supportive words. J.B. and J.B.j (the music was my motivation), Claude, Udo, Maxi, Johannes, Kevin, Flo, Kim, and Alex.

Without the support of my family, I would have never been able to get that far. Danke, dass ihr all die Jahre an mich geglaubt und mich unterstützt habt! Danke Mama und Papa, für jeden Anruf, die aufbauenden Worte und die Naschpakete. Danke für euer Verständnis und dass Ihr mir all das ermöglicht habt! Danke Martina, Johannes und Jakob, dass Ihr mir immer ein Lächeln ins Gesicht gezaubert habt!

My greatest thanks go to Marie. Your support at any time, your ability to motivate me, to make me happy and to make me dream is the most valuable thing I have!

Résumé

Les peintures extérieures des bâtiments peuvent contenir des biocides pour inhiber la croissance des algues, des champignons et des microbes sur les façades. Ces biocides urbains peuvent être libérés dans l'environnement lorsque l'eau de pluie ruissellent sur les façades. Par exemple, la terbutryne, biocide à base de triazine, est utilisée dans le monde entier dans les matériaux de construction, bien qu'il soit interdit pour les usages agricoles dans l'Union Européenne depuis 2003. Les émissions de biocides lors de chaque épisode de ruissellement sur les façades pendant des années peuvent présenter des risques écotoxicologiques dans les sols au pied des façades, dans les eaux pluviales, puis dans les rivières urbaines avec un risque d'accumulation dans le sol et les eaux souterraines.

Même si les voies de dégradation des biocides sont en partie connues, les études sur la contribution de chacune de ces voies dans le processus de dissipation lors du transport réactif des biocides urbains des façades vers les eaux de surface, le sol et les eaux souterraines restent rares. Bien que la présence de produits de transformation (PT) dans l'environnement indique une dégradation de la terbutryne, la dégradation de ces PTs, la sorption ou la dilution peuvent limiter l'identification et la quantification des voies de transformation spécifiques à l'aide des seules concentrations des biocides ou de leur PTs.

Dans ce contexte, le suivi des changements de la composition en isotopes stables (abondance des isotopes naturels d'un élément comme le carbone) de la fraction résiduelle non dégradée des biocides peut aider à évaluer la dégradation sans tenir compte des données de concentration du composé parent ou des PTs. En général, les isotopes légers (par exemple, ^{12}C) ont besoin d'une énergie d'activation plus faible pour le clivage des liaisons par rapport aux isotopes lourds (par exemple, ^{13}C), ce qui entraîne des temps de réaction plus rapides et un enrichissement des isotopologues lourds dans la fraction non dégradée. En revanche, les processus non dégradatifs comme la sorption, la dilution ou l'advection entraînent généralement un fractionnement isotopique non significatif. En particulier, l'analyse isotopique composé-spécifique (AICS) des biocides peut aider à identifier les voies de réaction en mesurant les changements dans les rapports d'isotopes stables (par exemple, $^{13}C/^{12}C$, $^{15}N/^{14}N$), qui sont souvent spécifiques à la réaction. Les changements des rapports isotopiques peuvent permettre de quantifier l'étendue de la dégradation en utilisant les valeurs de fractionnement isotopique (ε)

qui sont généralement dérivées à partir d'expériences en laboratoire dans des conditions contrôlées.

Compte tenu de l'exposition des façades au soleil, la photodégradation des biocides peut se produire dans les premiers millimètres des enduits et peintures et former une variété de PTs. Les ruissellements sur les façades peuvent donc entrainer le lessivage d'un cocktail de biocides et de PTs associés dont le risque écotoxicologique est largement inconnu. Les processus à l'origine du lessivage des PTs de biocides sont également méconnus, et les approches permettant d'estimer la contribution des PTs aux émissions globales de biocides font actuellement défaut.

Après avoir été lessivés depuis les façades, les biocides peuvent pénétrer dans les eaux souterraines à travers les interfaces surfaces urbaines-sol (par exemple, les graviers de drainage, les revêtements perméables et les sols végétalisés au pied des façades). Même si seule une petite partie des biocides atteint les eaux de surface et les systèmes d'évacuation, le devenir des biocides et la formation des PTs associés dans l'interface surface-sol urbain ne sont pas bien compris. Peu de données sont disponibles pour prédire la percolation et le transport réactif des biocides urbains au sein de ces interfaces. Pour prédire le transport réactif à long terme, des approches de modélisation sont nécessaires, dans le but de compléter les mesures in situ et renforcer les approches de bilan de masse (par exemple, l'estimation de la dégradation pendant l'infiltration par rapport à la sorption) ainsi que pour généraliser les processus de transport réactif sur de longues périodes depuis la construction des bâtiments. De plus, les modèles existants à l'échelle de quelques bâtiments comme FREWAB-PLUS ou COMLEAM ne permettent pas d'évaluer l'impact du lessivage des biocides aux échelles plus étendues depuis celles des unités de gestions alternatives des eaux pluviales (quelques dizaines d'hectares jusqu'à celle des communes).

Cette thèse vise à améliorer la compréhension du transport réactif des biocides urbains depuis les sources (matériaux de construction/façades) jusqu'aux compartiments récepteurs (eaux de surface, sol et eaux souterraines). Dans cette étude, un cadre méthodologique innovant couplant développements analytiques, expériences en conditions contrôlées et en extérieur et améliorations de modèles préexistants a été développé pour évaluer le devenir des biocides urbains et distinguer la contribution des processus de dégradation biotiques et abiotiques ainsi que les processus de dissipation des biocides par sorption, transport et dilution. Les questions de recherche suivantes ont été abordées pour combler les lacunes dans les connaissances actuelles:

1. Quelles sont les principales voies de dégradation dans l'environnement de la terbutryne, biocide urbain modèle utilisé dans cette thèse, et pouvons-nous utiliser l'AICS pour suivre et quantifier sa dégradation et identifier les mécanismes de dégradation ?

2. Quels sont les processus de dégradation des biocides urbains sur les façades et quels sont les facteurs clés d'apparition et de mobilisation des PTs dans les ruissellements de façade ?

3. Quelles sont les principales voies d'entrée et les processus clés lors du transport réactif du biocide urbain vers les eaux souterraines à travers les interfaces surfaces urbaines-sol urbain typiques ?

4. Peut-on utiliser l'AICS dans des conditions environnementales pour estimer l'étendue de la dégradation in situ et confirmer les voies de dégradation attendues ?

5. Peut-on estimer les émissions de biocides et leur distribution dans les différents compartiments de l'environnement à l'échelle du quartier ?

Après une introduction synthétisant l'état des connaissances, les enjeux et défis puis les questions de recherche et l'approche générale de la thèse, le chapitre 3 synthétise les méthodes, les expériences et le site d'étude retenus dans ce travail.

Dans le chapitre 3, des méthodes d'extraction robustes sont testées et validées pour l'analyse isotopique Multi-élément composé-spécifique (ME-AICS) à partir de différentes matrices environnementales pour les isotopes stables du carbone ($^{13}C/^{12}C$) et de l'azote ($^{15}N/^{14}N$). Dans le cadre de ces tests, neuf pesticides, dont six herbicides et trois fongicides, sont évalués, y compris le biocide urbain terbutryne et l'herbicide acétochlore. Les techniques d'extraction pour quatre différents types de sols et de sédiments, trois différents types d'eaux environnementales, et les parties aériennes et les racines des plantes sont développées afin de fournir une vue d'ensemble de l'applicabilité de l'AICS aux pesticides dont certains biocides urbains. Ici, nous étendons les recherches antérieures utilisant le SPE (Solid Phase extraction) et la ME-AICS à de nouvelles substances et matrices environnementales. Pour une application plus large de la ME-AICS dans l'environnement, nous étudions une méthode d'extraction modifiée assistée par ultrasons (MUSE) pour extraire les biocides urbains des sols, des sédiments et de la matière végétale.

Dans le chapitre 4, les taux de dégradation et le fractionnement des isotopes stables pendant l'hydrolyse abiotique, la biodégradation aérobie et la photodégradation de la terbutryne sont examinés afin d'améliorer l'interprétation de la dégradation de la terbutryne depuis les façades vers les écosystèmes récepteurs, tels que le sol et les eaux souterraines. Différentes voies de dégradation de la terbutryne peuvent conduire à la formation de PTs distincts et à des fractionnements des isotopes stables spécifiques. Nous examinons donc les cinétiques de la réaction (constante de vitesse), la formation de PT et le fractionnement des isotopes stables du carbone et de l'azote pour évaluer les mécanismes de dégradation de la terbutryne et le potentiel de l'AICS pour suivre sa dégradation in situ et distinguer les voies de dégradation. Les durées de demi-vies de biodégradation de la terbutryne sont élevées (> 80 d). La photodégradation sous une lumière solaire simulée et l'hydrolyse à des valeurs de pH extrêmes sont associées à une dégradation lente dans l'environnement. L'AISC de la terbutryne permet de différencier les voies de dégradation. Les valeurs de fractionnement isotopique du carbone (ε_C) vont de -3.4 ± 0.3‰ (hydrolyse pH 1) à +0.8 ± 0.1‰ (photodégradation sous lumière UV), tandis que les valeurs de fractionnement isotopique de l'azote vont de -1.0 ± 0.4‰ (photodégradation sous lumière solaire simulée en présence de nitrate) à +3.4 ± 0.2‰ (hydrolyse à pH 1). En revanche, le fractionnement isotopique au cours de la biodégradation se révèle insignifiant. Les valeurs $\Lambda N/C$ varient de -1.0 ± 0.1 (hydrolyse à pH 1) à 2.8 ± 0.3 (photodégradation sous UV), permettant de différencier les voies de dégradation. La combinaison de la formation des PTs et du fractionnement des isotopes stables permet donc d'identifier des voies de dégradation distinctes. Dans l'ensemble, cette étude souligne le potentiel de l'AICS pour suivre la dégradation de la terbutryne in situ et différencier les voies de dégradation dominantes, ce qui peut aider à évaluer l'efficacité des stratégies de remédiation et d'atténuation des biocides urbains.

Le chapitre 5 décrit la diffusion, le lessivage et la transformation de la terbutryne à partir de façades artificielles. Nous combinons des expériences au laboratoire de photodégradation, des expériences sur le terrain avec des modèles réduits de façade (1 m^2) et des tests d'immersion sur des façades artificielles peintes avec une formulation industrielle de terbutryne encapsulée pour (i) comprendre de façon mécaniste les processus de libération, de transport et de transformation de la terbutryne sur les façades, (ii) prédire la libération de la terbutryne et la contribution des PTs dans l'eau ruisselée sur les façades pour de longues périodes de temps et (iii) appliquer l'AICS sur l'eau ruisselée de façade pour suivre l'extension de la dégradation de la terbutryn.

Nous supposons que la photodégradation est la principale voie de transformation sur les façades, ce qui pourrait être confirmé par l'AICS. Nous supposons également que les émissions de PTs doivent être intégrées dans des fonctions d'émission des modèles de lessivage existants en tenant compte de variables hydro-climatiques telles que le rayonnement solaire. Nous comparons ainsi la contribution des PTs à la masse totale lessivée (terbutryne + PTs) sur les façades artificielles en extérieur d'avril à octobre pour la corréler avec les variables hydro-climatiques. De plus, nous utilisons des expériences en laboratoire avec une irradiation solaire simulée et des tests d'immersion pour estimer la contribution de processus de mobilisation et de dégradation individuels. Nous suggérons enfin un premier schéma conceptuel de modélisation pour l'implémentation des PTs dans les modèles de lessivage existants. En combinant des expériences sur le terrain et en laboratoire, nous montrons que le rayonnement solaire sur les façades contrôle la formation des PTs et peut être utilisé en combinaison avec le volume d'eau ruisselée pour estimer les émissions à long terme des PTs de la terbutryne à partir des façades des bâtiments. La photodégradation lente ($t_{1/2}$ > 90 jours) de la terbutryne dans la peinture dans les conditions environnementales est associée à un fractionnement isotopique non significatif ($\Delta\delta^{13}C < 2‰$) et provoque une libération de terbutryn-sulfoxyde (un des PTs formès) de 20% plus élevée que celle de la terbutryne dans l'eau ruisselée. Cela indique que la diffusion de la terbutryne vers la surface de la peinture est continue, la rendant accessible à la photodégradation. La contribution des PTs de la terbutryne dans l'eau ruisselée est simulée sur la durée d'existence du quartier ciblé (huit ans) en conditionnant l'intensité de dégradation journalière au rayonnement solaire et le volume d'eau ruisselé. Les émissions de PTs (77 mg m^{-2}) dans l'eau ruisselée sur les façades dépassent de près de 2 fois celles de la terbutryne (42 mg m^{-2}). Dans l'ensemble, cette étude fournit un cadre méthodologique pour estimer les émissions de PTs sur plusieurs années afin d'améliorer l'évaluation des risques environnementaux.

Le chapitre 6 décrit le transport réactif des biocides urbains diuron, terbutryne et octylisothiazolinone (OIT) à travers les interfaces surfaces urbaines-sols dans des conditions environnementales en utilisant différentes approches, y compris un traceur conservateur, des mesures de concentration des composés parents, des PTs et l'AICS. Pour identifier le risque de lixiviation des biocides vers les eaux souterraines, trois lysimètres de 0.23 m^3 différents ont été construits, simulant du gravier, des surfaces pavées avec des joints ou des surfaces végétalisées. Le modèle Hydrus-1D est utilisé pour accompagner l'interprétation du transport réactif des

biocides vers les eaux souterraines sur la base des données expérimentales, puis pour extrapoler le transport réactif des biocides sur les huit ans d'existence du site d'étude en utilisant comme entrée le ruissellement simulé des façades par le modèle COMLEAM. Nous réalisons donc une évaluation réaliste du transport réactif des biocides et des PTs associés vers les eaux souterraines. Pour la terbutryne dans le lysimètre de gravier, 9.5 % pénètrent dans les couches plus profondes sous forme de composé parent et 4.9 % sous forme de PTs. Pour les surfaces pavées avec des joints sur une couche de sable, 17 % de terbutryne sont libérés avec en plus 13.5 % sous forme de PTs, tandis que la masse percolée au travers de sols végétalisés ne dépasse pas 0.5 % de la masse de terbutryne appliquée, sans PTs quantifiables. Dans les trois lysimètres, de 8.5 à 9.4 % de la terbutryne initialement ajoutée sont retenus dans les matériaux constitutifs de ces lysimètres et extraits après l'expérience. De 4.2 à 5 % de la terbutryne appliquée sont retenus sous forme de PTs. Les résultats indiquent que les systèmes végétalisés peuvent agir en grande partie comme un puits pour les biocides. Au contraire, les zones de gravier autour des bâtiments peuvent favoriser le transfert rapide des biocides avec des capacités de rétention limitées vers les eaux souterraines sous-jacentes.

Dans le chapitre 7, nous explorons l'export de biocides urbains depuis les façades vers les systèmes de gestion alternatives des eaux pluviales à l'échelle du quartier en nous basant sur les données d'émission du quartier d'Adelshoffen (Schiltigheim, 67), les bilans massiques et la modélisation du transport réactif des biocides avec COMLEAM. Nous évaluons les tendances actuelles de la gestion durable des eaux pluviales qui vise à favoriser l'infiltration de l'eau mais qui peut aussi augmenter le risque de lixiviation des biocides vers les eaux souterraines. L'étude prouve que les biocides urbains sont disséminés au sein du quartier étudié au sein des sédiments du bassin d'infiltration, dans le sol, dans l'eau pluviale et au sein des plantes aquatiques des systèmes d'infiltration. L'infiltration de l'eau et des biocides joue un rôle important dans les bilans massiques des biocides à l'échelle du quartier, avec des taux d'infiltration des biocides au pied des façades importants compris entre 27 et 73 %, alors que seuls 7 à 39 % des biocides présents dans les façades aboutissent dans les bassins et fossés filtrants d'infiltration des eaux pluviales et les tranchées.

Le chapitre 8 discute les résultats des études mentionnées ci-dessus et synthétise les résultats dans la perspective de la mobilisation et du transport réactif des biocides urbains vers les eaux souterraines. Nous soulignons comment notre approche consistant à combiner les

expériences de terrain et de laboratoire avec la modélisation a amélioré la prédiction du transport réactif des biocides de la source au puits et discutons du cadre conceptuel pour quantifier la libération et la distribution des biocides à l'échelle du quartier et de la ville. En outre, le potentiel, les défis et les limites de l'AICS en tant qu'outil de suivi des biocides urbains dans l'environnement sont examinés en ce qui concerne le fractionnement isotopique de la terbutryne et les améliorations de la sensibilité de l'AICS.

Enfin, le chapitre 9 se termine par les implications et les perspectives sur la manière de prévenir la contamination de l'environnement par les biocides urbains. Deux perspectives principales sont abordées pour aller vers une ville sans biocides : (i) la réduction des rejets de biocides par les bâtiments existants et (ii) la construction de nouveaux bâtiments sans biocides avec des implications pour l'architecture future et les matériaux alternatifs. En outre, l'importance du transfert de connaissances aux dècideurs et aux parties prenantes est discutée.

Table of Contents

List of Tables

List of Figures

Chapter 1

General introduction: Urban biocides and their release into the environment

1 Planetary boundaries and micropollutants in the environment

The climate and ecosystem of Earth are increasingly influenced by an exponential growth of human activities (Hassan et al., 2005; IPCC, 2022). According to the planetary boundary concept, there are nine planetary limits within which mankind can expand and flourish for many more generations (Rockström et al., 2009). To reduce the likelihood of unfavourable or catastrophic environmental changes on a global scale, those boundaries are set as prerequisites that must be upheld. The boundaries include systemic processes at the planetary scale (climate change, ocean acidification, stratospheric ozone) and aggregated processes from local or regional scale (global phosphorous and nitrogen cycles, atmospheric aerosol loading, freshwater use, land use change, biodiversity loss and chemical pollution) (Figure 1. 1). The planetary boundaries of climate change, biodiversity loss and nitrogen cycle have already been crossed (Rockström et al., 2009). Recently the planetary boundary of chemical pollution was renamed into “novel entities” (Steffen et al., 2015) (Figure 1. 1). The novel entities encompass newly created substances, already-existing substances, altered organisms or materials, engineered materials, and naturally occurring components that have been mobilized by human activity (Steffen et al., 2015). Examples are radioactive compounds, heavy metals and a wide range of organic pollutants that can influence the earth system functioning through impacts on human health and

other organisms as well as though feedback reactions with other planetary boundaries (e.g., biodiversity). Chemicals can pose a threat to surpass a planetary boundary if they have disruptive effects on crucial processes of the Earth system, the disruptive effects are not discovered until it becomes a global problem and the effects are not readily reversible (MacLeod et al., 2014). According to a recent study, we are already operating beyond the boundary's safe operation space for novel entities (Persson et al., 2022) (Figure 1. 1). Additionally, the exceedance of the safe operation space of a single chemical class has firstly been described for per- and polyfluoroalkyl substances (Cousins et al., 2022). Even with an immediate reduction or stabilisation of the release of novel entities, the planetary boundary will be exceeding the safe operation space, due to persistence of several novel entities. Therefore, a global approach for reducing emissions of novel entities and implementation of precautionary principles are needed to return back into the safe operation space within the chemical and physical capacity of the Earth system (Persson et al., 2022). Operating outside the safe operation space does not only come with environmental and health risks but also a high cost for society (e.g., healthcare or remediation costs) (Grandjean and Bellanger, 2017; Landrigan et al., 2018).

A framework is thus needed to locate where the pressure on ecosystem health by chemical pollution is already exceeded while identifying sources and actors that contribute to the environmental contamination and reduce it. Such a framework might consider production, life cycle emissions, environmental fate and effects on ecosystems (Kosnik et al., 2022).

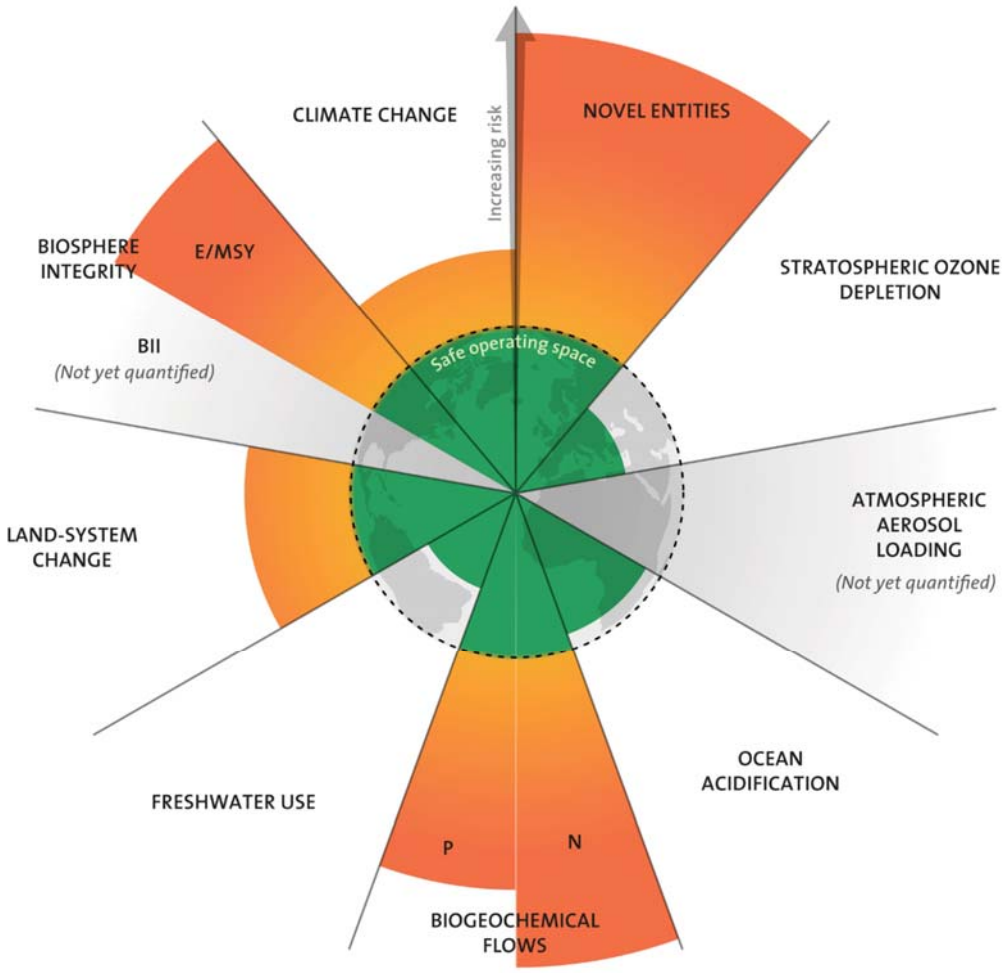

Figure 1. 1. Visualization of the nine planetary boundaries (Stockholm Resilience Centre based on analysis in Persson et al., 2022 and Steffen et al., 2015).

Regarding novel entities, the emission of micropollutants into the environment plays a crucial role. More than 350 000 chemicals and mixtures are on the global market, about 70 000 were registered in the past decade (Wang et al., 2020). Production of those chemicals can lead to unintended by-products, transformation products (TPs) might be formed and the environmental fate of many of the contaminants is unknown (Boxall et al., 2004; Fenner et al., 2013; Schwarzenbach et al., 2006). Micropollutants include a variety of artificial and natural organic compounds that are released to ground- and surface waters in trace quantities (i.e., at or below the microgram per liter level). Several micropollutants are classified as "emerging contaminants" largely due to being unmonitored or unregulated in environmental samples but have become of concern for public and environmental health in recent years. As the term of

emerging contaminants is only loosely defined with a list of compounds that changes over the years, we stick to the term "micropollutants" in this thesis (Kümmerer, 2011). The term micropollutants comprises industrial chemicals (e.g., solvents and petrochemicals), industrial products (e.g., additives), consumer products (e.g., pharmaceuticals, hormones), biocides (agricultural and nonagricultural pesticides), geogenic chemicals (e.g., heavy metals), disinfectants and TPs (metabolites) (Schwarzenbach et al., 2006). Although concentrations of the single contaminants may be low, toxicological effects might be induced, especially when complex contaminant mixtures might express synergistic toxicological effect (Schwarzenbach et al., 2006). To mitigate ecotoxicological effects of micropollutants, two main complementary approaches are needed: 1. Reducing the use of critical compounds and 2. Treating existing contamination (Schwarzenbach et al., 2006). The reduction of micropollutants in environments as proactive strategy to stay within the planetary boundaries of the novel entity must involve several stakeholders, including consumers, manufacturers and authorities (Schwarzenbach et al., 2006) and should focus strongly on the input prevention (Kümmerer et al., 2019).

Can we return into the safe operation space of a planetary boundary? Example of the stratospheric ozone layer

The stratospheric ozone layer is important as it filters ultraviolet irradiation from the sun and counts as a perfect example for crossing the threshold of an earth's boundary. In the late 1970s, chlorofluorcarbons (CFS) were identified to destroy the ozone in the stratospheric atmosphere (Molina and Rowland,1974) which was observed as a great ozone loss over Antarctica (Solomon et al., 1986). As the ozone is crucial for human health to filter sunlight irradiation in the low wavelengths (UVB), the depletion might result in adverse effects. The implementation of the Montreal Protocol in 1989 resulted in the reduction of production and therefore the emissions of CFCs (Solomon, 1999) following an international commitment and the promotion of existing alternatives. As a result, recent studies show a trend for the recovery of the ozone hole (Chipperfield et al., 2017) and attribute a success to the political intervention on CFCs production. According to the World Climate Research Program, the ozone hole might be closed by 2050 (Schrope, 2000).

"The science was listened to, policy-makers did something and it actually worked." – Drew Shindell, NASA Goddard Institute for Space Studies, Bueno Aires, 2000

Pesticides and biocides are two types of chemicals used for pest control, but they differ in their intended use and mode of action. Pesticides are substances with the aim to control pests in agriculture, horticulture, or forestry. They are used to protect crops from damage, to prevent the spread of plant diseases, and to eliminate pests that can cause health problems for humans or animals. On the other hand, biocides are used to control harmful organisms in a wide range of non-agricultural contexts, such as public health, industrial processes, and domestic situations to control bacteria, fungi and other organisms. In the European Union (EU), the regulation of pesticides is governed by the EU Pesticides Regulation (Regulation (EC) No 1107/2009), which was introduced in 2009. In contrary, biocides are regulated under the Biocidal Product Regulation (European Parliament and Council, 2012).

Besides the advantages of pesticides and biocides to control pests and plant disease vectors, vectors of animal disease and harmful organisms (e.g., to humans or materials), several risks, associated with pesticides in the environment have been identified. The risks include effects on human health such as cancer, diabetes or respiratory and neurological disorders (e.g., through direct handling of pesticides or residues in food, water or atmosphere), as well as environmental deterioration in water quality, adverse impact on aquatic species and soil ecosystems, and biodiversity loss (Rani et al., 2021). One use of biocides is to protect construction materials, especially facades, from microbial spoilage. Therefore, biocides are added into paint and render systems (Paijens et al., 2020). Even though, biocides for agricultural uses are well investigated and strictly regulated in the European Union, biocides prohibited for agricultural use are still used in construction materials, due to different regulation processes.

Biocidal products are defined under the Biocidal Product Regulation (BPR) as “any substance or mixture, in the form in which it is supplied to the user, consisting of, containing or generating one or more active substances, with the intention of destroying, deterring, rendering harmless, preventing the action of, or otherwise exerting a controlling effect on, any harmful organism by any means other than mere physical or mechanical action” (European Parliament and Council, 2012).

Chapter 1

2 Urban biocides in construction materials – history, types, application and measurement techniques

2.1 History of biocides in construction materials

Decoration of housings with paintings started as early as 40.000 b.c. with drawings in caves (Brumm et al., 2021). In caves, the paintings were protected from external environmental conditions such as precipitation or solar irradiation. A cave system, in Lascaux, France, contained paintings with an age of around 17 000 years. Those caves have been discovered in the 1940s and opened to public in the 1960s. After attracting around 1800 visitors per day, the caves had to be closed again in 1963, as the microclimate in the caves was distorted and the wall paintings were object to algae and fungi growth due to increased light and CO_2 levels (Bastian et al., 2010). A continuous treatment of the caves with biocides was necessary to preserve the wall paintings (Bastian et al., 2009; Bastian and Alabouvette, 2009).

Nowadays, facade coatings can improve live quality, as they are generally perceived as "key to beauty, charm, design and emotions" (Paulus, 2004). Nevertheless, the primary functions of facades are to provide shelter, facilitate air exchange with the exterior, enable light transmission to the interior and separate public and private areas (Herzog et al., 2012). Temperature (heat and frost), sunlight, rain, humidity, wind, air pollution and noise are needed to be taken into account (Sandak et al., 2019). Facades are thus denoted as a very complex and specific feature in architecture (Boswell, 2013) and urbanism worldwide.

Algae and fungi growth on facades is perceived as undesired or hazardous for the facade (Sandak et al., 2019). In recent years, solvent-based paint and render materials have largely been replaced by water-based paints to reduce volatile organic compound (VOC) emissions. Additionally, enhanced insulation systems on house walls, that are adapted to counteract climate change and reduce CO_2 emission (e.g., through less heating and air conditioning) alter the microclimate, as exterior parts of facades are more susceptible to condensation of water. Those factors result in a suitable growing environment for algae and fungi, moulds, lichens and mosses which might result in unwanted discoloration of the coating. Furthermore, those facades are often seen as damaged (Nordstierna et al., 2010), even though the microbial infestation remains an "aesthetical issue". To counteract the growth of algae, fungi or mould, biocides in form of in-can and film preservatives are added into the coatings. In-can preservatives are added to protect

the coating during storage from microbial growth from the point of production through retail and transportation to the point of usage. Film-preservatives, on the other hand are added to extend the life of coatings by keeping it clean and free from deterioration through infestation, therefore, to protect the aesthetics of the material (Gaylarde et al., 2003).

2.2 Types and application of urban biocides in construction materials

The use of 22 categories of biocidal products is currently regulated under the BPR of which 4 categories are applied in construction materials: (i): In-can preservatives (product type 6) to control microbial deterioration and ensure long storage, (ii) film preservatives (product type 7) for protection of surface materials e.g., paints, renders, sealants or wall adhesives (iii) wood preservatives (product type 8) for protection of wood from deteriorating organisms and (iv) masonry preservatives for the protection of masonry or composite materials from microbial or algal attack (European Parliament and Council, 2012). Paijens et al., 2020 identified the main application processes in urban areas, including the use of biocides in paint and renders, roof treatments (post-treatment of tiles and roof paints, herbicides in bitumen sheets) and treatment of wooden elements. Several different classes of molecules are used with a broad spectrum of physico-chemical properties, including azoles (e.g., propiconazole, tebuconazole), carbamates (e.g., carbendazim, iodopropyl carbamate), isothiazolinones (e.g., methylisothiazolinone, octylisothiazolinone (OIT)), triazines (e.g., terbutryn, cybutryn), phenylureas (e.g., diuron) and other groups (Table 1. 1). To have a broad spectrum of action against microbes, including algae, bacteria and fungi often a variety of up to five biocides are added together with a total mass contribution of up to 0.5% (w/w) in the final product (Burkhardt et al., 2011). In this work, we will focus mainly on film-preservatives, as they are exposed to and released into the environment. In Germany in 2011 the use of film preservatives (product type 7) in paint and render ranged between 200 and 400 t a^{-1}. The main biocides used where diuron, terbutryn and OIT, each with an estimated contribution of 50 – 100 t a^{-1}. (Burkhardt, 2015).

Throughout this work, the term biocide is used synonymous for film-preservatives (product type 7).

Table 1. 1. Molecules, molecular weight (MW), chemical structure, water solubility (WS), octanol-water partitioning coefficient (K_{OW}) and application of typical urban biocides.

Class of molecule	Name and MW (g mol^{-1})	Chemical structure	WS (mg L^{-1})	Log K_{OW}	Application
Azoles	Tebuconazole (307.82)	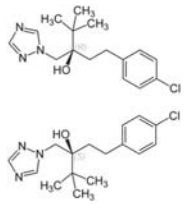	36[a]	3.7[a]	Roof paints[b] wood treatment[c], paint and render[d,e]
	Propiconazole (342.22)	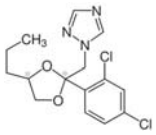	100[a]	3.72[a]	
Carbamates	Carbendazim (191.19)	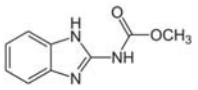	8[a]	1.6[a]	Roof paints[b], facade paint and render[f,g,h]
	Iodopropynyl butylcarbamate (Iodocarb/ IPBC) (281.09)	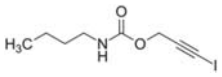	168[a]	2.8[a]	
Isothiazolinones	Benzisothiazolinon (151.18)	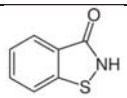	>1000[a]	0.64[i]	Paint/render[f,g,h,j,k,l] Roof paints[b] Post-treatment of roof tiles[m]
	Chloro-methylisothiazolinone (CMIT) (149.59)	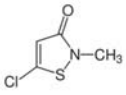	5000 [a]	0.4 [a]	
	Dichloro-octyl-isothiazolinone (DCOIT) (282.23)	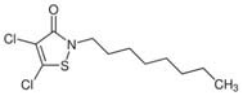	14 [a]	4.9 [a]	
	Methylisothiazolinone (115.15)		Infinite[a]	0.5 [a]	

[a] Paulus, 2004
[b] Jungnickel et al., 2008
[c] Janin et al., 2011
[d] Styszko et al., 2014
[e] Styszko et al., 2015
[f] Schoknecht et al., 2003
[g] Schoknecht et al., 2009
[h] Schoknecht et al., 2013
[i] Wittmer et al., 2010
[j] Bester and Lamani, 2010
[k] Burkhardt et al., 2011
[l] Burkhardt et al., 2012
[m] Pena-Poza et al., 2018

	Octylisothiazolinone (OIT) (213.34)		480[a]	2.45 [a]	
Phenylureas	Diuron (233.09)	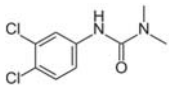	35 [i]	2.71 [a]	Roof Paints [b] Paint and render[d,e,f,g,h,k,l]
	Isoproturon (206.29)	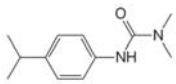	92 [n]	2.50[i]	
Triazines	Cybutryn (253.37)	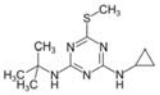	7 [a]	3.95 [a]	Paint and render [d,e,f,g,h,j,k,l,o] Roof paints[b] Post-treatment of roof tiles[m]
	Terbutryn (241.36)	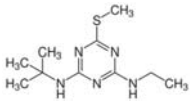	42[n]	3.65[n]	
Pyrithione	Zinc-pyrithione (317.72)	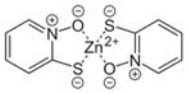	8 [a]	0.93 [a]	Roof paints[b] Facade paint and render[p]

2.3 Measuring urban biocides

2.3.1 Quantification and detection of urban biocides

Environmental samples for biocide quantification are usually commonly using chromatography coupled to a mass spectrometer (MS) as detector. In chromatographic techniques, analytes are separated on a stationary phase with a constant flow of a mobile phase. Most commonly, gas chromatography (GC) is used for volatile compounds, whereas (high performance-) liquid chromatography (HPLC) can be used to analyse non-volatile substances. MS detectors are used commonly as they are highly selective and provide a high sensitivity. Furthermore, some MS are able to provide information of the chemical structure of compounds and therefore enables non-targeted approaches for identification of unknown compounds. For targeted analysis with GC-

[n] Bollmann et al., 2014b [o] Bollmann et al., 2016 [p] Burkhardt et al., 2007

and HPLC-MS methods, reference standards are needed for a certain identification of compounds and calibration curves need to be prepared in the range of the targeted analyte for quantification.

GC-MS. GC-MS systems typically consist of an injector, followed by a GC, consisting of a GC-column in a temperature-controlled oven (McMaster, 2011). The samples run through the column with an inert carrier gas where the sample gets separated into different molecules, before entering the MS interface. In the MS, the sample gets ionized, producing charged molecules. Samples are then typically analysed with a quadrupole by filtering selected mass to charge ratios (m/z) that are able to escape the quadrupole and reach the detector (McMaster, 2011). Only few studies measured urban biocides using GC-MS (e.g., Quednow and Püttmann, 2007), as the low volatility of several compounds is not suitable for the instrumentation and therefore the parallel measurement of a variety of biocides is not possible.

HPLC-MS/MS. GC-MS methods are limited to volatile compounds and provides no possibility to directly inject water samples. Further, possible thermal degradation in the GC oven reduces the applicability of molecules for GC-MS analysis. Therefore, HPLC separation techniques gained more attention in the recent decades. HPLC columns can separate a great variety of compounds with the main prerequisite that the compound can be dissolved (McMaster, 2005). In MS/MS systems, molecules get fragmented and characteristic fragmentation patterns are used to identify and quantify compounds. Similar to GC systems, in LC systems, the separation of compounds is achieved on a stationary phase. For LC systems, the mobile phase consists of solvents, of which a gradient can be set to achieve better separation. Typically, samples are ionised using electrospray ionisation followed by analysis in a triple quadrupole mass spectrometer (QqQ). The first and third quadrupole act as mass filters while the second quadrupole is used as collusion cell for producing fragment ions. In suspect screening approaches, databases are used for identification of compounds based on fragment patterns (McMaster, 2005). Most studies use HPLC-MSMS for the quantification of urban biocides as well as for TPs (if reference analytical standards are available) (e.g., Bollmann et al., 2016; Linke et al., 2021; Paijens et al., 2021).

Non-target screenings. When no information about the dissolved compounds is known, non-target screenings can be conducted. In non-target approaches, compounds are identified by

a number of chemically structures that are associated with a chromatographic separated peak and exact mass measurements. This approach needs more accurate mass spectrometers, which is why quadrupole time of flight (QToF) or orbitrap MS are used (McMaster, 2005). Several studies used HPLC-QToF for the identification of TPs of urban biocides, e.g., for OIT (Bollmann et al., 2017b), terbutryn (Bollmann et al., 2016) or an HPLC coupled to an orbitrap for diuron, terbutryn and OIT TPs (Hensen et al., 2018).

2.3.2 Following contaminant degradation by using compound-specific isotope analysis

Several dissipation process in the environment (e.g., degradative (biodegradation or photodegradation) and non-degradative (dilution or sorption)) might occur simultaneously, making interpretation of reactive transport and degradative process based on concentration measurements difficult. Therefore, advances in monitoring of urban contaminants are necessary to estimate the contribution of degradation to the dissipation of contaminants, identify degradation mechanisms and improve remediation strategies. Compound-specific isotope analysis (CSIA) might help to fill this gap as a concentration independent tool to estimate the extent of degradation (Elsner and Imfeld, 2016). Additionally, CSIA has the potential to identify and distinguish degradation mechanisms, e.g., between hydrolytic biodegradation and alkaline hydrolysis (Elsner et al., 2005; Elsner and Imfeld, 2016).

Isotopes contain the same number of electrons and protons but vary in the number of neutrons and therefore have a distinct mass but the same chemical properties. Typical stable isotopes that are commonly measured for pollutants are carbon ($^{13}C/^{12}C$), hydrogen ($^{2}H/^{1}H$), nitrogen ($^{15}N/^{14}N$) and chlorine ($^{37}Cl/^{35}Cl$) (Elsner and Imfeld, 2016). The ratio of heavy to light isotopes is compared to an international standard (e.g., V-PDB – Vienna-Pee Dee Belemnite for carbon or atmospheric air for nitrogen) and written in the delta notation for the respective element E (δE_{sample}) in permill (‰) due to small changes in the isotope ratio.

$$\delta E_{sample} = \frac{R_{sample}}{R_{standard}} - 1 \qquad \textbf{(1.1)}$$

With the isotope ratio R_{sample} of the sample and the isotope ratio $R_{standard}$ of the reference material.

Degradation may result in isotope fractionation and therefore alteration of δ-values. The observed isotope fractionation is the result of a reaction rate difference between the heavy and light isotopologues (kinetic isotope effect, short KIE) (Elsner, 2010). Typically, bonds containing light isotopes tend to break faster, resulting in an enrichment of heavy isotopes in the non-degraded fraction of the molecule. Non-degradative processes such as sorption, volatilisation or advective transport usually only cause minor isotope fractionation for organic molecules (Elsner et al., 2005). The extend of degradation can be related to the isotope fractionation with the Rayleigh equation to calculate isotope fractionation values (ε) (Elsner, 2010):

$$\ln\left(\frac{R_{t,E}}{R_{0,E}}\right) = \ln\left(\frac{c_t}{c_0}\right) \cdot \frac{\varepsilon_{bulk}^{E}}{1000} \qquad \textbf{(1.2)}$$

With the isotope ratio R_t of element E and concentration c_t at time t as well as at the initial time ($R_{0,E}$ and c_0) the isotope fractionation value (ε) in permil. The isotope fractionation value can be used to estimate the extend of degradation *in situ* (Fischer et al., 2016) independent of the contaminant concentration:

$$B_E[\%] = 1 - f \cdot 100 = \left[1 - \left(\frac{\delta_{E,t} + 1000}{\delta_{E,0} + 1000}\right)^{\frac{1000}{\varepsilon_{bulk}^{E}}}\right] \cdot 100 \qquad \textbf{(1.3)}$$

Measuring stable isotope ratios of at least two elements in one molecule can reveal detailed information about reaction pathways and reaction mechanisms (Nijenhuis and Richnow, 2016; Vogt et al., 2016). The changes of two stable isotopes (multi element (ME) CSIA) can be used to be a quantitative parameter for respective degradation pathways, with the slope (Λ) denoting a transformation pathway specific value, for example for carbon (C) and nitrogen (N):

$$\Lambda^{N/C} = \frac{ln\left[\frac{\frac{\delta^{15}N_t}{1000}+1}{\frac{\delta^{15}N_0}{1000}+1}\right]}{ln\left[\frac{\frac{\delta^{13}C_t}{1000}+1}{\frac{\delta^{13}C_0}{1000}+1}\right]} \approx \frac{\varepsilon^N_{bulk}}{\varepsilon^C_{bulk}} \quad \textbf{(1.4)}$$

ME-CSIA was already applied for several chlorinated solvents, however only few studies exist for organic micropollutants (Drouin et al., 2021; Masbou et al., 2018).

3 Urban biocides – entry paths into the environment

3.1 Occurrence of biocide leaching from construction materials in the environment

Film-preservatives are intended to move into the coatings surface to act against the targeted microorganisms (Paulus, 2004). Therefore, with each rain event, biocides can be washed off from facade surfaces and enter the environment (Burkhardt et al., 2012). The release and entry pathways from facades and roof materials have been identified and discussed in laboratory and field emission studies (Bollmann et al., 2016, 2017b; Burkhardt et al., 2011, 2012; Schoknecht et al., 2009, 2013; Wangler et al., 2012). Urban biocides have been detected in various environmental compartments, such as stormwater, wastewater, rivers and groundwater (Paijens et al., 2020). Negative impacts (e.g., bioconcnetration and adverse ecotoxic effects) on the aquatic ecosystems might appear, even though the environmental concentrations for different biocides are mostly below acute toxicity values (Kresmann et al., 2018).

3.1.1 Release of biocides from construction materials

Several studies report high emissions shortly after the construction (several mg L^{-1}), followed by a decrease of emissions over time (concentrations of tens of µg L^{-1}) (Bollmann et al., 2017a, 2017b; Burkhardt et al., 2011, 2012; Wittmer et al., 2011). The release of film preservatives may continue for long time periods and was observed even from 14-year-old facades (Hensen et al.,

2018). Besides the previous mentioned physico-chemical parameters, emissions are dependent on the initial conditions, e.g., the mass of biocides in the coating and whether the biocides are encapsulated (Bollmann et al., 2017b, 2016; Burkhardt et al., 2012). Since 2001, biocides started to be encapsulated (Figure 1. 2) in microcapsules (or microspheres) to slow down biocide release and thus retain biocides in facade coatings for extended periods of time (Andersson Trojer et al., 2015; Burkhardt and Roger, 2011; Nordstierna et al., 2010; Vermeirssen et al., 2018). Encapsulated biocide formulations are used in construction materials since 2006. Those capsules often consist of different kind of organic or silica-based polymers in which biocides can be absorbed strongly, or as nanoparticles that are dispersed in the paint matrix (Burkhardt and Roger, 2011; Handa et al., 2006; Shtykova et al., 2009).

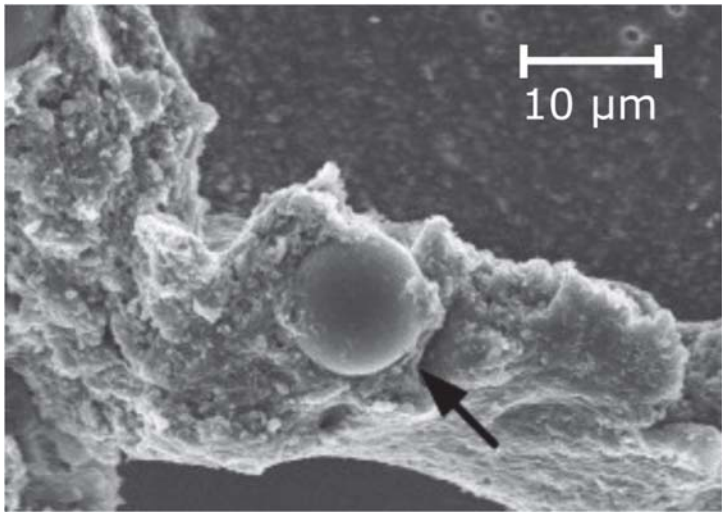

Figure 1. 2. Microsphere (encapsulation shown by black arrow) of biocides in the water-based paint (adapted from Nordstierna et al., 2010).

Several laboratory and environmental studies were conducted to monitor the release of urban biocides from render and paint surfaces (e.g., Bollmann et al., 2017b, 2016; Burkhardt et al., 2007; Schoknecht et al., 2013; Urbanczyk et al., 2016; Vega-Garcia et al., 2020; Wangler et al., 2012; Wittmer et al., 2011). In immersion and irrigation experiments, the release of eight biocides was investigated from different materials (Schoknecht et al., 2009). The biocide release was described using time dependent functions for the release. Emissions of different biocides were related to water solubility and partitioning coefficients of the biocides (Schoknecht et al., 2009). Styszko et al., 2015 tested the leaching of 11 different biocides in laboratory conditions from acrylate and silicone-based render systems. Acrylate and silicone render showed significant

different leaching behavior with stronger leaching in the acrylate render. Two studies described the leaching from acrylate and silicone render in the environment for 19 months for OIT and terbutryn, respectively (Bollmann et al., 2016, 2017b). Laboratory studies revealed, that the contact time with water is a main factor for the biocide release (Schoknecht et al., 2009). Jungnickel et al., 2008 observed high concentrations of the biocides carbendazim and terbutryn especially during small rain events. In contrast, biocide concentrations were lower during large rain events, although the total exported mass was higher.

In most studies examining biocide leaching, pure biocides were used in non-encapsulated formulations, which might lead to an overestimation of biocide release. An overestimation of biocide release may be especially observed in the beginning of the experiments, whereas biocide release may be underestimated for longer time periods and long-term emission scenarios. A comparison between field emissions and immersion tests was conducted for several painted surfaces (Schoknecht et al., 2016). The runoff amount was identified as a key parameter to compare field and laboratory experiments. The mass balances were not closed, highlighting the influence of degradation or evaporation of compounds on the biocide mass balance (Schoknecht et al., 2016). Less biocides were emitted during natural conditions than in standard immersion tests that were conducted according to European standard immersion tests (e.g. EN16105). This raises the difficulties to compare laboratory and field emissions (Schoknecht et al., 2016) and predict environmental release rates solely on laboratory experiments.

Leaching was described to happen in five steps (Uhlig et al., 2019): i) During rain events, water diffuses into the coating. ii) Biocides desorb from the hydrated microcapsules and are released into the water phase within the coating. iii) Biocides diffuse according to the concentration gradient to the outside layer of the facade. This process is dependent on the temperature and can be accelerated if the diffusion gradient is maintained through advective transport of the biocides at the surfaces of the coating. iv) Degradation via photolysis or hydrolysis at the outset layer of the façade system which reduces the number of biocide molecules. v) Continuous runoff and advective transport of biocides on the surface of the facade during the rain event. Even though, degradation of urban biocides on facade systems was already described, detailed knowledge about factors influencing specific degradation processes is missing.

3.1.2 Parameters influencing release of urban biocides from facades

There are two categories of parameters that were identified to influence the leaching of biocides from facades. Firstly, physico-chemical parameters, that are the physical and chemical parameters of biocides themselves and of the coating they are embedded in. This includes the solubility of biocides in the coating and water, and partitioning coefficients (e.g., log K_{OW} for the partitioning between octanol and water phase) which influence their release into water. These parameters can vary significantly between different biocides (Table 1. 1). Additionally, the material of the coating has influence on the biocide leaching: in silicon render less emissions were observed compared to acrylic render (e.g., Bollmann et al., 2016, 2017b; Styszko et al., 2014). This indicates that materials with higher organic content tend to retain biocides stronger in their matrix if the biocides have high K_{OW} values.

Secondly, environmental factors are key drivers for biocide release into the environment. Wind driven rain and therefore the volume of water in contact with the facade coating is the main factor for the amount of biocides released from a facade (Burkhardt et al., 2012; Vega-Garcia et al., 2020). Wind direction and speed influence wind driven rain, but also determine the facade orientation which is exposed most to those climatic conditions. Also, an influence of the temperature on the leaching has been observed (Burkhardt et al., 2012, 2011; Wangler et al., 2012) with increasing emission rates with increasing temperature, likely as a result of enhanced diffusion. However, there is a need to investigate further processes on the behaviour of biocide leaching. In particular, degradation, including biodegradation, photodegradation or hydrolysis, may control biocide emission in the environment by reducing the initial amount of parent compound that is released but potentially increasing the amount of TPs entering into the environment (Bollmann et al., 2016; Fenner et al., 2013). The effect of degradation on biocide release rates from facades has not been described yet.

3.1.3 Biocide transformation in the environment

3.1.3.1 Degradation

Following the release of biocides from the facade, biocides might undergo degradation either directly on the facade or in receiving compartments. To understand, quantify and predict the

environmental fate of biocides, factors affecting biocide degradation need to be understood. Degradation is the only process to remove biocides from the environment (Fenner et al., 2013), but also leads to the formation of TPs. Several degradative processes are involved in biocide dissipation, e.g., photodegradation, hydrolysis, biodegradation and reductive transformation. Those degradation pathways are mainly associated, but not restricted, to specific environmental compartments and conditions (Figure 1. 3). Degradation rates are typically given in half live times ($t_{1/2}$, the time a process needs to decrease the initial concentration of a compound by 50%).

Photodegradation typically occurs in surface waters but was already observed for biocides on facades (Figure 1. 3). Direct photodegradation is defined as the absorption of light by a molecule resulting in bond cleavage. Indirect photodegradation results typically from the excitation of other molecules, e.g., nitrate or dissolved organic carbon (DOC), which can react with other molecules, and subsequent in bond cleavage (Drouin et al., 2021; Schwarzenbach et al., 2005). Photodegradation of several urban biocides was tested under UV light and simulated sunlight in laboratory tests, as well as under environmental sunlight irradiation. UV-C irradiation (254 nm) resulted in fast degradation of terbutryn and diuron in deionized water, whereas carbendazim was not degraded. Under environmental conditions, none of the compounds showed significant degradation within 17 days (Minelgaite et al., 2017). The importance to select the correct irradiation setup (e.g., irradiation intensity and the use of wavelengths reproducing sunlight spectrum) in laboratory experiments was discussed and tested for terbutryn, mecoprop and penconazole (Hensen et al., 2019). Degradation rates were faster in presence of nitrates (indirect photodegradation) and results varied as a function of the chosen irradiation setup in terms of degradation rates and TP formation. Two studies combined UV-light induced laboratory experiments with field studies to monitor and identify photodegradation products of terbutryn and octylisothiazolinone (OIT) in facade leachates (Bollmann et al., 2016, 2017b). Seven photodegradation products were identified for terbutryn, eleven for OIT. The same studies observed photodegradation for both compounds directly on facades under environmental conditions (e.g., irradiation spectrum of sunlight). In another study, the degradation of urban biocides (carbendazim, diuron, OIT and terbutryn) in paint was tested through irradiation with UV-A (Urbanczyk et al., 2019). Carbendazim did not degrade significantly. For the other biocides, differences in degradation rates were observed dependant on added pigments and polymers in the paint, indicating the presence of different degradation mechanisms and light

absorption rates as well as a combination of direct and indirect photodegradation mechanisms (Urbanczyk et al., 2019).

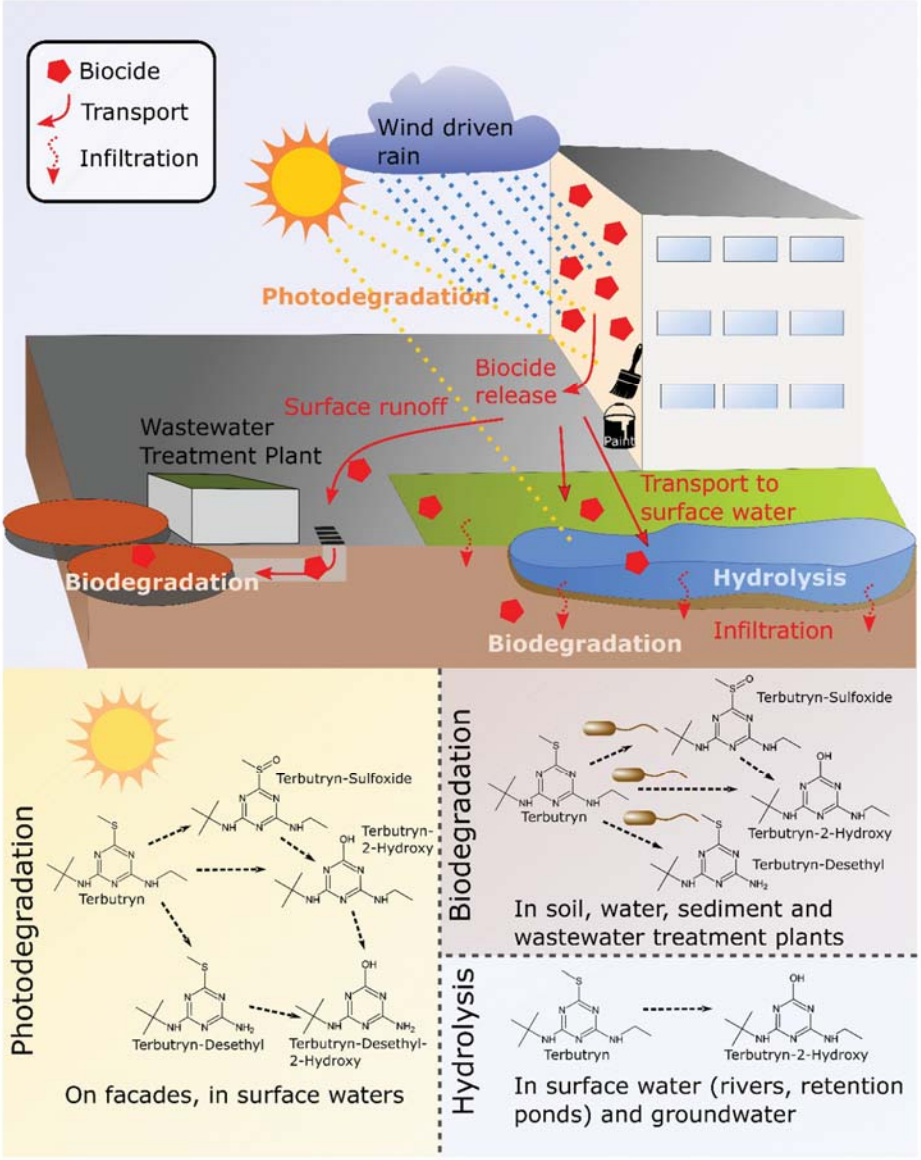

Figure 1. 3. Scheme of release and degradation processes of urban biocides in different compartments. Reactions and TPs based on the major TPs from literature and suggested degradation pathway for hydrolysis based on atrazine hydrolysis (similar, triazine herbicide) (Bollmann et al., 2017a, 2016; Luft et al., 2014; Masbou et al., 2018).

Biodegradation can be defined as transformation of molecules mediated by organisms. Typically, biodegradation is seen as the most important process of pesticide degradation (Fenner et al., 2013). Prokaryotes can metabolize pesticides for assimilation of nutrients and energy, whereas eukaryotes (plants, animals and fungi) transform pesticides with the aim of detoxification (Fenner et al., 2013). The aerobic biodegradation of several urban biocides has been examined in soil, including iodocarb, methylisothiazolinone, benzisothiazolinone, OIT, dichloroctylisothiazolinone, mecorop, isoproturun, terbutryn, propiconazole, tebuconazole and diuron (Bollmann et al., 2017a) (Figure 1. 3). Degradation half live times ($t_{1/2}$) ranged from several hours (methylisothiazolinone) to hundreds of days (terbutryn) with no observed degradation for diuron, tebuconazole and propiconazole. The mass balance for terbutryn was closed when including seven TPs. Transformation of terbutryn and irgarol (cybutryn) in activated sludge from wastewater treatment plants (WWTP) was monitored and $t_{1/2}$ ranged from 1.9 to 10.5 d, depending on the spike concentrations and used sludge (Luft et al., 2014). The estimated removal rates in WWTPs were 40-60%.

Hydrolysis. Another major pathway of pesticide degradation in the environment is hydrolysis (Figure 1. 3), which can either be biotic or abiotically mediated (Fenner et al., 2013). Hydrolysis is, generally speaking, any reaction with water and is dependent on pH and temperature (Mabey and Mill, 1978). Hydrolysis experiments for urban biocides are rare. Hydrolysis rates of two isothiazolinones were tested at pH 4, 7 and 9 and only slight hydrolysis of methylisothiazolinone at pH 9 was observed while chloromethylisothiazolinone was hydrolytically stable under the tested conditions (Park and Kwon, 2016). Similar triazine type pesticides than terbutryn showed only little hydrolytic degradability at extreme pHs (Masbou et al., 2018; Meyer et al., 2009; Torrentó et al., 2021).

Degradation generally results in (partial) removal of the parent compounds and often leads to the formation of TPs with different physico-chemical properties than those of the parent compounds. The contribution of different TPs depends on the degradation pathway. Only little is known so far on the contribution of different degradation pathways to the overall degradation of urban biocides in the environment.

3.1.3.2 Transformation products and degradation pathway identification

During degradation, the parent molecule is removed from the environment, however TPs are often formed (Figure 1. 3; Fenner et al., 2013). TPs are formed from a specific compound (e.g., biocide) as a result of metabolism of microorganisms, a chemical reaction or environmental processes (e.g., hydrolysis, UV irradiation in treatment systems or natural sunlight irradiation). TPs of some compounds are detected in higher frequency than their parent compounds and can be more persistent than their parent compound and therefore accumulate in the environment (Boxall et al., 2004). Mixtures of TPs and parent compounds might lead to additive or even synergistic toxicity effects, making it crucial to carefully monitor and consider TPs in environmental studies (Boxall et al., 2004; Escher and Fenner, 2011). Several studies identified already a variety of TPs from urban biocides. For six targeted pesticides, 45 TPs were identified, demonstrating, that the number of substances that need to be investigated is significantly higher when considering TPs compared to only parent compounds (Hensen et al., 2020). For penconazole (10), diuron (5), terbutryn (12), OIT (7) and mecoprop (4) TPs have been identified (Hensen et al., 2020) while other studies identified even more TPs for OIT (11) (Bollmann et al., 2017b), even though for some TPs a validation through an analytical standard was not available. Transformation products are included in the BPR if they are formed in large quantities (> 10%) at any time during degradation experiments. Transformation products have to be investigated in regard of their ecotoxicity, similar to parent compounds, however, reliable data is often missing.

Detailed degradation pathways have been suggested for terbutryn and OIT during photodegradation and biodegradation (Bollmann et al., 2017a, 2017b, 2016). For OIT during biodegradation, four TPs were identified: octylamide, octylmalonamic acid, octylacetamide and octylpropenamide. All TPs were further degraded, suggesting no further accumulation in the environment. Detailed degradation pathways were proposed for photodegradation of OIT in water with the formation of 3-octylthiazol-2(3H)-one, octylamine, octylformamide, octylprop-2-enamide, octylacetamide, octlymaolonamic acid and octyloxamic acid.

Environmental risk assessment usually does not integrate TPs. However, TPs can exhibit less, similar or even higher toxicity towards specific organisms and mixtures of different compounds or parent compounds with TPs might have synergistic toxicological effects (Boxall et al., 2004; Escher and Fenner, 2011). Increased ecotoxicity of a photolytic terbutryn solution (terbutryn and TPs) indicated that some TPs can be more toxic than the parent compound

(Hensen et al., 2020). Therefore, TPs need to be added to environmental studies. The contribution of TPs to overall urban biocide toxicity is rarely examined.

4 Distribution of biocides and transformation products in the environment and among compartments and their interfaces

4.1 The concept of sponge cities: improved rainwater management but an entry path of biocides towards groundwater?

In recent years, there is an increasing trend towards sustainable storm water management in cities, including local infiltration and stormwater retention systems at the district scale (Goulden et al., 2018). In China, the principle of sponge cities was established to face problems of flood management in highly urbanized areas and improving ecological aspects of cities and drainage infrastructure. Concepts include green roofs, artificial wetlands, stormwater infiltration ponds, biological retention facilities and permeable paving (Jia et al., 2017; Li et al., 2017, 2018; Wang et al., 2018). In contrast to conventional drainage systems (combined and separate sewer systems, Figure 1. 4) with the aim to remove stormwater as fast as possible from the city, sustainable stormwater management sees water as resource with several functions and benefits for society and the environment, such as better city climate, reduced wastewater treatment and flood control (Barbosa et al., 2012; Goulden et al., 2018; Hering and Ingold, 2012; Mitchell, 2006). Separate sewer systems use separate pipes for sanitary sewage and stormwater flow (Figure 1. 4). Stormwater flow is discharged directly into surface waters. In combined sewer systems, the same pipe is used for sanitary sewage and stormwater runoff. In case of high precipitation events, in which wastewater treatment plants cannot handle the sudden large amount of water, overflows can be activated from which water is then discharged into surface water without treatment. In sustainable stormwater management, water is infiltrated and evaporated on the district scale through ponds, wetlands or ditches. However, infiltration of urban biocides with stormwater towards groundwater is rarely addressed (Figure 1. 4).

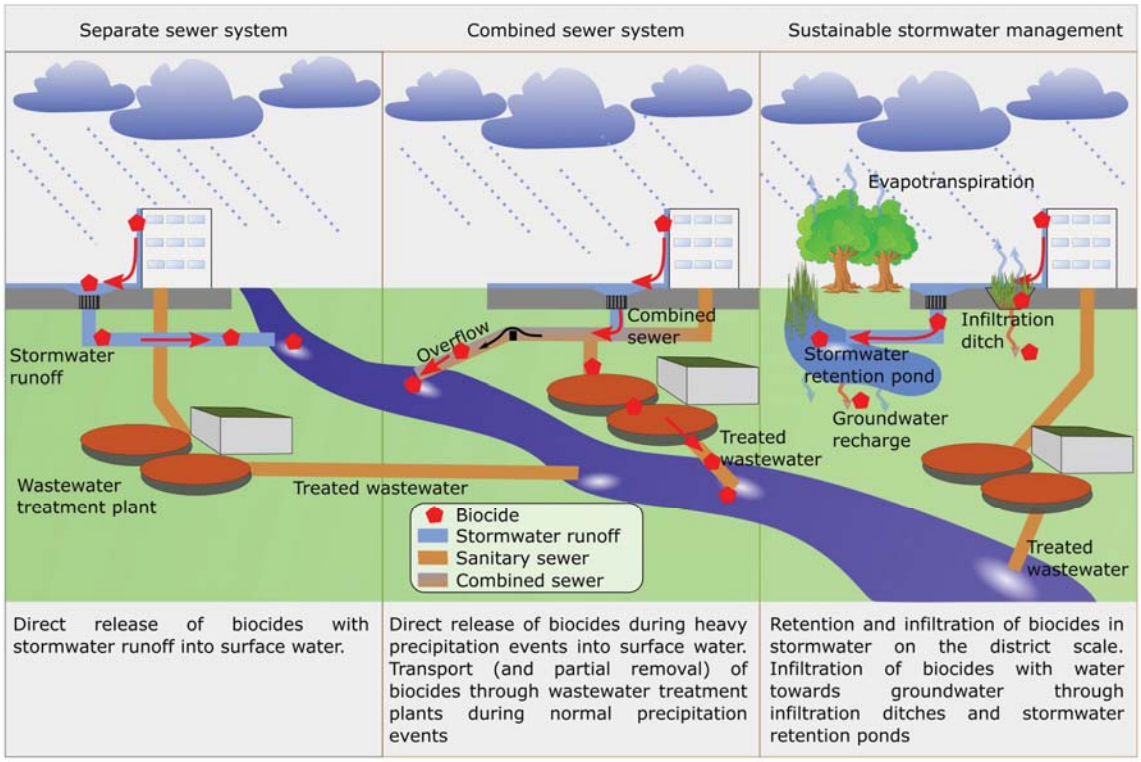

Figure 1. 4. Entry paths of biocides into the environment dependent on the stormwater management system.

A recent study indicated that urban stormwater infiltration systems are not reliable sinks of biocides (Bork et al., 2021). Biocides may enter the groundwater through preferential flow paths, e.g., macropores. Based on passive samplers, increasing groundwater concentrations downstream of stormwater infiltration systems were observed for carbendazim and diuron (Pinasseau et al., 2020). Overall, little is known about the retention capacities of urban biocides in sustainable stormwater management systems. There is a strong need to evaluate the benefits of sustainable stormwater management with the potential risk of groundwater contamination following direct infiltration of urban biocides at the district scale.

4.2 Urban biocides in soil

After the release from facades, biocides might enter directly into soil. So far, there is only little data about urban biocides accumulation, distribution, degradation and transport mechanisms in soil (Reiß et al., 2021). In urban soil sampling, six biocides were detected, including terbutryn,

diuron, OIT, tebuconazole, propiconazole and carbendazim (Bollmann et al., 2017a). Concentrations ranged from 0.001−0.1 µg g^{-1} dry soil. Besides parent compounds, also TPs of terbutryn were detected in the range of 0.1 to 20 ng g^{-1}, including terbutryn-sulfoxide (Ter-SO), terbutryn-desethyl (TerDesE), terbutryn-desethyl-2-hydroxy (TerDesEOH) and terbutryn-2-hydroxy (TerOH) (Bollmann et al., 2017a). The effects of leachate on soil organisms are rarely examined and effects of TPs are often disregarded (Vermeirssen et al., 2018).

4.3 Biocides in storm water basins, retention ponds and swales

Stormwater can be retained on the district scale to reduce stress on treatment systems and on rivers through separated sewers or swale systems and retention ponds (Figure 1. 4), which are part of a sustainable stormwater concept (Figure 1. 4). Retention ponds aim to hold water during rain events and slowly release it towards rivers or through evaporation and infiltration and therefore groundwater recharge. In swale systems, high concentrations above predicted no effect concentrations (PNEC) values were found for diuron (174 ng L^{-1}) and terbutryn (40 ng L^{-1}). Furthermore, the TPs TerOH and TerDesE, have been measured at some events at even higher concentrations than the parent compound terbutryn. Additionally, a TP of diuron was detected (diuron-desmethyl) (Linke et al., 2021).

Three targeted urban biocides (terbutryn, diuron and OIT) were detected in urban stormwater systems (swales and trenches) during rain events (Hensen et al., 2018). Besides the parent compounds, a variety of TPs have been detected (TerOH, TerDesE and terbumeton for terbutryn and diuron desmethyl of diuron). Another study in a separate sewer system with a stormwater retention pond found 11 different urban biocides draining from a residential catchment of 21.5 ha (Bollmann et al., 2014b). The highest median concentrations were found for terbutryn and carbendazim (45 ng L^{-1} and 52 ng L^{-1} respectively), with peak concentrations of up to 1800 ng L^{-1} for terbutryn. The total emission per house was estimated to 59 µg terbutryn per event and house. Furthermore, the study identified, that during rain events, biocides are introduced into the systems continuously rather than in a first flush event. However, little is known about the reactive transport behaviour of urban biocides in and from stormwater retention systems towards groundwater.

4.4 Wastewater treatment plants and combined sewer overflows

In combined sewer systems, urban stormwater discharge is entering wastewater treatment plants and can enter sewer overflows at heavy rain events (Figure 1. 4), therefore, by-passing the WWTP with a direct release in rivers. Concentrations of cybutryn, terbutryn; carbendazim, iodocarb, isoproturon, diuron, tebuconazole, propiconazole and mecoprop in the range of < 10 to 100 ng L^{-1} have been detected in WWTP influents in Denmark and Sweden (Bollmann et al., 2014a). Biocides occur in dry weather as well as during rain events. This indicates not only contribution of building runoff but may also reflect a contribution of biocides in combined sewer systems e.g., through washing of construction tools during construction (paint and render from brushes). Combined sewer overflows contribute significantly to the mass load of biocide emissions into river systems (Wittmer et al., 2010). A high contribution of terbutryn, diuron, isoproturon, carbendazim, tebuconazole and mecoprop in combined sewer overflows rather from stormwater (leaching from building materials) than from wastewater was also observed by Paijens et al., 2021. Contributions of nearly > 90% via combined sewer overflows (bypassing WWTPs) compared to WWTPs into surface waters were observed for several compounds (e.g., diuron, isoproturon, mecoprop). Nevertheless, the ubiquitous occurrence of 18 urban biocides in WWTPs was observed. Removal rates of biocides in treatment facilities were low with no removal at all for several biocides (Paijens et al., 2021). Abundance and poor (< 50%) removal rates of urban biocides such as OIT, mecoprop, irgarol and some TPs (e.g., TerDesE) were previously described (Singer et al., 2010). Discharge of those pollutants through WWTPs into surface waters could be reduced through advanced treatment systems (Guillossou et al., 2019). However, the implementation of advanced treatment systems is expensive and does not account for discharge from combined sewer overflows. Several other studies provided big datasets of the ubiquitous occurrence of urban biocides in WWTPs and respective input into other environmental compartments (e.g., rivers) (Launay et al., 2016; Liu et al., 2017; Östman et al., 2017; Wittmer et al., 2010). Altogether, this highlights the importance of WWTP as source of urban biocides in the environment.

4.5 Surface water

Rivers. A variety of studies indicate the occurrence of urban biocides in rivers (e.g., Ccanccapa et al., 2016; Öllers et al., 2001; Singer et al., 2010; Wittmer et al., 2010). Concentrations range typically from a few ng L^{-1} to several µg L^{-1} for detected biocides (Paijens et al., 2020). On the Paris catchment scale, up to 10 kg a^{-1} of DCOIT and IPBC, 100 kg a^{-1} of diuron, terbutryn and over 100 kg a^{-1} carbendazim and mecoprop were estimated to enter the Seine River via wastewater treatment plant effluents (Paijens et al., 2021). Generally, urban biocides have mainly been targeted in European rivers, however, studies also proof the occurrence in rivers in North America, Brazil, China, Australia and Tanzania (Paijens et al., 2020). However, it is to mention that in some countries, some biocides are additionally used in agricultural applications, whereas they are prohibited in Europe. Diuron was detected in all samples in five rivers in Switzerland with regular exceedance of annual average environmental quality standards (AA-EQS) (Moschet et al., 2014). A study monitored the concentrations of terbutryn in a small river in Germany for three years following the ban for agricultural use. The study concluded that the ban had no influence on terbutryn concentration in water. Maximum concentrations of 5.6 µg L^{-1} were measured with mean concentrations over 500 ng L^{-1} in two rivers (Quednow and Püttmann, 2009, 2007). The ubiquitous occurrence of urban biocides in rivers in varying concentrations indicates a strong need to closely monitor concentration dynamics in surface waters, while identifying main sources, to apply concrete measures to reduce surface water contamination.

Lakes. Only few data are available about urban biocide concentrations in lakes. Irgarol and terbutryn were detected in low concentrations up to 5 ng L^{-1} in the Greifensee, Switzerland (Öllers et al., 2001). The biocides irgarol, diuron and terbutryn were detected in sediments of lakes in northern Germany, with maximum concentrations of 45 ng g^{-1} TOC for terbutryn. Those biocides were identified as drivers of the toxicity resulting in a poor quality of the state of macrophytes (Machate et al., 2021). Another study identified increasing concentrations in lake sediments of irgarol over the recent years, with co-occurrence of terbutryn (Chiaia-Hernandez et al., 2013). Studies about urban biocides focus mainly on the discharge into rivers. However, plant protection products and urban biocides might accumulate over long time periods in the sediments (Chiaia-Hernández et al., 2020).

4.6 Groundwater

Stormwater infiltration is a current approach to improve urban stormwater management with the aim of sustainable stormwater management (Barbosa et al., 2012; Boller, 2004). Those stormwater infiltration systems may act as a source of urban biocides in groundwater. Urban stormwater infiltration systems might not retain biocides sufficiently and biocides might enter the groundwater under urban areas. The infiltration of urban biocides into groundwater is of great importance, as groundwater is used as the main drinking water source in Europe (European Environment Agency, 2022). An increasing risk of biocides leaching into groundwater with increasing number of macropores (e.g., from biological activity) was observed (Bork et al., 2021). Pinasseau et al., 2020 identified that infiltration of stormwater can alter the composition of pesticides in groundwater. By using passive samplers, they identified increasing concentrations of diuron and carbendazim in groundwater due to water infiltration while legacy compounds got diluted through the groundwater recharge. Terbutryn, diuron and OIT occurred in groundwater samples after stormwater infiltration systems in a residential catchment (Hensen et al., 2018), however concentrations were below the insignificance thresholds for the assessment of groundwater pollution for individual biocides (0.1 µg L^{-1}) and the sum of all measured biocides (0.5 µg L^{-1}) (Länderarbeitsgemeinschaft Wasser (LAWA), 2004). Additionally, TPs of all biocides were detected. Therefore, measures to protect groundwater quality need to be implemented to reduce pollution, especially in sensitive groundwater recharge areas (European Environment Agency, 2022). Additionally, the reactive transport processes towards groundwater need to be understood to forecast and mitigate biocide leaching and evaluate the formation of TPs.

5 Occurrence, transformation and risks of urban biocides using modelling approaches

Models can help to evaluate the contribution and impact of urban biocides to total chemical pollution in catchments. A facade leaching model was coupled to a runoff model on the catchment scale (Coutu et al., 2012a, 2012b). The model describes facade leaching from experimental data and underscores that the age of paint may play a minor role on the city scale. Indeed, on the city scale one has typically a distribution of old and new buildings and therefore

a distribution of the age of paint and biocide release. Several assumptions are considered for the models, e.g., biocides reaching soil are completely immobilized or degraded. The model was applied and validated for terbutryn, diuron and carbendazim with satisfactory results and estimated biocide release into rivers through separated sewers in the city of Lausanne, Switzerland, in the range of 900 kg a^{-1}. The model also predicted low probabilities to exceed PNEC values in rivers linked to the city of Lausanne for the three targeted compounds.

The model COMLEAM (COnstruction Material LEAching Model) was developed to assess the leaching of biocides and other substances from facades (Burkhardt et al., 2020). The model takes into account substance properties (e.g., through emission functions), real weather data (precipitation, wind direction and speed) for calculation of wind driven rain as main factor for biocide emissions, runoff coefficient for the different materials and the geometry of buildings to estimate facade leaching and effects on water quality. The model was already applied for a variety of studies, assessing exceedances of PNEC levels in water bodies receiving facade runoff (Wicke et al., 2022). The web-based model FReWaB-Plus is a simple and user-friendly tool, mainly intended for urban planners to simulate water volumes and potential biocide releases from urban catchments (Bork et al., 2022).

Another asset of models is their capacity to estimate biocide loads that are discharged to runoff. Using such models could be a first step to risk assessments but it relies on the availability of information, such as the consumption data or sale volumes, the amount of rainfall available for facade leaching or the facade surface area, which are often not readily accessible. Moreover, the variability of catchments and cities highlights limits of model genericity because of different land-uses and impervious surfaces, the age and the orientation of buildings or the weather conditions (Gaylarde et al. 2011). Many uncertainties remain to accurately estimate biocide release and transport into the environment, including the spatial variability of rainfall, particulate contamination for more hydrophobic biocides, such as benzalkonium chlorides, and the variety of sewer discharges (e.g., stormwater discharges, combined sewer overflows and WWTP discharges during wet weather). Further research should focus on biocide releases on the city-scale to address potential of groundwater contamination with implementation of TPs, which are currently disregarded in the mentioned models. Models for the reactive transport of pesticides towards groundwater exist, but are often very specific to agricultural uses, disregarding the different materials and complexity of urban systems. Further, current reactive degradation

models often use lumped half-live values for contaminants, disregarding the complex interaction between various degradative processes that might occur simultaneously (Höhener et al., 2022).

6 Risk evaluation: ecotoxicological effects of urban biocides

6.1 Ecotoxicological effects of urban biocides in water

The ecotoxicological risk of biocides is determined by comparing measured environmental concentrations to toxicity threshold data such as the PNEC (European Parliament and Council, 2008). Single measurements of urban biocides report repeatedly higher environmental concentrations than PNEC for single compounds in water (exemplary for terbutryn in Figure 1. 5). However, annual mean concentrations for proper risk assessments are generally missing. The evaluation of risk towards aquatic organisms based on single compounds neglects synergistic and cocktail effects. Besides the parent compounds, TPs can also induce toxic effects on organisms. This makes the evaluation of the risk based on a single compound even more difficult and uncertain (Hensen et al., 2020).

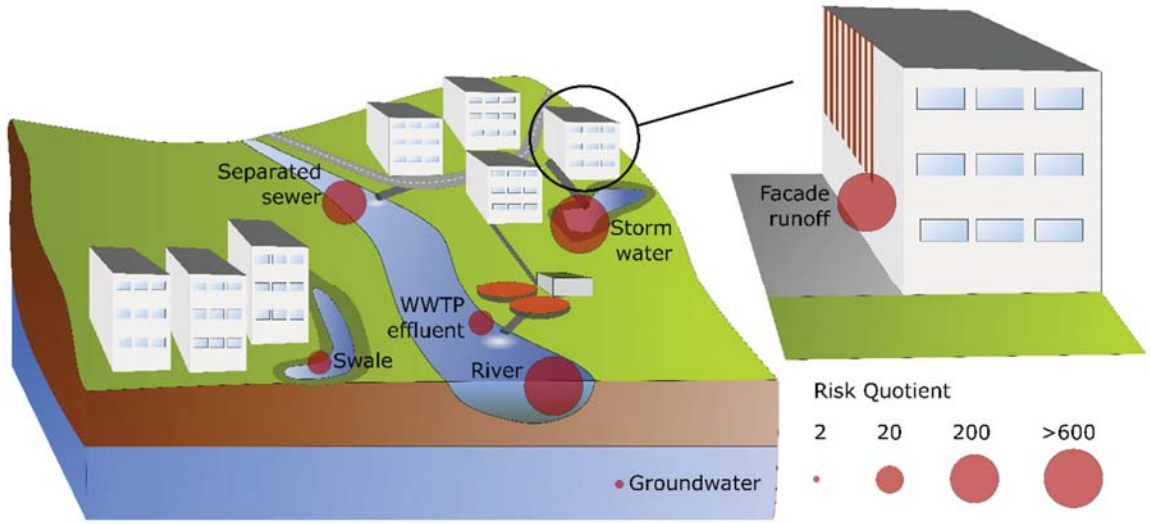

Figure 1. 5. Exceedance of PNEC values for terbutryn in different compartments, based on measurements and data from Bollmann et al., 2016, 2014a; Hensen et al., 2018; Kresmann et al., 2018; Linke et al., 2021; Masiá et al., 2013; Paijens et al., 2021; Quednow and Püttmann, 2007. The risk quotient is calculated as measured concentration divided by the PNEC. A risk quotient > 1 represents a potential risk towards the ecosystem.

PNEC values, determined based on literature research for terbutryn, OIT and methylisothiazolinone, were 0.003, 0.05 and 0.5 µg L^{-1}, respectively (Kresmann et al., 2018). In *Daphnia magna* tests, OIT indicated high toxicity (median effective concentration EC_{50}=156 µg L^{-1}) while terbutryn exhibited only low toxicity (EC_{50}=8390 µg L^{-1}). Other tests, e.g., the MTT assay with the ovarian cell line CHO-9 from Chinese hamster showed even lower toxicity. As the toxicity of terbutryn appears mainly as a reaction to photosynthesis inhibition, it is important to consider the correct target organisms and endpoints for ecotoxicological testing. Carazo-Rojas et al., 2018, reported high concentrations of terbutryn and other pesticides in water of an agricultural catchment in Costa Rica and classified it as a non-acceptable long-term risk to aquatic environment. Ecotoxicological tests with facade leachate revealed, that terbutryn is the main driver for toxicity towards algae growth (photosynthetic yield and growth inhibition), wherese OIT expresses high toxicity towards bacteria (Vermeirssen et al., 2018). Furthermore, the study suggested that toxicity towards water flea is mainly driven by isothiazolinones. In the environment, terbutryn, terbuthylazine and especially diuron were identified as main acute risk drivers in a river under wet and dry conditions (Beckers et al., 2018). The toxicity (calculated as toxicity units TU) in small streams with and without wastewater treatment plants (WWTP) were compared in Germany. In streams with WWTP, the compounds diuron, terbuthylazine, isoproturon, terbutryn and metazachlor were the most dominant contributors to toxicity (Le et al., 2017). A high contribution of terbutryn in WWTP effluents to ecotoxicological effects was identified, with risk quotients (RQ) reaching 348 (Gosset et al., 2021), indicating a potential risk for aquatic ecosystems, as RQs are generally defined as measured concentration divided by the PNEC. If this value exceeds 1, a potential risk exists. However, the study used calculated ecotoxicological data for the PNEC (Gosset et al., 2017). It is worthy to note, that acute and chronic ecotoxicological values do not consider synergistic and toxic cocktail effects although several studies have reported adverse effects of pesticide or biocide mixtures on aquatic organisms (e.g., Adam et al., 2009; Christen et al., 2014) and effects of TPs are often disregarded.

6.2 Ecotoxicological effects of urban biocides in soil

Terrestrial bioassays of artificial facade leachates of terbutryn, OIT and DCOIT showed no ecotoxicological effects for earthworm (*Eisenia Andrei*) avoidance and 21-d springtail (*Folsomia fimetaria*) reproduction (Vermeirssen et al., 2018). However, results were limited by

the applicable load of biocides: biocides were retrieved directly from immersion tests, limiting tested concentrations to the maximal released concentration from these laboratory experiments. Furthermore, bioavailability was limited to the terrestrial organisms due to sorption on the soil matrix. The microbial toxicity of terbutryn in soil was studied with bacterial and fungal growth as well as soil respiration as endpoints (Fernández-Calviño et al., 2021). The study showed a time dependent inhibition of microbial growth with increasing inhibition over longer time periods (up to 40 days) compared to short toxicity tests (0 – 7 days). The study highlighted, that guidelines to assess exoctoxicological parameters might underestimate the risk by chemicals. Microtox experiments towards the bacteria *Aliivibrio fischeri* were conducted for terbutryn, OIT and three respective TPs of each compound (desthiomethyl-terbutryn, desethyl-desthiomethyl-terbutryn, desethyl-desthiomethyl-terbutryn, octylacetamide, octylpropenamide, OIT) in a concentration range of 0 – 8 mg L^{-1} using inhibition of the luciferase activity as endpoint (Bollmann et al., 2017a). EC_{50} values were determined for OIT (0.05 mg L^{-1}), OIT (1.09 mg L^{-1}) and octylpropenamode (4.51 mg L^{-1}). The toxicity of terbutryn and octylacetamide was too little to calculate EC_{50} values and no toxicity was observed for the three TPs of terbutryn. Even though, low toxicity of terbutryn was measured, the mechanisms of action are different (photosynthesis inhibition of terbutryn) and therefore, the low toxicity are not representative for toxicity towards algae. Data on ecotoxicological effects of urban biocides is rare and the contribution of TPs and realistic test conditions are needed to be taken into account (Reiß et al., 2021). Furthermore, ecotoxicological tests might need to focus on the whole soil microbiome rather than on single organisms.

7 Terbutryn as a model compound for urban biocides

Based on the literature above, terbutryn has been identified as one of the most important urban biocides in external coatings. Terbutryn needs a special focus because: i) terbutryn has been detected in all investigated environmental compartments, including soil, surface waters and groundwater (e.g., Bollmann et al., 2017a; Hensen et al., 2018; Quednow and Püttmann, 2009), ii) terbutryn has a high toxicity towards algae and therefore might pose an ecotoxicological risk to aquatic ecosystems (Burkhardt et al., 2009; Kresmann et al., 2018), iii) terbutryn is degrading through photodegradation, whereas degradation in soil and wastewater treatment plants is slow, explaining its persistence in the environment (Bollmann et al., 2017a; Paijens et al., 2021; Wick

et al., 2010), and iv) besides the parent compound terbutryn, also TPs and mixtures of terbutryn with its TPs might cause ecotoxicological effects (Hensen et al., 2020).

Terbutryn was prohibited for agricultural use since 2003 (European Council Directive 91/414/EEC, 2002) due to high persistence and potential hazards towards water organisms but it is currently reviewed for the use as biocide in the EU as film preservative. The use of terbutryn is thus allowed in facade coatings (European Chemicals Agency (ECHA), 2022). As indicated previously, different PNEC values have been established for terbutryn. The lower value (attributing a higher toxicity) has been surpassed in all measured environmental compartments, including groundwater, river, swale systems, stormwater, facade runoff, separated and combined sewer systems and WWTP effluent (Figure 1. 5) (Bollmann et al., 2016, 2014a; Hensen et al., 2018; Kresmann et al., 2018; Linke et al., 2021; Masiá et al., 2013; Paijens et al., 2021; Quednow and Püttmann, 2007). Terbutryn was added to the list of priority substances under the water framework directive (European Council Directive 2013/39/EU, 2013).

The high toxicity in combination with high emission rates, high persistence and ubiquitous occurrence in the environment make terbutryn a compound of high interest for the research of urban biocides. Several studies already investigated degradation pathways during biodegradation and photodegradation of terbutryn and identified associated TPs. However, the contribution of respective degradation pathways to the environmental fate of terbutryn are not quantified yet.

According to Hensen et al., (2019), terbutryn degrades in the wavelength range of sunlight in laboratory tests, although photodegradation under environmental conditions is slow (Minelgaite et al., 2017). Photodegradation of terbutryn was studied in paints and on facades as well as in the environment (Bollmann et al., 2016; Schoknecht et al., 2021; Urbanczyk et al., 2019). Several TPs of terbutryn have been detected during direct and indirect photodegradation in aqueous solutions and on paint surfaces under exposure to UV light (Hensen et al., 2018) and artificial sunlight (Hensen et al., 2019; Urbanczyk et al., 2019). Photodegradation pathways for terbutryn were suggested (Bollmann et al., 2016). TPs were identified using their exact mass using high resolution mass spectroscopy (quadrupole-time-of-flight MS) and confirmed with analytical standards. The TP TerSO is formed through the insertion of oxygen (Figure 1. 6). The TP terbumeton can be formed through an exchange of the sulphur atom through oxygen.

Furthermore, TPs have been formed through the loss of side chains (desthiomethyl-terbutryn, desthiomethyl-desbutyl-terbutryn and desthimethyl-desethyl-terbutyrn). The hydroxyl-derivate (TerOH) is formed through replacement of the thiomethyl group by a hydroxyl group. This product can further be transformed to TerDesEOH or desbuthyl-2-hydroxy-terbutryn (TerDesBOH) through the abstraction of a side chains.

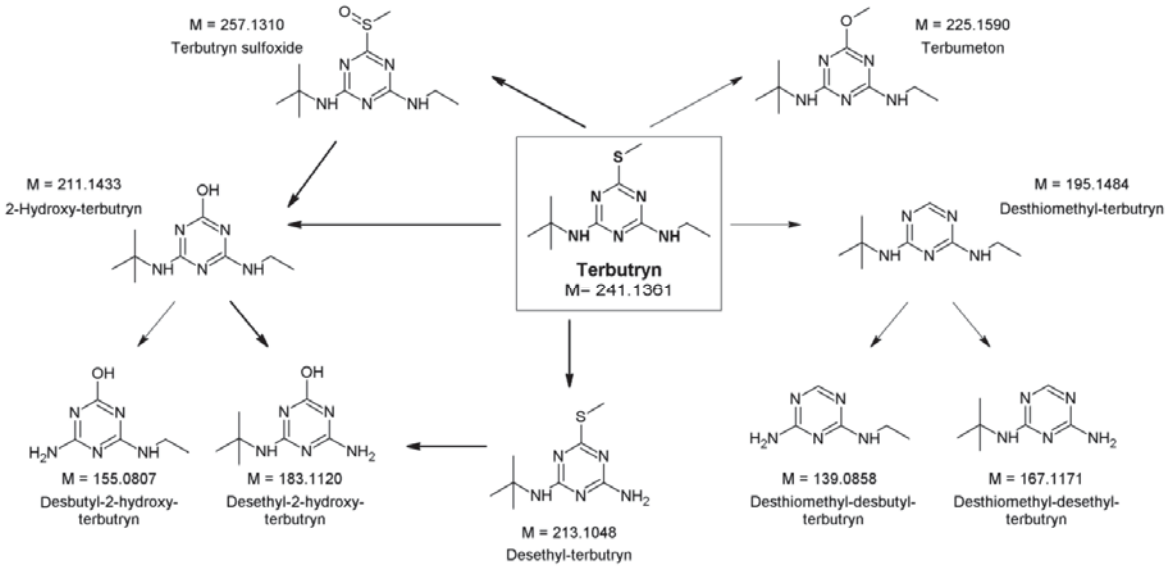

Figure 1. 6. Proposed degradation pathway of terbutryn (from Bollmann et al., 2016, supplementary information).

Biodegradation studies showed a high persistence of terbutryn in most studies ($t_{1/2}$ > 100 days) (Bollmann et al., 2017a; Lechón et al., 1997; Talja et al., 2008). In WWTP sludge, the TP TerSO was formed which further degraded to TerOH (Luft et al., 2014). In aerobic soil microcosms, TerSO was the prevailing product in the early phase of the experiment with higher contributions of TerOH, TerDesEOH and TerDesE with ongoing duration (Bollmann et al., 2017a).

Based on the conducted studies, terbutryn has been selected as target compound to investigate its environmental fate by conducting degradation studies, as well as release and reactive transport experiments, including TPs. Besides the monitoring based on concentrations, CSIA will be used to identify degradation mechanisms and proof *in situ* degradation. While CSIA has been used to study transformation of similar triazine type herbicides, such as atrazine and ametryn (Drouin et al., 2021; Hartenbach et al., 2008; Lihl et al., 2020; Masbou et al., 2018;

Meyer et al., 2009; Schürner et al., 2015; Torrentó et al., 2021), isotope fractionation of terbutryn has not been examined yet.

Chapter 1

References

Adam, O., Badot, P.-M., Degiorgi, F., Crini, G., 2009. Mixture toxicity assessment of wood preservative pesticides in the freshwater amphipod Gammarus pulex (L.). Ecotoxicol. Environ. Saf. 72, 441–449.

Andersson Trojer, M., Nordstierna, L., Bergek, J., Blanck, H., Holmberg, K., Nydén, M., 2015. Use of microcapsules as controlled release devices for coatings. Adv. Colloid Interface Sci., Reinhard Miller, Honorary Issue 222, 18–43.

Barbosa, A.E., Fernandes, J.N., David, L.M., 2012. Key issues for sustainable urban stormwater management. Water Res., Special Issue on Stormwater in urban areas 46, 6787–6798.

Bastian, F., Alabouvette, C., 2009. Lights and shadows on the conservation of a rock art cave: The case of Lascaux Cave. Int. J. of Speleol. 38.

Bastian, F., Alabouvette, C., Jurado, V., Saiz-Jimenez, C., 2009. Impact of biocide treatments on the bacterial communities of the Lascaux Cave. Sci. Nat. 96, 863–868.

Bastian, F., Jurado, V., Nováková, A., Alabouvette, C., Saiz-Jimenez, C.Y. 2010, 2010. The microbiology of Lascaux Cave. Microbiology 156, 644–652.

Beckers, L.-M., Busch, W., Krauss, M., Schulze, T., Brack, W., 2018. Characterization and risk assessment of seasonal and weather dynamics in organic pollutant mixtures from discharge of a separate sewer system. Water Research 135, 122–133.

Bester, K., Lamani, X., 2010. Determination of biocides as well as some biocide metabolites from facade run-off waters by solid phase extraction and high performance liquid chromatographic separation and tandem mass spectrometry detection. J. Chromatogr. A 1217, 5204–5214.

Boller, M., 2004. Towards sustainable urban stormwater management. Water Supply 4, 55–65.

Bollmann, U.E., Fernández-Calviño, D., Brandt, K.K., Storgaard, M.S., Sanderson, H., Bester, K., 2017a. Biocide runoff from building facades: degradation kinetics in soil. Environ. Sci. Technol. 51, 3694–3702.

Bollmann, U.E., Minelgaite, G., Schlüsener, M., Ternes, T., Vollertsen, J., Bester, K., 2016. Leaching of terbutryn and its photodegradation products from artificial walls under natural weather conditions. Environ. Sci. Technol. 50, 4289–4295.

Bollmann, U.E., Minelgaite, G., Schlüsener, M., Ternes, T.A., Vollertsen, J., Bester, K., 2017b. Photodegradation of octylisothiazolinone and semi-field emissions from facade coatings. Sci Rep 7, 41501.

Bollmann, U.E., Tang, C., Eriksson, E., Jönsson, K., Vollertsen, J., Bester, K., 2014a. Biocides in urban wastewater treatment plant influent at dry and wet weather: concentrations, mass flows and possible sources. Water Res. 60, 64–74.

Bollmann, U.E., Vollertsen, J., Carmeliet, J., Bester, K., 2014b. Dynamics of biocide emissions from buildings in a suburban stormwater catchment – concentrations, mass loads and emission processes. Water Res. 56, 66–76.

Bork, M., Engel, J., Krämer, A., Lange, J., 2022. FReWaB-PLUS (Freiburger Regenwasserbewirtschaftung plus Stofftransport) [WWW Document]. FReWaB-PLUS: Mobilisierung von Bioziden in Stadtgebieten. URL https://www.biozidauswaschung.de (accessed 10.1.22).

Bork, M., Lange, J., Graf-Rosenfellner, M., Hensen, B., Olsson, O., Hartung, T., Fernández-Pascual, E., Lang, F., 2021. Urban storm water infiltration systems are not reliable sinks for biocides: evidence from column experiments. Sci. Rep. 11, 7242.

Boswell, K., 2013. Exterior Building Enclosures: Design Process and Composition for Innovative Facades. John Wiley & Sons.

Boxall, A.B.A., Sinclair, C.J., Fenner, K., Kolpin, D., Maund, S.J., 2004. When synthetic chemicals degrade in the environment. Environ. Sci. Technol. 38, 368A-375A.

Brumm, A., Oktaviana, A.A., Burhan, B., Hakim, B., Lebe, R., Zhao, J., Sulistyarto, P.H., Ririmasse, M., Adhityatama, S., Sumantri, I., Aubert, M., 2021. Oldest cave art found in Sulawesi. Sci. Adv. 7, eabd4648.

Burkhardt, M., 2015. Reduction of environmental risks from the use of biocides: Environmental sound use of disinfectants, masonry preservatives and rodenticides Annex IV 36.

Burkhardt, M., Engelke, D., Gehrig, S., Hochstrasser, F., Rohr, M., Tietje, O., 2020. COMLEAM – Manual Version 3.0.

Burkhardt, M., Junghans, M., Zuleeg, S., Boller, M., Schoknecht, U., Lamani, X., Bester, K., Vonbank, R., Simmler, H., 2009. Biozide in Gebäudefassaden – ökotoxikologische Effekte, Auswaschung und Belastungsabschätzung für Gewässer. Environ. Sci. Eur. 21, 36–47.

Burkhardt, M., Kupper, T., Hean, S., Haag, R., Schmid, P., Kohler, M., Boller, M., 2007. Biocides used in building materials and their leaching behavior to sewer systems. Water Sci. Technol. 56, 63–67.

Burkhardt, M., Roger, V., 2011. Auswaschung von verkapselten Bioziden aus Fassaden.

Burkhardt, M., Zuleeg, S., Vonbank, R., Bester, K., Carmeliet, J., Boller, M., Wangler, T., 2012. Leaching of biocides from façades under natural weather conditions. Environ. Sci. Technol. 46, 5497–5503.

Burkhardt, M., Zuleeg, S., Vonbank, R., Schmid, P., Hean, S., Lamani, X., Bester, K., Boller, M., 2011. Leaching of additives from construction materials to urban storm water runoff. Water Sci. Technol. 63, 1974–1982.

Carazo-Rojas, E., Pérez-Rojas, G., Pérez-Villanueva, M., Chinchilla-Soto, C., Chin-Pampillo, J.S., Aguilar-Mora, P., Alpízar-Marín, M., Masís-Mora, M., Rodríguez-Rodríguez, C.E., Vryzas, Z., 2018. Pesticide monitoring and ecotoxicological risk assessment in surface water bodies and sediments of a tropical agro-ecosystem. Environ. Pollut. 241, 800–809.

Chapter 1

Ccanccapa, A., Masiá, A., Navarro-Ortega, A., Picó, Y., Barceló, D., 2016. Pesticides in the Ebro river basin: occurrence and risk assessment. Environ. Pollut. 211, 414–424.

Chiaia-Hernandez, A.C., Krauss, M., Hollender, J., 2013. Screening of Lake Sediments for Emerging Contaminants by Liquid Chromatography Atmospheric Pressure Photoionization and Electrospray Ionization Coupled to High Resolution Mass Spectrometry. Environ. Sci. Technol. 47, 976–986.

Chiaia-Hernández, A.C., Zander, P.D., Schneider, T., Szidat, S., Lloren, R., Grosjean, M., 2020. High-Resolution Historical Record of Plant Protection Product Deposition Documented by Target and Nontarget Trend Analysis in a Swiss Lake under Anthropogenic Pressure. Environ. Sci. Technol. 54, 13090–13100.

Chipperfield, M.P., Bekki, S., Dhomse, S., Harris, N.R.P., Hassler, B., Hossaini, R., Steinbrecht, W., Thiéblemont, R., Weber, M., 2017. Detecting recovery of the stratospheric ozone layer. Nature 549, 211–218.

Christen, V., Crettaz, P., Fent, K., 2014. Additive and synergistic antiandrogenic activities of mixtures of azol fungicides and vinclozolin. Toxicol. Appl. Pharmacol. 279, 455–466.

Cousins, I.T., Johansson, J.H., Salter, M.E., Sha, B., Scheringer, M., 2022. Outside the Safe Operating Space of a New Planetary Boundary for Per- and Polyfluoroalkyl Substances (PFAS). Environ. Sci. Technol.

Coutu, S., Del Giudice, D., Rossi, L., Barry, D.A., 2012a. Modeling of facade leaching in urban catchments. Water Resour. Res. 48.

Coutu, S., Rota, C., Rossi, L., Barry, D.A., 2012b. Modelling city-scale facade leaching of biocide by rainfall. Water Res. 46, 3525–3534.

Drouin, G., Droz, B., Leresche, F., Payraudeau, S., Masbou, J., Imfeld, G., 2021. Direct and indirect photodegradation of atrazine and S-metolachlor in agriculturally impacted surface water and associated C and N isotope fractionation. Environ. Sci. : Process. Impacts 23, 1791–1802.

Elsner, M., 2010. Stable isotope fractionation to investigate natural transformation mechanisms of organic contaminants: principles, prospects and limitations. J. Environ. Monit. 12, 2005–2031.

Elsner, M., Imfeld, G., 2016. Compound-specific isotope analysis (CSIA) of micropollutants in the environment — current developments and future challenges. Curr. Opin. Biotechnol., Analytical biotechnology 41, 60–72.

Elsner, M., Zwank, L., Hunkeler, D., Schwarzenbach, R.P., 2005. A new concept linking observable stable isotope fractionation to transformation pathways of organic pollutants. Environ. Sci. Technol. 39, 6896–6916.

Escher, B.I., Fenner, K., 2011. Recent Advances in Environmental Risk Assessment of Transformation Products. Environ. Sci. Technol. 45, 3835–3847.

European Chemicals Agency (ECHA), 2022. European Chemicals Agency (ECHA), Substance Information - Terbutryn [WWW Document]. URL https://echa.europa.eu/substance-information/-/substanceinfo/100.011.773 (accessed 8.3.22).

European Council Directive 91/414/EEC, 2002. Commission Regulation (EC) No 2076/2002 of 20 November 2002 extending the time period referred to in Article 8(2) of Council Directive 91/414/EEC and concerning the non-inclusion of certain active substances in Annex I to that Directive and the withdrawal of authorisations for plant protection products containing these substances (Text with EEA relevance), OJ L.

European Council Directive 2013/39/EU, 2013. Directive 2013/39/EU of the European Parliament and of the Council of 12 August 2013 amending Directives 2000/60/EC and 2008/105/EC as regards priority substances in the field of water policy Text with EEA relevance, OJ L.

European Environment Agency, 2022. Europe's groundwater — a key resource under pressure — European Environment Agency [WWW Document]. URL https://www.eea.europa.eu/publications/europes-groundwater (accessed 8.2.22).

European Parliament and Council, 2012. Regulation (EU) No 528/2012 of the European Parliament and of the Council of 22 May 2012 concerning the making available on the market and use of biocidal products. Text with EEA relevance.

European Parliament and Council, 2008. DIRECTIVE 2008/105/EC OF THE EUROPEAN PARLIAMENT AND OF THE COUNCIL of 16 December 2008 on environmental quality standards in the field of water policy.

Fenner, K., Canonica, S., Wackett, L.P., Elsner, M., 2013. Evaluating pesticide degradation in the environment: blind spots and emerging opportunities. Science.

Fernández-Calviño, D., Rousk, J., Bååth, E., Bollmann, U.E., Bester, K., Brandt, K.K., 2021. Short-term toxicity assessment of a triazine herbicide (terbutryn) underestimates the sensitivity of soil microorganisms. Soil Biol. Biochem. 154, 108130.

Fischer, A., Manefield, M., Bombach, P., 2016. Application of stable isotope tools for evaluating natural and stimulated biodegradation of organic pollutants in field studies. Curr. Opin. Biotechnol. 41, 99–107.

Gaylarde, C., Ribas Silva, M., Warscheid, Th., 2003. Microbial impact on building materials: an overview. Mat. Struct. 36, 342–352.

Gosset, A., Durrieu, C., Orias, F., Bayard, R., Perrodin, Y., 2017. Identification and assessment of ecotoxicological hazards attributable to pollutants in urban wet weather discharges. Environ. Sci.: Process. Impacts 19, 1150–1168.

Gosset, A., Wiest, L., Fildier, A., Libert, C., Giroud, B., Hammada, M., Hervé, M., Sibeud, E., Vulliet, E., Polomé, P., Perrodin, Y., 2021. Ecotoxicological risk assessment of contaminants of emerging concern identified by "suspect screening" from urban wastewater treatment plant effluents at a territorial scale. Sci. Total Environ. 778, 146275.

Goulden, S., Portman, M.E., Carmon, N., Alon-Mozes, T., 2018. From conventional drainage to sustainable stormwater management: Beyond the technical challenges. J. Environ. Manage. 219, 37–45.

Grandjean, P., Bellanger, M., 2017. Calculation of the disease burden associated with environmental chemical exposures: application of toxicological information in health economic estimation. Environ. Health 16, 123.

Guillossou, R., Le Roux, J., Mailler, R., Vulliet, E., Morlay, C., Nauleau, F., Gasperi, J., Rocher, V., 2019. Organic micropollutants in a large wastewater treatment plant: What are the benefits of an advanced treatment by activated carbon adsorption in comparison to conventional treatment? Chemosphere 218, 1050–1060.

Handa, P., Fant, C., Nydén, M., 2006. Antifouling agent release from marine coatings-ion pair formation/dissolution for controlled release. Prog. Org. Coat. 57, 376–382.

Hartenbach, A.E., Hofstetter, T.B., Tentscher, P.R., Canonica, S., Berg, M., Schwarzenbach, R.P., 2008. Carbon, hydrogen, and nitrogen isotope fractionation during light-induced transformations of atrazine. Environ. Sci. Technol. 42, 7751–7756.

Hassan, R.M., Scholes, R.J., Ash, N., Millennium Ecosystem Assessment (Program) (Eds.), 2005. Ecosystems and human well-being: current state and trends: findings of the Condition and Trends Working Group of the Millennium Ecosystem Assessment, The millennium ecosystem assessment series. Island Press, Washington, DC.

Hensen, B., Lange, J., Jackisch, N., Zieger, F., Olsson, O., Kümmerer, K., 2018. Entry of biocides and their transformation products into groundwater via urban stormwater infiltration systems. Water Res. 144, 413–423.

Hensen, B., Olsson, O., Kümmerer, K., 2020. A strategy for an initial assessment of the ecotoxicological effects of transformation products of pesticides in aquatic systems following a tiered approach. Environ. Int. 137, 105533.

Hensen, B., Olsson, O., Kümmerer, K., 2019. The role of irradiation source setups and indirect phototransformation: kinetic aspects and the formation of transformation products of weakly sunlight-absorbing pesticides. Sci. Total Environ. 695, 133808.

Hering, J.G., Ingold, K.M., 2012. Water Resources Management: What Should Be Integrated? Science 336, 1234–1235.

Herzog, T., Krippner, R., Lang, W., 2012. Facade Construction Manual. Walter de Gruyter.

Höhener, P., Guers, D., Malleret, L., Boukaroum, O., Martin-Laurent, F., Masbou, J., Payraudeau, S., Imfeld, G., 2022. Multi-elemental compound-specific isotope analysis of pesticides for source identification and monitoring of degradation in soil: a review. Environ. Chem. Lett.

IPCC, 2022. IPCC, 2022: Climate Change 2022: Impacts, Adaptation, and Vulnerability. Contribution of Working Group II to the Sixth Assessment Report of the Intergovernmental Panel on Climate Change.

Janin, A., Coudert, L., Riche, P., Mercier, G., Cooper, P., Blais, J.-F., 2011. Application of a CCA-treated wood waste decontamination process to other copper-based preservative-treated wood after disposal. J. of Hazard. Mater. 186, 1880–1887.

Jia, H., Wang, Z., Zhen, X., Clar, M., Yu, S.L., 2017. China's sponge city construction: A discussion on technical approaches. Front. Environ. Sci. Eng. 11, 18.

Jungnickel, C., Stock, F., Brandsch, T., Ranke, J., 2008. Risk assessment of biocides in roof paint. Part 1: experimental determination and modelling of biocide leaching from roof paint. Environ. Sci. Pollut. Res. Int. 15, 258–265.

Kosnik, M.B., Hauschild, M.Z., Fantke, P., 2022. Toward Assessing Absolute Environmental Sustainability of Chemical Pollution. Environ. Sci. Technol. 56, 4776–4787.

Kresmann, S., Arokia, A.H.R., Koch, C., Sures, B., 2018. Ecotoxicological potential of the biocides terbutryn, octhilinone and methylisothiazolinone: underestimated risk from biocidal pathways? Sci. Total Environ. 625, 900–908.

Kümmerer, K., 2011. Emerging Contaminants versus Micro-pollutants. Clean Soil Air Water 39, 889–890.

Kümmerer, K., Dionysiou, D.D., Olsson, O., Fatta-Kassinos, D., 2019. Reducing aquatic micropollutants – Increasing the focus on input prevention and integrated emission management. Sci. Total Environ. 652, 836–850.

Landrigan, P.J., Fuller, R., Acosta, N.J.R., Adeyi, O., Arnold, R., Basu, N. (Nil), Baldé, A.B., Bertollini, R., Bose-O'Reilly, S., Boufford, J.I., Breysse, P.N., Chiles, T., Mahidol, C., Coll-Seck, A.M., Cropper, M.L., Fobil, J., Fuster, V., Greenstone, M., Haines, A., Hanrahan, D., Hunter, D., Khare, M., Krupnick, A., Lanphear, B., Lohani, B., Martin, K., Mathiasen, K.V., McTeer, M.A., Murray, C.J.L., Ndahimananjara, J.D., Perera, F., Potočnik, J., Preker, A.S., Ramesh, J., Rockström, J., Salinas, C., Samson, L.D., Sandilya, K., Sly, P.D., Smith, K.R., Steiner, A., Stewart, R.B., Suk, W.A., van Schayck, O.C.P., Yadama, G.N., Yumkella, K., Zhong, M., 2018. The Lancet Commission on pollution and health. The Lancet 391, 462–512.

Launay, M.A., Dittmer, U., Steinmetz, H., 2016. Organic micropollutants discharged by combined sewer overflows – Characterisation of pollutant sources and stormwater-related processes. Water Res. 104, 82–92.

Le, T.D.H., Scharmüller, A., Kattwinkel, M., Kühne, R., Schüürmann, G., Schäfer, R.B., 2017. Contribution of waste water treatment plants to pesticide toxicity in agriculture catchments. Ecotoxicol. Environ. Saf. 145, 135–141.

Lechón, Y., Sánchez-Brunete, C., Tadeo, J.L., 1997. Influence of the laboratory incubation method on chlorotoluron and terbutryn degradation in soil. J. Agric. Food Chem. 45, 951–954.

Li, H., Ding, L., Ren, M., Li, C., Wang, H., 2017. Sponge City Construction in China: A Survey of the Challenges and Opportunities. Water 9, 594.

Li, Z., Dong, M., Wong, T., Wang, J., Kumar, A.J., Singh, R.P., 2018. Objectives and Indexes for Implementation of Sponge Cities—A Case Study of Changzhou City, China. Water 10, 623.

Lihl, C., Heckel, B., Grzybkowska, A., Dybala-Defratyka, A., Ponsin, V., Torrentó, C., Hunkeler, D., Elsner, M., 2020. Compound-specific chlorine isotope fractionation in biodegradation of atrazine. Environ. Sci.: Processes Impacts 22, 792–801.

Linke, F., Olsson, O., Preusser, F., Kümmerer, K., Schnarr, L., Bork, M., Lange, J., 2021. Sources and pathways of biocides and their transformation products in urban storm water infrastructure of a 2 ha urban district. Hydrol. Earth Syst. Sci. 25, 4495–4512.

Liu, W.-R., Yang, Y.-Y., Liu, Y.-S., Zhang, L.-J., Zhao, J.-L., Zhang, Q.-Q., Zhang, M., Zhang, J.-N., Jiang, Y.-X., Ying, G.-G., 2017. Biocides in wastewater treatment plants: Mass balance analysis and pollution load estimation. J. Hazard. Mater. 329, 310–320.

Luft, A., Wagner, M., Ternes, T.A., 2014. Transformation of biocides irgarol and terbutryn in the biological wastewater treatment. Environ. Sci. Technol. 48, 244–254.

Mabey, W., Mill, T., 1978. Critical review of hydrolysis of organic compounds in water under environmental conditions. J. Phys. Chem. Ref. Data 7, 383–415.

Machate, O., Dellen, J., Schulze, T., Wentzky, V.C., Krauss, M., Brack, W., 2021. Evidence for antifouling biocides as one of the limiting factors for the recovery of macrophyte communities in lakes of Schleswig-Holstein. Environ. Sci. Eur. 33, 57.

MacLeod, M., Breitholtz, M., Cousins, I.T., Wit, C.A. de, Persson, L.M., Rudén, C., McLachlan, M.S., 2014. Identifying Chemicals That Are Planetary Boundary Threats. Environ. Sci. Technol. 48, 11057–11063.

Masbou, J., Drouin, G., Payraudeau, S., Imfeld, G., 2018. Carbon and nitrogen stable isotope fractionation during abiotic hydrolysis of pesticides. Chemosphere 213, 368–376.

Masiá, A., Ibáñez, M., Blasco, C., Sancho, J.V., Picó, Y., Hernández, F., 2013. Combined use of liquid chromatography triple quadrupole mass spectrometry and liquid chromatography quadrupole time-of-flight mass spectrometry in systematic screening of pesticides and other contaminants in water samples. Anal. Chim. Acta 761, 117–127.

McMaster, M.C., 2005. LC/MS: A Practical User's Guide. John Wiley & Sons.

McMaster, M.C., 2011. GC/MS: A Practical User's Guide. John Wiley & Sons.

Meyer, A.H., Penning, H., Elsner, M., 2009. C and N isotope fractionation suggests similar mechanisms of microbial atrazine transformation despite involvement of different enzymes (AtzA and TrzN). Environ. Sci. Technol. 43, 8079–8085.

Minelgaite, G., Nielsen, A.H., Pedersen, M.L., Vollertsen, J., 2017. Photodegradation of three stormwater biocides. Urban Water J. 14, 53–60.

Mitchell, V.G., 2006. Applying Integrated Urban Water Management Concepts: A Review of Australian Experience. Environmental Management 37, 589–605.

Molina, M.J., Rowland, F.S., 1974. Stratospheric sink for chlorofluoromethanes: chlorine atom-catalysed destruction of ozone. Nature 249, 810–812.

Moschet, C., Wittmer, I., Simovic, J., Junghans, M., Piazzoli, A., Singer, H., Stamm, C., Leu, C., Hollender, J., 2014. How a Complete Pesticide Screening Changes the Assessment of Surface Water Quality. Environ. Sci. Technol. 48, 5423–5432.

Nijenhuis, I., Richnow, H.H., 2016. Stable isotope fractionation concepts for characterizing biotransformation of organohalides. Current Opinion in Biotechnology, Anal. Biotech. 41, 108–113.

Nordstierna, L., Abdalla, A.A., Masuda, M., Skarnemark, G., Nydén, M., 2010. Molecular release from painted surfaces: Free and encapsulated biocides. Progr. Org. Coat. 69, 45–48.

Öllers, S., Singer, H.P., Fässler, P., Müller, S.R., 2001. Simultaneous quantification of neutral and acidic pharmaceuticals and pesticides at the low-ng/l level in surface and waste water. J. Chromatogr. A 911, 225–234.

Östman, M., Lindberg, R.H., Fick, J., Björn, E., Tysklind, M., 2017. Screening of biocides, metals and antibiotics in Swedish sewage sludge and wastewater. Water Res. 115, 318–328.

Paijens, C., Bressy, A., Frère, B., Moilleron, R., 2020. Biocide emissions from building materials during wet weather: identification of substances, mechanism of release and transfer to the aquatic environment. Environ. Sci. Pollut. Res. 27, 3768–3791.

Paijens, C., Bressy, A., Frère, B., Tedoldi, D., Mailler, R., Rocher, V., Neveu, P., Moilleron, R., 2021. Urban pathways of biocides towards surface waters during dry and wet weathers: assessment at the Paris conurbation scale. J. Hazard. Mater. 402, 123765.

Park, S.-K., Kwon, J.-H., 2016. The fate of two isothiazolinone biocides, 5-chloro-2-methylisothiazol-3(2H)-one (CMI) and 2-methylisothiazol-3(2H)-one (MI), in liquid air fresheners and assessment of inhalation exposure. Chemosphere 144, 2270–2276.

Paulus, W., 2004. Directory of Microbiocides for the Protection of Materials –A Handbook. pp. 1–8.

Pena-Poza, J., Ascaso, C., Sanz, M., Pérez-Ortega, S., Oujja, M., Wierzchos, J., Souza-Egipsy, V., Cañamares, M.V., Urizal, M., Castillejo, M., García-Heras, M., 2018. Effect of biological colonization on ceramic roofing tiles by lichens and a combined laser and biocide procedure for its removal. Int. Biodeterior. Biodegradation 126, 86–94.

Persson, L., Carney Almroth, B.M., Collins, C.D., Cornell, S., de Wit, C.A., Diamond, M.L., Fantke, P., Hassellöv, M., MacLeod, M., Ryberg, M.W., Søgaard Jørgensen, P., Villarrubia-Gómez, P., Wang, Z., Hauschild, M.Z., 2022. Outside the Safe Operating Space of the Planetary Boundary for Novel Entities. Environ. Sci. Technol. 56, 1510–1521.

Pinasseau, L., Wiest, L., Volatier, L., Mermillod-Blondin, F., Vulliet, E., 2020. Emerging polar pollutants in groundwater: Potential impact of urban stormwater infiltration practices. Environ. Pollut. 266, 115387.

Quednow, K., Püttmann, W., 2009. Temporal concentration changes of DEET, TCEP, terbutryn, and nonylphenols in freshwater streams of Hesse, Germany: possible influence of mandatory regulations and voluntary environmental agreements. Environ. Sci. Pollut. Res. 16, 630–640.

Quednow, K., Püttmann, W., 2007. Monitoring terbutryn pollution in small rivers of Hesse, Germany. J. Environ. Monit. 9, 1337–1343.

Rani, L., Thapa, K., Kanojia, N., Sharma, N., Singh, S., Grewal, A.S., Srivastav, A.L., Kaushal, J., 2021. An extensive review on the consequences of chemical pesticides on human health and environment. J. Clean. Prod. 283, 124657.

Reiß, F., Kiefer, N., Noll, M., Kalkhof, S., 2021. Application, release, ecotoxicological assessment of biocide in building materials and its soil microbial response. Ecotoxicol. Environ. Saf. 224, 112707.

Rockström, J., Steffen, W., Noone, K., Persson, Å., Chapin, F.S.I., Lambin, E., Lenton, T., Scheffer, M., Folke, C., Schellnhuber, H.J., Nykvist, B., de Wit, C., Hughes, T., van der Leeuw, S., Rodhe, H., Sörlin, S., Snyder, P., Costanza, R., Svedin, U., Falkenmark, M., Karlberg, L., Corell, R., Fabry, V., Hansen, J., Walker, B., Liverman, D., Richardson, K., Crutzen, P., Foley, J., 2009. Planetary Boundaries: Exploring the Safe Operating Space for Humanity. Ecol. Soc. 14.

Sandak, A., Sandak, J., Marcin, B., Kutnar, A., 2019. Designing Building Skins with Biomaterials. pp. 65–97.

Schoknecht, U., Gruycheva, J., Mathies, H., Bergmann, H., Burkhardt, M., 2009. Leaching of biocides used in façade coatings under laboratory test conditions. Environ. Sci. Technol. 43, 9321–9328.

Schoknecht, U., Mathies, H., Lisec, J., 2021. Leaching and transformation of film preservatives in paints induced by combined exposure to ultraviolet radiation and water contact under controlled laboratory conditions. Water 13, 2390.

Schoknecht, U., Mathies, H., Wegner, R., 2016. Biocide leaching during field experiments on treated articles. Environ. Sci. Eur. 28, 6.

Schoknecht, U., Sommerfeld, T., Borho, N., Bagda, E., 2013. Interlaboratory comparison for a laboratory leaching test procedure with façade coatings. Prog. Org. Coat. 76, 351–359.

Schoknecht, U., Wegner, R., Horn, W., Jann, O., 2003. Emission of biocides from treated materials test procedures for water and air. Environ. Sci. Pollut. Res. 10, 154–161.

Schrope, M., 2000. Successes in fight to save ozone layer could close holes by 2050. Nature 408, 627–627.

Schürner, H.K.V., Seffernick, J.L., Grzybkowska, A., Dybala-Defratyka, A., Wackett, L.P., Elsner, M., 2015. Characteristic isotope fractionation patterns in s-triazine degradation have their origin in multiple protonation options in the s-triazine hydrolase TrzN. Environ. Sci. Technol. 49, 3490–3498.

Schwarzenbach, R.P., Escher, B.I., Fenner, K., Hofstetter, T.B., Johnson, C.A., Gunten, U. von, Wehrli, B., 2006. The challenge of micropollutants in aquatic systems. Science.

Schwarzenbach, R.P., Gschwend, P.M., Imboden, D.M., 2005. Environmental organic chemistry. John Wiley & Sons.

Shtykova, L., Fant, C., Handa, P., Larsson, A., Berntsson, K., Blanck, H., Simonsson, R., Nydén, M., Ingelsten Härelind, H., 2009. Adsorption of antifouling booster biocides on metal oxide nanoparticles: Effect of different metal oxides and solvents. Prog. Org. Coat. 64, 20–26.

Singer, H., Jaus, S., Hanke, I., Lück, A., Hollender, J., Alder, A.C., 2010. Determination of biocides and pesticides by on-line solid phase extraction coupled with mass spectrometry and their behaviour in wastewater and surface water. Environ. Pollut. 158, 3054–3064.

Solomon, S., 1999. Stratospheric ozone depletion: A review of concepts and history. Reviews of Geophysics 37, 275–316.

Solomon, S., Garcia, R.R., Rowland, F.S., Wuebbles, D.J., 1986. On the depletion of Antarctic ozone. Nature 321, 755–758.

Steffen, W., Richardson, K., Rockström, J., Cornell, S.E., Fetzer, I., Bennett, E.M., Biggs, R., Carpenter, S.R., de Vries, W., de Wit, C.A., Folke, C., Gerten, D., Heinke, J., Mace, G.M., Persson, L.M., Ramanathan, V., Reyers, B., Sörlin, S., 2015. Planetary boundaries: Guiding human development on a changing planet. Science 347, 1259855.

Styszko, K., Bollmann, U.E., Bester, K., 2015. Leaching of biocides from polymer renders under wet/dry cycles--rates and mechanisms. Chemosphere 138, 609–615.

Styszko, K., Bollmann, U.E., Wangler, T.P., Bester, K., 2014. Desorption of biocides from renders modified with acrylate and silicone. Chemosphere 95, 188–192.

Talja, K.M., Kaukonen, S., Kilpi-Koski, J., Malin, I., Kairesalo, T., Romantschuk, M., Tuominen, J., Kontro, M.H., 2008. Atrazine and terbutryn degradation in deposits from groundwater environment within the boreal region in Lahti, Finland. J. Agric. Food Chem. 56, 11962–11968.

Torrentó, C., Ponsin, V., Lihl, C., Hofstetter, T.B., Baran, N., Elsner, M., Hunkeler, D., 2021. Triple-element compound-specific stable isotope analysis (3D-CSIA): added value of Cl isotope ratios to assess herbicide degradation. Environ. Sci. Technol. 55, 13891–13901.

Uhlig, S., Colson, B., Schoknecht, U., 2019. A mathematical approach for the analysis of data obtained from the monitoring of biocides leached from treated materials exposed to outdoor conditions. Chemosphere 228, 271–277.

Urbanczyk, M.M., Bester, K., Borho, N., Schoknecht, U., Bollmann, U.E., 2019. Influence of pigments on phototransformation of biocides in paints. J. Hazard. Mater. 364, 125–133.

Urbanczyk, M.M., Bollmann, U.E., Bester, K., 2016. Partition of biocides between water and inorganic phases of renders with organic binder. Sci. Total Environ. 573, 639–644.

Vega-Garcia, P., Schwerd, R., Scherer, C., Schwitalla, C., Johann, S., Rommel, S.H., Helmreich, B., 2020. Influence of façade orientation on the leaching of biocides from building façades covered with mortars and plasters. Sci. Total Environ. 734, 139465.

Vermeirssen, E.L.M., Campiche, S., Dietschweiler, C., Werner, I., Burkhardt, M., 2018. Ecotoxicological assessment of immersion samples from facade render containing free or encapsulated biocides. Environ. Toxicol. Chem. 37, 2246–2256.

Vogt, C., Dorer, C., Musat, F., Richnow, H.-H., 2016. Multi-element isotope fractionation concepts to characterize the biodegradation of hydrocarbons — from enzymes to the environment. Curr. Opin. Biotechnol. Anal. biotechnol. 41, 90–98.

Wang, H., Mei, C., Liu, J., Shao, W., 2018. A new strategy for integrated urban water management in China: Sponge city. Sci. China Technol. Sci. 61, 317–329.

Wang, Z., Walker, G.W., Muir, D.C.G., Nagatani-Yoshida, K., 2020. Toward a Global Understanding of Chemical Pollution: A First Comprehensive Analysis of National and Regional Chemical Inventories. Environ. Sci. Technol. 54, 2575–2584.

Wangler, T.P., Zuleeg, S., Vonbank, R., Bester, K., Boller, M., Carmeliet, J., Burkhardt, M., 2012. Laboratory scale studies of biocide leaching from façade coatings. Build. Environ. 54, 168–173.

Wick, A., Fink, G., Ternes, T.A., 2010. Comparison of electrospray ionization and atmospheric pressure chemical ionization for multi-residue analysis of biocides, UV-filters and benzothiazoles in aqueous matrices and activated sludge by liquid chromatography–tandem mass spectrometry. J. Chromatogr. A. 1217, 2088–2103.

Wicke, D., Tatis-Muvdi, R., Rouault, P., Zerball-van Baar, P., Dünnbier, U., Rohr, M., Burkhardt, M., 2022. Emissions from building materials—a threat to the environment? Water 14, 303.

Wittmer, I.K., Bader, H.-P., Scheidegger, R., Singer, H., Lück, A., Hanke, I., Carlsson, C., Stamm, C., 2010. Significance of urban and agricultural land use for biocide and pesticide dynamics in surface waters. Water Res. 44, 2850–2862.

Wittmer, I.K., Scheidegger, R., Stamm, C., Gujer, W., Bader, H.-P., 2011. Modelling biocide leaching from facades. Water Res. 45, 3453–3460.

Chapter 2
Aims, research questions and general approach of the thesis

This thesis aims to improve the understanding of the reactive transport of urban biocides and their transformation products from their sources (construction materials/facades) to the receiving compartments (surface water, soil, and groundwater). A framework was developed to evaluate the behaviour of urban biocides and the contribution of biotic and abiotic degradation processes to the overall biocide dissipation, including sorption and transport and dilution (Figure 2. 1). Terbutryn was selected as a model compound for the experiments because of (i) ubiquitous occurrence in the environment, (ii) high persistence (iii) high and constant emission rates and (iii) high ecotoxicological potential. Based on the literature review in Chapter 1, the following research questions were addressed to fill the existing gaps of knowledge:

1. What are the degradation pathways of the urban biocide terbutryn in the environment and can we use CSIA to evaluate terbutryn degradation and identify degradation pathways?
2. What are the processes controlling the degradation of urban biocides on facades and thus the contribution of transformation products in facade leachates?
3. What are the prevailing entry paths and reactive transport processes of urban biocides towards groundwater through typical urban surface-soil interfaces?
4. What is the potential and limits of CSIA to estimate the extent of degradation *in situ* and identify degradation pathways under environmental conditions?
5. Can we quantify and predict biocide emissions and distribution into environmental compartments on the district scale?

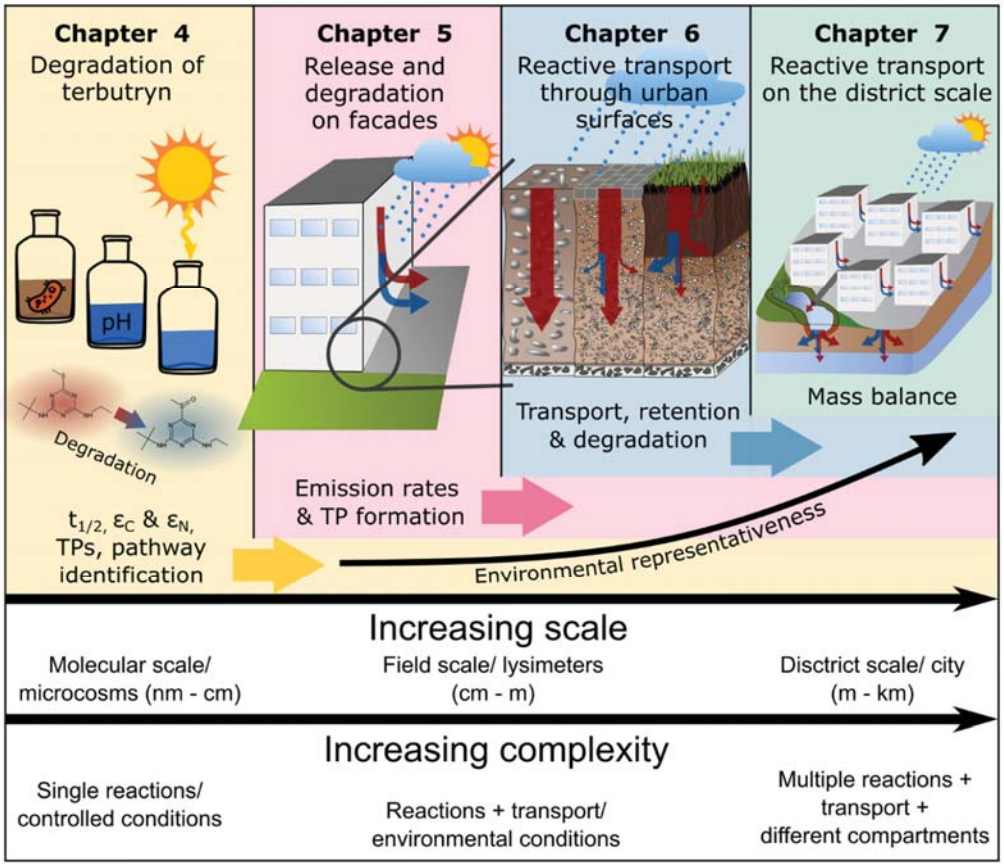

Figure 2. 1. Graphical outline of the thesis with increasing scale and complexity with the aim to represent real environmental conditions.

In Chapter 3, an overview of the used methods is given. Further, extraction methods were tested and validated for multi-element compound-specific isotope analysis (ME-CSIA) from different environmental matrixes for carbon ($^{13}C/^{12}C$) and nitrogen ($^{15}N/^{14}N$) stable isotopes. Within the tests, nine pesticides, including six herbicides and three fungicides were evaluated, including the urban biocide terbutryn and the herbicide acetochlor. Extraction techniques for four different types of soils and sediments, three different types of environmental waters, and plant aerial parts and roots were examined to provide an overview for the applicability of pesticide CSIA. Here, we expanded earlier research using SPE and ME-CSIA to new substances and environmental matrices. For a broader application of ME-CSIA in the environment, we investigated a modified ultrasonic-assisted extraction method (MUSE) approach for extracting pesticides from soils, sediments, and plant matter.

In Chapter 4, the degradation rates and stable isotope fractionation during abiotic hydrolysis, aerobic biodegradation and photodegradation of terbutryn were examined to improve the interpretation of terbutryn degradation from facades to sink ecosystems, such as soil and groundwater. Different terbutryn degradation pathways may lead to distinct patterns of TP formation and stable isotope fractionation. We thus examined the reaction kinetic rate constants, the TP formation, and carbon and nitrogen stable isotope fractionation to evaluate degradation mechanisms of terbutryn and the potential of CSIA to follow up terbutryn degradation *in situ* and distinguish degradation pathways.

Chapter 5 describes the leaching and transformation of terbutryn from artificial facades. We combined photodegradation experiments, field experiments and immersion tests on artificial facades with a paint coating containing an industrial encapsulated terbutryn formulation to (i) understand the mechanisms associated with the release and transformation of terbutryn on facades, (ii) predict the release of terbutryn and the contribution of TPs in leachate over long time periods, and (iii) apply CSIA on facade leachate to follow the extent of degradation of terbutryn. We assumed that photodegradation is the main transformation pathway on facades, which might be confirmed by CSIA. We further assumed that TP emissions can be implemented into emission functions by considering hydro-climatic variables such as solar irradiation. We thus compared the contribution of TPs to the total leached mass (terbutryn + TPs) to correlate it with hydro-climatic variables. Further, we used laboratory experiments with simulated sunlight irradiation and immersion tests to estimate the contribution of single processes to biocide release. We finally suggested a first modeling framework to implement TPs into existing leaching models.

Chapter 6 describes the reactive transport of the urban biocides diuron, terbutryn and OIT through typical urban surfaces under environmental conditions by using complementary approaches, including a conservative tracer, concentration measurements of parent biocides, TPs and CSIA. To identify the risk of biocide leaching towards groundwater, three different lysimeters were built to simulate gravel, paved surfaces with joints and vegetated surfaces. We calibrated the reactive transport of the biocides towards the groundwater based on experimental data using a simple 1-D finite element model (Hydrus-1D) and extrapolated biocide leachate into subsurfaces over eight years using simulated facade runoff. This enabled to realistically evaluate the transport of biocide and TP toward groundwater.

Chapter 2

In Chapter 7, we examined the release and export of urban biocides on the district scale based on field-emission data, hydrological mass balances and modeling of biocide reactive transport. We evaluated current trends of sustainable stormwater management in terms of water infiltration versus the risks of biocide leaching towards groundwater and identified areas with high risk of biocide infiltration.

The Chapter 8 discusses the results of the above-mentioned studies and synthesizes them with emphasize on the release and reactive transport of urban biocides towards groundwater. Further, chances, challenges and limitations of CSIA as a tool to follow-up urban biocides in the environment are reviewed based on terbutryn isotope fractionation, and improvements for CSIA sensitivity.

Chapter 9 concludes the thesis by providing implications and perspectives on opportunities to prevent urban biocides contamination in the environment. Two main perspectives are addressed on the path towards a biocide free city: (i) reducing the release of biocides from existing buildings, and (ii) developing biocide-free construction for new buildings, with implications for future architecture and alternative materials. Additionally, the relevance of knowledge transfer to policy and stakeholders is discussed.

Chapter 3
General Methodology

This chapter describes the study site and sample collection strategy and summaries methods and experiments developed in a broader study (Gilevska et al., 2022) on the validation of extraction methods for pesticide compound specific isotope analysis. The study validated the methods for terbutryn extraction, quantification and multi element (ME)-CSIA from water, soil, sediment and plants.

Gilevska, T., Wiegert, C., Droz, B., Junginger, T., Prieto-Espinoza, M., Borreca, A., Imfeld, G., 2022. Simple extraction methods for pesticide compound-specific isotope analysis from environmental samples. MethodsX 101880

Chapter 3

1 Description of the study site

Within the work of this thesis, several field experiments were conducted at a study site north of Strasbourg, France (Schiltigheim, Adelshoffen, 48°36'31.7"N 7°44'54.8"E) (Figure 3. 1). The sampling site is an "Eco-quartier", constructed from 2014 to 2015, on an area of 2.4 ha. An Eco-quartier is defined as a neighborhood built to promote both better living together and the sustainable use of resources. A detailed monitoring campaign to estimate mass balances of biocide release was conducted between April and August 2021 (Chapter 7). Furthermore, experimental setups were installed (artificial facades and lysimeters, detailed in Chapter 5 and Chapter 6) to monitor biocide release from facades and reactive transport towards groundwater under environmental conditions.

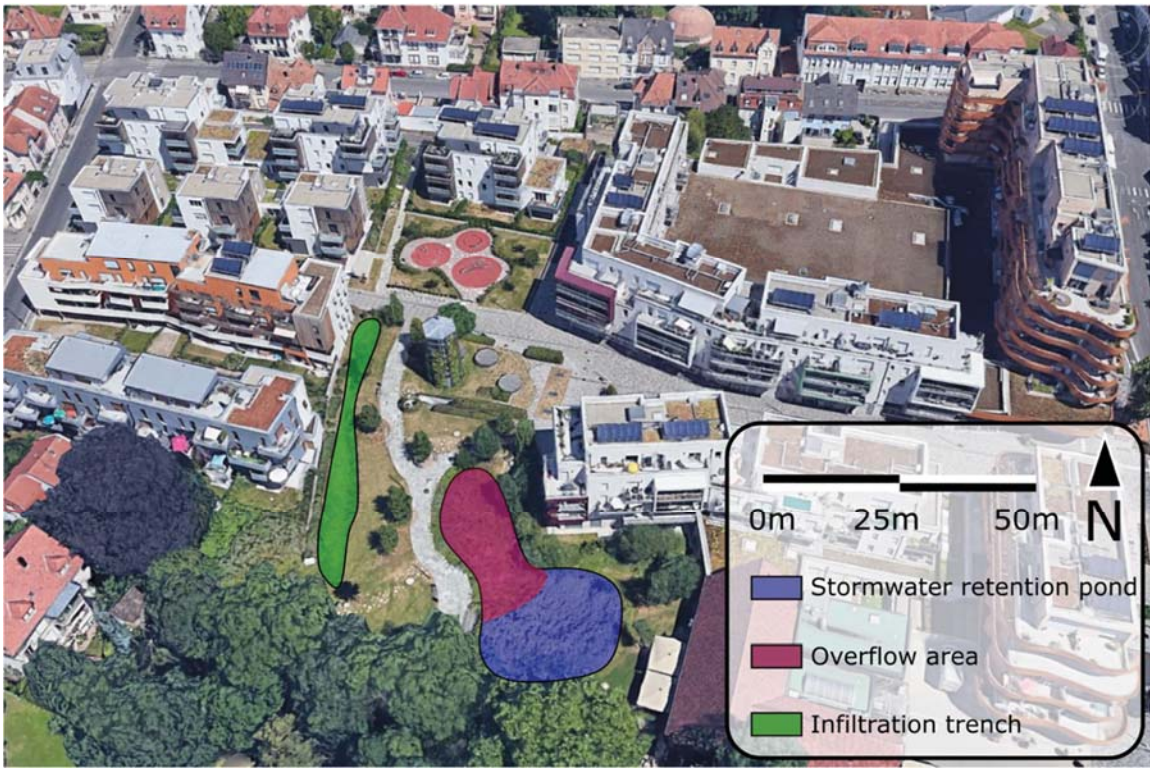

Figure 3. 1. Aerial overview of the investigated field site with the stormwater infiltration pond (blue), overflow area (red) and the infiltration trench (green).

The field site includes a vegetated stormwater infiltration pond with an overflow area and infiltration wells as well as an infiltration trench (Figure 3. 1, Figure 3. 2). Surface runoff in the catchment is drained through pipes towards the stormwater infiltration system (detailed in Chapter 7). Buildings and type of urban surfaces have been characterized, including the land use (e.g., vegetated soil, pavement with joints, drainage gravel or impermeable surfaces such as asphalt) and the characterization of the buildings (e.g., building height, exposition of each facade, material of facades and contribution of balconies and windows to total facade area). During the field campaigns and outdoor experiments, devices were installed to monitor hydroclimatic conditions, enable automated event sampling and monitor water levels (detailed in Chapter 7).The hydraulic functioning of the system was characterized in spring and summer 2021 (Chapter 7). Collected data was used for preliminary modeling with the facade leaching model FreWaB-PLUS (Bork et al., 2022) and the leaching model COMLEAM (Burkhardt et al., 2020), as well as for a risk characterization of the catchment for its risk of biocide release (Chapter 7). Data was further analyzed and visualized in GIS (Figure 3. 3 and Figure 3. 4).

Figure 3. 2. Infiltration trench (left) and vegetated stormwater infiltration pond (right).

Figure 3. 3. Categorization of buildings and land use in the Adelshoffen district.

Figure 3. 4. Analysis of building height in the Adelshoffen district.

1.1 Water and soil collection

Water samples were collected during rainfall-runoff events using either flow-proportional automated samplers (detailed in Chapter 7) or by weekly grab sampling. Grab samples in stormwater pond and trench, collected with a clean telescope sampling scoop from random locations within the pond or trench, consisted typically of 5-10 L water. Water samples were successively filtered at 11 µm (Whatmann 1001-047) followed by 0.45 µm (CA Membrane filter) and stored at 4°C until further analysis.

Soil and sediment samples were taken according to US EPA soil sampling procedure. Briefly, surface material, like grass, roots and debris (top 5 cm) was removed with a cleaned shovel. 5 subsamples of about 20 g were collected in labelled plastic bags and mixed to obtain homogeneity. Samples were sieved to 2 mm prior to extraction. Samples were transported to the laboratory within 2 h and prepared for extraction within 24 h. Samples were stored at 4°C prior to extraction.

2 Extraction methods

Water samples were extracted using an automated solid phase extraction (SPE) procedure. Two different approaches were chosen and optimized for high recoveries of the respective compounds.

SPE Method 1 for pesticides terbutryn, acetochlor, atrazine, alachlor, butachlor, metalaxy, s-metolachlor, tebuconazole, dimetomorph Z and dimetomorph E: The extraction procedure was performed with an AutoTrace 280 SPE system (Dionex®, CA, USA) for the simultaneous extraction of 6 samples. SPE cartridges, SolEx C18 cartridges (1 g, Dionex®, CA, USA) were washed with 5 mL of Ethyl acetate (EtOAc), followed by 5 mL of acetonitrile (ACN). The cartridges were then sequentially conditioned by 10 mL of ultrapure water. Cartridges were loaded with the samples and dried under nitrogen flux for 10 min. Elution of pesticides was performed by 5 mL of EtOAc followed by 5 mL of ACN. The extract was subsequently concentrated under gentle nitrogen flux to 1 droplet and suspended in 0.5 mL of ACN for quantification and isotope analyses.

SPE Method 2 for terbutryn, diuron, OIT and transformation products of terbutryn: Samples were enriched using Chromabond HR-X cartridges (6 mL, 500 mg, particle size 85 µm). Cartridges were conditioned with 10 ml of methanol, followed by 10 ml of H_2O. The full volume of the sample was loaded onto the cartridge followed by drying of cartridges for 15 min with N_2. Cartridges were soaked with chloroform:methanol (1:1, V:V) and 10 ml solvent was collected. Solvent was evaporated under gentle N_2 flux and resuspended in 1 mL acetonitrile.

Soil, sediment and other solid materials (e.g., paint samples): Pesticides in sediment, soil, plant materials and paint were extracted using an adapted solid-liquid extraction (Anastassiades et al., 2003; Ivdra et al., 2014). Five grams of soil or sediment (dry weight) were placed in an amber glass centrifuge tube. Due to the large (~85%) water content of plants, 3 g of plant dry weight was used for extraction. Water in the sample was adjusted prior to extraction to reach 100% water content for better separation between solvent and sample. 3 mL of DCM:pentane (3:1, V:V) were added and vortexed for 5 s, followed by 5 min in an ultrasonic bath (Branson 5510, 40 kHz) for homogenization. The sample was vortexed for 1 min, followed by centrifugation (2400 rpm) for 20 min. The supernatant was transferred to an amber glass vial, and the extraction method was repeated two more times. The supernatants were pooled and concentrated at room temperature under a gentle nitrogen stream to the last drop before resuspension into acetonitrile to a volume of 1 mL by vortexing (5 s) and ultrasonication (5 min) to collect pesticide residues. Then 75 mg of anhydrous magnesium sulfate ($MgSO_4$) was added to remove residual water and 13 mg of primary-secondary amine (PSA bonded silica, Supelco P/N 52738) as a clean-up agent (Anastassiades et al., 2003). The vial was vortexed for 30 s, centrifuged at 2400 rpm for 5 min, and the supernatant was transferred to a clean amber glass vial for further analysis. Minor changes of the extraction procedure were adapted to enhance extraction yields and are detailed in the respective chapters.

3 Quantification of urban biocides, pesticides and transformation products using GC-MS and UHPLC-MS/MS

Quantification of pesticide concentrations for extraction method validation using GC-MS. For a general method validation, pesticides were analyzed with gas chromatography (GC, Trace

1300, ThermoFisher Scientific) coupled to a mass spectrometer (MS, ISQ™, ThermoFisher Scientific). Chromatographic separation was performed with a TG –5MS column (30 m × 0.25 mm ID, 0.25 µm film thickness). *S*-metolachlor d-11 or atrazine d-5 were used as internal standards and injected with every sample to account for reproducibility of the autosampler. All samples were diluted to be within the linear calibration range (0.1 to 1 mg L^{-1}). The sample (1.5 µL) with the internal standard were injected together via a split/splitless injector in splitless mode at 280°C with helium as carrier gas at a 1.5 mL min^{-1} flow rate. The temperature program of the GC consisted of a 2 min hold time at 50°C, heating with 15°C min^{-1} to 250°C, heating at 40°C min^{-1} to 340°C, and holding the temperature for 2 min. The MS transfer line and source were heated at 320°C. Compounds were identified by their specific mass in a selective ion mode (SIM) (Table A 1).

UHPLC-MS/MS measurements for urban biocide and transformation product quantification. Within this study, terbutryn, diuron, OIT, acetochlor and four TPs of terbutryn (TerSO, TerOH, TerDesE and TerDesEOH) were quantified using ultra high-pressure liquid chromatography (UHPLC) (Dionex/ Thermo Scientific UltiMate Dionex 3000) using a C18 column (Accucore 100 x 2.1, particle size 2.6 µm) coupled to a triple quadrupole mass spectrometer (Thermo Scientific TSQ Quantiva). Samples were measured in positive ESI mode. Water (A) with 0.05% formic acid and acetonitrile (B) with 0.1% formic acid were used as mobile phase. In the first 8 minutes, solvent B was increased from 10% to 90% with a hold phase of 1 min at 90% solvent B, decrease of solvent B to 10% within one minute, followed by 2 min at initial solvent composition (10% solvent B). Flow was 0.4 ml min^{-1}. A static spray voltage was used (1800 V). Sheath gas was 55 Arb, Aux gas 20 Arb and Sweep gas 2 Arb. The ion transfer tube was heated to 280°C. Vaporizer temperature was set to 300°C. The mass spectrometer was run in selected reaction monitoring (SRM) mode. The resolution in Q1 and Q3 was 0.7 full width at half maximum (FWHM). The CID gas was set to 1.5 mTorr. Compounds were identified and quantified based on their precursor and two fragment ions (Table A 2).

Chapter 3

4 Development and validation of extraction methods for terbutryn, acetochlor and other pesticides for CSIA using GC-IRMS

A multielement (ME)-CSIA approach may help to interpret reaction pathways in complex pollution scenarios, such as multiple contamination sources or concurrent degradation processes. The application of ME-CSIA for pesticides requires validated and efficient extraction approaches from environmental matrices. Extraction methods for pesticide residues from environment matrices for ME-CSIA should: (i) provide sufficient analyte mass for reliable isotope analysis, (ii) cause no stable isotope effect ($\Delta\delta^{H}E$), (iii) be applicable to a wide range of pesticides and matrices, and (iv) limit matrix co-enrichment to avoid co-elution during chromatographic separation.

Previously, SPE for pesticide extraction from water for CSIA has been tested for atrazine, acetochlor, *S*-metolachlor, metalaxyl, butachlor, alachlor, terbutryn, chlordizon, and several of their metabolites (Chen et al., 2019; Drouin, 2021; Droz, 2021; Masbou et al., 2018a; Ponsin et al., 2019; Schreglmann et al., 2013; Torrentó et al., 2019). Pesticide extraction methods from soil, sediment and plants for reliable pesticide CSIA have been used in both laboratory and field studies (Alvarez-Zaldivar et al., 2018; Masbou et al., 2018b; Pérez-Rodríguez et al., 2021; Wu et al., 2019). Ivdra et al., 2014 proposed a modified ultrasonic-assisted extraction (MUSE) method without carbon isotope fractionation ($\Delta\delta^{13}C \leq 0.4‰$) for soil. Other studies used accelerated solvent extraction (ASE) for the extraction of hexachlorocyclohexanes (HCHs) from soil and plants for C, H, and Cl isotopes analysis (Liu et al., 2021, 2020; Wu et al., 2019). The application of Quick, Easy, Cheap, Effective, Rugged and Safe procedure (QuEChERS) for the extraction of metolachlor from two agricultural soils led to a systematic but reproducible isotope fractionation for Cl ($\Delta\delta^{37}Cl$ between +2.5 and +3.5‰) (Torrentó et al., 2021).

In this context, we tested and compared simple extraction methods for pesticide ME-CSIA from various environmental matrices, with emphasis on carbon ($^{13}C/^{12}C$) and nitrogen ($^{15}N/^{14}N$) stable isotope ratios. Efficient pesticide extraction from diverse matrices can improve ME-CSIA's ability to assess pesticide degradation and help develop monitoring and remediation strategies. To develop an overview for the application of pesticide extraction methods for CSIA, four types of soils and sediments, three types of environmental waters, and aerial parts and roots

of plants were tested. We selected six commonly used herbicides, i.e., atrazine, terbutryn, acetochlor, alachlor, butachlor, and *S*-metolachlor, and three fungicides, i.e., dimethomorph, tebuconazole, metalaxyl, representing a wide range of physicochemical properties and belonging to four chemical families (Table A 3). Here, we extend previous findings for SPE and ME-CSIA to new compounds and environmental matrices. We further tested a MUSE method for extracting selected pesticides from soils, sediments, and plant material, thus paving the way for wider application of ME-CSIA in the environment.

4.1 Materials and methods

Used chemicals are described in detail in the Appendix A.

Sampling and characterisation of water, sediment and plants

Water. Three types of water matrices were tested: i) buffered ultrapure water (> 18 MΩ cm), ii) storm water from a vineyard catchment (Rouffach, France) (Imfeld et al., 2020), iii) runoff and river water from two different crop catchments (Alteckendorf and Souffel, France) (Elsayed et al., 2014; Pérez-Rodríguez et al., 2021). Field samples were successively filtered at 11 µm trough grade one cellulose (Whatmann 1001-047) and 0.45 µm cellulose acetate membrane filters and stored at 4°C until further analysis. The hydrochemical composition (Table A 4) was analyzed by ionic chromatography (IC) and inductively coupled plasma atomic emission spectroscopy (ICP-AES) using standard analytical procedures (NF/ISO), as described elsewhere (Droz et al., 2021).

Soil and sediment. The top 0–10 cm of i) river sediments from the Souffel river, France, (Droz, 2021), ii) vineyard soils from the Rouffach catchment (Imfeld et al., 2020; Pérez-Rodríguez et al., 2021), iii) vineyard storm water basin sediments (Rouffach, France (Maillard et al., 2011)), iv) forest soils (Strengbach, France (Pérez-Rodríguez et al., 2021)) were sampled with a shovel cleaned with ultrapure water and ethanol and wiped between collections. Soil and sediment samples were mixed and sieved through a 2-mm mesh and stored at 4°C before spiking. The physicochemical characteristics of the sieved soil and sediment samples (Table A 5) were measured using standard analytical procedures (NF/ISO) (Droz et al., 2021).

Plants. Mature common reed (*Phragmites australis*, *n*=20) were sampled from the Rouffach storm water basin, separated into roots and aerial parts, which were extracted

separately. Plant material was washed by shaking the roots and rhizosphere for 10 min in ultrapure water. The water was replaced several times until all the sediment rhizosphere was separated from the roots (Barillot et al., 2013). A 0.9% NaCl solution was used to rinse the plant material twice to remove rhizosphere and rhizoplane sediment. Plant material was homogenized with a hand blender (Bosch MSM66110) and frozen at –20ºC until further use.

Extraction methods

Extraction from water. Pesticide stock solutions (1 g L^{-1}) of pesticides in DCM or ACN were added to buffered (13.6 g L^{-1} monopotassium phosphate, 4 g L^{-1} sodium hydroxide) ultrapure water or environmental water and stirred until complete solvent evaporation to reach concentrations ranging from 0.5 µg L^{-1} to 6 mg L^{-1}. The extraction method is described in detail above (SPE method 1 for pesticides). Tested water volumes were: 0.01, 0.5, 1, 2, 4, and 8 L.

Extraction from soil, sediment, and plant material. MUSE method. Triplicate or duplicate samples were spiked (0.5 to 50 µg g^{-1}) with aqueous solutions of pesticides. Spiking included adding 25 – 500 µL of 100 – 500 mg L^{-1} pesticide mix, while filling remaining volume with acetonitrile (to reach 500 µL in each sample). Samples were vortexed, shaken (orbital shaker 80 rpm) for at least 30 min, and incubated in the dark for three days at 4°C. Pesticides in sediment, soil or plant were extracted using the method described above

Quantification and CSIA

Quantification. Pesticides were quantified using the GC-MS method described above, allowing the simultaneous quantification of all targeted pesticides with one injection.

Compound-specific isotope analysis. Carbon and nitrogen stable isotope analysis was conducted using a GC-IRMS system consisting of a gas chromatograph (GC, TRACE Ultra ThermoFisher Scientific) coupled to an isotope ratio mass spectrometer (IRMS, DeltaV plus, ThermoFisher Scientific) via a GC combustion interface (IsoLink/Conflow IV, ThermoFisher Scientific) equipped with a TG-5MS column (60 m × 0.25 mm ID, 0.25 µm film thickness). The samples (0.3 - 3 µL) were injected via a split/splitless injector at 250°C with helium as carrier gas at a 1.5 mL min^{-1} flow rate. The GC-IRMS temperature program for carbon and nitrogen started with a 2 min hold time at 50°C, heating to 150°C with 20°C min^{-1}, heating to 245°C with 5°C min^{-1} heating with 30°C min^{-1} to 320°C and holding the temperature for 0.5 min. For carbon,

analytes were combusted to CO_2, for nitrogen to N_2 respectively in a reactor oven (P/N 1255321, NiO tube and CuO-NiO-Pt wires, Thermo Fischer Scientific) at 1000°C. During nitrogen isotope measurements, liquid N_2 was used for cryogenic trapping of CO_2. Samples were bracketed with standards (after every 9 samples for C and every 3 samples for N). For C, the standard was BTEX with known isotopic signature (benzene, toluene, ethylbenzene and o-Xylene). For N measurements, Caffeine (international reference material AIEA600) was used at 100 mg L^{-1} in acetone. Additionally, standards of the respective compounds (100 mg L^{-1} in DCM) were injected after each BTEX or Caffeine measurement. Pesticide standards were previously characterized using an elemental analyzer to get the reference isotope signature (Flash EA IsoLinkTM CN IRMS, Thermo Fisher Scientific). The range of injected amount of contaminant for which carbon and nitrogen isotope values are within a ± 0.5‰ interval was established for peak amplitudes (e.g., for terbutryn between 221 and 2558 for $\delta^{13}C$ (m/z = 44) and 221 and 1477 for $\delta^{15}N$ (m/z = 28)). The reproducibility of $\delta^{13}C$ and $\delta^{15}N$ measurements ranged from ± 0.4 to ± 0.6‰ and from ± 0.4 to ± 0.5‰, while the total uncertainty, including accuracy and reproducibility, ranged, from ± 0.6 to ± 0.8‰ and from ± 0.6 to ± 0.7‰ for the respective compounds.

4.2 Results and discussion

Extraction from environmental water

SPE recoveries. The mean extraction recovery of pesticide analysis with SPE ranged from 77 ± 8% (butachlor) up to 115 ± 12% (*S*-metolachlor) (Figure 3. 5, Table A 7) across all conditions tested. Extraction recoveries for atrazine, acetochlor, *S*-metolachlor, metalaxyl, and alachlor were similar than those previously obtained for different sorbents and amounts (Drouin, 2021; Droz, 2021; Masbou et al., 2018a; Schreglmann et al., 2013; Torrentó et al., 2019). Overall, octanol-water partition constant of pesticides (log K_{ow};, Table A 3) did not correlate with pesticide recoveries.

Effect of SPE on stable isotope signatures. Results show that SPE can be effectively used for the pre-concentration of tested pesticides prior to carbon and nitrogen CSIA. The deviation from the initial isotope value can be expressed as $\Delta\delta^{13}C$ for carbon and $\Delta\delta^{15}N$ for nitrogen. Both carbon and nitrogen isotopes signatures of pesticides were not affected by the matrix, extracted

water volume, or concentration of tested pesticides ($\Delta\delta^{13}C < 0.9‰$ and $\Delta\delta^{15}N < 1.0‰$) (Figure 3. 5, Figure A 5, Figure A 6, Table A 8). These results confirm the applicability of SPE for carbon and nitrogen CSIA of atrazine, acetochlor, *S*-metolachlor, metalaxyl, butachlor, and alachlor (Drouin, 2021; Droz, 2021; Elsayed et al., 2014; Masbou et al., 2018a; Pérez-Rodríguez et al., 2021; Schreglmann et al., 2013; Torrentó et al., 2019) and extend the use to the urban biocide terbutryn and fungicides dimethomorph and tebuconazole.

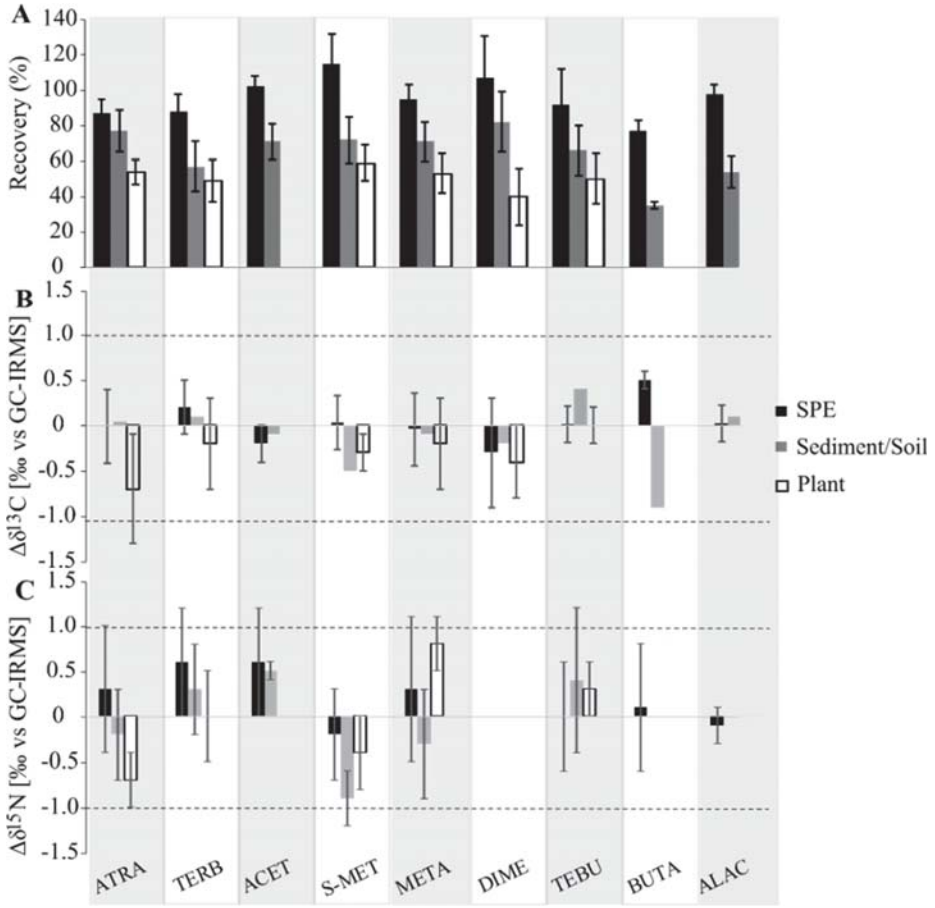

Figure 3. 5. A - Extraction recovery, B – Effect on $\delta^{13}C$ ($\Delta\delta^{13}C$ [‰ vs GC-IRMS].), C – Effect on $\delta^{15}N$ ($\Delta\delta^{15}N$ [‰ vs GC-IRMS]) of SPE (water samples), and MUSE with DCM:Pentane (3:1) (sediment, soil, plant) for pesticides and all matrices combined. ATRA – atrazine, TERB – terbutryn, ACET – acetochlor, S-MET – S-metolachlor, META – metalaxyl, DIME – dimethomorph, TEBU – tebuconazole, BUTA – butachlor, ALAC – alachlor. Error bars denote standard deviation (1 σ, n ≥ 8). Dashed lines represent ± 1‰ (significance threshold) from reference isotope values of in-house standards measured with GC-IRMS.

Besides the targeted compounds, sample pre-concentration can co-enrich other organic compounds in environmental samples, leading to a matrix effect during GC-IRMS separation, especially for larger volumes (> 4 L). Hence, field variables, such as the dynamics of the matrix composition, pesticide concentrations and the occurrence of vegetation, should be accounted for in a preliminary matrix screening prior to sampling. For instance, the co-elution of terbutryn with the wetland water matrix did not enable carbon CSIA when the water was collected in summer from the tested storm water wetland. In contrast, no matrix interferences were observed for water collected in winter. Typically, compounds eluting first, such as atrazine, metalaxyl, or terbutryn, were affected stronger by co-eluting peaks.

To address the issue of co-enrichment, several clean-up procedures can be applied to maximize the analytical performance of pesticide CSIA extraction from environmental matrices without altering the isotope ratios of the target pesticide. These include: i) the addition of a sorbent, such as PSA, florisil, or graphitized carbon black, etc. (Anastassiades et al., 2003; Ivdra et al., 2014; Muhammad et al., 2020; Wilkowska and Biziuk, 2011), ii) chromatography HPLC separation (Schreglmann et al., 2013), and iii) the use of molecularly imprinted polymers (MIP) (Bakkour et al., 2018). MIP is likely the most effective cleanup method for CSIA. However, MIP is not commercially available for all classes of compounds, and therefore must be specifically synthesized prior to cleanup.

Extraction from soil and sediment

Pesticide recoveries. The mean extraction recoveries for MUSE with DCM:Pentane (3:1) ranged from 35 ± 2% (butachlor) up to 82 ± 17% (dimethomorph) across the soil and sediment samples (Figure 3. 5, Table A 7). The extraction recoveries were above 70% for atrazine, acetochlor, *S*-metolachlor, metalaxyl, and dimethomorph. The results partly mirror the main parameters governing pesticide sorption capacities in soil/sediment matrices, including the physicochemical characteristics of the pesticide, such as the hydrophobicity and the acid dissociation constant (pKa, Table A 3), and soil characteristics, such as soil pH, organic matter content and its surface functional group (Table A 5) (Sigmund et al., 2022). We observed lowest extraction recovery for butachlor, correlating with the highest log K_{ow} (Table A 3). The other pesticides, i.e. terbutryn, alachlor, tebuconazole, with log K_{ow} above 3 also had an extraction recovery below 70%. A detailed discussion of effects of soil properties on extraction efficiencies can be found in the Appendix A.

Effect on stable isotope signatures. Carbon and nitrogen stable isotope composition of pesticides were not significantly affected ($\Delta\delta^{13}C < 0.5‰$ and for $\Delta\delta^{15}N < 0.8‰$) by the soil type or the pesticide concentrations (Figure 3. 6, Figure A 5). This is in line with the literature for soil extraction with MUSE method for both carbon and nitrogen CSIA of atrazine, terbutryn, acetochlor and *S*-metolachlor, metalaxyl, butachlor and alachlor (Alvarez-Zaldivar et al., 2018; Drouin, 2021; Droz, 2021; Droz et al., 2021; Masbou et al., 2018b; Pérez-Rodríguez et al., 2021). This study is the first report of soil extraction of dimethomorph and tebuconazole for carbon and nitrogen CSIA.

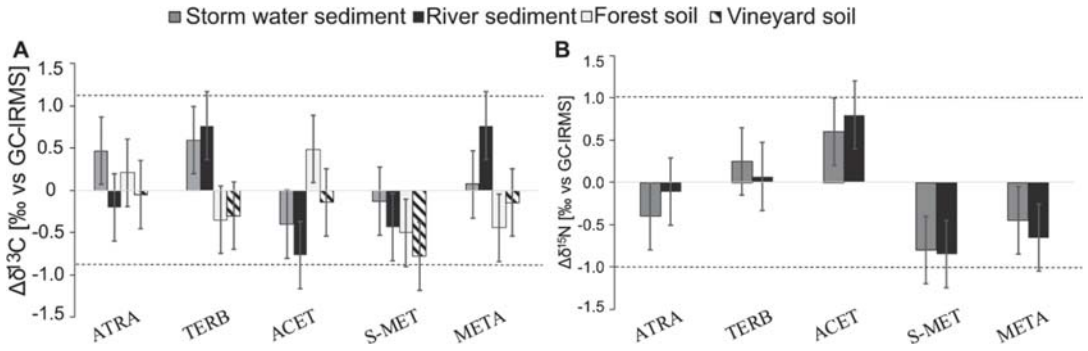

Figure 3. 6. Effect of the MUSE extraction method on A – Carbon isotope values ($\Delta\delta^{13}C_{[‰\ vs\ GC\text{-}IRMS]}$) for the different types of soils and sediments and B – Nitrogen isotope values ($\Delta\delta^{15}N_{[‰\ vs\ GC\text{-}IRMS]}$) for the different types of soil and sediment. Dashed lines represent ±1‰ (significance threshold) from the measured isotope values of in-house standards. ATRA– atrazine, TERB –terbutryn, ACET - acetochlor, S-MET - S-metolachlor, META – metalaxyl. Error bars denote standard deviation for all concentrations.

Overall, these results highlight that pesticide extraction from soil samples for CSIA requires consideration of several practical aspects. First, pre-concentration of soil extracts may increase the chromatogram baseline during GC-IRMS measurements, especially for $\delta^{13}C$ analysis. This may severely compromise the analytical performance (higher method detection limit (MDL) and lower accuracy), even when co-elution is limited. The application of MIP with high specificity in the pre-concentration step may significantly reduce the matrix effect of soil compounds and thus reduce the MDL (Bakkour et al., 2018). Finally, injection of high sample loads containing organics, especially for $\delta^{15}N$ measurements, may significantly increase the maintenance of IRMS system, including frequent oven and column replacement, and capillaries blockage.

Extraction from plants

Extraction recovery and effect on stable isotope signatures. The mean extraction recovery for plant material ranged from 40 ± 16% (Dimethomorph) up to 59 ± 10% (*S* -metolachlor) (Figure 3. 5, Table A 5). Overall, extraction recoveries from plant were lower than those for soil and sediment, suggesting that pesticide sorption in the plant matrix was higher. However, extraction efficiencies were similar to those reported for ASE extraction for HCHs from wheat and grass (Liu et al., 2021, 2020; Wu et al., 2019). Despite low extraction efficiencies, $\delta^{13}C$ of $\delta^{15}N$ of pesticides were not affected by the extraction from plant material (Figure 3. 5, Table A 7).

In the future, other extraction methods of pesticides from plants, such as solid-phase microextraction, QuEChERS, superfluid extraction, and Soxhlet extraction, routinely tested for concentration analysis, could also be evaluated for CSIA to increase the recovery (Barriada-Pereira et al., 2003; Obuseng et al., 2013; Yousefi et al., 2021).

4.3 Implications for ME-CSIA from environmental matrices

Reliable ME-CSIA requires both a high extraction recovery (≥70%), especially for pollutants with low environmental concentrations, and the absence of isotope effects in extraction methods. For all tested extraction methods, the stable isotope composition of pesticides was not significantly altered ($\Delta\delta^{13}C$ and $\Delta\delta^{15}N$ < 1‰) during pesticide extraction from water, soil, sediment, and plant matrixes (Figure 3. 5, Table A 7).

Most importantly, the applicability of extraction methods for ME-CSIA to environmental samples is an essential step. The tested SPE methods allowed carbon CSIA from water samples for all studied pesticides at concentrations above 100 to 200 ng L^{-1} (Table A 7). In contrast, nitrogen CSIA required several µg L^{-1} of pesticides in water. In a previous study, concentrations of *S*-metolachlor and acetochlor in water ranged from < 100 to 66100 ng L^{-1} at the plot or at the outlet of the agricultural catchment (Lutz et al., 2017). In urban catchments, biocides, such as terbutryn, leach from the facade materials, leading to highly polluted runoff water (up to several mg L^{-1}) (Bollmann et al., 2016; Burkhardt et al., 2012). Hence, carbon CSIA of pesticides and biocides appears feasible from agricultural samples across the agricultural season, and from most

construction material leachates in urban settings. For some compounds, the SPE method for carbon CSIA can also be used for nonpoint sources of pollution (Smith et al., 2012), although wider application would require reaching levels of pg L^{-1} to several ng L^{-1}. In contrast, nitrogen CSIA may be restricted to areas close to the pollution source, following application, and/or during runoff events (Table A 8).

The tested extraction method enabled carbon CSIA from soil/sediment and plant samples with pesticide concentrations ranging from 300 to 1000 ng g^{-1} and 300 to 500 ng g^{-1}, respectively (Table A 7). Although *S*-metolachlor concentrations in soil can reach 8 µg g^{-1} following application (Alvarez-Zaldivar et al., 2018), pesticide concentrations typically range from pg g^{-1} to several ng g^{-1} in agricultural soils (Hvězdová et al., 2018) or in soil receiving facade runoff (Bollmann et al., 2017). This mainly restricts pesticide CSIA to source areas, following application. Furthermore, nitrogen CSIA in soils and plants would typically require more than 10 µg g^{-1}, currently restricting its application to laboratory studies.

Developing simple and isotope fractionation free clean-up methods for environmental matrices and pesticides might reduce current concentration ranges of ME-CSIA. Despite promising results (Bakkour et al., 2018), MIP is still not widely used due to its high selectivity and the requirement of self-preparation of the polymer. Nevertheless, recently MIP phase, which offers excellent selectivity for a broad range of triazines (SupelMIP Triazines, Merck, model 53208-U) has been introduced. Altogether, this study illustrates the diversity of candidate compounds and environmental matrices for ME-CSIA and current limitations of pesticide extraction methods, paving the way for wider use of ME-CSIA to assess pesticide degradation in environmental compartments.

References

Alvarez-Zaldivar, P., Payraudeau, S., Meite, F., Masbou, J., Imfeld, G., 2018. Pesticide degradation and export losses at the catchment scale: Insights from compound-specific isotope analysis (CSIA). Water Res. 139, 197–207.

Anastassiades, M., Lehotay, S.J., Štajnbaher, D., Schenck, F.J., 2003. Fast and easy multiresidue method employing acetonitrile extraction/partitioning and "dispersive solid-phase extraction" for the determination of pesticide residues in produce. J. AOAC Int. 86, 412–431.

Bakkour, R., Bolotin, J., Sellergren, B., Hofstetter, T.B., 2018. Molecularly Imprinted Polymers for Compound-Specific Isotope Analysis of Polar Organic Micropollutants in Aquatic Environments. Anal. Chem. 90, 7292–7301.

Barillot, C.D.C., Sarde, C.-O., Bert, V., Tarnaud, E., Cochet, N., 2013. A standardized method for the sampling of rhizosphere and rhizoplan soil bacteria associated to a herbaceous root system. Ann. Microbiol. 63, 471–476.

Barriada-Pereira, M., Concha-Grana, E., Gonzalez-Castro, M.J., Muniategui-Lorenzo, S., López-Mahıa, P., Prada-Rodrıguez, D., Fernandez-Fernandez, E., 2003. Microwave-assisted extraction versus Soxhlet extraction in the analysis of 21 organochlorine pesticides in plants. J. Chromatogr. A 1008, 115–122.

Beulke, S., Brown, C.D., Fryer, C.J., van Beinum, W., 2004. Influence of kinetic sorption and diffusion on pesticide movement through aggregated soils. Chemosphere 57, 481–490.

Bollmann, U.E., Fernández-Calviño, D., Brandt, K.K., Storgaard, M.S., Sanderson, H., Bester, K., 2017. Biocide runoff from building facades: degradation kinetics in soil. Environ. Sci. Technol. 51, 3694–3702.

Bollmann, U.E., Minelgaite, G., Schlüsener, M., Ternes, T., Vollertsen, J., Bester, K., 2016. Leaching of terbutryn and its photodegradation products from artificial walls under natural weather conditions. Environ. Sci. Technol. 50, 4289–4295.

Bork, M., Engel, Johannes, Krämer, Alexander, Lange, Jens, 2022. FReWaB-PLUS (Freiburger Regenwasserbewirtschaftung plus Stofftransport) [WWW Document]. FReWaB-PLUS: Mobilisierung von Bioziden in Stadtgebieten. URL https://www.biozidauswaschung.de (accessed 10.1.22).

Burkhardt, M., Engelke, D., Gehrig, S., Hochstrasser, F., Rohr, M., Tietje, O., 2020. COMLEAM - Manual Version 3.0. HSR University of Applied Sciences Rapperswil, Switzerland.

Burkhardt, M., Zuleeg, S., Vonbank, R., Bester, K., Carmeliet, J., Boller, M., Wangler, T., 2012. Leaching of biocides from façades under natural weather conditions. Environ. Sci. Technol. 46, 5497–5503.

Chapter 3

Chen, S., Zhang, K., Jha, R.K., Chen, C., Yu, H., Liu, Y., Ma, L., 2019. Isotope fractionation in atrazine degradation reveals rate-limiting, energy-dependent transport across the cell membrane of gram-negative rhizobium sp. CX-Z. Environ. Pollut. 248, 857–864.

Drouin, G., 2021. Micropollutant dissipation at the sediment-water interface by coupling modelling and Compound-Specific Isotope Analysis. University of Strasbourg.

Droz, B., 2021. Pesticide Dissipation at the sediment-water interface: insights from compound-specific isotope analysis (CSIA). University of Strasbourg.

Droz, B., Drouin, G., Maurer, L., Villette, C., Payraudeau, S., Imfeld, G., 2021. Phase Transfer and Biodegradation of Pesticides in Water–Sediment Systems Explored by Compound-Specific Isotope Analysis and Conceptual Modeling. Environ. Sci. Technol. 55, 4720–4728.

Elsayed, O.F., Maillard, E., Vuilleumier, S., Nijenhuis, I., Richnow, H.H., Imfeld, G., 2014. Using compound-specific isotope analysis to assess the degradation of chloroacetanilide herbicides in lab-scale wetlands. Chemosphere 99, 89–95.

Gilevska, T., Wiegert, C., Droz, B., Junginger, T., Prieto-Espinoza, M., Borreca, A., Imfeld, G., 2022. Simple extraction methods for pesticide compound-specific isotope analysis from environmental samples. MethodsX 101880.

Hvězdová, M., Kosubová, P., Košíková, M., Scherr, K.E., Šimek, Z., Brodský, L., Šudoma, M., Škulcová, L., Sáňka, M., Svobodová, M., 2018. Currently and recently used pesticides in Central European arable soils. Sci. Total Environ. 613, 361–370.

Imfeld, G., Meite, F., Wiegert, C., Guyot, B., Masbou, J., Payraudeau, S., 2020. Do rainfall characteristics affect the export of copper, zinc and synthetic pesticides in surface runoff from headwater catchments? Sci. Total Environ. 741, 140437.

Ivdra, N., Herrero-Martín, S., Fischer, A., 2014. Validation of user-and environmentally friendly extraction and clean-up methods for compound-specific stable carbon isotope analysis of organochlorine pesticides and their metabolites in soils. J. Chromatogr. A 1355, 36–45.

Liu, X., Wu, L., Kümmel, S., Merbach, I., Lal, R., Richnow, H.H., 2020. Compound-Specific Isotope Analysis and Enantiomer Fractionation to Characterize the Transformation of Hexachlorocyclohexane Isomers in a Soil–Wheat Pot System. Environ. Sci. Technol. 54, 8690–8698.

Liu, X., Wu, L., Kümmel, S., Richnow, H.H., 2021. Characterizing the biotransformation of hexachlorocyclohexanes in wheat using compound-specific stable isotope analysis and enantiomer fraction analysis. J. Hazard. Mat. 406, 124301.

Lutz, S.R., Velde, Y. van der, Elsayed, O.F., Imfeld, G., Lefrancq, M., Payraudeau, S., Breukelen, B.M. van, 2017. Pesticide fate on catchment scale: conceptual modelling of stream CSIA data. Hydrol. Earth Syst. Sci. 21, 5243–5261.

Maillard, E., Payraudeau, S., Faivre, E., Grégoire, C., Gangloff, S., Imfeld, G., 2011. Removal of pesticide mixtures in a stormwater wetland collecting runoff from a vineyard catchment. Sci. Total Environ. 409, 2317–2324.

Masbou, J., Drouin, G., Payraudeau, S., Imfeld, G., 2018a. Carbon and nitrogen stable isotope fractionation during abiotic hydrolysis of pesticides. Chemosphere 213, 368–376.

Masbou, J., Meite, F., Guyot, B., Imfeld, G., 2018b. Enantiomer-specific stable carbon isotope analysis (ESIA) to evaluate degradation of the chiral fungicide Metalaxyl in soils. J. Hazard. Mat. 353, 99–107.

Muhammad, R., Ahad, K., Mehboob, F., 2020. Extraction techniques for pesticide residues analysis in edible oils and role of sorbents in cleanup. Sep. Sci. Plus 3, 51–62.

Obuseng, V.C., Mookantsa, B.M., Okatch, H., Mosepele, K., Torto, N., 2013. Extraction of pesticides from plants using solid phase microextraction and QuEChERS. S. Afr. J. Chem. 66, 183–188.

Pérez-Rodríguez, P., Schmitt, A.-D., Gangloff, S., Masbou, J., Imfeld, G., 2021. Plants affect the dissipation and leaching of anilide pesticides in soil mesocosms: Insights from compound-specific isotope analysis (CSIA). Agric. Ecosyst. Environ. 308, 107257.

Ponsin, V., Torrentó, C., Lihl, C., Elsner, M., Hunkeler, D., 2019. Compound-specific chlorine isotope analysis of the herbicides atrazine, acetochlor, and metolachlor. Anal. Chem. 91, 14290–14298.

Schreglmann, K., Hoeche, M., Steinbeiss, S., Reinnicke, S., Elsner, M., 2013. Carbon and nitrogen isotope analysis of atrazine and desethylatrazine at sub-microgram per liter concentrations in groundwater. Anal. Bioanal. Chem. 405, 2857–2867.

Sigmund, G., Arp, H.P.H., Aumeier, B.M., Bucheli, T.D., Chefetz, B., Chen, W., Droge, S.T.J., Endo, S., Escher, B.I., Hale, S.E., Hofmann, T., Pignatello, J., Reemtsma, T., Schmidt, T.C., Schönsee, C.D., Scheringer, M., 2022. Sorption and mobility of charged organic compounds: how to confront and overcome limitations in their assessment. Environ. Sci. Technol. 56, 4702–4710.

Smith, R., Middlebrook, R., Turner, R., Huggins, R., Vardy, S., Warne, M., 2012. Large-scale pesticide monitoring across Great Barrier Reef catchments–paddock to reef integrated monitoring, modelling and reporting program. Mar. Pollut. Bull. 65, 117–127.

Torrentó, C., Bakkour, R., Glauser, G., Melsbach, A., Ponsin, V., Hofstetter, T.B., Elsner, M., Hunkeler, D., 2019. Solid-phase extraction method for stable isotope analysis of pesticides from large volume environmental water samples. Analyst 144, 2898–2908.

Torrentó, C., Ponsin, V., Lihl, C., Hofstetter, T.B., Baran, N., Elsner, M., Hunkeler, D., 2021. Triple-Element Compound-Specific Stable Isotope Analysis (3D-CSIA): Added Value of Cl Isotope Ratios to Assess Herbicide Degradation. Environ. Sci. Technol. 55, 13891–13901.

Wilkowska, A., Biziuk, M., 2011. Determination of pesticide residues in food matrices using the QuEChERS methodology. Food Chem. 125, 803–812.

Wu, L., Moses, S., Liu, Y., Renpenning, J., Richnow, H.H., 2019. A concept for studying the transformation reaction of hexachlorocyclohexanes in food webs using multi-element compound-specific isotope analysis. Anal. Chim. Acta. 1064, 56–64.

Chapter 3

Yousefi, M., Rahimi-Nasrabadi, M., Mirsadeghi, S., Pourmortazavi, S.M., 2021. Supercritical fluid extraction of pesticides and insecticides from food samples and plant materials. Crit. Rev. Anal. Chem. 51, 482–501.

Preface to Chapter 4

In Chapter 3, we validated extraction methods for the use of compound-specific isotope analysis (CSIA) for a variety of pesticides. This knowledge was then applied in Chapter 4 to evaluate and examine different terbutryn degradation pathways using CSIA. The chapter discusses transformation processes of terbutryn based on carbon and nitrogen isotope fractionation and transformation product measurements in order to retrieve reference isotope fractionation values (ε_C and ε_N) during biodegradation, photodegradation and abiotic hydrolysis. To evaluate single pathways, microcosm experiment under controlled laboratory experiments were conducted.

In this study, we report first carbon and nitrogen isotope fractionation values of terbutryn for photodegradation, hydrolysis and biodegradation. We highlight that degradation pathways can be distinguished using multi-element CSIA. Additionally, underlying degradation mechanisms were consolidated by considering both, transformation products and carbon and nitrogen isotope fractionation. Altogether, this study lays the foundation for using carbon and nitrogen stable isotope analysis of terbutryn in environmental studies by providing reference isotope fractionation values.

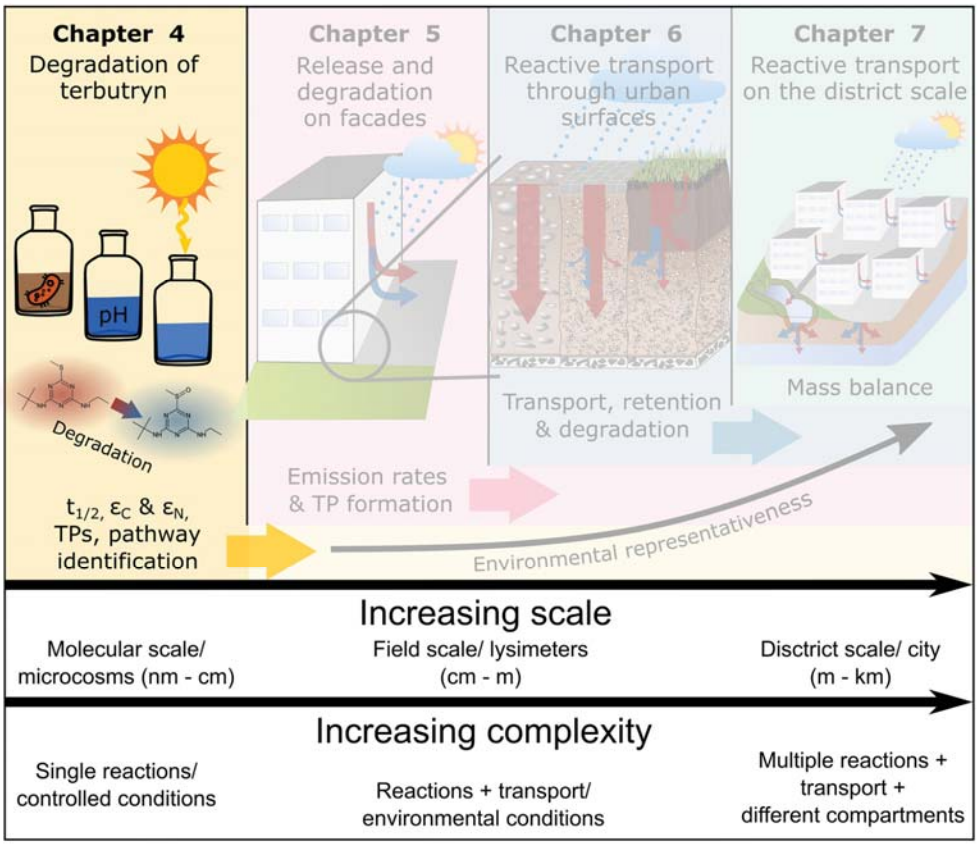

Chapter 4
Transformation and stable isotope fractionation of the urban biocide terbutryn during biodegradation, photodegradation and abiotic hydrolysis

This chapter is an edited version of the peer reviewed article:

Junginger, T., Payraudeau, S., & Imfeld, G. (2022). Transformation and stable isotope fractionation of the urban biocide terbutryn during biodegradation, photodegradation and abiotic hydrolysis. *Chemosphere*, *305*, 135329.

Graphical abstract:

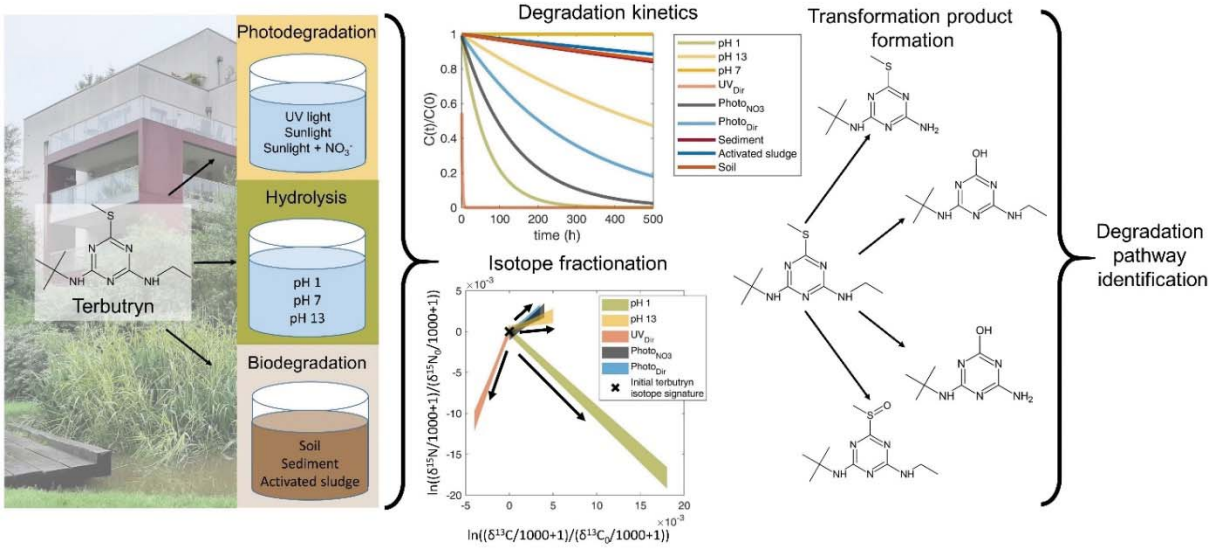

Chapter 4

Abstract

Terbutryn is a widely used biocide in construction materials like paint and render to prevent the growth of microorganisms, algae and fungi. Terbutryn is released from the facades into the environment during rainfall, contaminating surface waters, soil and groundwater. Knowledge of terbutryn dissipation from the facades to aquatic ecosystems is scarce. Here, we examined in laboratory microcosms degradation half-lives, formation of transformation products and carbon and nitrogen isotope fractionation during terbutryn direct (UV light with λ = 254 nm and simulated sunlight) and indirect (simulated sunlight with nitrate) photodegradation, abiotic hydrolysis (pH = 1, 7 and 13), and aerobic biodegradation (stormwater pond sediment, soil and activated sludge). Biodegradation half-lives of terbutryn were high (> 80 d). Photodegradation under simulated sunlight and hydrolysis at extreme pH values indicated slow degradability and potential accumulation in the environment. Photodegradation resulted in a variety of transformation products, whereas abiotic hydrolysis lead solely to terbutryn-2-hydroxy in acidic and alkaline conditions. Biodegradation indicates degradation to terbutryn-2-hydroxy through terbutryn-sulfoxide. Compound-specific isotope analysis (CSIA) of terbutryn holds potential to differentiate degradation pathways. Carbon isotope fractionation values (ε_C) ranged from –3.4 ± 0.3‰ (hydrolysis pH 1) to +0.8 ± 0.1‰ (photodegradation under UV light), while nitrogen isotope fractionation values ranged from –1.0 ± 0.4‰ (simulated sunlight photodegradation with nitrate) to +3.4 ± 0.2‰ (hydrolysis at pH 1). In contrast, isotope fractionation during biodegradation was insignificant. $\Lambda^{N/C}$ values ranged from –1.0 ± 0.1 (hydrolysis at pH 1) to 2.8 ± 0.3 (photodegradation under UV light), allowing to differentiate degradation pathways. Combining the formation of transformation products and stable isotope fractionation enabled identifying distinct degradation pathways. Altogether, this study highlights the potential of CSIA to follow terbutryn degradation in situ and differentiate prevailing degradation pathways, which may help to monitor urban biocide remediation and mitigation strategies

1 Introduction

Biocides are added as in-can and film preservatives in building materials to prevent algae and microbial growth on facade materials like paints and renders. During rainfall events, biocides and their transformation products (TPs) are washed out from building materials and enter into the environment (Bollmann et al., 2016; Burkhardt et al., 2012; Linke et al., 2021; Schoknecht et al., 2009; Wittmer et al., 2011). Lab-scale experiments have demonstrated the export of urban biocides from silicone render, acrylate render, roof paint and facade paints (Burkhardt et al., 2012; Jungnickel et al., 2008; Schoknecht et al., 2009; Styszko et al., 2015). However, knowledge of the contribution of dissipation processes controlling the reactive transport of urban biocides from facades to surface waters, soil and groundwater remains scarce.

Among urban biocides, an active compound of major concern is terbutryn, acting as a photosynthesis inhibitor (Jurado et al., 2011). Terbutryn is still used as a pre-emergent or post-emergent herbicide in agriculture in several countries (Carazo-Rojas et al., 2018; LeBaron et al., 2008). In the EU, terbutryn is prohibited for agricultural applications since 2003 (European Council Directive 91/414/EEC, 2002) and is defined as a priority substance since 2013 according to the Water Framework Directive (WFD) (European Council Directive 2013/39/EU, 2013). Terbutryn, measured in concentrations up to 5.6 µg L^{-1} in German rivers exceeds predicted no-effect concentrations (PNEC, 0.003 to 0.034 µg L^{-1}) (Burkhardt et al., 2009; Kresmann et al., 2018; Quednow and Püttmann, 2007) and is detected in groundwater (Hensen et al., 2018). The redundant detection of terbutryn in waters may be related to its low removal in wastewater treatment plants (WWTP) (Luft et al., 2014; Paijens et al., 2021). Altogether, this emphasizes significant, and possibly ecotoxic, release of terbutryn into surface water. However, the contribution of degradative processes (i.e., photodegradation, hydrolysis and biodegradation) and non-degradative process (i.e., sorption and dilution) to the overall dissipation of terbutryn and its TPs is largely unknown.

Photodegradation may either occur directly on the facades or in water bodies, such as retention ponds or rivers (Bollmann et al., 2016; Minelgaite et al., 2017; Sakkas et al., 2006; Urbanczyk et al., 2019). Direct photodegradation refers to the absorption of light by a molecule leading to bond cleavage, whereas indirect photodegradation results from the excitation of other molecules, e.g., nitrate or dissolved organic carbon (DOC), and the formation of radical reactive

species mediating bond cleavages (Schwarzenbach et al., 2005). Terbutryn degrades in the range of sunlight wavelengths (Hensen et al., 2019), although degradation is slow under environmental conditions (Minelgaite et al., 2017). Terbutryn photodegradation occurred in paint and on facades under controlled laboratory conditions and in the environment (Bollmann et al., 2016; Schoknecht et al., 2021; Urbanczyk et al., 2019). Several TPs of terbutryn have been identified under irradiation with UV light (Hensen et al., 2018) and under simulated sunlight during direct and indirect photodegradation in aqueous solutions and on paint surfaces (Hensen et al., 2019; Urbanczyk et al., 2019). This raises the issue of the formation of photodegradation TPs and their release from facades.

Hydrolysis is a major pathway of pesticide degradation, which can be abiotically or biologically mediated (Fenner et al., 2013), depending on pH and temperature (Mabey and Mill, 1978). Some studies indicate only minor abiotic hydrolysis of other triazine pesticides, such as atrazine, under moderate acidic or alkaline pHs and degradation mainly occurring at extreme pHs (< 4 or > 12) (Masbou et al., 2018; Meyer et al., 2009; Torrentó et al., 2021).

Biodegradation of terbutryn may occur in soils collecting runoff from facades, in WWTPs and in water bodies receiving discharges from separated sewers. Biodegradation half-lives of terbutryn in laboratory soil microcosms ranged from 7 (32°C, 10% soil moisture content) to 227 days (4°C with 10% soil moisture content) (Lechón et al., 1997), and from 180 to 240 days in water with river sediment under aerobic conditions (Muir and Yarechewski, 1982), and up to 650 days under anaerobic conditions (Talja et al., 2008). Biodegradation in activated WWTP sludge resulted mainly in the formation of terbutryn-sulfoxide (TerSO). TerSO was further degraded to the hydroxy-derivate terbutryn-2-hydroxy (TerOH) under acidic conditions (Luft et al., 2014). TerSO prevailed in the early state of degradation under aerobic soil biodegradation experiments, with declining concentrations throughout the experiment. TerOH, desbutyl-2-hydroxy-terbutryn (TerDesBOH) and desethyl-terbutryn (TerDesE) were gradually formed, with minor contribution of desethyl-2-hydroxy-terbutryn (TerDesEOH) (Bollmann et al., 2017a). Although the occurrence of TPs in the environment indicates terbutryn degradation, further TP degradation, sorption or dilution may limit the identification and the quantification of specific transformation pathways.

In this context, following up changes of the stable isotope composition (natural isotope abundance) of the residual, non-degraded fraction of a pollutant may help to evaluate degradation without considering concentration data of parent compound or TPs (Alvarez-Zaldívar et al., 2018; Elsner et al., 2012; Elsner and Imfeld, 2016; Schmidt et al., 2004). Typically, light isotopes (e.g., ^{12}C) need a lower activation energy for bond cleavage compared to heavy isotopes (e.g., ^{13}C), resulting in faster reaction times and enrichment of heavy isotopologues in the non-degraded fraction (Elsner, 2010). In contrast, non-degradative processes like sorption, dilution or advection generally cause insignificant isotope fractionation (Höhener and Yu, 2012; Schüth et al., 2003). In particular, compound-specific isotope analysis (CSIA) of pollutants may help to identify reaction pathways by measuring changes in stable isotope ratios (e.g., $^{13}C/^{12}C$, $^{15}N/^{14}N$), which are often reaction-specific (Alvarez-Zaldívar et al., 2018; Elsner, 2010; Elsner and Imfeld, 2016; Fischer et al., 2016; Meyer et al., 2009; Torrentó et al., 2021). Changes in isotope ratios may be related to the extent of degradation using isotope fractionation values (ε) that are typically retrieved from laboratory experiments under controlled conditions (Coplen, 2011; Hoefs, 2015). While CSIA has been used to study transformation of similar triazine type herbicides, such as atrazine and ametryn (Drouin et al., 2021; Hartenbach et al., 2008; Lihl et al., 2020; Masbou et al., 2018; Meyer et al., 2009; Schürner et al., 2015; Torrentó et al., 2021), isotope fractionation of terbutryn during degradation has not been examined yet.

The purpose of this study was to examine the degradation rates and stable isotope fractionation during abiotic hydrolysis, biodegradation and photodegradation of terbutryn to improve the interpretation of terbutryn degradation from the facades to sink ecosystems, such as soil and groundwater, in urban settings. Different terbutryn degradation pathways may lead to distinct patterns of TP formation and stable isotope fractionation. We thus examined the reaction kinetic rate constants, the TP formation, and carbon and nitrogen CSIA data to evaluate degradation pathways of terbutryn and the potential of CSIA to follow up terbutryn degradation in situ and distinguish degradation processes.

Chapter 4

2 Material and Methods

2.1 Chemicals

Solvents (dichloromethane (DCM) and n-Pentane) were HPLC-grade (> 99.9%) and purchased from Sigma-Aldrich (St. Louis, MO, USE). Analytical standards with purity >9 8% (terbutryn and alachlor D-13) were purchased from PESTANAL (St. Louis, MO, USA). Standards of terbutryn TPs TerOH, TerDesE and TerDesEOH (purity > 98%) were purchased from HPC Standards GmbH (Borsdorf, Germany), TerSO (purity > 97%) was purchased from MicroCombiChem GmbH (Wiesbaden, Germany). Water, acetonitrile and formic acid for analysis with HPLC-MS were LC/MS grade (Biosolve, France). Buffer solutions were prepared using DI-water (> 18 MΩ), hydrochloric acid (37%, AnalaR NORMAPUR), potassium phosphate monobasic (> 99.5%, Sigma Aldrich), potassium chloride (> 99.5%, VWR Chemicals BDH) and sodium hydroxide (> 95%, Sigma Aldrich). Nitrate solutions for photodegradation experiments were prepared with calcium nitrate tetrahydrate (> 99%, Sigma Aldrich).

2.2 Experimental setup

Photodegradation experiment. Photodegradation experiments in aqueous solutions were conducted under UV irradiation (UV_{Dir}), under simulated sunlight in pure water ($Photo_{Dir}$) and under simulated sunlight with 20 mg L^{-1} nitrate ($Photo_{NO3}$) to mimic environmental conditions in surface waters. UV_{Dir} was conducted using a temperature-controlled black box with a low-pressure mercury lamp (Philips, TUV 6W G6T5) providing a single-band light at $\lambda = 254$ nm. Simulated sunlight was replicated using a QSUN XE-1 test chamber (Q-LAB, Westlake, OH USA) with a xenon arc lamp and a daylight-Q filter with a nominal cut-on at 295 nm. The irradiation intensity was set to 0.68 W m^{-2} nm^{-1} at 340 nm which matches best with maximum solar irradiation and represents an intensity of ≈1200 W m^{-2} integrated over all wavelengths (QSun/QLab, 2011). Initial terbutryn concentrations were 10 mg L^{-1} in the aqueous solutions. Three independent beakers (50 mL beakers containing 40 mL solution) for sacrificial sampling were prepared for each sampling. Additionally, dark controls and process blanks were prepared for three successive samplings throughout the experiment. Sample preparation and sampling are detailed in Table B 1. Effects of degradation on solution pH were tested by measuring the pH of

several mixtures of terbutryn and TPs in the relevant concentration range (1 – 10 mg L^{-1}), with and without calcium nitrate tetrahydrate ($Ca(NO_3)_2$ 4 H_2O). For all tested solutions, the pH was 7 ± 0.5 (Appendix B).

Hydrolysis experiment. Hydrolysis experiments were carried out in triplicate in 400 mL Schott glass bottles under dark and sterile conditions. Three aqueous buffer solutions were prepared with sterilized DI water at pH = 1, 7 and 13 and sterilized by filtration through sterile 0.2 µm PTFE filters (Rotilabo®, Carl Roth®, France). Extreme pH values were chosen to increase degradation kinetics and study reaction pathways and associated isotope fractionation. Buffer solutions were spiked with terbutryn to a final concentration of 10 mg L^{-1}. Additional process blanks without terbutryn were prepared for each pH and sampled three times throughout the experiment. Solutions were incubated at 60°C to accelerate the reaction. The preparation of buffer solutions, sample preparation and sampling procedures are detailed in Table B 1 and Table B 2.

Biodegradation experiment. Terbutryn biodegradation in different systems exposed to biocide effluent was examined in microcosm experiments: (i) water from stormwater retention pond with 100 mg L^{-1} of 2 mm-sieved pond sediment (PondSed), (ii) soil from a stormwater swale system (soil) and (iii) activated sludge from WWTP diluted 1:10 (v:v) in milliQ water. Composite samples (n > 5 subsamples) of either soil, pond water or sediment exposed to facade runoff through drainage pipes and surface flow were collected in the Aldelshoffen district in Schiltigheim (Strasbourg Eurometropolis, Bas-Rhin, France) and the respective samples were mixed together thoroughly. The activated sludge was collected in the main WWTPs of Strasbourg, receiving diluted urban runoff through combined sewer systems. The frequent exposure of sediment, soil and activated sludge to terbutryn from facade runoff may lead to microbial adaptation and favor terbutryn biodegradation (Poursat et al., 2019; Spain et al., 1980). The collection procedure and physico-chemical characteristics of the samples used in the biodegradation experiments are detailed in the Appendix B.

Aerobic biodegradation microcosms consisted in 50 mL vials crimped with butyl/PTFE caps filled either with 30 mL of spiked stormwater retention pond water with sediment, 30 mL spiked diluted sewage sludge or 5 g of spiked soil. A needle with a 0.2 µm syringe filter was stuck through the cap to maintain oxic conditions without water loss (Torabi et al., 2020). For

each soil sample, 5 g of soil were spiked with terbutryn, to reach a final concentration of 120 µg g^{-1}, adjusted to a water content of 40% and thoroughly mixed. Concentrations are representative for accumulation of terbutryn on small receiving surfaces exposed to repeated facade runoff with emission rates of several mg m^{-2} $event^{-1}$ (Bollmann et al., 2017b, 2016; Burkhardt et al., 2012). Stormwater retention pond and activated sludge samples were spiked with terbutryn at 10 mg L^{-1} and divided into the different microcosms for sacrificial sampling. Concentrations are representative for direct facade runoff from new buildings (Bollmann et al., 2017b, 2016; Burkhardt et al., 2012). Process blanks without terbutryn and sterile controls were prepared for all setups. Microcosms were incubated at room temperature (21°C) and constantly shaken on an orbital shaker at 120 rpm. During each sampling time (Table B 1), triplicate microcosms were retrieved for extraction and analysis.

2.3 Terbutryn extraction and quantification

Liquid samples were extracted using liquid-liquid extraction. Briefly, the entire sample for biodegradation experiments and 30 mL for photodegradation experiments were transferred into 40 mL amber glass vials and terbutryn was extracted with DCM (3 mL). Samples were shaken (600 rpm) for 5 min, ultrasonicated for 15 min, shaken again for 5 seconds and centrifuged at 1500 rpm for 5 min. Solvent was recovered and the whole procedure was repeated three times. The extracts were pooled and evaporated under gentle N_2 stream. Samples were resuspended in 0.5 mL DCM. Soil samples followed a modified solid-liquid extraction with 3:1 Pentane:DCM (v:v) and purification procedure (Droz et al., 2021; Ivdra et al., 2014), described in details in Chapter 3. Water subsamples (1 mL) were collected at different time points and filtered at 0.2 µm for TP analysis (Table B 1 and sections B1.2 – B1.4). All samples were stored in the freezer at –20°C until analysis. Recoveries of extraction methods and validation for CSIA (i.e., absence of stable isotope fractionation associated with the methods) are provided in SI (section B1.5)

Terbutryn and four main TPs TerSO, TerOH, TerDesE and TerDesEOH (Table B 7) were quantified using ultra high-pressure liquid chromatography (UHPLC) (Dionex/ Thermo Scientific UltiMate Dionex 3000) coupled to a triple quadrupole mass spectrometer (Thermo Scientific TSQ Quantiva), using a C18 column (Accucore 100 x 2.1, particle size 2.6 µm).

Solvent gradients, mass transitions, limit of detection (LOD) and limit of quantification (LOQ) were determined based on calibration curves and are provided in section B1.7.

Carbon and nitrogen stable isotope analysis was conducted using a GC/IRMS system consisting of a gas chromatograph (GC, TRACE Ultra ThermoFisher Scientific) coupled to an isotope ratio mass spectrometer (IRMS, DeltaV plus, ThermoFisher Scientific) via a GC combustion interface (IsoLink/Conflow IV, ThermoFisher Scientific) equipped with a TG-5MS column (60 m × 0.25 mm ID, 0.25 µm film thickness). Details about instrument conditions, quality checks and reference materials are provided in section B1.8.

2.4 Data analysis

For all degradation experiments, concentrations were plotted against experimental time and fitted using first order degradation kinetics with Matlab R2020 b using the fit function.

Isotope ratios were normalized to Vienna Pee Dee Belemnite (VPDB) and air standards for carbon and nitrogen stable isotopes respectively and written in the delta notation (Elsner, 2010):

$$\delta_{\text{sample}}\text{E}\,[‰] = \left(\frac{\text{R}_{\text{sample}}}{\text{R}_{\text{standard}}} - 1\right) \cdot 1000 \qquad \textbf{(4.1)}$$

The Rayleigh equation was used to calculate the isotope values of the residual (non-degraded) fraction of terbutryn (Elsner, 2010):

$$\ln\left(\frac{\text{R}_{\text{t,E}}}{\text{R}_{\text{0,E}}}\right) = \ln\left(\frac{\text{C}_{\text{t,E}}}{\text{C}_{\text{0,E}}}\right) \cdot \frac{\varepsilon^{\text{E}}_{\text{bulk}}}{1000} \qquad \textbf{(4.2)}$$

Where $R_{t,E}$ / $R_{0,E}$ is the isotope ratio of the element E (e.g., $^{13}C/^{12}C$ or $^{15}N/^{14}N$), $C_{t,E}$ and $C_{0,E}$ are concentrations of terbutryn at a specific time t and at the start of the experiment (0) and ε^{E}_{bulk} is the apparent isotope fractionation value. Apparent isotope values were derived from linear regression by taking into account each of the triplicate microcosms/samples individually (Scott et al., 2004). Given uncertainties correspond to the 95% confidence interval (CI) of the slope of the linear regression. $\Lambda^{N/C}$ values were derived using the York regression, accounting for

uncertainties in C and N isotope measurements (Höhener and Imfeld, 2021; Ojeda et al., 2019) according to:

$$\Lambda^{N/C} = \frac{\ln\left[\left(\frac{\delta^{15}N_t}{1000}+1\right)/\left(\frac{\delta^{15}N_0}{1000}+1\right)\right]}{\ln\left[\left(\frac{\delta^{13}C_t}{1000}+1\right)/\left(\frac{\delta^{13}C_0}{1000}+1\right)\right]} \quad \textbf{(4.3)}$$

For analysis of $\Lambda^{N/C}$ values, the R package IsoplotR was used (Vermeesch, 2018).

3 Results and discussion

3.1 Terbutryn photodegradation

Terbutryn photodegradation was faster under UV light than under simulated sunlight (Table 4. 1), due to the absorption spectrum of terbutryn and irradiation intensity (Bollmann et al., 2016; Hensen et al., 2019; Minelgaite et al., 2017). Slower terbutryn degradation under simulated sunlight likely reflects the slight overlap of the absorption spectrum of terbutryn with simulated sunlight at wavelengths 290 – 300 nm (Figure B 4). Selecting a representative irradiation source, such as a filtered Xenon arc lamp, is thus crucial to infer environmentally relevant photodegradation kinetics, especially for compounds weakly absorbing sunlight, such as terbutryn (Hensen et al., 2019).

Photodegradation rate constants were twice higher with than without nitrate (Table 4. 1). Nitrate concentrations are often above 20 mg L^{-1} in agricultural surface waters as well as effluents of WWTPs, where urban biocides are present as well. Irradiation of nitrate may form hydroxy radicals ($NO_3^- + H_2O \xrightarrow{hv} NO_2 + OH\cdot + OH$) acting as photocatalyst during indirect photodegradation of terbutryn (Schwarzenbach et al., 2005). Hence, terbutryn degradation rate constants increase with increasing formation of hydroxy radicals (Hensen et al., 2019; Lam et al., 2003). It is worth mentioning, that direct and indirect photodegradation can co-occur in water, limiting the estimation of the contribution of nitrate-mediated degradation. Direct and indirect terbutryn photodegradation may also already occur on facades (Bollmann et al., 2016; Schoknecht et al., 2021; Urbanczyk et al., 2019) then in sink aquatic ecosystems, including storm water retention systems (swale systems), rivers and lakes where terbutryn was frequently

detected (Ccanccapa et al., 2016; Linke et al., 2021; Machate et al., 2021; Quednow and Püttmann, 2007). Besides nitrate, other substances (e.g., humic acids or dissolved organic matter) can catalyze photodegradation by providing radicals or decelerate photodegradation through absorption and shielding of the contaminant (Drouin et al., 2021; Wu et al., 2021; Zhang et al., 2015). Degradation kinetics, however, may be overestimated as they represent constant irradiation with light intensities of peak natural daylight (CIE, 1989; QSun/QLab, 2011). Considering the mean annual solar surface irradiation in northern Europe (100 – 200 W/m², accounting for e.g., diurnal and annual variation) (Pfeifroth et al., 2018), photodegradation half-lives in the environment may increase by one order of magnitude compared to half-lives estimated in the laboratory experiments.

Table 4. 1. Terbutryn degradation half-life ($t_{1/2}$) and degradation rate constant (k), isotope fractionation values for carbon (ε_C) and nitrogen (ε_N) and $\Lambda^{N/C}$ values. Uncertainties are given as 95% confidence interval (± 95% CI). NS: non-significant degradation or isotope fractionation ($\Delta\delta^{13}C$ or $\Delta\delta^{15}N$ < 0.5‰ in biodegradation experiments).

	Degradation process	$t_{1/2}$	k [s^{-1}]	ε_C [‰]	ε_N [‰]	$\Lambda^{N/C}$
UV_{Dir}	Photodegradation	68.7 ± 24.6 min	1.7×10^{-4}± 9.4×10^{-5}	+0.8 ± 0.1	+2.2 ± 0.3	2.8 ± 0.3
$Photo_{NO3}$		93.6 ± 37.2 h	2.1×10^{-6} ± 1.4×10^{-6}	–0.6 ± 0.2	–1.0 ± 0.4	0.8 ± 0.1
$Photo_{Dir}$		202.3 ± 83.3 h	9.5×10^{-7} ± 6.7×10^{-7}	–0.7 ± 0.3	–0.5 ± 0.3	0.7 ± 0.2
pH 1	Abiotic Hydrolysis	45.4 ± 15.2 h	4.2×10^{-6} ± 2.1×10^{-6}	–3.4 ± 0.3	+3.4 ± 0.2	–1.0 ± 0.1
pH 7		NS	NS	NS	NS	NS
pH 13		462.3 ± 173.3 h	4.2×10^{-7} ± 2.5×10^{-7}	–1.3 ± 0.2	–0.4 ± 0.3	0.3 ± 0.1
Pond + sediment	Biodegradation	83.6 ± 27.6 d	$9.6\text{x}10^{-8}$ ± $4.7\text{x}10^{-8}$	NS	NS	NS
Soil		90.2 ± 34.5 d	$8.9\text{x}10^{-8}$ ± $5.5\text{x}10^{-8}$	NS	NS	NS
Activated sludge		117.1 ± 34.4 d	$6.9\text{x}10^{-8}$ ± $2.9\text{x}10^{-8}$	NS	NS	NS

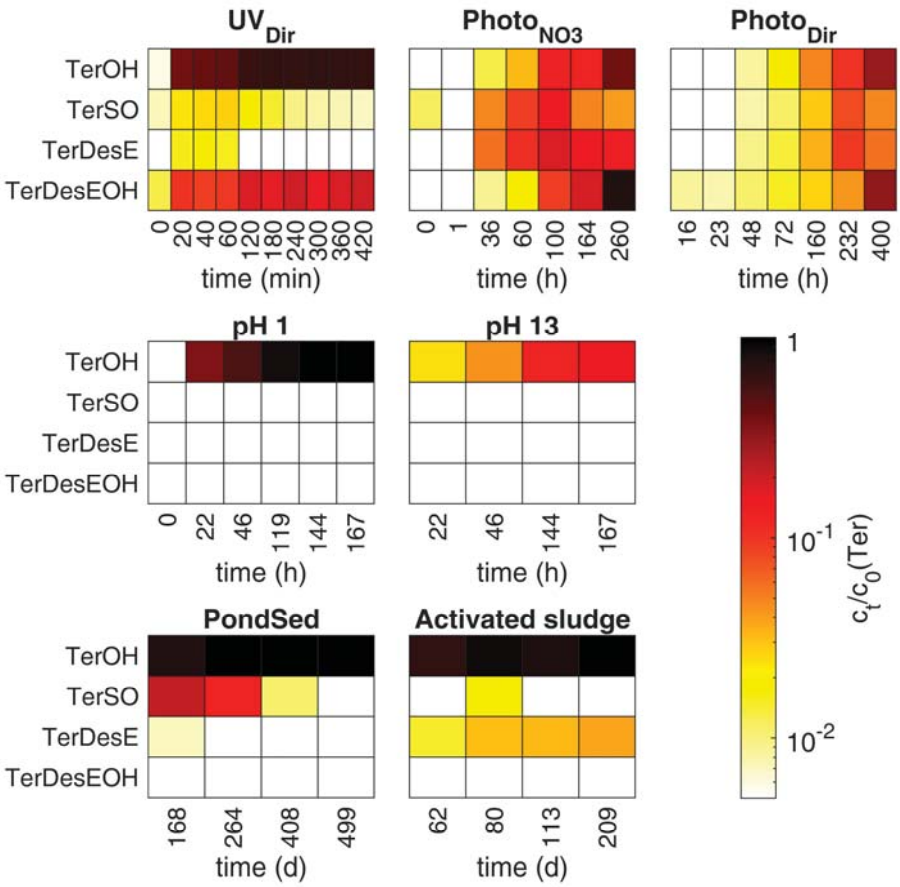

Figure 4. 1 Transformation products formed during terbutryn photodegradation (top), abiotic hydrolysis (middle) and biodegradation (bottom). Results are given in molar concentrations normalized to the initial concentration of terbutryn (ter). No degradation was observed at pH 7. Transformation products in soil microcosms were only measured for one sampling.

TerOH mainly formed during photodegradation under UV light, followed by TerDesEOH. In contrast, TerSO and TerDesE concentrations initially increased and gradually decreased during the experiment (Figure 4. 1). Similar trends were observed during photodegradation under artificial sunlight (Figure 4. 1). For UV light induced transformation, TerOH was formed either through substitution of the methylthio group by a hydroxy group through hydroxy radicals, or through an oxidation of the methylthio group, leading to TerSO, and further substitution of the oxidized methylthio group by a hydroxy group. This is supported by an increase of TerSO concentrations, followed by TerSO depletion (Figure 4. 1). A similar pattern was observed for TerDesE formation through the loss of an ethyl group at the side chain

of terbutryn. TerDesEOH was likely formed through TerDesE by a cleavage of the methylthio group and substitution through a hydroxy group. In contrast, the formation of TerDesEOH through TerOH is unlikely as supported by constant TerOH concentrations up to the end of the experiment. Desthiomethyl-terbutryn (TerDesS) was previously identified as a main TP formed through the loss of the -SCH_3 sidechain during photodegradation under UV irradiation (Bollmann et al., 2016 and Hensen et al., 2018). Although the contribution of TerDesS to the overall mass balance could not be quantified in our experiment due to the lack of an analytical standard, it was likely limited as the mass balance was nearly closed (> 80% recovery) with TerOH, TerDesEOH, TerSO and TerDesE.

The dominant TPs in photodegradation experiment with simulated sunlight were TerDesEOH, TerOH, with lower and decreasing concentrations of TerDesE and TerSO at the end of the experiment. TP patterns were similar in experiments with nitrate and distilled water. The dominance of terbutryn hydroxylation and/or dealkylation pathways suggest similar degradation patterns during direct and indirect photodegradation (Burrows et al., 2002; Hensen et al., 2019). However, on paint surfaces, TP formation patterns in photodegradation assays with UVB irradiation suggested a dependency on pigments and polymers that can get excited and cause indirect photodegradation (Urbanczyk et al., 2019). In pigment free paint, where most degradation occurred, TerSO increased before gradually decreasing, whereas TerDesEOH steadily increased, while TerOH concentrations reached a constant level (Urbanczyk et al., 2019). This latter pattern of TP formation is coherent with that of our study (Figure 4. 1), highlighting the relevance to consider transformation processes on the facades.

Carbon and nitrogen stable isotope fractionations differed for photodegradation under UV light and with simulated sunlight but were similar for direct and indirect photodegradation under simulated sunlight. Photodegradation under UV light resulted in inverse isotope fractionation values, i.e., an enrichment of light isotopes in non-degraded fraction, for both carbon (ε_C = +0.8 ± 0.10‰) and nitrogen (ε_N = +2.2 ± 0.3). In contrast, simulated sunlight resulted in normal isotope fractionation (Table 4. 1, Figure B 6 and Figure B 7). An inverse isotope effect for triazine transformation by UV light was related to excitation and relaxation processes or magnetic isotope effects (Drouin et al., 2021; Hartenbach et al., 2008; Knossow et al., 2020). An inverse isotope fractionation value during photodegradation under UV light was previously observed for atrazine, with a similar isotope fractionation value for nitrogen

($\varepsilon_{N(Atrazine)}$ = +2.4 ± 0.3‰) and more pronounced effect for carbon ($\varepsilon_{C(Atrazine)}$ = +2.7 ± 0.3‰) compared to isotope fractionation values for terbutryn degradation (Drouin et al., 2021; Hartenbach et al., 2008). A less pronounced carbon isotope fractionation during terbutryn degradation suggests terbutryn degradation to TerSO and then to TerOH, rather than the direct formation of TerOH. This idea is also supported by decreasing TerSO concentrations. The formation of TerSO may not significantly affect carbon or nitrogen isotope fractionation since carbon and nitrogen are not directly involved in bond cleavage or formation. In addition, constant TerOH concentrations indicate the formation of TerDesEOH through TerDesE rather than through TerOH. An inverse isotope fractionation may thus be caused by excitation at the triazine ring (Figure 4. 1, Figure 4. 2A). The excitation may result in the formation of the singlet state and conversion to the triplet state with cleavage of the C-N bond, e.g., during the formation of TerDesE. During the transition state, the bond is either cleaved or the molecule recombines. A recombination of the initial molecule is likelier for bonds containing light isotopes, resulting in enrichment of the light isotope in the non-degraded fraction. In addition, isotope fractionation may be more pronounced for nitrogen than for carbon, due to dilution effects for carbon isotopes.

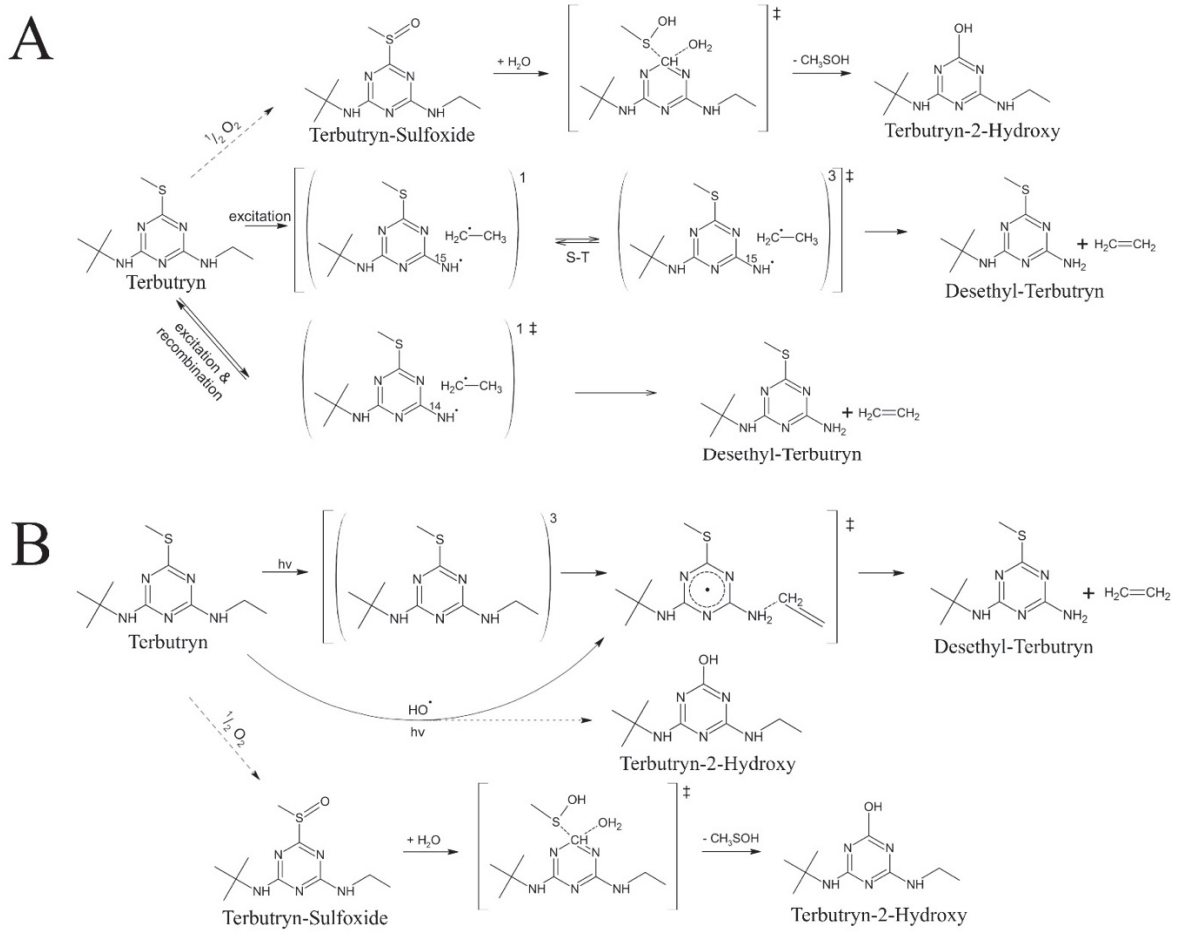

Figure 4. 2. Suggested pathways for photodegradation of terbutryn under UV irradiation (λ = 254 nm) (A) and under simulated sunlight (B) modified from Knossow et al., 2020. Numbers at the brackets represent the singlet (1) or triplet (3) state of the molecule. The double-cross (‡) indicates the transition state. The dashed arrow in the reaction to TerSO implies that no carbon or nitrogen isotope fractionation is expected.

3.2 Terbutryn Hydrolysis

Overall, our results emphasize limited hydrolysis of terbutryn under most common environmental conditions. Terbutryn hydrolysis occurred at pH = 1 and pH = 13 but was insignificant at pH = 7 (Table 4. 1). Acidic hydrolysis at pH = 1 was ten times faster than hydrolysis at pH = 13. Acidic hydrolysis occurs through bond cleavage catalyzed by H^+, whereas

hydrolysis at pH = 13 occurs through a base mediated reaction with OH^- as nucleophile (Wolfe et al., 1990).

Studies on hydrolysis of terbutryn are scarce, although previous studies on triazine pesticides indicated high hydrolytic stability between pH = 5 and pH = 9 (Lewis et al., 2016; Masbou et al., 2018), slow degradation at pH < 4 and insignificant degradation at pH = 7 and pH = 9 (Comber, 1999). While acidic rain (pH ~ 5; Keresztesi et al., 2019) may slightly hydrolyze terbutryn in facade runoff, surface waters in Europe and Northern America typically have higher pH values (Austnes et al., 2018). Alkaline pH values are rarely observed in the environment but might occur, for example, in soda lakes (pH > 10) (Grant and Sorokin, 2011) or directly in the pores of facade material (pH = 9.5) (Styszko et al., 2014). Considering faster degradation due to higher temperature in our microcosms underlines that typical environmental pHs result in negligible contribution of hydrolysis to terbutryn degradation.

Only TerOH was detected during abiotic hydrolysis at pH = 1 and pH = 13, indicating nucleophile substitution of the methylthio group under alkaline conditions (pH = 13) (Figure 4. 3A). Under acidic conditions, we hypothesize an intermediate step through the protonation of the triazine ring followed by the cleavage of the SCH_3 group, as suggested for atrazine (Meyer et al., 2009; Russell et al., 1968 Meyer et al., 2008), and in agreement with the formation of TerOH during terbutryn acidic hydrolysis (Figure 4. 3B).

Although TerOH was formed during both alkaline and acidic hydrolysis of terbutryn, carbon and nitrogen isotope fractionation significantly differed, indicating distinct degradation pathways (Table 4. 1). Under alkaline hydrolysis, isotope fractionation was observed for carbon (ε_C = –1.3 ± 0.2), and to lesser extent for nitrogen (ε_N= –0.4 ± 0.3). The carbon isotope fractionation may be due to nucleophilic substitution of the methylthio group during the formation of TerOH. The less pronounced nitrogen fractionation likely results from a secondary isotope effect since no N atom is directly involved in the bond cleavage (Figure 4. 3A). In contrast, acidic hydrolysis resulted in a normal isotope fractionation for carbon (ε_C = –3.4 ± 0.7) and an inverse isotope fractionation for nitrogen (ε_N = +3.4 ± 0.1). Protonation of a nitrogen atom in the triazine ring is leading to a polarization of the C-SCH_3 bond and the formation of TerOH (Figure 4. 3B). The bond cleavage at the methylthio group is expected to result in carbon isotope fractionation, as previously described for atrazine (Masbou et al., 2018; Meyer et al., 2009).

Protonation of a nitrogen atom in the triazine ring would lead to an inverse isotope effect for nitrogen, as observed in this study. Such bonding is more stable for heavy isotopes in the transition state, resulting in an enrichment of light isotopes in the non-degraded fraction. Even though extreme pH values are unlikely to occur in the environment, slower degradation at less extreme pHs might result in similar TP formation and isotope fractionation since the reaction pathway is identical.

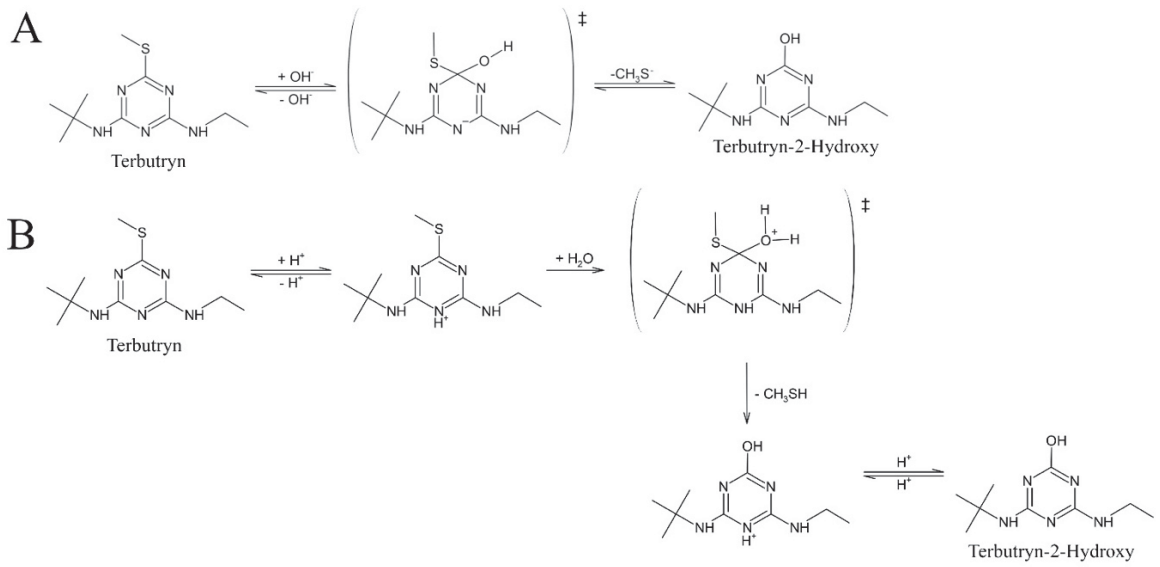

Figure 4. 3. Suggested pathways of terbutryn transformation during abiotic hydrolysis at pH 13 (A) and pH 1 (B) (modified from Meyer et al., 2009). The double-cross (‡) indicates the transition state.

3.3 Terbutryn biodegradation

Half-lives for terbutryn biodegradation, ordered from the lowest to the highest half-lives: PondSed < Soil < activated sludge, were 4 to 62-fold higher than half-lives for terbutryn photodegradation under simulated sunlight and hydrolysis (Table 4. 1). However, biodegradation rates and sunlight induced degradation of terbutryn may be in the same order of magnitude since environmental photodegradation half-lives were overestimated in our study as discussed previously.

Overall, these results suggest slow terbutryn biodegradation in the environment. Microbial adaptation may explain faster terbutryn degradation in pond-sediment and soil experiments than in the activated sludge experiment (Poursat et al., 2019; Spain et al., 1980). Indeed, pond water and sediment in the PondSed, and soil in the soil experiments, were chronically exposed to direct release of terbutryn from facades at the sampling site. It is also worth noting that a wide range of half-lives (7 up to > 240 days) for terbutryn degradation in previous laboratory studies underscores a strong dependency on the incubation method and matrix (Bollmann et al., 2017a; Lechón et al., 1997; Muir and Yarechewski, 1982). Half-lives for terbutryn degradation in activated WWTP sludge were two orders of magnitude higher than those in previous experiments with activated sewage sludge (2.1 to 7 days) (Luft et al., 2014). The initial amount and activity of degrading microorganisms in activated sewage inoculum may strongly vary among experiments, thereby affecting terbutryn degradation kinetics. In general, terbutryn degradation in WWTPs is expected to be limited as hydraulic retention times in WWTPs (< 24 h) are typically lower than half-lives (Verlicchi et al., 2012). Terbutryn and other urban biocides were frequently detected in effluents and downstream of WWTPs, underlining the limited degradation in treatment facilities (Le et al., 2017; Paijens et al., 2021).

TerOH was the prevailing TP formed during biodegradation (Figure 4. 1). TPs in soil microcosm experiments were only measured at one time point (Figure B 5). We hypothesize that terbutryn degraded to TerSO, which was further degraded to TerOH (Luft et al., 2014). The degradation of methylthio-s-triazines through sulfoxides to the respective hydroxyl derivates has been described previously (Kaufman and Kearney, 1976), and confirmed in degradation experiments with Bacillus cereus strain JUN7 (Harada et al., 2006). The prevalence of biodegradation via TerSO is also supported in our experiment by decreasing TerSO concentrations in sediment microcosms (PondSed), coinciding with increasing TerOH concentrations. A similar trend was observed in soil biodegradation experiments, alongside the formation of other TPs, including Desbutyl-2-hydroxy-terbutryn through a dealkylation of the TerOH sidechain (Bollmann et al., 2017a).

Terbutryn biodegradation did not lead to significant carbon and nitrogen stable isotope fractionation ($\Delta\delta^{13}C$ and $\Delta\delta^{15}N < 0.5‰$) (Table 4. 1). This further supports the hypothesis of an initial terbutryn degradation to TerSO, although TerOH was the main TP detected during biodegradation. Indeed, the oxidation of the methylthio group to form TerSO could only lead to

a secondary carbon or nitrogen isotope effect since carbon or nitrogen are not directly involved in bond cleavage (Figure 4. 4). Further transformation from TerSO to TerOH is not affecting terbutryn stable isotope composition.

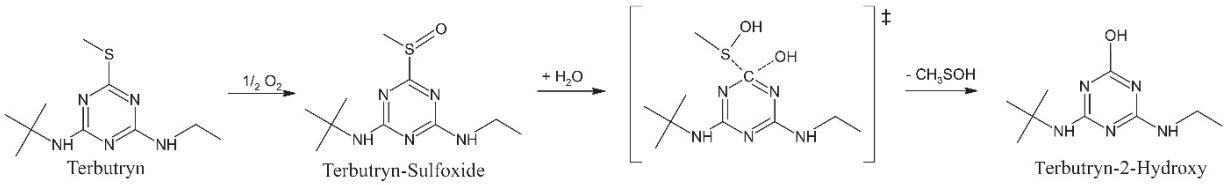

Figure 4. 4. Suggested pathway of terbutryn biodegradation. The double-cross (‡) indicates the transition state.

Altogether, both CSIA and TP data confirmed that degradation through the sulfoxide to the 2-hydroxy derivate is a major biodegradation pathway of terbutryn, in agreement with previous studies (Harada et al., 2006; Luft et al., 2014).

3.4 Contribution of terbutryn degradation pathways in the environment

The dual carbon and nitrogen isotope plot shows that stable isotope fractionation patterns may help differentiate degradation pathways of terbutryn in the environment (Figure 4. 5). This is relevant since classical concentration-based approaches cannot tease apart the contribution of sorption, dilution and degradation to the overall terbutryn dissipation. While single element CSIA provides a footprint of degradation when isotope values change due to kinetic isotope effect, distinct degradation pathways often occur simultaneously or consecutively, and thus may be mistaken. For instance, terbutryn direct photodegradation on facades may be followed by biodegradation in soil, and indirect photodegradation in a river or storm water retention pond.

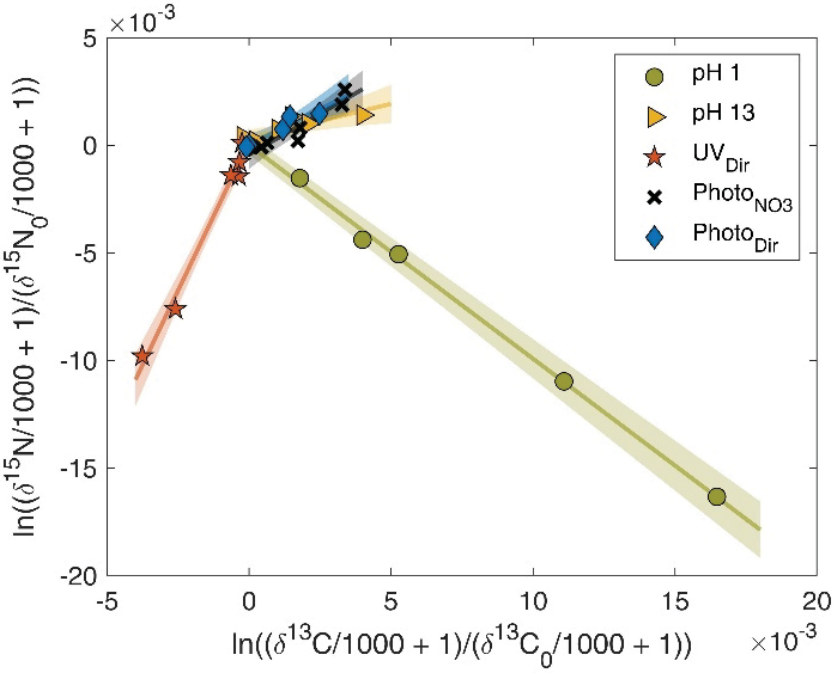

Figure 4. 5. Dual C and N isotope plot for terbutryn degradation. Stable isotope fractionation patterns are represented at pH 1 (green circles), pH 13 (yellow triangles), irradiation with UV light (orange stars), irradiation under simulated sunlight in presence of nitrate (black crosses) and irradiation under simulated sunlight in pure water (blue diamonds). Shaded areas represent the 95% confidence interval (CI) according to the York method (Ojeda et al., 2019). The origin (0,0) represents the original terbutryn isotope signature prior to degradation.

In this case, the dual element plot representing $\delta^{15}N$ against $\delta^{13}C$ values may help to identify degradation pathways of terbutryn. For instance, $\Lambda^{N/C}$ patterns for terbutryn photodegradation under UV light and with simulated sunlight indicate distinct transformation pathways (Figure 4. 5). Hence, terbutryn photodegradation experiments under UV light have limited value to evaluate environmental photo-transformation because pathways differ from natural sunlight conditions but can be used to follow UV based remediation processes of water and wastewater (Yang et al., 2014). On the other hand, isotope fractionation patterns during direct and indirect terbutryn photodegradation are similar under simulated sunlight. This emphasizes that carbon and nitrogen stable isotope fractionation may help to distinguish terbutryn photodegradation from biodegradation or hydrolysis in environmental studies.

However, the contribution of direct and indirect photodegradation may not be differentiated using carbon and nitrogen CSIA (Figure 4. 5).

In addition, the direction and extent of isotope fractionation may indicate underlying reactions, reflecting degradation mechanisms, as shown for $^{15}N/^{14}N$ in terbutryn. Although TerOH is formed during both alkaline and acidic hydrolysis, the dual isotope plot highlights that the underlying degradation mechanisms differ substantially for abiotic acidic ($\Lambda^{N/C} = -1.0 \pm 0.1$) and alkaline ($\Lambda^{N/C} = 0.3 \pm 0.1$) hydrolysis of terbutryn (Figure 4. 5). For instance, an unusual trend to more negative $\delta^{15}N$ values (inverse isotope effect) occurs during protonation of the nitrogen atoms during acidic hydrolysis as ^{15}N protonation is more stable than ^{14}N in the transition state. In contrast, the nucleophilic substitution of the methylthio group during alkaline hydrolysis of terbutryn results in normal isotope effect. This highlights the reaction specificity of multi element (ME) CSIA to identify degradation mechanisms, even when the same TP is eventually formed.

Altogether, combining TP analysis with carbon and nitrogen isotope CSIA allows to identify and compare pathways of terbutryn photodegradation under UV and simulated sunlight irradiation, abiotic acidic and alkaline hydrolysis and biodegradation (Figure 4. 6).

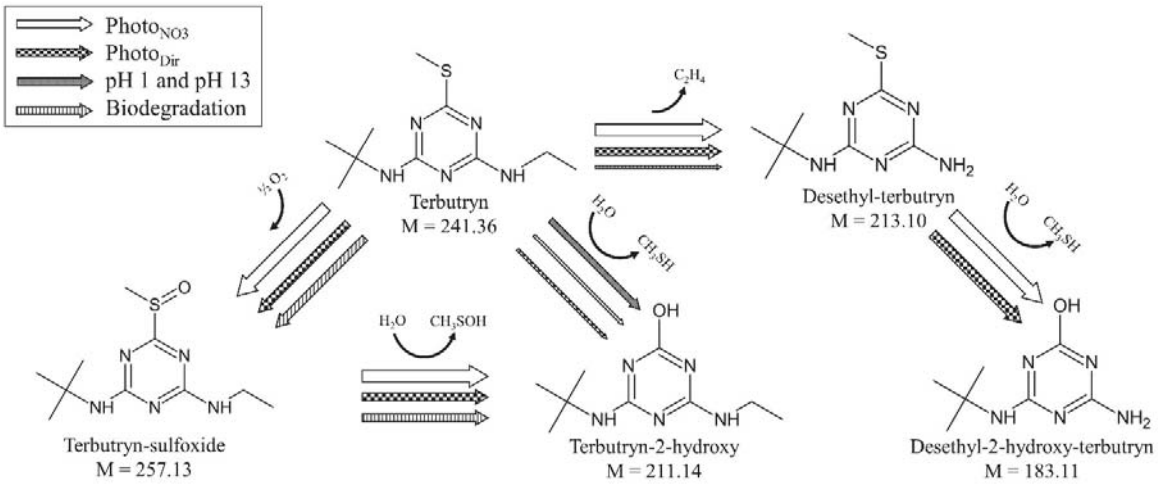

Figure 4. 6. Putative degradation pathways of terbutryn in the environment. The thickness of the arrows indicates the contribution of each process to the overall degradation. Thick arrows indicate the main contribution while thinner arrows indicate minor contribution of the respective degradation pathway to the overall terbutryn transformation.

Chapter 4

4 Conclusion

Better knowledge of degradation kinetics and pathways of terbutryn in different environmental compartments may help to evaluate the terbutryn reactive transport across the facade-soil-water continuum. Our results emphasize that photodegradation may contribute to terbutryn degradation on the facade and in waters. Since setups and irradiation intensities of simulated sunlight experiments require correction for the local irradiation intensities, degradation rates indicate further terbutryn accumulation in the environment. Terbutryn released from facades during rainfall events may accumulate in soil receiving facade wash-off due to limited biodegradation and hydrolysis. In particular, the contribution of abiotic hydrolysis to terbutryn degradation appears negligible under most environmental conditions.

Most importantly, the combination of ME-CSIA data and TP quantification allowed to identify and tease apart degradation pathways of terbutryn. While terbutryn TPs help to identify degradation pathways, distinct degradation pathways may lead to the same TPs, thereby limiting the interpretation. Our results highlight that terbutryn CSIA can help identifying underlying degradation pathways based on a dual isotope approach and differentiate pathways in situ, even without TP measurements. Isotope fractionation patterns during direct and indirect terbutryn photodegradation under simulated sunlight are similar, and terbutryn biodegradation does not lead to significant isotope fractionation. Hence, carbon and nitrogen stable isotope fractionation may help to distinguish terbutryn photodegradation from biodegradation in environmental studies.

In the future, insights into degradation pathways from ME-CSIA may be gained with sulphur stable isotope fractionation ($\delta^{34}S$) during terbutryn degradation based on GC-MS-ICPMS measurements (Kümmel et al., 2020; Torrentó et al., 2021). Sulphur stable isotope values may significantly change during biodegradation through the formation of TerSO, while the formation of a bond between the sulphur and oxygen atoms may cause an inverse isotope effect (i.e., more negative $\delta^{34}S$ values) (Figure 4. 4). It is thus expected that sulphur stable isotope fractionation may help teasing apart biodegradation and photodegradation during terbutryn leaching from the facade up to groundwater.

Altogether, we anticipate our study to be a starting point for a new strategy including ME-CSIA to examine terbutryn transformation on facades and in receiving environmental compartments to follow-up mitigation measures to limit biocide release.

Chapter 4

References

Alvarez-Zaldívar, P., Payraudeau, S., Meite, F., Masbou, J., Imfeld, G., 2018. Pesticide degradation and export losses at the catchment scale: insights from compound-specific isotope analysis (CSIA). Water Res. 139, 198–207.

Austnes, K., Aherne, J., Arle, J., Čičendajeva, M., Couture, S., Fölster, J., Garmo, Ø.A., Hruska, J., Monteith, D., Posch, M., Rogora, M., Sample, J.E., Skjelkvåle, B.L., Steingruber, S., Stoddard, J.L., Ulańczyk, R., Van Dam, H., Velasco, M.T., Vuorenmaa, J., Wright, R.F., de Wit, H., 2018. Regional assessment of the current extent of acidification of surface waters in Europe and North America, 134. Norwegian institute for water research.

Bollmann, U.E., Fernández-Calviño, D., Brandt, K.K., Storgaard, M.S., Sanderson, H., Bester, K., 2017a. Biocide runoff from building facades: degradation kinetics in soil. Environ. Sci. Technol. 51, 3694–3702.

Bollmann, U.E., Minelgaite, G., Schlüsener, M., Ternes, T., Vollertsen, J., Bester, K., 2016. Leaching of terbutryn and its photodegradation products from artificial walls under natural weather conditions. Environ. Sci. Technol. 50, 4289–4295.

Bollmann, U.E., Minelgaite, G., Schlüsener, M., Ternes, T.A., Vollertsen, J., Bester, K., 2017b. Photodegradation of octylisothiazolinone and semi-field emissions from facade coatings. Sci. Rep. 7, 41501.

Burkhardt, M., Junghans, M., Zuleeg, S., Boller, M., Schoknecht, U., Lamani, X., Bester, K., Vonbank, R., Simmler, H., 2009. Biozide in Gebäudefassaden – ökotoxikologische Effekte, Auswaschung und Belastungsabschätzung für Gewässer. Environ. Sci. Eur. 21, 36–47.

Burkhardt, M., Zuleeg, S., Vonbank, R., Bester, K., Carmeliet, J., Boller, M., Wangler, T., 2012. Leaching of biocides from façades under natural weather conditions. Environ. Sci. Technol. 46, 5497–5503.

Burrows, H.D., Canle L, M., Santaballa, J.A., Steenken, S., 2002. Reaction pathways and mechanisms of photodegradation of pesticides. J. Photochem. Photobiol. B: Biol. 67, 71–108.

Carazo-Rojas, E., Pérez-Rojas, G., Pérez-Villanueva, M., Chinchilla-Soto, C., Chin-Pampillo, J.S., Aguilar-Mora, P., Alpízar-Marín, M., Masís-Mora, M., Rodríguez-Rodríguez, C.E., Vryzas, Z., 2018. Pesticide monitoring and ecotoxicological risk assessment in surface water bodies and sediments of a tropical agro-ecosystem. Environ. Pollut. 241, 800–809.

Ccanccapa, A., Masiá, A., Navarro-Ortega, A., Picó, Y., Barceló, D., 2016. Pesticides in the Ebro river basin: occurrence and risk assessment. Environ. Pollut. 211, 414–424.

CIE, 1989. CIE 85 - Solar Spectral Irradiance (1st Edition) (E) | Engineering360, International Comission on Illumination (CIE).

Comber, S.D.W., 1999. Abiotic persistence of atrazine and simazine in water. Pesticide Science 55, 696–702.

Coplen, T.B., 2011. Guidelines and recommended terms for expression of stable-isotope-ratio and gas-ratio measurement results. Rapid Commun. Mass Spectrom. 25, 2538–2560.

Drouin, G., Droz, B., Leresche, F., Payraudeau, S., Masbou, J., Imfeld, G., 2021. Direct and indirect photodegradation of atrazine and S-metolachlor in agriculturally impacted surface water and associated C and N isotope fractionation. Environ. Sci.: Processes Impacts 23, 1791–1802.

Droz, B., Drouin, G., Maurer, L., Villette, C., Payraudeau, S., Imfeld, G., 2021. Phase transfer and biodegradation of pesticides in water–sediment systems explored by compound-specific isotope analysis and conceptual modeling. Environ. Sci. Technol. 55, 4720–4728.

Elsner, M., 2010. Stable isotope fractionation to investigate natural transformation mechanisms of organic contaminants: principles, prospects and limitations. J. Environ. Monit. 12, 2005–2031.

Elsner, M., Imfeld, G., 2016. Compound-specific isotope analysis (CSIA) of micropollutants in the environment — current developments and future challenges. Curr. Opin. Biotechnol., Analytical biotechnology 41, 60–72.

Elsner, M., Jochmann, M.A., Hofstetter, T.B., Hunkeler, D., Bernstein, A., Schmidt, T.C., Schimmelmann, A., 2012. Current challenges in compound-specific stable isotope analysis of environmental organic contaminants. Anal. Bioanal. Chem. 403, 2471–2491.

European Council Directive 91/414/EEC, 2002. Commission Regulation (EC) No 2076/2002 of 20 November 2002 extending the time period referred to in Article 8(2) of Council Directive 91/414/EEC and concerning the non-inclusion of certain active substances in Annex I to that Directive and the withdrawal of authorisations for plant protection products containing these substances (Text with EEA relevance), OJ L.

European Council Directive 2013/39/EU, 2013. Directive 2013/39/EU of the European Parliament and of the Council of 12 August 2013 amending Directives 2000/60/EC and 2008/105/EC as regards priority substances in the field of water policy Text with EEA relevance, OJ L.

Fenner, K., Canonica, S., Wackett, L.P., Elsner, M., 2013. Evaluating pesticide degradation in the environment: blind spots and emerging opportunities. Science.

Fischer, A., Manefield, M., Bombach, P., 2016. Application of stable isotope tools for evaluating natural and stimulated biodegradation of organic pollutants in field studies. Curr. Opin. Biotechnol. 41, 99–107.

Grant, W.D., Sorokin, D.Yu., 2011. Distribution and diversity of soda lake alkaliphiles, in: Horikoshi, K. (Ed.), Extremophiles Handbook. Springer Japan, Tokyo, pp. 27–54.

Harada, N., Takagi, K., Fujii, K., Iwasaki, A., 2006. Transformation of methylthio-s-triazines via sulfur oxidation by strain JUN7, a Bacillus cereus species. Soil Biol. Biochem. 38, 2952–2957.

Hartenbach, A.E., Hofstetter, T.B., Tentscher, P.R., Canonica, S., Berg, M., Schwarzenbach, R.P., 2008. Carbon, hydrogen, and nitrogen isotope fractionation during light-induced transformations of atrazine. Environ. Sci. Technol. 42, 7751–7756.

Hensen, B., Lange, J., Jackisch, N., Zieger, F., Olsson, O., Kümmerer, K., 2018. Entry of biocides and their transformation products into groundwater via urban stormwater infiltration systems. Water Res. 144, 413–423.

Hensen, B., Olsson, O., Kümmerer, K., 2019. The role of irradiation source setups and indirect phototransformation: kinetic aspects and the formation of transformation products of weakly sunlight-absorbing pesticides. Sci. Total Environ. 695, 133808.

Hoefs, J., 2015. Stable isotope geochemistry. Springer International Publishing, Cham.

Höhener, P., Imfeld, G., 2021. Quantification of Lambda (Λ) in multi-elemental compound-specific isotope analysis. Chemosphere 267.

Höhener, P., Yu, X., 2012. Stable carbon and hydrogen isotope fractionation of dissolved organic groundwater pollutants by equilibrium sorption. J. Contam. Hydrol. 129–130, 54–61.

Ivdra, N., Herrero-Martín, S., Fischer, A., 2014. Validation of user- and environmentally friendly extraction and clean-up methods for compound-specific stable carbon isotope analysis of organochlorine pesticides and their metabolites in soils. J. Chromatogr. A 1355, 36–45.

Jungnickel, C., Stock, F., Brandsch, T., Ranke, J., 2008. Risk assessment of biocides in roof paint. Part 1: experimental determination and modelling of biocide leaching from roof paint. Environ. Sci. Pollut. Res. Int. 15, 258–265.

Jurado, A., Fernandes, M., Videira, R., Peixoto, F., Vicente, J., 2011. Herbicides: the face and the reverse of the coin. An in vitro approach to the toxicity of herbicides in non-target organisms, Herbicides and Environment. IntechOpen.

Kaufman, D.D., Kearney, P.C., 1976. Microbial transformations in the soil. Herbicides: Physiology.

Keresztesi, Á., Birsan, M.-V., Nita, I.-A., Bodor, Z., Szép, R., 2019. Assessing the neutralisation, wet deposition and source contributions of the precipitation chemistry over Europe during 2000–2017. Environ. Sci. Eur. 31, 50.

Knossow, N., Siebner, H., Bernstein, A., 2020. Isotope analysis method for the herbicide bromoxynil and its application to study photo-degradation processes. J. Hazard. Mater. 388, 122036.

Kresmann, S., Arokia, A.H.R., Koch, C., Sures, B., 2018. Ecotoxicological potential of the biocides terbutryn, octhilinone and methylisothiazolinone: underestimated risk from biocidal pathways? Sci. Total Environ. 625, 900–908.

Kümmel, S., Horst, A., Gelman, F., Strauss, H., Richnow, H.H., Gehre, M., 2020. Simultaneous compound-specific analysis of δ^{33} S and δ^{34}S in organic compounds by GC-MC-ICPMS using medium- and low-mass-resolution modes. Anal. Chem. 92, 14685–14692.

Lam, M.W., Tantuco, K., Mabury, S.A., 2003. PhotoFate: a new approach in accounting for the contribution of indirect photolysis of pesticides and pharmaceuticals in purface waters. Environ. Sci. Technol. 37, 899–907.

Le, T.D.H., Scharmüller, A., Kattwinkel, M., Kühne, R., Schüürmann, G., Schäfer, R.B., 2017. Contribution of waste water treatment plants to pesticide toxicity in agriculture catchments. Ecotoxicol. Environ. Saf. 145, 135–141.

LeBaron, H.M., McFarland, J.E., Burnside, O., 2008. The triazine herbicides: 50 years revolutionizing agriculture. Elsevier.

Lechón, Y., Sánchez-Brunete, C., Tadeo, J.L., 1997. Influence of the laboratory incubation method on chlorotoluron and terbutryn degradation in soil. J. Agric. Food Chem. 45, 951–954.

Lewis, K.A., Tzilivakis, J., Warner, D.J., Green, A., 2016. An international database for pesticide risk assessments and management. Hum. Ecol. Risk Assess. 22, 1050–1064.

Lihl, C., Heckel, B., Grzybkowska, A., Dybala-Defratyka, A., Ponsin, V., Torrentó, C., Hunkeler, D., Elsner, M., 2020. Compound-specific chlorine isotope fractionation in biodegradation of atrazine. Environ. Sci.: Processes Impacts 22, 792–801.

Linke, F., Olsson, O., Preusser, F., Kümmerer, K., Schnarr, L., Bork, M., Lange, J., 2021. Sources and pathways of biocides and their transformation products in urban storm water infrastructure of a 2 ha urban district. Hydrol. Earth Syst. Sci. 25, 4495–4512.

Luft, A., Wagner, M., Ternes, T.A., 2014. Transformation of biocides irgarol and terbutryn in the biological wastewater treatment. Environ. Sci. Technol. 48, 244–254.

Mabey, W., Mill, T., 1978. Critical review of hydrolysis of organic compounds in water under environmental conditions. J. Phys. Chem. Ref. Data 7, 383–415.

Machate, O., Dellen, J., Schulze, T., Wentzky, V.C., Krauss, M., Brack, W., 2021. Evidence for antifouling biocides as one of the limiting factors for the recovery of macrophyte communities in lakes of Schleswig-Holstein. Environ. Sci. Eur. 33, 57.

Masbou, J., Drouin, G., Payraudeau, S., Imfeld, G., 2018. Carbon and nitrogen stable isotope fractionation during abiotic hydrolysis of pesticides. Chemosphere 213, 368–376.

Meyer, A.H., Penning, H., Elsner, M., 2009. C and N isotope fractionation suggests similar mechanisms of microbial atrazine transformation despite involvement of different enzymes (AtzA and TrzN). Environ. Sci. Technol. 43, 8079–8085.

Minelgaite, G., Nielsen, A.H., Pedersen, M.L., Vollertsen, J., 2017. Photodegradation of three stormwater biocides. Urban Water J. 14, 53–60.

Muir, D.C., Yarechewski, A.L., 1982. Degradation of terbutryn in sediments and water under various redox conditions. J. Environ. Sci. Health - B Pestic. Food Contam. Agric. Wastes 17, 363–380.

Chapter 4

Ojeda, A.S., Phillips, E., Mancini, S.A., Lollar, B.S., 2019. Sources of uncertainty in biotransformation mechanistic interpretations and remediation studies using CSIA. Anal. Chem. 91, 9147–9153.

Paijens, C., Bressy, A., Frère, B., Tedoldi, D., Mailler, R., Rocher, V., Neveu, P., Moilleron, R., 2021. Urban pathways of biocides towards surface waters during dry and wet weathers: assessment at the Paris conurbation scale. J. Hazard. Mater. 402, 123765.

Pfeifroth, U., Sanchez-Lorenzo, A., Manara, V., Trentmann, J., Hollmann, R., 2018. Trends and variability of surface solar radiation in Europe based on surface- and satellite-based data records. J. Geophys. Res. Atmos. 123, 1735–1754.

Poursat, B.A.J., van Spanning, R.J.M., de Voogt, P., Parsons, J.R., 2019. Implications of microbial adaptation for the assessment of environmental persistence of chemicals. Crit. Rev. Environ. Sci. Technol. 49, 2220–2255.

QSun/QLab, 2011. Q-Lab QSun Technical bulletin LU-0822: sunlight, weathering & light stability testing [WWW Document]. URL https://www.q-lab.com/documents/public/cd131122-c252-4142-86ce-5ba366a12759.pdf (accessed 2.9.22).

Quednow, K., Püttmann, W., 2007. Monitoring terbutryn pollution in small rivers of Hesse, Germany. J. Environ. Monit. 9, 1337–1343.

Russell, J.D., Cruz, M., White, J.L., Bailey, G.W., W. R. Payne, J., J. D. Pope, J., Teasley, J.I., 1968. Mode of chemical degradation of s-triazines by montmorillonite. Science.

Sakkas, V.A., Konstantinou, I.K., Albanis, T.A., 2006. Photochemical fate of organic booster biocides in the aquatic environment, in: Konstantinou, I.K. (Ed.), Antifouling Paint Biocides, The Handbook of Environmental Chemistry. Springer, Berlin, Heidelberg, pp. 171–200.

Schmidt, T.C., Zwank, L., Elsner, M., Berg, M., Meckenstock, R.U., Haderlein, S.B., 2004. Compound-specific stable isotope analysis of organic contaminants in natural environments: a critical review of the state of the art, prospects, and future challenges. Anal. Bioanal. Chem. 378, 283–300.

Schoknecht, U., Gruycheva, J., Mathies, H., Bergmann, H., Burkhardt, M., 2009. Leaching of biocides used in façade coatings under laboratory test conditions. Environ. Sci. Technol. 43, 9321–9328.

Schoknecht, U., Mathies, H., Lisec, J., 2021. Leaching and transformation of film preservatives in paints induced by combined exposure to ultraviolet radiation and water contact under controlled laboratory conditions. Water 13, 2390.

Schürner, H.K.V., Seffernick, J.L., Grzybkowska, A., Dybala-Defratyka, A., Wackett, L.P., Elsner, M., 2015. Characteristic isotope fractionation patterns in s-triazine degradation have their origin in multiple protonation options in the s-triazine hydrolase TrzN. Environ. Sci. Technol. 49, 3490–3498.

Schüth, C., Taubald, H., Bolaño, N., Maciejczyk, K., 2003. Carbon and hydrogen isotope effects during sorption of organic contaminants on carbonaceous materials. J. Contam. Hydrol. 64, 269–281.

Schwarzenbach, R.P., Gschwend, P.M., Imboden, D.M., 2005. Environmental organic chemistry. John Wiley & Sons.

Scott, K.M., Lu, X., Cavanaugh, C.M., Liu, J.S., 2004. Optimal methods for estimating kinetic isotope effects from different forms of the Rayleigh distillation equation. Geochim. Cosmochim. Acta 68, 433–442.

Spain, J.C., Pritchard, P.H., Bourquin, A.W., 1980. Effects of adaptation on biodegradation rates in sediment/water cores from estuarine and freshwater environments. Appl. Environ. Microbiol. 40, 726–734.

Styszko, K., Bollmann, U.E., Bester, K., 2015. Leaching of biocides from polymer renders under wet/dry cycles--rates and mechanisms. Chemosphere 138, 609–615.

Styszko, K., Bollmann, U.E., Wangler, T.P., Bester, K., 2014. Desorption of biocides from renders modified with acrylate and silicone. Chemosphere 95, 188–192.

Talja, K.M., Kaukonen, S., Kilpi-Koski, J., Malin, I., Kairesalo, T., Romantschuk, M., Tuominen, J., Kontro, M.H., 2008. Atrazine and terbutryn degradation in deposits from groundwater environment within the boreal region in Lahti, Finland. J. Agric. Food Chem. 56, 11962–11968.

Torabi, E., Wiegert, C., Guyot, B., Vuilleumier, S., Imfeld, G., 2020. Dissipation of S-metolachlor and butachlor in agricultural soils and responses of bacterial communities: insights from compound-specific isotope and biomolecular analyses. J. Environ. Sci. 92, 163–175.

Torrentó, C., Ponsin, V., Lihl, C., Hofstetter, T.B., Baran, N., Elsner, M., Hunkeler, D., 2021. Triple-element compound-specific stable isotope analysis (3D-CSIA): added value of Cl isotope ratios to assess herbicide degradation. Environ. Sci. Technol. 55, 13891–13901.

Urbanczyk, M.M., Bester, K., Borho, N., Schoknecht, U., Bollmann, U.E., 2019. Influence of pigments on phototransformation of biocides in paints. J. Hazard. Mater. 364, 125–133.

Verlicchi, P., Al Aukidy, M., Zambello, E., 2012. Occurrence of pharmaceutical compounds in urban wastewater: removal, mass load and environmental risk after a secondary treatment—a review. Sci. Total Environ. 429, 123–155.

Vermeesch, P., 2018. IsoplotR: a free and open toolbox for geochronology. Geosci. Front. 9, 1479–1493.

Wittmer, I.K., Scheidegger, R., Bader, H.-P., Singer, H., Stamm, C., 2011. Loss rates of urban biocides can exceed those of agricultural pesticides. Sci. Total Environ. 409, 920–932.

Wolfe, N.L., Mingelgrin, U., Miller, G.C., 1990. Abiotic transformations in water, sediments, and soil, in: Pesticides in the Soil Environment: Processes, Impacts and Modeling. John Wiley & Sons, Ltd, pp. 103–168.

Chapter 4

Wu, B., Arnold, W.A., Ma, L., 2021. Photolysis of atrazine: role of triplet dissolved organic matter and limitations of sensitizers and quenchers. Water Res. 190, 116659.

Yang, W., Zhou, H., Cicek, N., 2014. Treatment of organic micropollutants in water and wastewater by UV-based processes: a literature review. Crit. Rev. Environ. Sci. Technol. 44, 1443–1476.

Zhang, N., Schindelka, J., Herrmann, H., George, C., Rosell, M., Herrero-Martín, S., Klán, P., Richnow, H.H., 2015. Investigation of humic substance photosensitized reactions via carbon and hydrogen isotope fractionation. Environ. Sci. Technol. 49, 233–242.

Preface to Chapter 5

Within Chapter 4, we conducted laboratory experiments required to apply compound specific isotope analysis *in situ* and patterns of transformation products dependent on the transformation mechanism were identified. This fundamental information was further used in chapter 5 to identify the processes controlling degradation of the urban biocide terbutryn on facades and thus the contribution of transformation products in facade leachates. In chapter 5, we explored the potential and limitations of CSIA to follow terbutryn degradation directly on facades under both laboratory and environmental conditions. Finally, we implemented results in a leaching model to estimate the contribution of terbutryn transformation products in facade leachate over a period of eight years.

The novelty of our study lies in the combination of field experiments with laboratory immersion tests to determine the dependence of transformation product emissions from facades on hydroclimatic variables. We highlight the significant contribution of transformation products in facade leachates and that sunlight irradiation drives the formation of transformation products. In addition, implementing the leaching of transformation products of terbutryn into an emission function by integrating hydroclimatic variables enabled us to estimate the contribution of photodegradation to terbutryn leaching over years. Altogether, this study indicates that transformation products of biocides should be integrated for a more accurate and robust evaluation and prediction of the environmental impacts of biocide leaching from facade paints. On contrary, disregarding the emission of transformation products can lead to a severe underestimation of biocide leaching and associated ecotoxicological risk in receiving compartments.

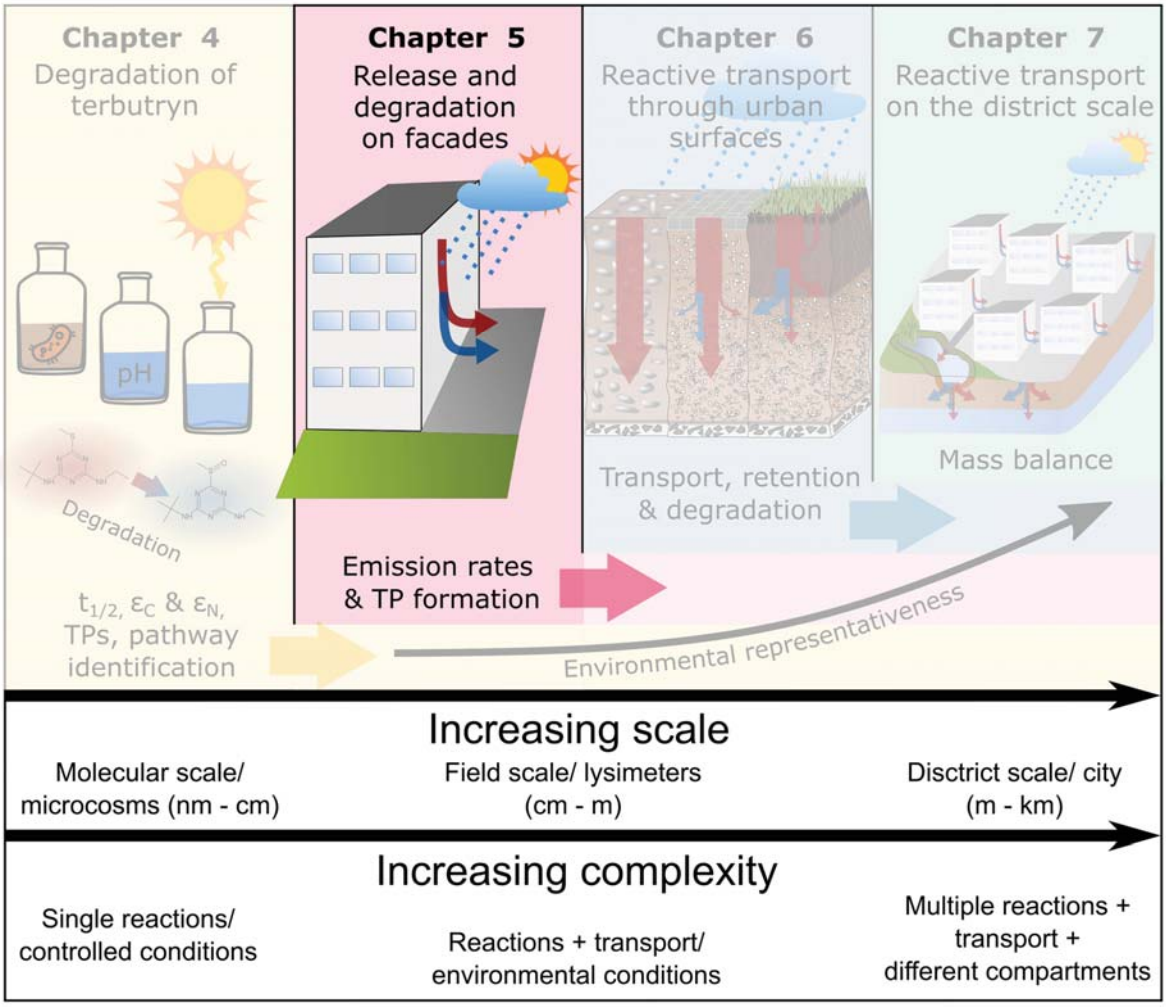
Chapter 4
Degradation of terbutryn
pH
Degradation
$t_{1/2}$, ε_C & ε_N, TPs, pathway identification
Chapter 5
Release and degradation on facades
Emission rates & TP formation
Chapter 6
Reactive transport through urban surfaces
Transport, retention & degradation
Chapter 7
Reactive transport on the district scale
Mass balance
Environmental representativeness
Increasing scale
Molecular scale/ microcosms (nm - cm)
Field scale/ lysimeters (cm - m)
Disctrict scale/ city (m - km)
Increasing complexity
Single reactions/ controlled conditions
Reactions + transport/ environmental conditions
Multiple reactions + transport + different compartments

Chapter 5
Emissions of the urban biocide terbutryn from facades: the contribution of transformation products

This chapter is an edited version of the submitted article:

Junginger, T., Payraudeau, S., & Imfeld, G: Emissions of the urban biocide terbutryn from facades: the contribution of transformation products. Environmental Science & Technology

Chapter 5

Abstract

Biocides are added to facade paints and renders to prevent algal and fungal growth. The release of biocides from facades during wind-driven rain contaminates surface waters, soil and groundwater. Although both the concentrations and ecotoxicity of biocide transformation products may be higher than biocides, their formation and release from facades is not well understood. Combining field and lab-scale experiments, we show that solar irradiation on facades controls the formation of transformation products and can be used in combination with runoff volume to estimate the long-term emissions of terbutryn transformation products from building facades. The slow ($t_{1/2}$ > 90 d) photodegradation of terbutryn in paint under environmental conditions was associated with insignificant isotope fractionation ($\Delta\delta^{13}C < 2‰$) and caused 20% higher release of terbutryn-sulfoxide than terbutryn in leachates. This indicates that the diffusion of terbutryn toward the paint surface was continuous, making it accessible for photodegradation. The contribution of terbutryn transformation products in leachate was predicted based on irradiation and facade runoff as key variables over 8 years. The emissions of transformation products (77 mg m^{-2}) in facade leachates exceeded that of terbutryn (42 mg m^{-2}) by nearly 2-fold. Altogether, this study provides a framework to estimate the emissions of transformation products over years to improve the assessment of environmental risks.

Graphical abstract:

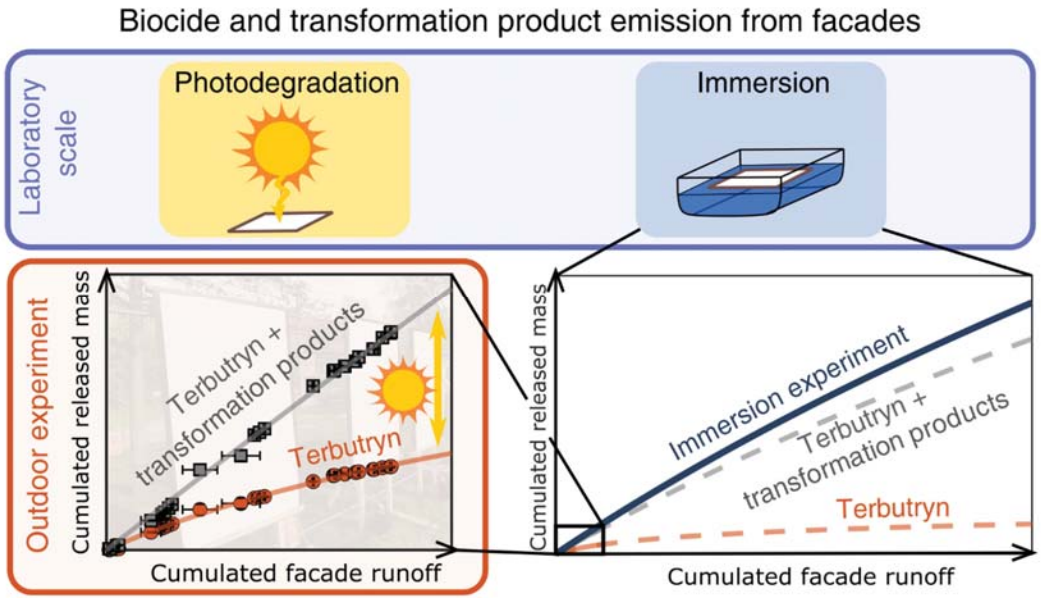

1 Introduction

Urban biocides added as film preservatives to paints inhibit algae, fungi, and microbial growth on facades and can be released into the environment during wind-driven rain (Burkhardt et al., 2012; Paijens et al., 2020). For instance, the triazine biocide terbutryn is used worldwide in construction materials (Paz-Villarraga et al., 2022), although it has been banned for agricultural use in the EU since 2003 (European Council Directive 91/414/EEC, 2002; Paijens et al., 2020). Terbutryn is toxic to algae, while emissions of several terbutryn transformation products (TPs), classified as probably toxic, may exceed terbutryn emissions in facade leachates (Bollmann et al., 2016; Hensen et al., 2020; Schoknecht et al., 2021). Biocides are generally entrapped in microcapsules, slowing down their release from facades (Andersson Trojer et al., 2015; Nordstierna et al., 2010; Vermeirssen et al., 2018). Continuous biocide emissions with facade runoff over years (Hensen et al., 2018; Linke et al., 2021) may pose ecotoxicological risks in receiving soil, stormwater, surface water, and eventual accumulation in soil and groundwater (Bollmann et al., 2017a, 2017b, 2014; Burkhardt et al., 2011; Hensen et al., 2018; Kresmann et al., 2018; Linke et al., 2021; Quednow and Püttmann, 2007; Schoknecht et al., 2016; Vega-Garcia et al., 2020; Vermeirssen et al., 2018). In addition, the photodegradation of biocides on facades may form a variety of TPs (Bollmann et al., 2017b, 2016; Urbanczyk et al., 2019), resulting in leaching of biocide-TP mixtures with largely unknown ecotoxicological risk (Hensen et al., 2020). Overall, the processes driving the leaching of biocide TPs are largely unknown, while approaches to estimate the contribution of TPs to overall biocide emissions are currently lacking.

A framework combining laboratory and field emission experiments is thus needed to evaluate the emissions of both biocides and TPs from facades over time. Biocide leaching from facades involves the dissolution of encapsulated biocides and their diffusion from deeper layers to the surface, followed by photodegradation and advective transport on the coating surface (Uhlig et al., 2019). Although laboratory immersion tests can simulate long-term biocide emissions (Schoknecht et al., 2016; Wangler et al., 2012), their design, i.e., abiotic conditions in the dark, is not appropriate for quantifying TP formation throughout the life cycle of facades. This severely limits the use of laboratory immersion tests to estimate field emissions of biocides and their TPs in long-term scenarios. For instance, terbutryn emissions have been estimated previously (Bollmann et al., 2016; Burkhardt et al., 2011; Uhlig et al., 2019; Vega-Garcia et al.,

2020), but emission models have not included TPs (Burkhardt et al., 2020; Coutu et al., 2012b, 2012a). Currently, field emission experiments under environmental conditions have often included TP measurements but have generally run for short periods (e.g., weeks or months) and have thus failed to cover the lifecycle of facades over years. As a result, both the short-term emission data from field studies and immersion tests are limited for the long-term estimation of biocide and TP leaching. In this context, compound-specific isotope analysis (CSIA) may help to evaluate terbutryn degradation relying on changes in its stable isotope composition (natural isotope abundance) (Alvarez-Zaldívar et al., 2018; Elsner et al., 2012; Elsner and Imfeld, 2016; Fischer et al., 2016; Schmidt et al., 2004). Indeed, nondegradative processes, such as advection, dilution and sorption, generally cause insignificant isotope fractionation (Höhener and Yu, 2012; Schüth et al., 2003). In a previous study, we showed that CSIA has the potential to differentiate pathways of terbutryn degradation (Junginger et al., 2022). Although reaction-specific isotope fractionation values (ε) may be used to relate the extent of degradation to changes in isotope ratios (e.g., $\delta^{13}C$) (Elsner, 2010; Hoefs, 2015; Meyer et al., 2009), the potential of CSIA still needs to be examined to follow up on terbutryn degradation in situ, assuming photodegradation on facades as the main transformation process.

Overall, more lines of evidence of biocide degradation on facades are needed to estimate the long-term emissions of biocides and TPs. Hence, we examined the degradation and leaching of terbutryn and its TPs by combining laboratory photodegradation experiments with simulated sunlight, field experiments with artificial facades and lab-scale immersion tests from facades coated with a paint formulation containing encapsulated terbutryn. Our results highlighted the significant contribution of TPs in facade leachate and that sunlight irradiation drives TP formation. We also underlined the limits of CSIA to follow terbutryn degradation and factors driving the leaching of terbutryn TPs. We improved predictive models to estimate the total emissions of biocides (terbutryn + TPs) by implementing the leaching of terbutryn TPs into an emission function by integrating hydroclimatic variables. Our approach allowed us to estimate the contribution of photodegradation and terbutryn leaching over years, accounting for its TPs. Recognition of biocide TPs leaching from facades and their key drivers leads to realistic estimates of urban biocide release into the environment that may guide future biocide mitigation policies and better risk assessments, including TPs.

2 Material and Methods

All chemicals used and suppliers are described in the Supporting Information (Appendix C).

2.1 Terbutryn photodegradation in paint under simulated sunlight

Terbutryn photodegradation experiments were conducted on (i) encapsulated terbutryn, as currently used commercially in paints; (ii) nonencapsulated terbutryn, as used in recent decades (Burkhardt and Roger, 2011) in facade paint and render; and (iii) two paints (Paint A and B, Table C 1) containing encapsulated terbutryn. Paint A and B varied in hydrophobicity, binders, and fillers (detailed recipe confidential); are commercially available and widely used in Europe; and were obtained without film preservatives from Sto SE & Co. KGaA. The encapsulated terbutryn formulation (Troysan CR280, 28% terbutryn in encapsulated formulation) was added to paints at 4 g kg^{-1}, which is the upper range of industrial concentrations and enables terbutryn CSIA. For each sample, 250 mg of paint (i.e., 278 g paint m^{-2} with 1.1 g terbutryn m^{-2}) was added to Whatman glass microfiber filters (Grade GF/F 47 mm diameter). The pure encapsulated and a nonencapsulated industrial terbutryn formulation (Troysan V662, 48% terbutryn) were diluted to 4 g L^{-1} terbutryn and spread on filters as 5×50 µL strips with an automated syringe. All experiments, blanks (paint or empty filters without terbutryn) and dark controls (wrapped in aluminum foil) were dried for one week in the dark. Photodegradation experiments were carried out in a QSun-XE1 test chamber using a xenon arc lamp with a Daylight-Q filter with nominal cut-on at 295 nm. The irradiation intensity was 0.68 W m^{-2} nm^{-1} at 340 nm (i.e., maximum midday solar irradiation), corresponding to an intensity of ≈1200 W m^{-2} across wavelengths (QSun/QLab, 2011). Filters were collected over time using a sacrificial approach (

Table **C 2**).

2.2 Field facade panel leaching experiment

Four 1 m² panels (0.65 × 1.54 m) were constructed according to the guidelines for external thermal insulation composite systems (ETICS). Briefly, a polystyrene plate was glued to a wooden panel protected with a plastic frame and covered with fiberglass reinforcement mesh within two layers of a biocide-free rendered material (StoSilico blue® K/MP). Three panels were painted with 350 g of Paint A at 2.5 g kg^{-1} of encapsulated terbutryn (0.875 g terbutryn m^{-2}). A fourth panel with Paint A without terbutryn addition was used as the process blank. To collect facade runoff from each facade, a gutter coated with Teflon was connected to brown glass bottles and covered under a tarp (Figure C 1). All panels were exposed to the outdoors from April 13th, 2021 (Day 0) to October 24th (Day 194) in Schiltigheim, district of Adelshoffen, Bas-Rhin, France (48°36'31.7"N; 7°44'54.8"E), facing west (prevailing wind direction). Wind direction, humidity, temperature, and rainfall data (Table C 3) were recorded on site using a Davis Vantage Vue weather station equipped with a WeatherLink data logger (10 min intervals). The daily irradiation was obtained from the MeteoFrance station of Entzheim (10 km to the southwest). In parallel, four panels (20 × 20 cm) were prepared similarly for immersion tests and sampled on Days 0, 33, 160 and 194. Collected samples for immersion were wrapped in three layers of aluminum foil and frozen at −22°C.

2.3 Lab-scale immersion tests for long-term release assessment

Panel pieces (10 × 10 cm) were cut from the 1 m² panels at the end of the experiment and from each small facade panel that was collected throughout the study to not only account for new facades but also consider physical aging through outdoor exposition. The immersion test followed European standards (*DIN EN 16105*; Vermeirssen et al., 2018) (detailed in Appendix C). Individual facade pieces were placed in glass cases and plunged face down in deionized water (100 mL), which limited the effects of biotic degradation. The experiment was carried out for 18 days in the dark to prevent photodegradation and consisted of nine immersion days, including

two immersion cycles per immersion day. Nine immersion days correspond to a runoff of 10 to 25 years on a facade facing west (Wicke et al., 2022a).

2.4 Analysis of terbutryn and TPs

Samples from lab-scale photodegradation experiments were extracted using a modified solid–liquid extraction protocol (Droz et al., 2021; Ivdra et al., 2014). Filters were cut into 0.5 cm² pieces and transferred into 40 mL amber glass vials to extract terbutryn using 3×3 mL Pentane:DCM (3:1, V:V) (detailed in Appendix C).

Facade leachate samples were filtered using 0.45 µm PTFE membranes (25 mm ∅, VWR chemicals). Depending on the concentration, aqueous samples were either directly injected or extracted using solid phase extraction (SPE) with Chromabond HR-X cartridges (detailed in Appendix C). Terbutryn, terbutryn-sulfoxide (TerSO), terbutryn-2-hydroxy (TerOH), terbutryn-desethyl (TerDesE) and terbutryn-desethyl-2-hydroxy (TerDesEOH) were quantified using HPLC–MS/MS as described previously (Table C 4) (Junginger et al., 2022).

Carbon stable isotope analysis was conducted using a GC-IRMS system consisting of a gas chromatograph (GC, TRACE Ultra ThermoFisher Scientific) coupled to an isotope ratio mass spectrometer (IRMS, DeltaV plus, ThermoFisher Scientific) via a GC combustion interface (IsoLink/Conflow IV, ThermoFisher Scientific) as described previously (Junginger et al., 2022). No effect on the isotope fractionation was observed for the extraction of the encapsulated terbutryn formulation (Troysan CR280) and in Paints A and B (Figure C 2).

2.5 Data analysis

Predictive emission functions. The cumulative biocide emissions (E_{log}) in the field experiments were described with a logarithmic emission function (Tietje et al., 2018):

$$E_{\log}(q) = a_{char} \cdot \ln\left(1 + 1.72\frac{q}{q_{char}}\right) \quad \textbf{(5.1)}$$

with q, the cumulative facade runoff and fitted parameters are the characteristic discharge q_{char} and the characteristic substance fraction a_{char}, representing the proportion of the applied biocide quantity emitted up to the characteristic discharge q_{char}. Parameters were fitted using the fit function in MATLAB R2020b.

Correlation between hydroclimatic variables and TPs. Pearson correlation coefficients were calculated to examine the relationships between weather data, leachates of terbutryn, TerSO and TP/terbutryn ratios. The statistical significance level was set at $p < 0.05$. Weather data included rain (mL): cumulative rain since the last sampling event; temperature: mean temperature (°C) since the last sampling event; runoff (mL): collected facade runoff since the last sampling event; humidity (%): mean humidity since the last sampling event; dry period (d): time since the last sampling; and irradiation (W m^{-2}): cumulative irradiation since the last sampling.

Modeling terbutryn and TP leaching. Terbutryn emissions since the year of building construction were simulated using the leaching model COMLEAM (Burkhardt et al., 2020). The model calculates runoff from building components by calculating wind-driven rain from weather data. The leaching of biocides was simulated by emission functions. Precipitation, wind direction and wind speed were used at a 1 h resolution from 01.01.2014 (building construction of the Adelshoffen district in Schiltigheim) to 31.12.2021 (end of experiment). Emissions were calculated for the west facade of a standardized building (OECD house; Table C 5, Figure C 3, Figure C 4). Two scenarios were considered to evaluate the emission functions of terbutryn and TPs as a function of climate variables: Scenario A relied on emission functions from the field experiment (April 2021 to October 2021) for i) terbutryn only and ii) the sum of terbutryn + TPs as a function of facade runoff. Scenario A was created from data covering only a part of seasonal variability (i.e., March to October) with associated high irradiation to directly estimate emissions of terbutryn and its TPs as a function of runoff.

Scenario B was implemented to consider the full seasonal irradiation variability with low values in winter. It relied on the emission function of terbutryn + TPs from the field experiment. The contribution of TPs to the total biocide emissions was estimated from the ratio of leached TPs to terbutryn (TPs/Ter) as a function of solar irradiation and runoff volume (Eq. 2). Rain events were defined as days with a rain volume > 0.2 mm. Precipitation lasting for several days

was accounted for as one single event. Irradiation was calculated as the sum of solar irradiation from the end of the previous rain event to the beginning of the rain event causing biocide emissions. Scenario B used the main drivers of TP formation and release (e.g., irradiation and facade runoff) as predictors for the time series. The total biocide emissions ($E_{Ter+TPs}$) between both scenarios were thus identical. However, the contribution of TPs differed among scenarios. The nonlinear relationship was fitted in MATLAB R2021b with the nlinfit function using the field data for the ratio of TPs/Ter, irradiation since the last rain event (Irr), and facade runoff volume (q):

$$\frac{TPs}{Ter}(t) = a * \ln\big(\mathrm{Irr(t)}\big) + \mathrm{b} * e^{c*q(t)} \qquad \textbf{(5.2)}$$

3 Results

3.1 Effect of encapsulation and paint type on terbutryn photodegradation

Terbutryn photodegradation prevailed on facades (Bollmann et al., 2016; Hensen et al., 2019; Junginger et al., 2022), although it was limited by both paint and encapsulation. Less than 30% of the terbutryn in the pure encapsulated formulation was degraded after 1000 h ($t_{1/2}$=110 ± 49 d) of maximum daily solar irradiation onto a horizontal surface (Figure 5. 1). This indicates that encapsulation limited terbutryn photodegradation. Hence, encapsulation not only slowed the leaching of biocides from facades but also decreased terbutryn photodegradation in paint by shielding terbutryn molecules from sunlight. Accordingly, the carbon isotope composition of terbutryn did not change significantly ($\Delta\delta^{13}C$ = 0.8 ± 0.5‰). The extent of terbutryn degradation was insufficient to cause significant isotope fractionation, in agreement with the low carbon isotope fractionation values (ε_C = -0.7 ± 0.3 and -0.6 ± 0.2 for direct and indirect photodegradation, respectively) (Junginger et al., 2022). In contrast, fast degradation ($t_{1/2}$ = 27.5 ± 1.6 h) of terbutryn in the nonencapsulated industrial formulation and significant stable isotope fractionation ($\Delta\delta^{13}C$ = 2.9 ± 0.4‰) indicated terbutryn photodegradation in the paint. The extent of degradation (99.7%) based on mass balance fitted with the degradation estimates (99.3%) based on change in isotope signatures and isotope fractionation values of terbutryn photodegradation in water (ε_C = -0.7‰) (Elsner and Imfeld, 2016; Junginger et al., 2022). This

underscores the potential of CSIA to evaluate the extent of terbutryn photodegradation on facades.

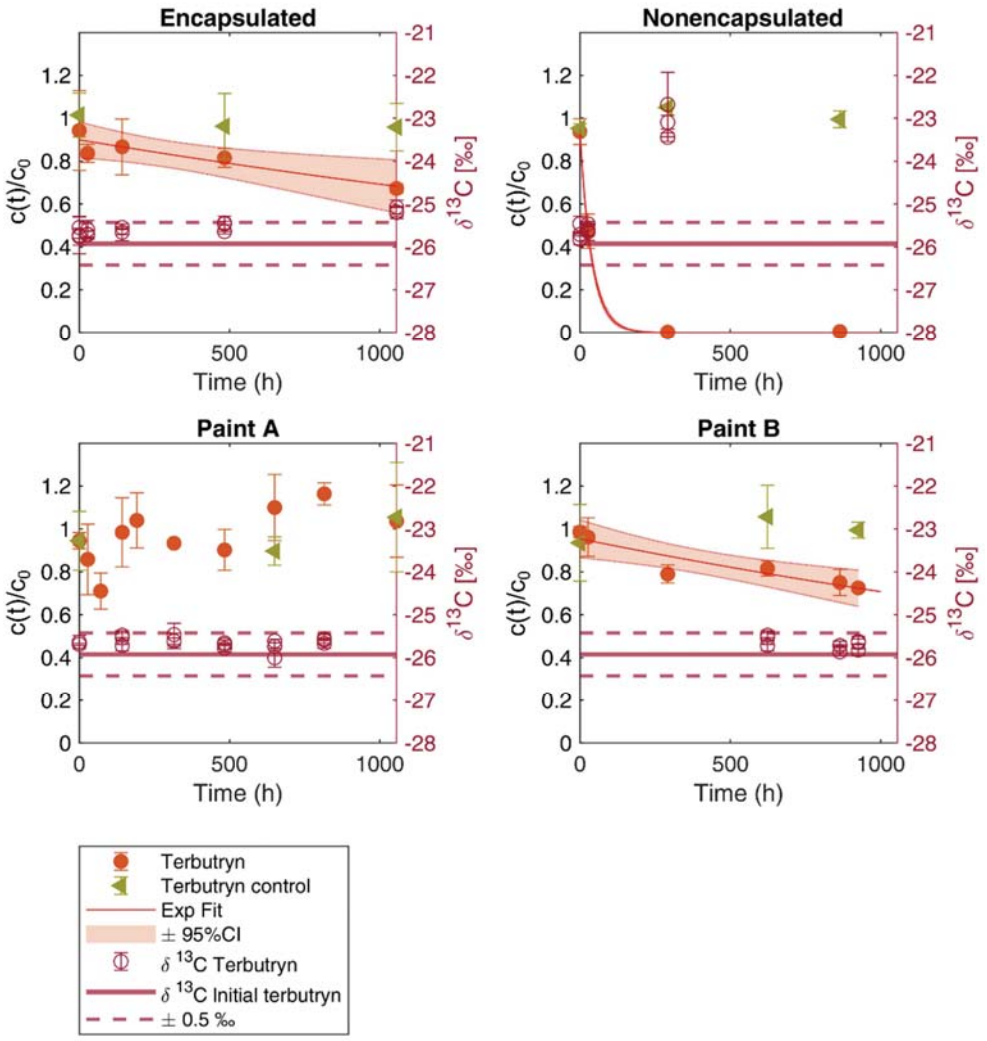

Figure 5. 1. Terbutryn fraction ($C(t)/C_0$) in paints and terbutryn formulations during photodegradation under simulated sunlight and for dark controls as a function of time and associated change of carbon stable isotope ratios of terbutryn ($\Delta\delta^{13}C$).

Terbutryn degradation in Paint A (< 15%) was lower than that in Paint B (25%; $t_{1/2}$ = 97 ± 36 d) (Figure 5. 1). However, the measurement uncertainty among replicates and the dark control limited the detection of minor (< 15%) changes in terbutryn concentrations. Light penetration was likely restricted to a few µm of the outer paint layer, thereby controlling terbutryn photodegradation (Uhlig et al., 2019). The degradation kinetics of terbutryn on vertical

facades under environmental conditions are expected to be even lower due to diurnal cycles, seasonal changes in irradiation intensities and facade orientation (i.e., vertical vs. horizontal) compared to constant irradiation with simulated sunlight at > 1000 W m^{-2}. In addition, different paint compositions, including pigments and polymers, may favor distinct photodegradation mechanisms (Urbanczyk et al., 2019). This can affect the degradation kinetics and the leaching rates of both biocides and TPs. For instance, Paint B may either favor deeper light penetration or higher photolytic activity through indirect photodegradation mechanisms. Even though TPs were not extractable from our samples, previous studies of photodegradation in pain indicated the formation of TerSO with further degradation to TerOH or direct degradation to TerOH with further degradation to TerDesEOH (Urbanczyk et al., 2019).

Carbon isotope fractionation in Paint A and B was insignificant ($\Delta\delta^{13}C$ < 1‰), confirming the moderate extent (< 77%) of terbutryn degradation (Junginger et al., 2022). In laboratory studies with fresh paints, the potential of CSIA to follow terbutryn degradation may be limited since a large fraction of terbutryn is not affected by irradiation. However, in older facades subject to physical deterioration of the paint and continuous terbutryn diffusion to surface layers of the paint, CSIA of terbutryn may help evaluate the degradation extent and prevailing pathway on the facades. Most importantly, the variability of stable isotope ratios of terbutryn in commercial formulations at the source must be narrow to avoid confounding effects of source isotopic heterogeneity. The terbutryn isotope compositions of different commercially available paints (n=11) were similar (mean $\delta^{13}C = -26.8 \pm 0.8$‰; Figure C 2). This suggests a homogeneous signature of terbutryn sources, enabling the application of terbutryn CSIA in urban environments.

3.2 Release of terbutryn and transformation products from field experimental facades

Even though laboratory experiments indicated limited photodegradation of terbutryn in paint, a significant contribution of TPs in field facade leachate was observed. Terbutryn emissions from facades were detected in all leachates, with concentrations ranging from 12 to 387 µg L^{-1}. Less than 0.02 mmol m^{-2} terbutryn (i.e., 0.4% of the initial mass of terbutryn) leached from the facades within 194 days (Figure 5. 2). When including the terbutryn TPs, the total leached mass

accounted for 1.1% of the initially applied terbutryn for the same duration. Mass balance, considering the remaining terbutryn in facades, was not applicable due to the high analytical uncertainties of extractions from paint. This supports the idea of slow but continuous terbutryn photodegradation, leading to leaching-driven release of terbutryn and TPs over years. In contrast, hydrolysis and biodegradation of terbutryn on facades are expected to be negligible due to its high hydrolytic stability and slow biodegradation (Bollmann et al., 2017a; Junginger et al., 2022).

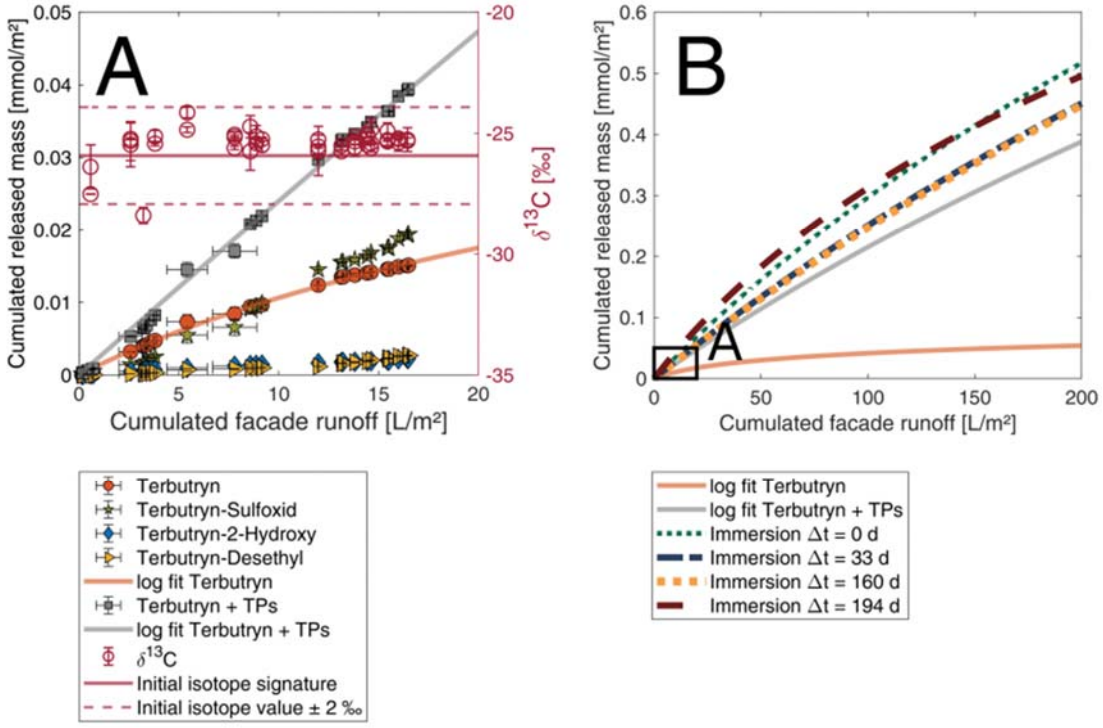

Figure 5. 2. Cumulative mass export of terbutryn and its transformation products (TerSO, TerOH, and TerDesE) in leachate from the field experimental facades. A: Emission functions for terbutryn (orange) and the sum of terbutryn and TPs (gray) and carbon isotope fractionation of terbutryn in facade leachates. Error bars for runoff and mass exports indicate standard deviation (1σ, n=3 facades) and reproducibility for carbon stable isotope analysis ($\delta^{13}C$ of terbutryn, n=3 measurements). B: Logarithmic fit of emission functions for the field experiments for terbutryn (orange), the sum of terbutryn and TPs from field experiments (gray) and emissions for the immersion tests of field facades (dotted and dashed lines, by using freshly painted (Δt = 0d) and older facades collected at 33, 160 and 194 d). The black rectangle in the bottom left corner represents the timeframe of the field facade experiment.

TerSO, TerOH and TerDesE were detected in facade leachates, whereas TerDesEOH could not be detected. The cumulative mass of leached TerSO exceeded that of terbutryn by 20% after a cumulative facade runoff of 16.5 L m^{-2} (Figure 5. 2A). This indicates that terbutryn was initially degraded to TerSO. Both direct and indirect photodegradation of terbutryn may form TerSO as an initial TP, which can sequentially degrade to TerOH and TerDesEOH, although degradation of TerDesE may also result in TerDesEOH (Bollmann et al., 2016; Junginger et al., 2022). Other TPs, such as TerOH, may also be formed on facades but might be mobilized to a lesser extent, depending on the physicochemical properties of the facade and the TPs. For instance, a previous study with render material showed that more than 20% of the initial mass of terbutryn was retained in the facades as TerDesE, TerOH and TerDesEOH after 18 months of exposure (Bollmann et al., 2016).

Based on the measured concentrations and emission functions fitted for terbutryn (E_{Ter}) and the total emissions ($E_{Ter+TPs}$) of terbutryn and its major TPs, the emissions of $E_{Ter+TPs}$ were twice as high as those of E_{Ter} across the season (Figure 5. 2A). Nevertheless, the contribution of TPs might be underestimated due to leaching of additional TPs that were not accounted for in this study but that were previously identified in facade leachates from render (Bollmann et al., 2016). Our results highlight the significant contribution of TPs to biocide leaching, in agreement with previous observations, and underscores the need for implementing TPs in biocide mass balances and ecotoxicological risk assessment (Bollmann et al., 2016). In contrast to field emission experiments, standard laboratory immersion experiments typically exclude photodegradation, and emission functions are typically restricted to parent biocides, as immersed facades are not exposed to environmental conditions (Jungnickel et al., 2008; Schoknecht et al., 2013; Styszko et al., 2015). This severely limits the transposability of results from the laboratory immersion tests to environmental conditions and highlights that irradiation and immersion tests should be combined with field experiments to quantify the parent biocide and TP releases.

A logarithmic emission function (Eq. 1) fitted the observations of the cumulative emissions of terbutryn and TPs from facades. Hence, emissions decreased over time (Figure 5. 2A) (Tietje et al., 2018), which may be due to diffusion-controlled release of terbutryn. The limited terbutryn photodegradation in paint in the laboratory photodegradation experiments and the high contribution of TerSO in facade leachates under environmental conditions indicate that photodegradation mainly occurred following terbutryn leaching from the capsules and diffusive

transport toward the paint surface. It cannot be excluded that continuous terbutryn diffusion toward the paint surface occurred by residual water in the facade during dry periods, making more terbutryn accessible for solar irradiation. Hence, we hypothesize that cumulative irradiation since the last rain event is a key predictor of the TP contribution in leachates from facades.

Although terbutryn TPs contributed to > 50% of the released mass in the leachate, the $\delta^{13}C$ of terbutryn did not change throughout the experiment (Figure 5. 2A). Indeed, the constant diffusion of nondegraded terbutryn bearing its initial isotope signature from the deeper layer to the facade surface likely diluted the signal of the remaining pool of terbutryn subject to photodegradation. Moreover, only a small carbon isotope fractionation is expected since terbutryn degradation should reach 90% before significant isotope fractionation (> 2‰) is expected (Hunkeler et al., 2008). Significant carbon isotope fractionation reflecting terbutryn degradation may be, however, theoretically observed in leachates from small rain events hydrating the outer paint layers after a long period of terbutryn photodegradation. The insignificant change in the stable isotope ratios of terbutryn also supports the idea that nondegraded terbutryn continuously diffuses toward the surface.

The limited isotope fractionation of terbutryn in leachates of freshly painted facades reduces the applicability of C-CSIA to follow-up degradation. In this case, a homogeneous isotopic source of terbutryn (i.e., mean $\delta^{13}C$ of terbutryn in paints = –26.8 ± 0.8‰) may enable subsequent terbutryn degradation with CSIA in environmental compartments receiving facade leachates. Nevertheless, CSIA based on carbon alone may not be sufficient to tease apart pathways of terbutryn transformation, and multielement CSIA (ME-CSIA) is needed. Larger nitrogen isotope fractionation during indirect photodegradation of terbutryn (ε= –1.0 ± 0.4‰) indicates the potential of nitrogen CSIA to follow terbutryn degradation (Junginger et al., 2022). In addition, sulfur stable isotope measurements ($\delta^{34}S$) using GC-MC-ICPMS hold great potential to evaluate terbutryn degradation and TerSO and TerOH formation (Kümmel et al., 2020), as the bond formation between the sulfur and oxygen atoms may cause an inverse isotope effect (i.e., more negative $\delta^{34}S$ values).

3.3 Factors controlling transformation and leaching of terbutryn and transformation products from facades

The cumulative irradiation intensity mainly controlled the contribution of TPs to the overall terbutryn leaching from facades. Both Terbutryn and TerSO emissions in leachates correlated with the runoff amount ($p < 0.005$, Figure 5. 3, Figure C 5 and Figure C 6). It is expected that longer and more intense rain events generate a continuous diffusion gradient of biocide and TP concentrations from the inner to the outer paint layers, resulting in rainfall-proportional emissions. Notably, TerSO leaching correlated with air temperature ($\rho = 0.42$, $p < 0.05$), which was not the case for terbutryn, suggesting either temperature dependent TerSO diffusion and leaching (Wangler et al., 2012) or convolution with irradiation and dry periods.

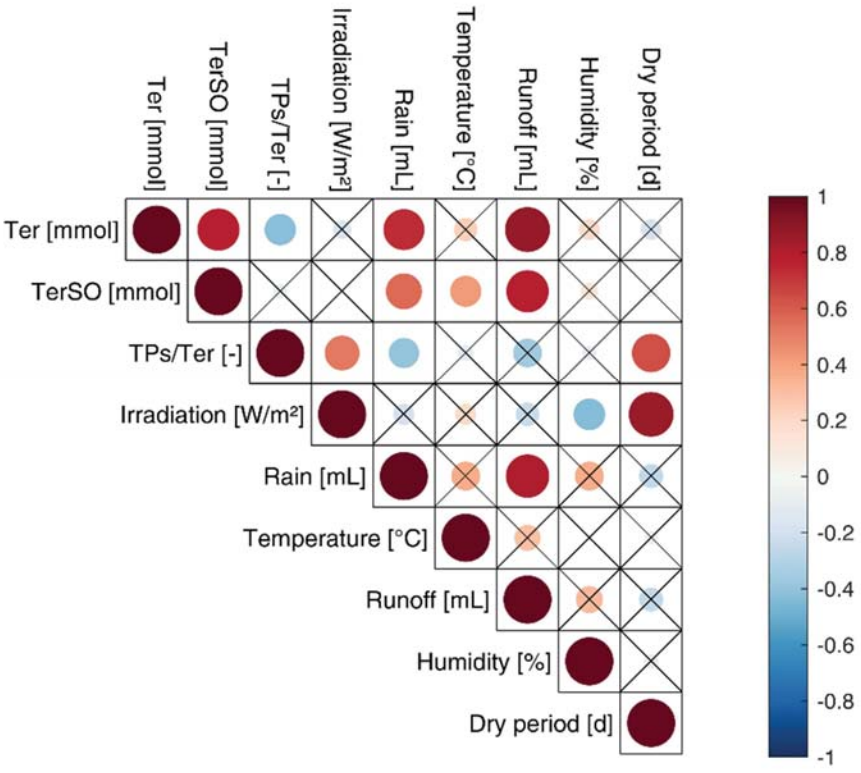

Figure 5. 3. Pearson correlation coefficients between event-based emissions of terbutryn (Ter) and terbutryn-sulfoxide (TerSO), the ratio of all TPs to terbutryn (TPs/Ter) and hydroclimatic variables. Crossed out cells indicate nonsignificant correlations ($p > 0.05$). The size of the circle indicates the value of the correlation coefficient.

The ratio of leached TPs to terbutryn (TPs/terbutryn) correlated positively ($p < 0.05$) with the cumulative irradiation intensities and time since the last rainfall and negatively ($p < 0.1$) with rainfall and runoff volumes. This confirms that solar radiation is the main degradation mechanism and can be used as a predictor of TPs in leachate and indicates that TPs are formed predominantly during spells with high irradiation and low precipitation before leaching from the outer paint layer during strong and long-lasting rain events. In contrast, terbutryn was continuously mobilized from the facade. Hence, the contribution of TPs is limited to the photodegraded terbutryn fraction on the paint surface, whereas the large pool of terbutryn may diffuse continuously during long rain events. Heavy and long rain events may also increase the residual water content in the facade after rain events, thereby increasing the terbutryn diffusion and the renewal of the photodegradable pool of terbutryn in the paint surface. Regarding the contribution of TPs to the overall biocide leaching, TerOH and TerDesE may diffuse at a slower rate than TerSO and thus contribute less to the total leaching (Bollmann et al., 2016).

3.4 Predicting leaching of terbutryn and transformation products from facades

The difference between the logarithmic fit of emission functions (Eq. 1) for terbutryn and for terbutryn + TPs (Figure 5. 2, Table C 6) highlights that considering terbutryn without TPs leads to underestimation of biocide leaching by > 50% after 194 d. Extrapolating the emission functions increased the estimated contribution of TPs over time (Figure 5. 2B), since experiments were conducted in spring and summer under high irradiation. When considering TPs, the biocide emissions from the field facades and from the immersion tests are in good agreement for the same simulated water runoff volume (Figure 5. 2B). Hence, the amount of water in contact with the facade controls the total biocide emissions. This supports the notion that diffusion-controlled leaching of biocides is well accounted for in laboratory immersion tests. Older facades retrieved from the field experiment after Δt = 33 d, 160 d and 194 d had similar leaching patterns to those of freshly painted facades (Figure 5. 2B, Table C 6). This suggests that physical deterioration of the facades during a few months had a minor impact on emissions. However, physical deterioration over the lifespan of facade paints, generally exceeding one decade, may gradually enhance biocide leaching.

A comparison of emissions from immersion tests with extrapolated emissions from field experiments indicated that emissions of Ter + TPs were underestimated by < 25%. This may be due to the minor contribution of unquantified TPs in leachates (i.e., terbutryn-desbutyl-2-hydroxy, terbutryn-desbutyl, terbutryn-desthiomethyl-desbutyl, and terbutryn-desthiomethyl-desethyl) that were not targeted in this study but identified in previous studies (Bollmann et al., 2016; Hensen et al., 2020, 2019). The facade runoff (q) needed releasing 1 or 10% of biocides from the facade can be estimated from Eq. 1 considering terbutryn only or both terbutryn and TPs and indicates the large underestimation of biocide release (e.g., estimated runoff of 1.25 × 10^9 L for 10% terbutryn release vs. 184 L when considering TPs) (Table C 6).

Although the release of terbutryn decreases over time, different TPs may accumulate in the facade material and increasingly contribute to biocide leachate over time until emissions of the parent biocide are exceeded (Schoknecht et al., 2021). Even though no degradation during the immersion tests was expected, TerOH was continuously released with a minor contribution of TerSO, especially from panels previously exposed to field conditions (e.g., for 160 d and 194 d, Figure C 7). Additionally, TerDesEOH and TerDesE were released in the immersion experiment (Figure C 7), confirming that some TPs formed over time of environmental exposition but were likely retained in the facade material and were mobilized only after contact with a large amount of water. This is also in line with previous field experiments with render as an external coating showing that TerOH and other TPs, such as TerDesE, can be retained in the facade, leading to small but continuous release (Bollmann et al., 2016). Additionally, elution experiments with 1 L water per 0.25 m² on 13-year-old facades indicated a high release of TerOH (one order of magnitude higher than that of terbutryn), while grab samples after natural rain events showed higher concentrations of terbutryn (Linke et al., 2021), indicating primary retention of TerOH and release after long time periods and with heavy rain events.

The implementation of biocide emission curves into the COMLEAM model allowed us to estimate the contribution of TPs to the overall biocide emissions over time (i.e., eight years for building construction in 2014). For both scenarios and same initial conditions (e.g., $c_{0\ Terbutryn}$=1416 mg m^{-2}), the emission functions for the total emissions ($E_{Ter+TPs}$) underscored the release of 8.4% (118 mg m^{-2}) of the initial applied mass but varying contributions of terbutryn and TPs (Figure 5. 4). Scenario A, based on the field emissions (Table C 6), overestimated the contribution of TPs since the experimental data were obtained predominantly in summer,

corresponding to higher irradiation and rates of TP formation. The contribution of terbutryn was negligible at the end of the simulation period (Figure 5. 4), although the simulated TP emissions prevailed. For Scenario A, cumulative emissions of 19 mg m^{-2} terbutryn and 99 mg m^{-2} TPs emphasized the bias when extrapolating over eight years using data based on summer irradiation only. Even though field observations in over 10-year-old districts showed a high contribution of terbutryn TPs (Hensen et al., 2018; Linke et al., 2021), the simulated ratio of 1:5 terbutryn:TPs (after eight years in each event, even 1:10) exceeded those severely.

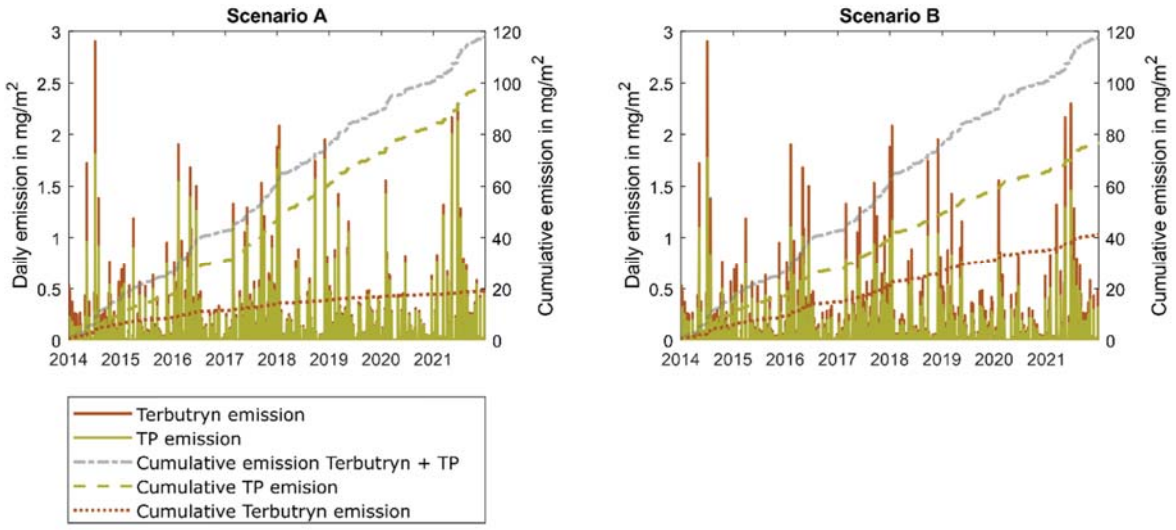

Figure 5. 4. Total emissions of terbutryn and TPs and cumulative emissions per m^2 of facade from 2014 to 2021 for Scenario A, based on field experimental emission curves and Scenario B, based on runoff and irradiation correlation for the contribution of TPs in leachate.

In contrast, the contribution of TPs over time in Scenario B was lower (2:3 ratio of terbutryn:TPs), accounting for both summer and winter irradiation conditions. The fitted values for Eq. 2 were a = 0.164, b = 1.422 and c = -0.858, yielding a good fit (R^2 = 0.97) between the measured and modeled ratios of TPs/Ter (Figure C 8). In Scenario B, the simulated emissions of TPs (77 mg m^{-2}) were twice as high as those of terbutryn (42 mg m^{-2}) over eight years (Figure 5. 4). Although other parameters may influence the contribution of TPs in leachate, irradiation and facade runoff are sufficient predictors of biocide and TP leaching from facades. The ratio of simulated terbutryn:TPs is in agreement with grab samples close to facades in old districts (> 10 years) (Hensen et al., 2018; Linke et al., 2021). Hence, Scenario B could be used to implement

release models of mixtures of TPs and parent biocides to predict the emissions and potential ecotoxicological risks in compartments receiving leachates from facades.

4 Environmental implications for the estimation of biocide leaching from facades

Previous studies underscored the significant leaching of terbutryn TPs from facades (Bollmann et al., 2016; Hensen et al., 2018; Linke et al., 2021; Wicke et al., 2022b). However, key drivers controlling TP leaching have not yet been identified, and the contribution of TPs to the overall biocide leaching has not been quantified. Thus, by combining field experiments with laboratory immersion tests, the dependence of TP emissions on hydroclimatic variables could be determined. Our results confirmed that photodegradation is mainly responsible for degradation. This supports the idea that degradation occurs predominantly after terbutryn diffusion from microcapsules toward the outer paint layer (Figure 5. 5), as also evidenced by CSIA. Even though no significant isotope fractionation (> 2‰) was observed in the field experiments, this study opens the door for broader application of CSIA to various urban organic contaminants. In particular, the absence of isotope fractionation for terbutryn in facade leachates may help to evaluate terbutryn degradation in compartments receiving biocide leachates and runoffs, assuming a homogeneous source isotope signature in terbutryn in the facades.

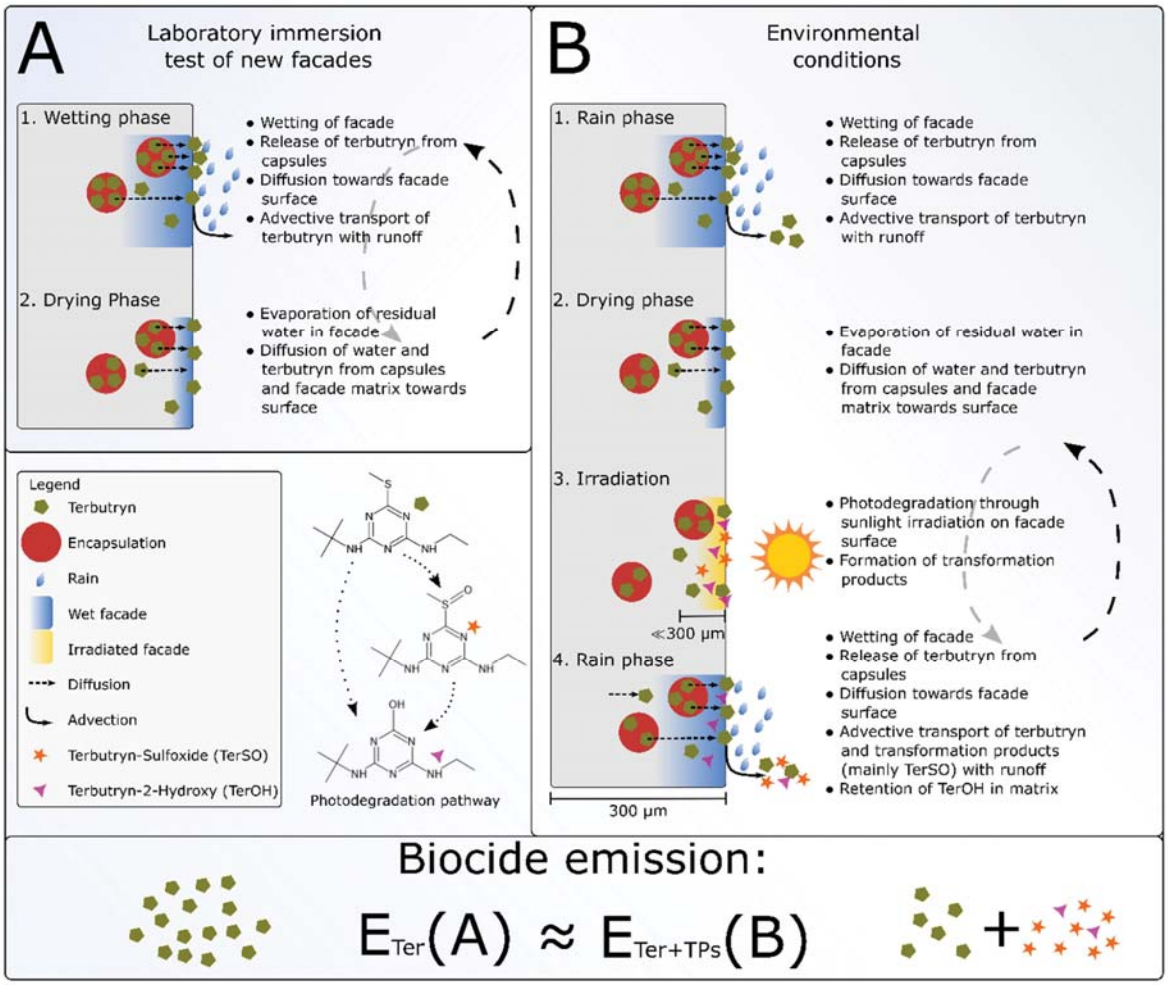

Figure 5. 5. Proposed leaching sequence of terbutryn (Ter) and TPs (TerSO and TerOH) from facades in four steps (adapted from Uhlig et al., 2019). Under environmental conditions, Steps 2 and 3 might occur simultaneously.

Overall, our results confirm the sequence of terbutryn leaching and degradation suggested previously (Uhlig et al., 2019). During immersion tests, no degradation is expected, and release is dependent on diffusion. For terbutryn under field conditions, diffusion of terbutryn is also the main release process. However, it is accompanied by degradative processes during the drying phase of the facades (Figure 5. 5). Because the release rates of terbutryn and TPs are mainly dependent on terbutryn diffusion, emissions ($E_{Ter}(A)$) in immersion tests are similar to those of terbutryn and TPs ($E_{Ter+TPs}(B)$) in the field emission experiments. Thus, immersion tests can be used to evaluate long-term biocide emissions, but accounting for TP formation is required to deliver realistic environmental emission scenarios (Figure 5. 5). Most importantly, solar

irradiation and facade runoff are the main predictors to estimate the contribution of TPs to the overall biocide leaching and to estimate the release of TPs over long time periods. Our results showed that > 60% of terbutryn may be released from the facades as TPs over long time periods (e.g., 8 years). Disregarding the emissions of biocide TPs can lead to an essential underestimation of both biocide leaching and associated toxicological risks in receiving compartments. Therefore, we anticipate our results to be a starting point to integrate TPs for a more accurate and robust evaluation and prediction of the environmental impacts of biocide leaching from facade paints.

Chapter 5

References

Alvarez-Zaldívar, P., Payraudeau, S., Meite, F., Masbou, J., Imfeld, G., 2018. Pesticide degradation and export losses at the catchment scale: insights from compound-specific isotope analysis (CSIA). Water Res. 139, 198–207.

Andersson Trojer, M., Nordstierna, L., Bergek, J., Blanck, H., Holmberg, K., Nydén, M., 2015. Use of microcapsules as controlled release devices for coatings. Adv. Colloid Interface Sci., Reinhard Miller, Honorary Issue 222, 18–43.

Bollmann, U.E., Fernández-Calviño, D., Brandt, K.K., Storgaard, M.S., Sanderson, H., Bester, K., 2017a. Biocide runoff from building facades: degradation kinetics in soil. Environ. Sci. Technol. 51, 3694–3702.

Bollmann, U.E., Minelgaite, G., Schlüsener, M., Ternes, T., Vollertsen, J., Bester, K., 2016. Leaching of terbutryn and its photodegradation products from artificial walls under natural weather conditions. Environ. Sci. Technol. 50, 4289–4295.

Bollmann, U.E., Minelgaite, G., Schlüsener, M., Ternes, T.A., Vollertsen, J., Bester, K., 2017b. Photodegradation of octylisothiazolinone and semi-field emissions from facade coatings. Sci. Rep. 7, 41501.

Bollmann, U.E., Vollertsen, J., Carmeliet, J., Bester, K., 2014. Dynamics of biocide emissions from buildings in a suburban stormwater catchment – concentrations, mass loads and emission processes. Water Res. 56, 66–76.

Burkhardt, M., Engelke, D., Gehrig, S., Hochstrasser, F., Rohr, M., Tietje, O., 2020. COMLEAM - Manual Version 3.0. HSR University of Applied Sciences Rapperswil, Switzerland.

Burkhardt, M., Roger, V., 2011. Auswaschung von verkapselten Bioziden aus Fassaden.

Burkhardt, M., Zuleeg, S., Vonbank, R., Bester, K., Carmeliet, J., Boller, M., Wangler, T., 2012. Leaching of biocides from facades under natural weather conditions. Environ. Sci. Technol. 46, 5497–5503.

Burkhardt, M., Zuleeg, S., Vonbank, R., Schmid, P., Hean, S., Lamani, X., Bester, K., Boller, M., 2011. Leaching of additives from construction materials to urban storm water runoff. Water Sci. Technol. 63, 1974–1982.

Coutu, S., Del Giudice, D., Rossi, L., Barry, D.A., 2012a. Modeling of facade leaching in urban catchments. Water Resour. Res. 48.

Coutu, S., Rota, C., Rossi, L., Barry, D.A., 2012b. Modelling city-scale facade leaching of biocide by rainfall. Water Res. 46, 3525–3534.

DIN EN 16105:2011-12 Beschichtungsstoffe - Laborverfahren zur Bestimmung der Freisetzung von Substanzen aus Beschichtungen in intermittierendem Kontakt mit Wasser; Deutsche Fassung EN_16105:2011, n.d. Beuth Verlag GmbH.

Droz, B., Drouin, G., Maurer, L., Villette, C., Payraudeau, S., Imfeld, G., 2021. Phase transfer and biodegradation of pesticides in water–sediment systems explored by compound-specific isotope analysis and conceptual modeling. Environ. Sci. Technol. 55, 4720–4728.

Elsner, M., 2010. Stable isotope fractionation to investigate natural transformation mechanisms of organic contaminants: principles, prospects and limitations. J. Environ. Monit. 12, 2005–2031.

Elsner, M., Imfeld, G., 2016. Compound-specific isotope analysis (CSIA) of micropollutants in the environment — current developments and future challenges. Curr. Opin. Biotechnol., Analytical biotechnology 41, 60–72.

Elsner, M., Jochmann, M.A., Hofstetter, T.B., Hunkeler, D., Bernstein, A., Schmidt, T.C., Schimmelmann, A., 2012. Current challenges in compound-specific stable isotope analysis of environmental organic contaminants. Anal. Bioanal. Chem. 403, 2471–2491.

European Council Directive 91/414/EEC, 2002. Commission Regulation (EC) No 2076/2002 of 20 November 2002 extending the time period referred to in Article 8(2) of Council Directive 91/414/EEC and concerning the non-inclusion of certain active substances in Annex I to that Directive and the withdrawal of authorisations for plant protection products containing these substances (Text with EEA relevance), OJ L.

Fischer, A., Manefield, M., Bombach, P., 2016. Application of stable isotope tools for evaluating natural and stimulated biodegradation of organic pollutants in field studies. Curr. Opin. Biotechnol. 41, 99–107.

Hensen, B., Lange, J., Jackisch, N., Zieger, F., Olsson, O., Kümmerer, K., 2018. Entry of biocides and their transformation products into groundwater via urban stormwater infiltration systems. Water Res. 144, 413–423.

Hensen, B., Olsson, O., Kümmerer, K., 2020. A strategy for an initial assessment of the ecotoxicological effects of transformation products of pesticides in aquatic systems following a tiered approach. Environ. Int. 137, 105533.

Hensen, B., Olsson, O., Kümmerer, K., 2019. The role of irradiation source setups and indirect phototransformation: kinetic aspects and the formation of transformation products of weakly sunlight-absorbing pesticides. Sci. Total Environ. 695, 133808.

Hoefs, J., 2015. Stable isotope geochemistry. Springer International Publishing, Cham.

Höhener, P., Yu, X., 2012. Stable carbon and hydrogen isotope fractionation of dissolved organic groundwater pollutants by equilibrium sorption. J. Contam. Hydrol. 129–130, 54–61.

Hunkeler, D., Meckenstock, R.U., Lollar, B.S., Schmidt, T.C., Wilson, J.T., 2008. A Guide for Assessing Biodegradation and Source Identification of Organic Ground Water Contaminants using Compound Specific Isotope Analysis (CSIA). (No. PB2009105967). US EPA, Ada.

Ivdra, N., Herrero-Martín, S., Fischer, A., 2014. Validation of user- and environmentally friendly extraction and clean-up methods for compound-specific stable carbon isotope analysis of organochlorine pesticides and their metabolites in soils. J. Chromatogr. A 1355, 36–45.

Chapter 5

Junginger, T., Payraudeau, S., Imfeld, G., 2022. Transformation and stable isotope fractionation of the urban biocide terbutryn during biodegradation, photodegradation and abiotic hydrolysis. Chemosphere 305, 135329.

Jungnickel, C., Stock, F., Brandsch, T., Ranke, J., 2008. Risk assessment of biocides in roof paint. Part 1: experimental determination and modelling of biocide leaching from roof paint. Environ. Sci. Pollut. Res. Int. 15, 258–265.

Kresmann, S., Arokia, A.H.R., Koch, C., Sures, B., 2018. Ecotoxicological potential of the biocides terbutryn, octhilinone and methylisothiazolinone: underestimated risk from biocidal pathways? Sci. Total Environ. 625, 900–908.

Kümmel, S., Horst, A., Gelman, F., Strauss, H., Richnow, H.H., Gehre, M., 2020. Simultaneous compound-specific analysis of δ^{33} S and δ^{34}S in organic compounds by GC-MC-ICPMS using medium- and low-mass-resolution modes. Anal. Chem. 92, 14685–14692.

Linke, F., Olsson, O., Preusser, F., Kümmerer, K., Schnarr, L., Bork, M., Lange, J., 2021. Sources and pathways of biocides and their transformation products in urban storm water infrastructure of a 2 ha urban district. Hydrol. Earth Syst. Sci. 25, 4495–4512.

Meyer, A.H., Penning, H., Elsner, M., 2009. C and N isotope fractionation suggests similar mechanisms of microbial atrazine transformation despite involvement of different enzymes (AtzA and TrzN). Environ. Sci. Technol. 43, 8079–8085.

Nordstierna, L., Abdalla, A.A., Masuda, M., Skarnemark, G., Nydén, M., 2010. Molecular release from painted surfaces: Free and encapsulated biocides. Prog. Org. Coat. 69, 45–48.

Paijens, C., Bressy, A., Frère, B., Moilleron, R., 2020. Biocide emissions from building materials during wet weather: identification of substances, mechanism of release and transfer to the aquatic environment. Environ. Sci. Pollut. Res. 27, 3768–3791.

Paz-Villarraga, C.A., Castro, Í.B., Fillmann, G., 2022. Biocides in antifouling paint formulations currently registered for use. Environ. Sci. Pollut. Res. 29, 30090–30101.

QSun/QLab, 2011. Q-Lab QSun Technical bulletin LU-0822: sunlight, weathering & light stability testing [WWW Document]. URL https://www.q-lab.com/documents/public/cd131122-c252-4142-86ce-5ba366a12759.pdf (accessed 2.9.22).

Quednow, K., Püttmann, W., 2007. Monitoring terbutryn pollution in small rivers of Hesse, Germany. J. Environ. Monit. 9, 1337–1343.

Schmidt, T.C., Zwank, L., Elsner, M., Berg, M., Meckenstock, R.U., Haderlein, S.B., 2004. Compound-specific stable isotope analysis of organic contaminants in natural environments: a critical review of the state of the art, prospects, and future challenges. Anal. Bioanal. Chem. 378, 283–300.

Schoknecht, U., Mathies, H., Lisec, J., 2021. Leaching and transformation of film preservatives in paints induced by combined exposure to ultraviolet radiation and water contact under controlled laboratory conditions. Water 13, 2390.

Schoknecht, U., Mathies, H., Wegner, R., 2016. Biocide leaching during field experiments on treated articles. Environ. Sci. Eur. 28, 6.

Schoknecht, U., Sommerfeld, T., Borho, N., Bagda, E., 2013. Interlaboratory comparison for a laboratory leaching test procedure with façade coatings. Prog. Org. Coat. 76, 351–359.

Schüth, C., Taubald, H., Bolaño, N., Maciejczyk, K., 2003. Carbon and hydrogen isotope effects during sorption of organic contaminants on carbonaceous materials. J. Contam. Hydrol. 64, 269–281.

Styszko, K., Bollmann, U.E., Bester, K., 2015. Leaching of biocides from polymer renders under wet/dry cycles--rates and mechanisms. Chemosphere 138, 609–615.

Tietje, O., Burkhardt, M., Rohr, M., Borho, N., Schoknecht, U., 2018. Emissions- und Übertragungsfunktionen für die Modellierung der Auslaugung von Bauprodukten. Umweltbundesamt, 28/2018 58.

Uhlig, S., Colson, B., Schoknecht, U., 2019. A mathematical approach for the analysis of data obtained from the monitoring of biocides leached from treated materials exposed to outdoor conditions. Chemosphere 228, 271–277.

Urbanczyk, M.M., Bester, K., Borho, N., Schoknecht, U., Bollmann, U.E., 2019. Influence of pigments on phototransformation of biocides in paints. J. Hazard. Mater. 364, 125–133.

Vega-Garcia, P., Schwerd, R., Scherer, C., Schwitalla, C., Johann, S., Rommel, S.H., Helmreich, B., 2020. Influence of façade orientation on the leaching of biocides from building façades covered with mortars and plasters. Sci. Total Environ. 734, 139465.

Vermeirssen, E.L.M., Campiche, S., Dietschweiler, C., Werner, I., Burkhardt, M., 2018. Ecotoxicological assessment of immersion samples from facade render containing free or encapsulated biocides. Environ. Toxicol. Chem. 37, 2246–2256.

Wangler, T.P., Zuleeg, S., Vonbank, R., Bester, K., Boller, M., Carmeliet, J., Burkhardt, M., 2012. Laboratory scale studies of biocide leaching from façade coatings. Build. Environ. 54, 168–173.

Wicke, D., Tatis-Muvdi, R., Rouault, P., Zerball-van Baar, P., Dünnbier, U., Rohr, M., Burkhardt, M., 2022a. Bauen und Sanieren als Schadstoffquelle in der urbanen Umwelt. Umweltbundesamt 108.

Wicke, D., Tatis-Muvdi, R., Rouault, P., Zerball-van Baar, P., Dünnbier, U., Rohr, M., Burkhardt, M., 2022b. Emissions from building materials—a threat to the environment? Water 14, 303.

Preface to chapter 6

Urban biocides have been previously detected in groundwater, however their reactive transport in urban districts through typical urban surfaces is unknown. Therefore, we aimed to identify prevailing entry paths of urban biocides towards groundwater through typical urban surfaces and to identify the contribution of transport, sorption and degradation. Three lysimeters were set up, representing typical urban surfaces that are often in direct contact to facades. Lysimeters were spiked with a non-reactive tracer (NaCl) as well as with the urban biocides terbutryn, diuron and octylisothiazolinone. Additionally, the herbicide acetochlor was used as a reactive tracer. To interpret the results, findings from chapter 4 and 5 were used. Finally, we set up a model to evaluate urban biocide entry paths into the subsurface over a period of eight years, using simulated facade leachate as input.

This study provides first experimental data of biocide leaching through typical urban surface-soil interfaces. We highlight the potential of vegetated surfaces to retain biocides during leaching of water towards groundwater. In contrary, pavement and gravel result in higher mass fractions of biocides in leachate. CSIA was applicable for peak concentrations, allowing to estimate the extent of degradation for the reactive tracer acetochlor. Coupling models for long-term biocide emissions with our calibrated reactive transport model allows us to estimate mass-fluxes towards groundwater over eight years. Altogether, this study identifies gravel and pavement as main sources of biocide leaching towards groundwater and indicates that large fractions of biocides might enter groundwater before entering stormwater infiltration systems.

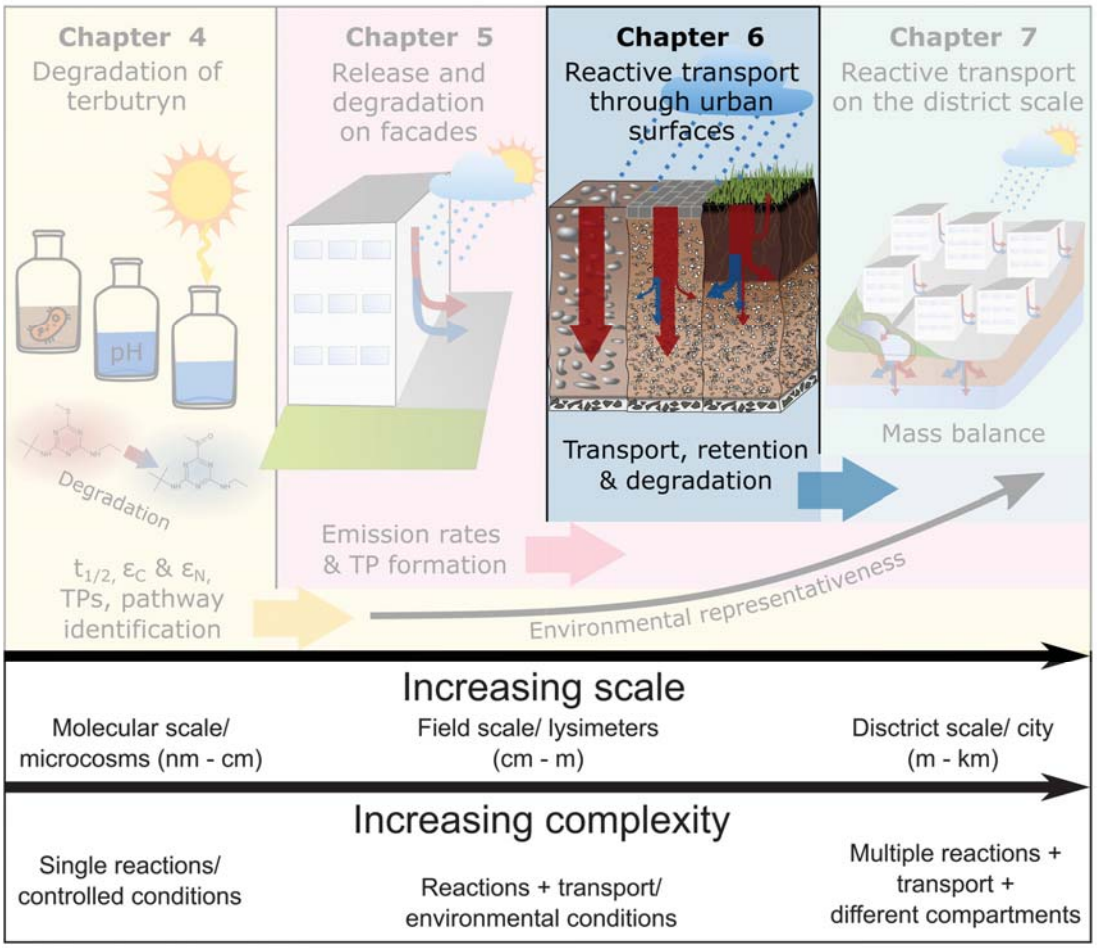
Chapter 4
Degradation of terbutryn
pH
Degradation
$t_{1/2}$, ε_C & ε_N, TPs, pathway identification
Chapter 5
Release and degradation on facades
Emission rates & TP formation
Chapter 6
Reactive transport through urban surfaces
Transport, retention & degradation
Chapter 7
Reactive transport on the district scale
Mass balance
Environmental representativeness
Increasing scale
Molecular scale/ microcosms (nm - cm)
Field scale/ lysimeters (cm - m)
Disctrict scale/ city (m - km)
Increasing complexity
Single reactions/ controlled conditions
Reactions + transport/ environmental conditions
Multiple reactions + transport + different compartments

Chapter 6
Transport, retention and degradation of the urban biocides terbutryn, diuron and octylisothiazolinone in typical urban surface-soil interfaces

This chapter is an edited version of the article under preparation:

Junginger, T., Payraudeau, S., Linke, F., Lange, J., & Imfeld, G.: Transport, retention and degradation of the urban biocides terbutryn, diuron and octylisothiazolinone in typical urban surface-soil interfaces. Environmental Science & Technology

Chapter 6

Abstract

Urban biocides, such as terbutryn, diuron and octylisothiazolinone, are released from facade paint and render, and enter groundwater through permeable surfaces. Although urban biocides have been detected in groundwater, their pathways and reactive transport through surface-soil interfaces is not well understood. Using field lysimeter experiments and reactive transport modeling, we show that pavement and drainage gravel have only limited biocide retention potential, while mass fluxes through vegetated soil systems were limited. After 207 d, up to 9% of the initially applied mass of terbutryn was extractable in all lysimeters of which a significant fraction (7 to 18%) was still accessible for leaching. Compound-specific isotope analysis highlighted a higher contribution of degradation in the pavement than in the gravel lysimeter. Over a period of eight years, 36% and 22% of terbutryn reaches deep (> 30 cm) soil layers through gravel and pavement, respectively, as terbutryn or transformation products. In contrast, only 0.2% of terbutryn may leach through vegetated soils. Altogether, we anticipate this study to be a starting point for integrating biocide leaching when planning sustainable stormwater management strategies.

1 Introduction

Urban biocides used in building materials to prevent growth of algae, mosses, fungi and bacteria (Paijens et al., 2020) are released over years from facades during rainfall events, posing a risk for soil, surface water and groundwater contamination (Bollmann et al., 2017b, 2016; Burkhardt et al., 2011, p. 20127; Hensen et al., 2018; Linke et al., 2021; Paijens et al., 2021; Quednow and Püttmann, 2007; Schoknecht et al., 2016; Vega-Garcia et al., 2020; Wittmer et al., 2010). In contrast to conventional drainage systems removing stormwater quickly from the city, sustainable stormwater management favours local infiltration and stormwater retention at the district scale through artificial facilities (often vegetated) and permeable paving (Ahammed, 2017; Barbosa et al., 2012; Goulden et al., 2018; Hering and Ingold, 2012; Mitchell, 2006; Wang et al., 2018). Urban biocides and transformation products (TP) were previously detected in groundwater (Hensen et al., 2018). However, their main entry paths, distribution dynamics and transformation in urban surface-soil interfaces, e.g., paved or vegetated surfaces with underlying soils, are not well understood. For instance, in different districts > 88% of facade emissions of the urban biocide diuron and terbutryn did not reach stormwater systems (Linke et al., 2022; Wicke et al., 2022), and may thus contribute to groundwater contamination by infiltration through permeable urban surfaces. However, urban biocides may also infiltrate into groundwater through stormwater infiltration (e.g., ponds or ditches) (Pinasseau et al., 2020; Bork et al., 2021). Although organic rich material and retention systems can effectively retain contaminants (Bester et al., 2011), biocide infiltration through gravel and paved surfaces with joints has not been examined yet. Overall, reference experiments and predictive models on the reactive transport of biocide in urban surface-soil interface remain scarce, thus limiting the assessment of ecotoxicological risks (Reiß et al., 2021).

Current modelling of urban biocide infiltration toward groundwater relies mainly on physio-chemical parameters of soil and biocides (Vega-Garcia et al., 2022), while validation with experimental data is mostly missing. Although the reactive transport of pesticides and their TP from agricultural plots toward groundwater is well described (Arias-Estévez et al., 2008; Hildebrandt et al., 2008; Melsbach et al., 2020; Torrentó et al., 2018), soil properties and runoff infiltration may differ from urban soil. In addition, agricultural pesticides are typically applied seasonally, whereas urban biocides are systematically released from facades during rain events.

As a result, current models can estimate biocide emissions from facade and release into surface waters (Burkhardt et al., 2020; Coutu et al., 2012a, 2012b) but infiltration into subsurface and groundwater is not accounted for. To assess the risk of biocide leaching through urban surfaces, reactive transport models considering TP (Gassmann, 2021) and validated with field data are needed to estimate the contribution of processes driving biocide dissipation.

In this context, compound-specific isotope analysis (CSIA) may help to identify (bio-) chemical degradation reactions by relating changes in contaminant stable isotope ratios (e.g., $^{13}C/^{12}C$) with isotope fractionation values (ε_C) to estimate the contribution of degradation to the overall biocide dissipation (Elsner, 2010; Elsner and Imfeld, 2016). In a previous study, we reported reference fractionation values (ε_C) for the urban biocide terbutryn (Junginger et al., 2022), and showed the potential of CSIA to estimate terbutryn degradation in facade leachate. Therefore, CSIA might be used as concentration independent tool to estimate the extent of degradation and consequently assess degradation rates. Similarly, lysimeter studies using pesticide CSIA allowed to follow pesticide degradation (Melsbach et al., 2020). However, reference lysimeter experiments for urban biocides in typical urban surface-soil interfaces are currently missing.

Here, we use complementary approaches of concentration and transformation product measurements, isotope fractionation and a modelling approach to describe reactive transport processes (e.g., sorption, advection and degradation) and estimate degradation rates of biocides during leaching towards groundwater. Therefore, we aim to identify hot-spots of biocide infiltration through typical urban surface-soil interfaces.

We evaluate the transport, retention and degradation of urban biocides in typical urban surface-soil interfaces (i.e., gravel, paved, vegetated) receiving leachate from facades and their reactive transport towards groundwater. Three biocides, i.e., terbutryn, diuron and octylisothiazolinone (OIT), are selected as model biocides based on their ubiquitous detection and distinct physico-chemical properties (Burkhardt et al., 2012, 2011, 2007; Hensen et al., 2018; Linke et al., 2021; Paijens et al., 2021; Wittmer et al., 2011). The herbicide acetochlor is used as a reactive tracer, assuming significant stable isotope fractionation during degradation in surface-soil interfaces (Droz et al., 2021; Elsayed et al., 2014; Torrentó et al., 2021). We inject one pulse of the three biocides and the tracers (NaCl, acetochlor) in mixture in each urban surface-soil

interface to evaluate the transport parameters, the degradation rates, the formation of terbutryn TP, and changes in $\delta^{13}C$ isotope signatures of acetochlor and terbutryn. A 1-D reactive transport model (Hydrus-1D) (Šimůnek et al., 2013) is calibrated and used to estimate degradation rates for the campaign with the experimental data. Further, Hydrus-1D is coupled to COMLEAM (Burkhardt et al., 2020), a model to estimate biocide release from facades, to assess biocide reactive transport through urban surfaces over eight years to evaluate long term risk of biocide leaching towards groundwater. This enables to estimate mass fluxes through typical urban surfaces towards groundwater and to identify the contribution of TP in leachate over time to support the design of measures and sustainable stormwater management by identifying entry paths and ecotoxicological risks.

2 Material and Methods

All chemicals and suppliers are described in the Supporting Information (Appendix D)

2.1 Experimental setup and sampling

Three major urban surface-soil interfaces serving as entry point of urban biocides toward groundwater that may differ in solute transport properties were selected: (i) drainage gravel as buildings are typically surrounded by drainage gravel ("splash strips") to enhance water infiltration, reduce moisture and reduce splashing toward facades. Drainage gravel does not generate surface runoff due to fast infiltration with limited evaporation (Timm et al., 2018), (ii) permeable pavements, that may significantly contribute of water infiltration through joints and cracks with limited runoff and evaporation (Timm et al., 2018, Schaffitel et al., 2020) and (iii) vegetated soil since facades may be connected to gardens and urban stormwater can be retained in vegetated ditches or swale systems to limit discharge into sewer systems while promoting groundwater recharge (Bork et al., 2021; Hensen et al., 2018; Linke et al., 2021; Vijayaraghavan et al., 2021).

Three 0.23 m^3 outdoor lysimeters (0.7 m × 1.1 m × 0.3 m), i.e. gravel, pavement and vegetated soil, were set in Schiltigheim, district of Adelshoffen, France (48°36'31.7"N; 7°44'54.8"E) (Figure D 1). Lysimeters had a slope of 2° at the bottom to collect leachates in sampling bottles. The lysimeter composition is detailed in the appendix (Figure D 2, Table D 2).

Briefly, the gravel lysimeter consisted of coarse gravel (28 cm) followed by a geotextile layer and 2 cm of filter gravel (Figure D 2). Pavement lysimeter was covered with pavement stones (20 × 9.5 × 8 cm) with joints filled with sand, a sand layer (20 cm), a layer of geotextile and 2 cm filter gravel. The vegetated lysimeter consisted of 10 cm soil planted with grass on 17 cm of sand, geotextile and 2 cm of filter gravel. Sensors (SMT 100 connected to Truebner TrueLog100) of soil water content and temperature were installed in the lysimeters at 15 and 20 cm depth (Figure D 2). Lysimeters were set-up and monitored in the field site 2 months before the experiment (15.02.2021) for acclimatization. Weather data, i.e., temperature, wind speed and direction, pressure, humidity, and rain volume (10 min intervals) were recorded on site (Davis Vantage Vue weather station and WeatherLink data logger) (Table D 3, Figure D 3).

The lysimeters were spiked on 16.04.2021 (Day 0) with 1.5 L of aqueous solution containing NaCl (1.5 g L^{-1}), terbutryn, diuron, acetochlor and OIT (10 mg L^{-1}) using a sprinkle watering can. Another liter of tab water water was added to each lysimeter surface for biocide infiltration. Leachates were collected after each rain event (> 2 L m^{-2}) and at least weekly until 09. Nov (Day 207). Leached water was transferred into clean containers, transported to the lab at 4°C, filtered to 0.45 µm (PTFE, 25 mm ∅, VWR) and stored at 4°C < 24 h before extraction. For each sample, electrical conductivity was measured on site to determine breakthrough curves (BTC) for the conservative tracer (NaCl). At the end of the experiment, lysimeters were dismantled to collect solid samples from all layers (see Figure D 2). The material of one layer was thoroughly mixed prior to sampling. Aerial and root parts of the vegetation were sampled from the vegetated lysimeter. The roots were cleaned prior to extraction (Gilevska et al., 2022).

2.2 Sample extraction and analysis

Biocides in the filtered water samples were extracted using an automated solid phase extraction (SPE), using Chromabond HR-X cartridges (6 mL, 500 mg, particle size 85 µm) (Chapter 5). Biocides in sand, soil and plant materials were extracted in triplicates using a solid-liquid extraction adapted for CSIA using the solvents DCM and n-pentane (Gilevska et al., 2022). Additionally, the water accessible fraction of biocides in solid material in lysimeter layers was defined as the biocide fraction that may leach during rain events saturating the concerned layer and extracted independently of solvent extraction. To calculate the mass of water accessible

biocides, 250 g of lysimeter material was weighted in triplicates, 200 mL of water were added, followed by horizontal shaking at 30 rpm. After 24 hours, the water was collected and filtered to extract biocides as described above.

Acetochlor, diuron, OIT, terbutryn and four terbutryn TP (terbutryn-sulfoxide (TerSO), terbutryn-2-hydroxy (TerOH), terbutryn-desethyl (TerDesE), terbutryn-desethyl-2-hydroxy (TerDesEOH)) were quantified using HPLC-MS/MS (Junginger et al., 2022 and Chapter 5) (recoveries for soil extraction and SPE are provided in Table D 4).

Carbon stable isotope analysis of terbutryn and acetochlor was conducted using a GC-IRMS system consisting of a gas chromatography (GC, TRACE Ultra ThermoFisher Scientific) coupled to an isotope ratio mass spectrometer (IRMS, DeltaV plus, ThermoFisher Scientific). Diuron and OIT were not suitable for IRMS measurements due to absence of reference isotope fractionation values and limited GC applicability. GC-IRMS measurement conditions and methods were reported previously (Junginger et al., 2022 and Chapter 3-5). The range in which $\delta^{13}C$ values are independent of signal intensity (± 0.5‰) was established for terbutryn (reported (Junginger et al., 2022)) and acetochlor (Figure D 4). Samples with high biocide concentrations in the enriched extract (> 13 mg L^{-1} terbutryn and > 40 mg L^{-1} acetochlor) were selected for measurements with limited matrix effect. Some samples with similar high concentrations in the enriched extracts, originating from large leachate volumes, were not measurable due to co-enrichment with other organic species.

Based on literature isotope fractionation values (ε_C), the extend of degradation (B_C) can be calculated with the modified Rayleigh equation (Elsner, 2010; Fischer et al., 2016) using the initial ($\delta^{13}C_0$) and isotope value after time t ($\delta^{13}C_t$):

$$B_C[\%] = 1 - f \cdot 100 = \left[1 - \left(\frac{\delta^{13}C_t + 1000}{\delta^{13}C_0 + 1000}\right)^{\frac{1000}{\varepsilon_C}}\right] \cdot 100 \qquad \textbf{(6.5)}$$

2.3 Modeling of biocide reactive transport

The finite element numerical model Hydrus-1D (Šimůnek et al., 2013) was used to examine the reactive transport of terbutryn and its major TP, TerSO, in the lysimeters. The soil hydraulic parameters were optimized to fit soil water content. Initial values were obtained from the neural

network prediction using Rosetta Lite DLL (Schaap et al., 2001) from the soil textural distribution to predict van Genuchten's water retention parameters (van Genuchten, 1980) and saturated hydraulic conductivity (Table D 5). Results were further calibrated with measured water content (Figure D 5, Table D 6). BTC of terbutryn and TerSO were used to estimate degradation half-lives of Terbutryn and TerSO in the lysimeters (Figure D 6). To predict biocide infiltration over eight years (from 01.01.2014 (building construction of the Adelshoffen district in Schiltigheim) to 31.12.2021), concentrations of terbutryn in facade runoff were estimated using COMLEAM (Burkhardt et al., 2020) with precipitation and wind data from the nearby Entzheim weather station from 2014 to 2021, for a 10 m high facade (≈ 3 story building), facing west (Figure D 7, Figure D 8). Results of COMLEAM were used as input data for HYDRUS-1D considering facade runoff and rainfall directly on 1 m² of respective simulated surface. The parametrization of Hydrus-1D with results of the lysimeter experiments is detailed in the Appendix D.

3 Results

3.1 Biocide leaching in gravel, pavement and vegetated surface-soil interfaces

The rainfall volume recovered in the total leaching from lysimeters reached 89%, 90% and 43% in the gravel, pavement, and vegetated lysimeters, respectively. The significant water loss in the vegetated lysimeter was attributed to evapotranspiration, whereas fast percolation after precipitation occurred in the gravel and pavement lysimeters as indicated by fast changes in measured water content (Figure D 9). The first arrival of peak concentrations of NaCl in the gravel and paved lysimeters occurred earlier than in the vegetated lysimeter, underscoring higher water retention capacity in the latter (Figure D 10, Table D 7). A second NaCl peak in the pavement lysimeter after 53 d (Figure D 10) indicated parallel, slower flow paths (Maliva, 2016), due to non-uniform entry paths through the pavement joints. The hydraulic dynamics in all lysimeters could be reproduced by optimizing van Genuchten's water retention parameters in Hydrus-1D (Table D 6, Figure D 5).

OIT was never detected in leachates and lysimeter layers, indicating fast degradation (Bollmann et al., 2017a). In contrast, terbutryn, acetochlor and diuron were detected in the gravel and the paved lysimeter 3 days after spiking, coinciding with NaCl and peak concentrations (Figure 1, Table D 7). This indicates fast transport through preferential flow paths during rain events, while sorption retains a limited mass of biocide (Koroša et al., 2020). However, drying following a rain event reduced water content (< 1%, Figure D 9), thus increasing biocide sorption (Delle Site, 2001). Most of the biocide leached mass, i.e., 67%, 84% and 88% for terbutryn, acetochlor and diuron, respectively, leached out from the gravel lysimeter within the first 32 d (Figure 6. 1). However, biocides were chronically released, even after 100 d, with concentrations for all compounds ranging from 0.1 to 3 µg L^{-1} (Figure 6. 1). Lower terbutryn peak concentrations and lower contribution of terbutryn in the first 32 d compared to acetochlor and diuron indicated stronger sorption and higher retardation of terbutryn. This reflects the lower water solubility of terbutryn than acetochlor (Bollmann et al., 2017a; Droz et al., 2021), and its higher sorption coefficients than diuron (Bollmann et al., 2014). TerSO peaked after 11 d, indicating terbutryn degradation. The first arrival of all compounds also occurred after 3 d in the pavement lysimeter, while peak concentrations arrived later (21 d for NaCl, 25 d for acetochlor and terbutryn, 32 d for diuron) (Figure 6. 1, Table D 7). TerSO peak concentrations arrived after 39 d, together with the occurrence of TerOH and TerDesE (Figure 6. 1), indicating terbutryn biodegradation. A high fraction of total biocides in leachate of pavement was released within the first 32 days (58%, 85% and 42% of terbutryn, acetochlor and diuron, respectively). Higher retardation, lower contribution in the first 32 d and lower peak concentrations for diuron indicated stronger sorption in the pavement lysimeter. Stronger sorption of diuron in pavement than in the gravel is also reflected in less overall released mass, later peak arrival and lower contribution of diuron in the first 32 d, while continuous leaching occurred even after 100 d (Figure 6. 1). Sorption based on K_{OW} alone does not explain diuron retention since the K_{OW} of diuron is lower than that of terbutryn and acetochlor (Table D 1). Therefore, sorption to non-organic fraction may strongly influence diuron, e.g., through sorption to clay minerals (Muendo et al., 2021).

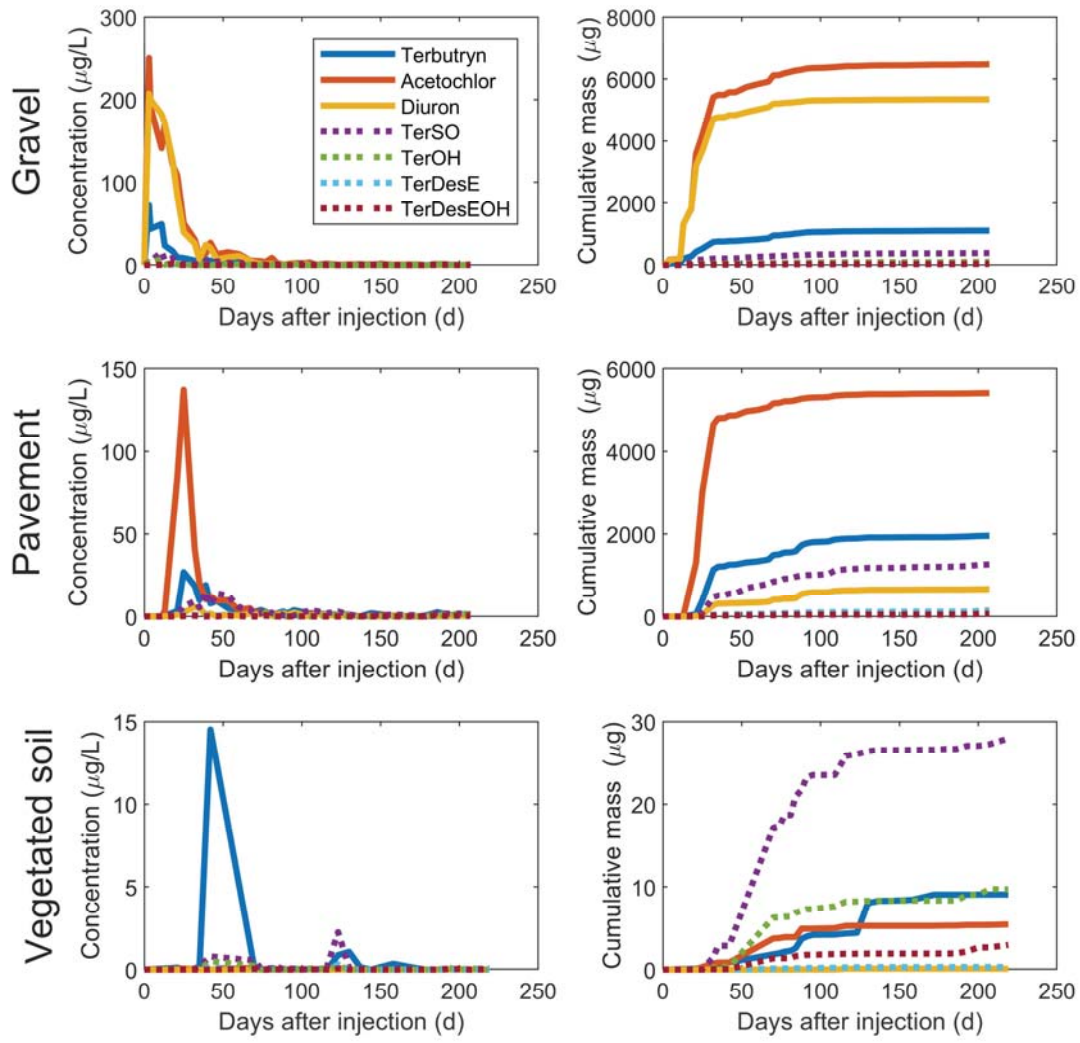

Figure 6. 1. Breakthrough curves of terbutryn (and its TP), acetochlor and diuron concentrations (left) and cumulated leached masses (right) from the lysimeters.

In the vegetated lysimeter, acetochlor, terbutryn and TerSO leached after 21 days and diuron after 81 d (Figure 6. 1, Table D 7), while peak concentrations arrived later than in gravel and pavement lysimeter (Figure 6. 1). This underscores the higher water retention and biocide sorption in the vegetated lysimeter, which may be due to the higher organic carbon content (Table D 2). In contrary to pavement and gravel lysimeter, the lower leached masses and small contribution of biocide leaching compared to overall leached mass in the first 32 d (< 14%) confirms stronger sorption and thus biocide retardation in the vegetated lysimeter.

3.2 Distribution of biocides among lysimeter layers

Even at the end of the experiment (207 d), biocides could be extracted from different layers of the lysimeters, indicating biocide sorption on the lysimeter material. The water accessible fraction confirmed that biocides and TP may still be released. The water accessible fraction reflects the potentially releasable biocide masses during heavy precipitation and saturation of soils. Hydrophilic transformation products were solely extractable with water because solvent extraction resulted in low recoveries (Table D 4).

Gravel lysimeter. About 9% of the initial mass of terbutryn was retained in the lysimeter, confirming terbutryn sorption on gravel (Figure 6. 2). In contrast, the low retention of TerSO (1.5%), despite its high log K_{OW} and low water solubility, indicated limited TP accumulation on the solid phase. More hydrophilic TPs, i.e., TerOH and TerDesEOH, were found in similar proportion (1.7% for both) than TerSO, but only in the water accessible fraction in the top layer of the gravel lysimeter (Figure 6. 2). The occurrence of hydrophilic TP indicates ongoing degradation with potential TP accumulation. While only small amounts of hydrophilic TP were released during the experiment, accumulated terbutryn and TP in gravel may be further degraded, released and transported toward groundwater during heavy rain events. In contrast, acetochlor mainly accumulated in the second gravel layer but to a much lower extent than terbutryn (< 1% of added mass), confirming that acetochlor degradation was a prominent process. Only small amounts of acetochlor were found in the water accessible fraction. Diuron mainly accumulated in the filter gravel (28 µg), while 36% of the extractable mass of diuron was still accessible for water, indicating weak sorption and potential diuron release from gravels.

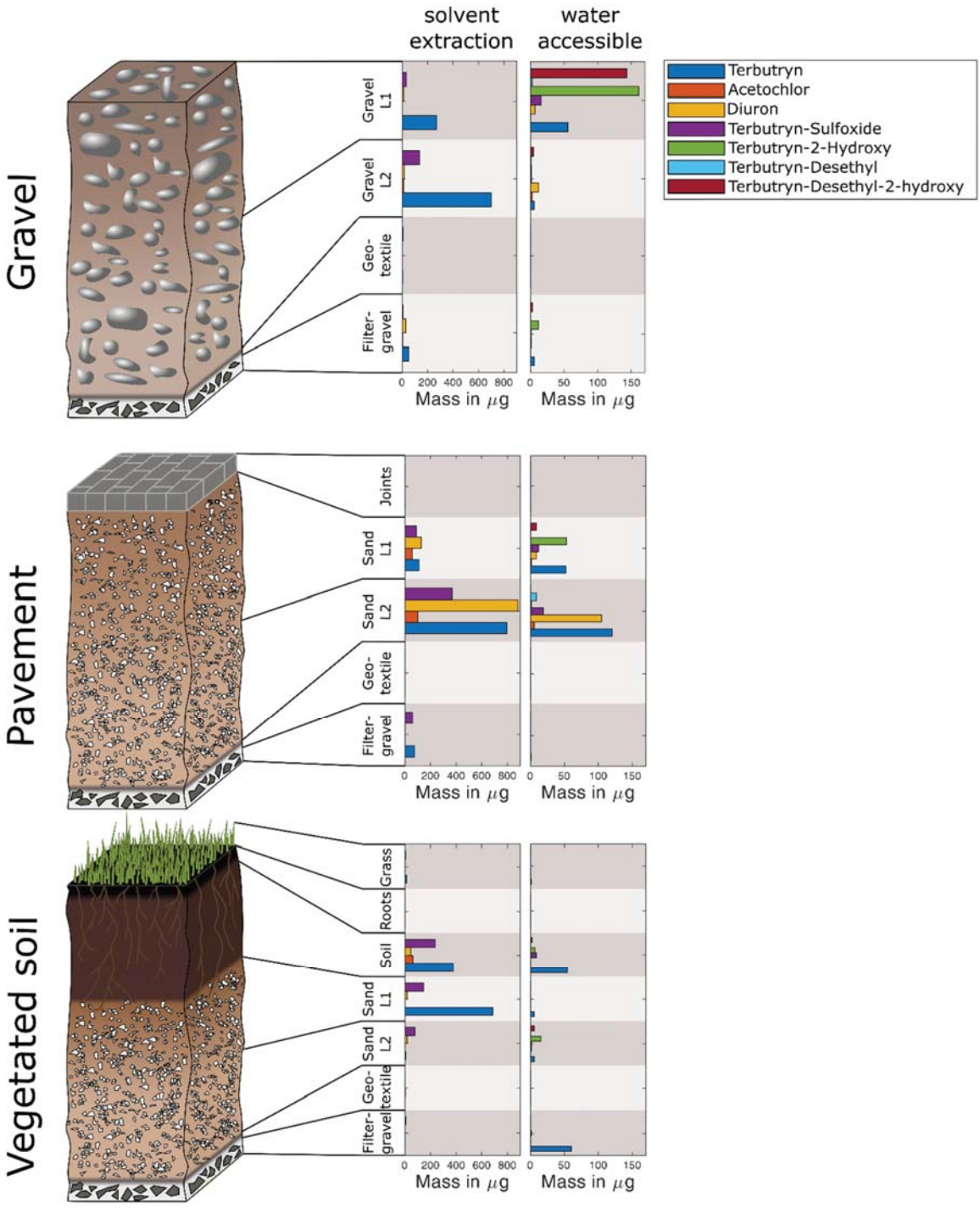

Figure 6. 2. Mass of biocides extracted with solvent and water (i.e., water accessible fraction) from material of the different lysimeter layers.

Pavement lysimeter. The mass of terbutryn and TerSO increased with depth from the pavement joints to the sand layers (Figure 6. 2). The water accessible fraction accounted for 50% and 15% of solvent extracted terbutryn in the first and second sand layer, respectively. This indicates potential terbutryn leaching toward groundwater, even after 200 days. Water extractable TerOH and TerDesEOH was found in high amount in the top sand (53 µg and 9 µg respectively), while water accessible TerDesE prevailed in the second layer (9 µg). Overall, the water accessible fraction of TP in the pavement lysimeter was lower than in the gravel lysimeter indicating that some TP might have been further degraded to secondary TP. Similarly, the largest acetochlor amount was found in the top and second sand layer (59 and 101 µg, contributing 1.2% of spiked solution, Figure 6. 2), although masses were less than of those of terbutryn, indicating fast acetochlor degradation. Only small masses (4% of recovered mass) were water accessible, indicating low risk of further release of acetochlor. Diuron masses extracted from the pavement lysimeter showed similar mass distributions than other compounds (Figure 6. 2). The mass contributions were highest in the second sand layer (881 µg), followed by the top sand layer (127µg). This confirms stronger retention of diuron in the pavement than in the gravel lysimeter (7.7% of spiked mass) and compared to other compounds within the same lysimeter. Results confirm the strong sorption of diuron to minerals. Diuron was mainly water accessible in the second sand layer (105 µg, 11% of recovered diuron), explaining leaching following rain events.

Vegetated soil. High amount of terbutryn sorbed to soil (377 µg, i.e., 2.5% of application) of which 54 µg was water accessible. Even higher amount was extracted from the first sand layer (697 µg, 4.6% of application) of which only 5 µg was found in the water accessible fraction (Figure 6. 2). This indicates terbutryn sorption to the top layer containing the highest carbon content (7.2%), with low desorption potential. Under environmental conditions with continuous input from facades, terbutryn may thus accumulate in the topsoil layer. The abundance of TerSO in soil (236 µg) and the top sand layer (147 µg) confirms ongoing degradation and low desorption potential (9 and 0.1 µg, respectively). The other TPs were found in low amount (< 15 µg) in the water accessible fraction, suggesting that targeted TP might already have been degraded to secondary TP (Bollmann et al., 2017a). The highest mass of acetochlor was found in the soil layer (61 µg, < 1% of applied mass) with only minor contributions to the overall mass in all other layers (< 1 µg) besides the geotextile (4.7 µg). The retained masses were generally lower for acetochlor than for terbutryn, confirming faster

acetochlor degradation. Consequently, water accessible fraction of acetochlor from all layers was < 1 µg. The mass of diuron contributions were 47 µg in soil, and 37 µg in the sand layers. Although diuron was strongly retained in soil, diuron was also retained in the sand layers of vegetated lysimeter. The water accessible fraction was below 2 µg in all layers, confirming its low leaching potential through soil and sand towards groundwater.

Remarkably, the highest concentrations for all compounds were observed in plant material (Figure D 12). However, the overall contribution of plants to the mass balance was low (< 1% of applied mass). Nevertheless, constant growth of plants over time, associated with uptake and transformation of biocides in the plants may be significant in the mass balance and contribute to reduce biocide transport toward groundwater. Plant uptake may play a significant role for the fate of urban biocide in vegetated systems and SSM. Plant uptake has been previously reported for acetochlor (Ju et al., 2020; Lu et al., 2022), and for terbutryn (Turgut, 2005), but reference experiments for urban biocides are scarce and uptake rates are missing.

In contrast to a single pulse injection, facades chronically emit biocides during rain events, which may lead to biocide accumulation in vegetated systems. Ecotoxicological tests of biocides on soil microbial communities are rare and mixtures of various biocides as well as TP have rarely been tested on soil ecotoxicology (Reiß et al., 2021). At the end of the experiment, acetochlor and diuron masses retained in vegetated lysimeter were low, indicating that these compounds were degraded, thus reducing their leaching potential. In contrary, higher amounts of terbutryn and TP were found in the lysimeter, indicating slower degradation and potential accumulation in soil.

3.3 Biocide mass balance and retention in the lysimeters

The mass recoveries were higher in leachate of gravel and paved, than in the vegetated lysimeter but also varied significantly among compounds. For instance, 10% of terbutryn, 47% of acetochlor and 40% of diuron masses were recovered in leachates from the gravel lysimeter (Figure 6. 3). The sum of the leached terbutryn TP accounted for 4.9% of the initial terbutryn mass, indicating limited degradation and confirming terbutryn retention in the gravel lysimeter. Indeed, most terbutryn TP are more water soluble than terbutryn, thus higher leaching potentials are expected. A higher mass of terbutryn (16.8%), but lower masses of acetochlor (39.5%) and

diuron (5%), leached from the paved than from the gravel lysimeters (Figure 6. 3, Table D 8). Higher terbutryn leaching may reflect larger residual water content in the paved lysimeter (Figure D 9), resulting in lower sorption. Accordingly, longer water retention time in the paved lysimeter favored acetochlor and terbutryn degradation, as also underscored by a higher contribution of TP to the overall terbutryn leaching, and lower recoveries in leachate of acetochlor. Similarly, the recovery of diuron was low, with later peak breakthrough and continuous leaching after 100 d at high concentrations (30 µg L^{-1}), although diuron has a lower K_{OW} value. This supports the idea that distinct sorption mechanisms, e.g., sorption to clay minerals (Muendo et al., 2021), may drive diuron retention in the paved lysimeter. In contrast, the terbutryn mass leaching from the vegetated lysimeter was 0.1% and 0.4% as TP, whereas less than 0.1% of acetochlor and diuron leached out (Figure 6. 3). The high water holding capacity and long retention times in the lysimeter may enhance strong biocide sorption in the organic rich layers, thus resulting in a strong retention of biocides.

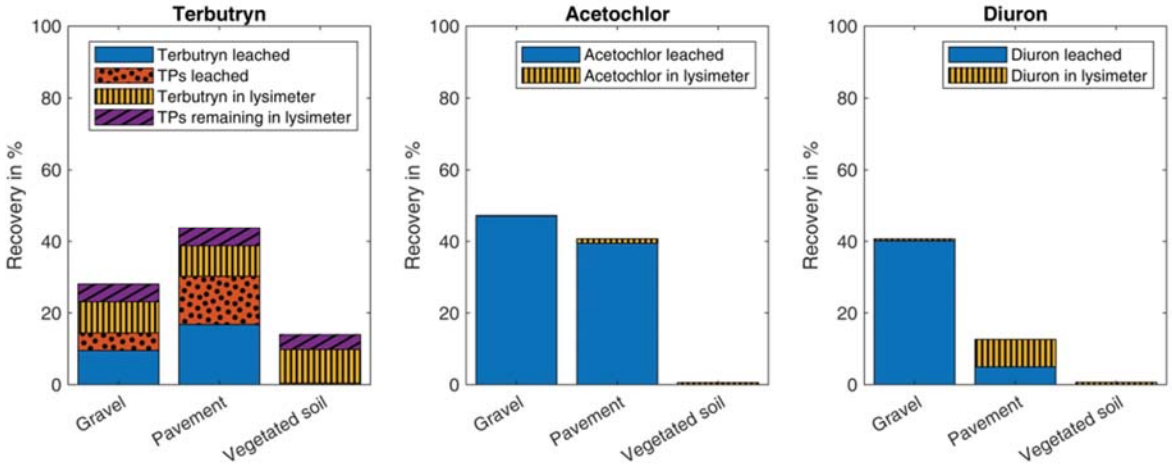

Figure 6. 3. Mass recoveries of terbutryn (including TP), acetochlor and diuron in the lysimeters, including the leached and remaining masses at the end of the experiment.

The extractable mass of terbutryn (8.5 – 9.4%) and TP (4.2 – 5%) at the end of the experiment did not vary widely among lysimeters, yielding in a total mass recovery in the lysimeter of 28% (gravel), 44% (paved) and 14% (vegetated) (Figure 6. 3). Hence, more than 50% of the terbutryn mass could not be recovered in the lysimeters or in leachates, although TP were included in the mass balances. This indicates degradation and transformation to secondary, untargeted TP (Figure 6. 3). A suspect screening for TP detected in previous degradation studies

identified the terbutryn TP TerDesS (desthiomethyl-terbutryn) and MEBT (Terbumeton) based on precursor and two product ions (Table D 9, Figure D 11). In addition, decreasing concentrations of TerSO with higher concentrations of desbutyl-2-hydroxy terbutryn than hydroxy-terbutryn was also previously reported (Bollmann et al., 2017a), suggesting further terbutryn transformation to secondary TP.

The recovered mass of acetochlor in the lysimeter, i.e., retained in the lysimeter material, was 0.1%, 1.2% and 0.5% in gravel, pavement and vegetated soil (Figure 6. 3), indicating that > 50% acetochlor was degraded accounting of the leached mass (i.e., 47% from gravel and 40% from pavement lysimeters). Since a negligible mass of acetochlor leached out from the vegetated lysimeter and mass recovery was low, most acetochlor was likely degraded in the vegetated soil lysimeter.

The recovered mass of diuron from lysimeter material was 0.4% (gravel), 7.7% (pavement) and 0.7% (vegetated soil), respectively (Figure 6. 3), confirming sorption of diuron in the sand material of the pavement and the soil in the vegetated lysimeters. Although previous microcosm studies indicated no biotic degradation of diuron (Bollmann et al., 2017a), the TP diuron-desmethyl was previously detected in urban field sites, suggesting that diuron may degrade in the urban environment, explaining the low recoveries in vegetated soil (Hensen et al., 2018; Linke et al., 2021).

3.4 Biocide degradation in the lysimeters

Carbon stable isotope analysis was possible for peak concentration of terbutryn and acetochlor in leachates from the pavement and the gravel lysimeters (Figure 6. 4). The absence of significant (< 2‰ (Hunkeler, 2009)) isotope fractionation for terbutryn suggests that the extent of degradation was insufficient to cause isotope fractionation. In addition, the main degradation pathway through TerSO would only lead to secondary carbon isotope fractionation (Junginger et al., 2022). In contrast, significant carbon stable isotope fractionation was observed for acetochlor in the pavement lysimeter ($\Delta\delta^{13}C$ = 3.3‰) and to a lower extent in the gravel lysimeter ($\Delta\delta^{13}C$ = 1.5‰) (Figure 6. 4). Interestingly, carbon isotope fractionation in the pavement was higher than in the gravel lysimeter for the corresponding sampling times,

suggesting higher degradation rates in the pavement than in the gravel lysimeters. The extend of degradation after 42 days in the pavement lysimeter (and after 34 days in gravel lysimeter) was calculated based on reported carbon isotope fractionation values for acetochlor biodegradation (i.e., ε_C = -5.0‰ under oxic, -3.6‰ under anoxic conditions in water/sediment microcosms, and -3.4‰ in wetlands) (Droz et al., 2021; Elsayed et al., 2014). The contribution of acetochlor degradation to the overall dissipation was estimated to 48 - 61% in the pavement lysimeter ($t_{1/2}$= 30 – 44 d) after 42 days, and between 24 – 33% in the gravel lysimeter after 32 days ($t_{1/2}$= 70 – 103 d).

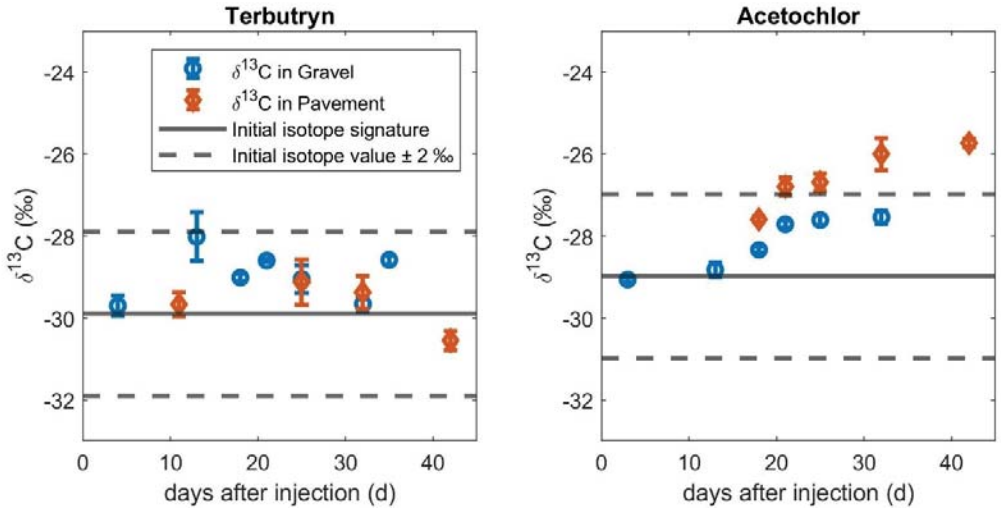

Figure 6. 4. Carbon stable isotope fractionation ($\delta^{13}C$) of terbutryn and acetochlor in leachates. Error bars represent the standard error of carbon isotope value measurements in triplicates.

Our results highlighted that CSIA can provide another line of evidence of ongoing degradation in the lysimeter and higher bioactivity through faster degradation in the pavement lysimeter compared to gravel. Nevertheless, in urban environments with continuous entry of biocides from facades into urban surfaces, CSIA is limited, as enriched isotope values near the facade surfaces are subsequently diluted by non-degraded terbutryn with initial isotope composition (Chapter 5).

For terbutryn, degradation rates were estimated based on the Hydrus-1D parametrization (detailed in SI). Good agreement (r^2 = 0.84) between modelled and measured BTC were observed for terbutryn in the gravel lysimeter. However, concentrations of TerSO resulted in poor (r^2 <

0.5) model fit, while concentration were overestimated in the BTC tailing (Figure D 6). As a results, the half live time of terbutryn ($t_{1/2}$ = 2.9 d in liquid phase and 28.8 d in solid phase) estimated with the model is likely underestimated. Indeed, previous biodegradation experiments in soil, sediment and water microcosm yielded terbutryn half-lives to $t_{1/2}$ > 80 d (Bollmann et al., 2017a; Junginger et al., 2022). The low concentrations of secondary, more soluble, terbutryn TP, such as TerOH and TerDesEOH also support the idea that Hydrus-1D underestimated half-lives. Estimated half-live times were $t_{1/2}$ = 3.3 d in water, and $t_{1/2}$ = 34.0 d in the solid phase in the pavement lysimeter. The parametrization of terbutryn and TerSO BTC resulted in a good fit (r^2 > 0.7) between measured and modeled concentrations in pavement lysimeter, nevertheless, half-live times are lower than from reference experiments. Due to the low concentrations of terbutryn in leachate from the vegetated lysimeter, Hydrus-1D could not be parametrized and literature values were used for reaction parameters (Table D 10).

Besides with Hydrus-1D, bulk half-lives of terbutryn were estimated based on remaining mass in the lysimeters considering the leached masses (detailed in Appendix D). Estimated half-lives were $t_{1/2}$= 64, 68 and 61 d in gravel, pavement and vegetated lysimeter, similar to previous experiments (Junginger et al., 2022). For acetochlor, the estimated half-live times were $t_{1/2}$= 38, 45 and 27 d in gravel, pavement and vegetated lysimeter, respectively, which is in line with previous studies ($t_{1/2}$ = 14 – 31 d) (Droz et al., 2021; Lewis et al., 2016). Even though faster degradation was estimated based on isotope fractionation values for acetochlor in pavement than in gravel, estimation of degradation rates from mass balances consistently estimated faster degradation in gravel for all compounds (Figure D 13). As isotope fractionation was solely measured in leached water, we suggest faster degradation in water than in the sorbed phase due to limited bioavailability (Gamerdinger et al., 1997; Guo et al., 2000), therefore, half-lives estimated from isotope fractionation in leachates represent degradation half-lives in water while mass balance approaches give bulk-half-live values considering sorbed and dissolved biocide.

3.5 Biocide reactive transport towards groundwater

Since outdoor experiments are time-limited, reactive transport models may help to predict the main entry paths and mass fluxes of urban biocides through urban surfaces to evaluate the associated risks over years. The modeled terbutryn and TP leaching through gravel, pavement and vegetated soil largely varied (Figure 6. 5). Terbutryn was mainly exported from the gravel

lysimeter, with little contribution of TerSO, supporting the idea of fast transport during rain and strong sorption during dry periods. 36% of terbutryn reached deeper layers, while only 1% leached as TerSO. The remaining terbutryn was either sorbed or further degraded to TerOH or TerDesEOH. Worthy of note, TerOH and TerDesEOH may be mobilized into water, due to lower Kow and higher water solubility. Highest biocide masses in leachate (in 30 cm depth) were observed in the first year, coinciding with highest inflows of biocides from modeled facade (Figure 6. 5, Figure D 7).

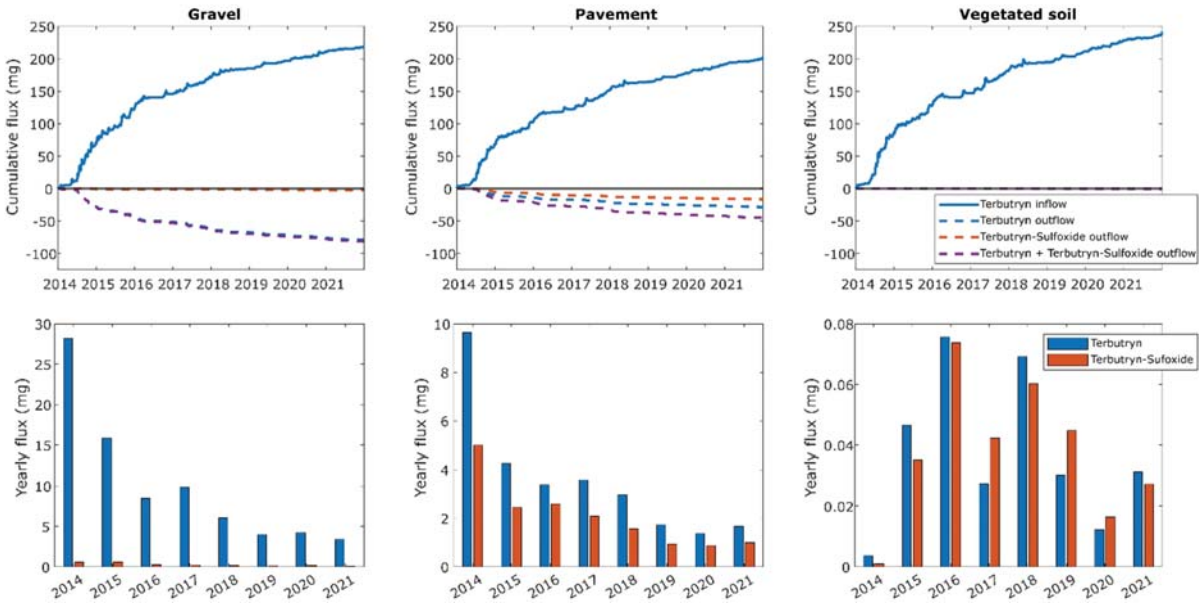

Figure 6. 5. Top: Cumulative flux of terbutryn leached from facades into sub-surface materials (positive values) and of terbutryn and terbutryn-sulfoxide leached under the 30 cm surface-soil interfaces for 1 m² surface connected to a facade. Bottom: yearly terbutryn and terbutryn-sulfoxide export towards deeper soil layer and groundwater.

In the pavement lysimeter, 22% of infiltrated terbutryn reaches 30 cm depth either as terbutryn or TerSO. This indicates stronger retention time terbutryn and TerSO in the paved lysimeter, which may favor degradation to TerSO and its release into leachate. Yearly fluxes of terbutryn have a similar pattern (decreasing fluxes over time dependent on input fluxes) than in the gravel lysimeter with highest fluxes in the first year, related to the low water retention capacity. In contrast, cumulated biocide emissions of terbutryn and TerSO toward groundwater were two orders of magnitude lower in the vegetated than in the gravel and paved lysimeters (Figure 5). Only 0.2% of terbutryn and TerSO was exported over time, emphasizing that the

reactive transport of terbutryn and TerSO in the vegetated soil was driven mainly by sorption. Strong retention in organic rich soil layers for different urban biocide was also modelled by another study (Vega-Garcia et al., 2022). In the first year, when highest concentrations entered the vegetated soil, lowest concentrations were exported, which is in line with observed concentrations. Heavy rainfall events were the main drivers for solute fluxes towards groundwater (Figure D 14, Figure D 15), as they result in high porewater content and water saturation, thus reducing the water travel times and sorption.

4 Environmental implications

Pavement and drainage gravel around buildings can be seen as main input sources of biocides towards groundwater if no underlying soil can retain the biocides. On contrary, terbutryn leaching from undisturbed soil and vegetated surfaces, as in artificial ditches designed for SSM is significantly lower but leads to accumulation in soil and plants. Natural SSM systems can therefore be accounted for as temporary sinks of biocides. Nevertheless, simulation over eight years showed low concentrations of terbutryn and TerSO being constantly released. Furthermore, secondary TP with higher solubility and lower sorption affinity (e.g., TerOH or TerDesEOH) might be translocated towards groundwater. In aged SSM systems, macropores might also enhance preferential flow and fast transport of a fraction of biocides (Bork et al., 2021).

Based on our results, we suggest that a large proportion of urban biocides might enter the subsurface (e.g., through gravel or permeable pavement) prior to reaching SSM systems such as infiltration ponds and trenches. Infiltration systems might then act largely as a sink with low biocide emissions over long time periods. We also found that heavy rain events might be drivers for both, biocide release from facades (Vega-Garcia et al., 2020 and Chapter 5) and reactive transport towards groundwater through saturated surface-soil interfaces.

Stormwater retention through permeable urban surfaces is relevant for flood management in urban areas and to improve ecological aspects in cities and drainage infrastructure by implementing e.g., artificial wetlands, infiltration ponds and ditches and permeable paving (Barbosa et al., 2012; Bork et al., 2021; Goulden et al., 2018; Hering and Ingold, 2012; Li et al.,

2018; Mitchell, 2006; Wang et al., 2018). Especially fast draining systems (e.g., drainage gravel and pavement directly connected to facades) can have adverse effects as source of biocide contamination for groundwater resources when no underlying soil buffers these fluxes. Even though vegetated infiltration systems can significantly reduce biocide emissions towards groundwater, slow leaching of parent compounds over long time periods and significant contribution of TP might still occur. This highlights the importance for a strong input prevention (Kümmerer et al., 2019, 2018), for example with biocide free materials or readily biodegradable compounds (Kümmerer, 2007) and regulation of individual chemicals or construction-based solutions e.g., through facade greening.

Chapter 6

References

Ahammed, F., 2017. A review of water-sensitive urban design technologies and practices for sustainable stormwater management. Sustain. Water Resour. Manag. 3, 269–282.

Arias-Estévez, M., López-Periago, E., Martínez-Carballo, E., Simal-Gándara, J., Mejuto, J.-C., García-Río, L., 2008. The mobility and degradation of pesticides in soils and the pollution of groundwater resources. Agric. Ecosyst. Environ. 123, 247–260.

Barbosa, A.E., Fernandes, J.N., David, L.M., 2012. Key issues for sustainable urban stormwater management. Water Res., Special Issue on Stormwater in urban areas 46, 6787–6798.

Bester, K., Banzhaf, S., Burkhardt, M., Janzen, N., Niederstrasser, B., Scheytt, T., 2011. Activated soil filters for removal of biocides from contaminated run-off and waste-waters. Chemosphere 85, 1233–1240.

Bollmann, U.E., Fernández-Calviño, D., Brandt, K.K., Storgaard, M.S., Sanderson, H., Bester, K., 2017a. Biocide runoff from building facades: degradation kinetics in soil. Environ. Sci. Technol. 51, 3694–3702.

Bollmann, U.E., Minelgaite, G., Schlüsener, M., Ternes, T., Vollertsen, J., Bester, K., 2016. Leaching of terbutryn and its photodegradation products from artificial walls under natural weather conditions. Environ. Sci. Technol. 50, 4289–4295.

Bollmann, U.E., Minelgaite, G., Schlüsener, M., Ternes, T.A., Vollertsen, J., Bester, K., 2017b. Photodegradation of octylisothiazolinone and semi-field emissions from facade coatings. Sci. Rep. 7, 41501.

Bollmann, U.E., Vollertsen, J., Carmeliet, J., Bester, K., 2014. Dynamics of biocide emissions from buildings in a suburban stormwater catchment – concentrations, mass loads and emission processes. Water Res. 56, 66–76.

Bork, M., Lange, J., Graf-Rosenfellner, M., Hensen, B., Olsson, O., Hartung, T., Fernández-Pascual, E., Lang, F., 2021. Urban storm water infiltration systems are not reliable sinks for biocides: evidence from column experiments. Sci. Rep. 11, 7242.

Burkhardt, M., Engelke, D., Gehrig, S., Hochstrasser, F., Rohr, M., Tietje, O., 2020. COMLEAM - Manual Version 3.0. HSR University of Applied Sciences Rapperswil, Switzerland.

Burkhardt, M., Kupper, T., Hean, S., Haag, R., Schmid, P., Kohler, M., Boller, M., 2007. Biocides used in building materials and their leaching behavior to sewer systems. Water Sci. Technol. 56, 63–67.

Burkhardt, M., Zuleeg, S., Vonbank, R., Bester, K., Carmeliet, J., Boller, M., Wangler, T., 2012. Leaching of biocides from facades under natural weather conditions. Environ. Sci. Technol. 46, 5497–5503.

Burkhardt, M., Zuleeg, S., Vonbank, R., Schmid, P., Hean, S., Lamani, X., Bester, K., Boller, M., 2011. Leaching of additives from construction materials to urban storm water runoff. Water Sci. Technol. 63, 1974–1982.

Coutu, S., Del Giudice, D., Rossi, L., Barry, D.A., 2012a. Modeling of facade leaching in urban catchments. Water Resour. Res. 48.

Coutu, S., Rota, C., Rossi, L., Barry, D.A., 2012b. Modelling city-scale facade leaching of biocide by rainfall. Water Res. 46, 3525–3534.

Delle Site, A., 2001. Factors Affecting Sorption of Organic Compounds in Natural Sorbent/Water Systems and Sorption Coefficients for Selected Pollutants. A Review. J. Phys. Chem. Ref. Data 30, 187–439.

Droz, B., Drouin, G., Maurer, L., Villette, C., Payraudeau, S., Imfeld, G., 2021. Phase transfer and biodegradation of pesticides in water–sediment systems explored by compound-specific isotope analysis and conceptual modeling. Environ. Sci. Technol. 55, 4720–4728.

Elsayed, O.F., Maillard, E., Vuilleumier, S., Nijenhuis, I., Richnow, H.H., Imfeld, G., 2014. Using compound-specific isotope analysis to assess the degradation of chloroacetanilide herbicides in lab-scale wetlands. Chemosphere 99, 89–95.

Elsner, M., 2010. Stable isotope fractionation to investigate natural transformation mechanisms of organic contaminants: principles, prospects and limitations. J. Environ. Monit. 12, 2005–2031.

Elsner, M., Imfeld, G., 2016. Compound-specific isotope analysis (CSIA) of micropollutants in the environment — current developments and future challenges. Curr. Opin. Biotechnol., Analytical biotechnology 41, 60–72.

Fischer, A., Manefield, M., Bombach, P., 2016. Application of stable isotope tools for evaluating natural and stimulated biodegradation of organic pollutants in field studies. Curr. Opin. Biotechnol. 41, 99–107.

Gamerdinger, A.P., Achin, R.S., Traxler, R.W., 1997. Approximating the Impact of Sorption on Biodegradation Kinetics in Soil-Water Systems. Soil Sci. Soc. Am. J. 61, 1618–1626.

Gassmann, M., 2021. Modelling the fate of pesticide transformation products from plot to catchment scale—state of knowledge and future challenges. Front. Environ. Sci. 9.

Gilevska, T., Wiegert, C., Droz, B., Junginger, T., Prieto-Espinoza, M., Borreca, A., Imfeld, G., 2022. Simple extraction methods for pesticide compound-specific isotope analysis from environmental samples. MethodsX 101880.

Goulden, S., Portman, M.E., Carmon, N., Alon-Mozes, T., 2018. From conventional drainage to sustainable stormwater management: Beyond the technical challenges. J. Environ. Manage. 219, 37–45.

Guo, L., Jury, W.A., Wagenet, R.J., Flury, M., 2000. Dependence of pesticide degradation on sorption: nonequilibrium model and application to soil reactors. J. Contam. Hydrol. 43, 45–62.

Chapter 6

Hensen, B., Lange, J., Jackisch, N., Zieger, F., Olsson, O., Kümmerer, K., 2018. Entry of biocides and their transformation products into groundwater via urban stormwater infiltration systems. Water Res. 144, 413–423.

Hensen, B., Olsson, O., Kümmerer, K., 2020. A strategy for an initial assessment of the ecotoxicological effects of transformation products of pesticides in aquatic systems following a tiered approach. Environ. Int. 137, 105533.

Hering, J.G., Ingold, K.M., 2012. Water Resources Management: What Should Be Integrated? Science 336, 1234–1235.

Hildebrandt, A., Guillamón, M., Lacorte, S., Tauler, R., Barceló, D., 2008. Impact of pesticides used in agriculture and vineyards to surface and groundwater quality (North Spain). Water Res. 42, 3315–3326.

Hunkeler, D., 2009. A Guide for Assessing Biodegradation and Source Identification of Organic Ground Water Contaminants using Compound Specific Isotope Analysis (CSIA) 82.

Ju, C., Zhang, H., Wu, R., Dong, S., Yao, S., Wang, F., Cao, D., Xu, S., Fang, H., Yu, Y., 2020. Upward translocation of acetochlor and atrazine in wheat plants depends on their distribution in roots. Sci. Total Environ. 703, 135636.

Junginger, T., Payraudeau, S., Imfeld, G., 2022. Transformation and stable isotope fractionation of the urban biocide terbutryn during biodegradation, photodegradation and abiotic hydrolysis. Chemosphere 305, 135329.

Koroša, A., Brenčič, M., Mali, N., 2020. Estimating the transport parameters of propyphenazone, caffeine and carbamazepine by means of a tracer experiment in a coarse-gravel unsaturated zone. Water Res. 175, 115680.

Kümmerer, K., 2007. Sustainable from the very beginning: rational design of molecules by life cycle engineering as an important approach for green pharmacy and green chemistry. Green Chem. 9, 899–907.

Kümmerer, K., Dionysiou, D.D., Olsson, O., Fatta-Kassinos, D., 2019. Reducing aquatic micropollutants – Increasing the focus on input prevention and integrated emission management. Sci. Total Environ. 652, 836–850.

Kümmerer, K., Dionysiou, D.D., Olsson, O., Fatta-Kassinos, D., 2018. A path to clean water. Science 361, 222–224.

Lewis, K.A., Tzilivakis, J., Warner, D.J., Green, A., 2016. An international database for pesticide risk assessments and management. Hum. Ecol. Risk Assess. 22, 1050–1064.

Li, Z., Dong, M., Wong, T., Wang, J., Kumar, A.J., Singh, R.P., 2018. Objectives and Indexes for Implementation of Sponge Cities—A Case Study of Changzhou City, China. Water 10, 623.

Linke, F., Olsson, O., Preusser, F., Kümmerer, K., Schnarr, L., Bork, M., Lange, J., 2021. Sources and pathways of biocides and their transformation products in urban storm water infrastructure of a 2 ha urban district. Hydrol. Earth Syst. Sci. 25, 4495–4512.

Linke, F., Olsson, O., Schnarr, L., Kümmerer, K., Preusser, F., Bork, M., Leistert, H., Lange, J., 2022. Discharge and fate of biocide residuals to ephemeral stormwater retention pond sediments. Hydrol. Res. nh2022075.

Lu, Q., Shen, Z., Zheng, K., Chang, Q., Xue, J., Wu, X., 2022. Estimating the bioavailability of acetochlor to wheat using in situ pore water and passive sampling. Sci. Total Environ. 833, 155239.

Maliva, R.G., 2016. Tracer Tests, in: Maliva, R.G. (Ed.), Aquifer Characterization Techniques: Schlumberger Methods in Water Resources Evaluation Series No. 4, Springer Hydrogeology. Springer International Publishing, Cham, pp. 403–443.

Melsbach, A., Torrentó, C., Ponsin, V., Bolotin, J., Lachat, L., Prasuhn, V., Hofstetter, T.B., Hunkeler, D., Elsner, M., 2020. Dual-Element Isotope Analysis of Desphenylchloridazon to Investigate Its Environmental Fate in a Systematic Field Study: A Long-Term Lysimeter Experiment. Environ. Sci. Technol. 54, 3929–3939.

Mitchell, V.G., 2006. Applying Integrated Urban Water Management Concepts: A Review of Australian Experience. Environ. Manage. 37, 589–605.

Muendo, B.M., Shikuku, V.O., Getenga, Z.M., Lalah, J.O., Wandiga, S.O., Rothballer, M., 2021. Adsorption-desorption and leaching behavior of diuron on selected Kenyan agricultural soils. Heliyon 7, e06073.

Paijens, C., Bressy, A., Frère, B., Moilleron, R., 2020. Biocide emissions from building materials during wet weather: identification of substances, mechanism of release and transfer to the aquatic environment. Environ. Sci. Pollut. Res. 27, 3768–3791.

Paijens, C., Bressy, A., Frère, B., Tedoldi, D., Mailler, R., Rocher, V., Neveu, P., Moilleron, R., 2021. Urban pathways of biocides towards surface waters during dry and wet weathers: assessment at the Paris conurbation scale. J. Hazard. Mater. 402, 123765.

Pinasseau, L., Wiest, L., Volatier, L., Mermillod-Blondin, F., Vulliet, E., 2020. Emerging polar pollutants in groundwater: Potential impact of urban stormwater infiltration practices. Environ. Pollut. 266, 115387.

Quednow, K., Püttmann, W., 2007. Monitoring terbutryn pollution in small rivers of Hesse, Germany. J. Environ. Monit. 9, 1337–1343.

Reiß, F., Kiefer, N., Noll, M., Kalkhof, S., 2021. Application, release, ecotoxicological assessment of biocide in building materials and its soil microbial response. Ecotoxicol. Environ. Saf. 224, 112707.

Schaap, M.G., Leij, F.J., van Genuchten, M.Th., 2001. rosetta: a computer program for estimating soil hydraulic parameters with hierarchical pedotransfer functions. J. Hydrol. 251, 163–176.

Schaffitel, A., Schuetz, T., Weiler, M., 2020. A distributed soil moisture, temperature and infiltrometer dataset for permeable pavements and green spaces. Earth System Science Data 12, 501–517.

Schoknecht, U., Mathies, H., Wegner, R., 2016. Biocide leaching during field experiments on treated articles. Environ. Sci. Eur. 28, 6.

Šimůnek, J., Šejna, M., Saito, H., Sakai, M., van Genuchten, M. Th., 2013. The HYDRUS-1D Software Package for Simulating the Movement of Water, Heat, and Multiple Solutes in Variably Saturated Media, HYDRUS Software Series 3. Department of Environmental Sciences, University of California Riverside, Riverside, California, USA.

Timm, A., Kluge, B., Wessolek, G., 2018. Hydrological balance of paved surfaces in moist mid-latitude climate – A review. Landsc. Urban Plan. 175, 80–91.

Torrentó, C., Ponsin, V., Lihl, C., Hofstetter, T.B., Baran, N., Elsner, M., Hunkeler, D., 2021. Triple-element compound-specific stable isotope analysis (3D-CSIA): added value of Cl isotope ratios to assess herbicide degradation. Environ. Sci. Technol. 55, 13891–13901.

Torrentó, C., Prasuhn, V., Spiess, E., Ponsin, V., Melsbach, A., Lihl, C., Glauser, G., Hofstetter, T.B., Elsner, M., Hunkeler, D., 2018. Adsorbing vs. Nonadsorbing Tracers for Assessing Pesticide Transport in Arable Soils. Vadose Zone J. 17, 170033.

Turgut, C., 2005. Uptake and Modeling of Pesticides by Roots and Shoots of Parrotfeather (Myriophyllum aquaticum) (5 pp). Environ. Sci. Pollut. Res. Int. 12, 342–346.

van Genuchten, M.Th., 1980. A Closed-form Equation for Predicting the Hydraulic Conductivity of Unsaturated Soils. Soil Sci. Soc. Am. J. 44, 892–898.

Vega-Garcia, P., Lok, C.S.C., Marhoon, A., Schwerd, R., Johann, S., Helmreich, B., 2022. Modelling the environmental fate and behavior of biocides used in façades covered with mortars and plasters and their transformation products. Build. Environ. 216, 108991.

Vega-Garcia, P., Schwerd, R., Scherer, C., Schwitalla, C., Johann, S., Rommel, S.H., Helmreich, B., 2020. Influence of façade orientation on the leaching of biocides from building façades covered with mortars and plasters. Sci. Total Environ. 734, 139465.

Vijayaraghavan, K., Biswal, B.K., Adam, M.G., Soh, S.H., Tsen-Tieng, D.L., Davis, A.P., Chew, S.H., Tan, P.Y., Babovic, V., Balasubramanian, R., 2021. Bioretention systems for stormwater management: Recent advances and future prospects. J. Environ. Manage. 292, 112766.

Wang, H., Mei, C., Liu, J., Shao, W., 2018. A new strategy for integrated urban water management in China: Sponge city. Sci. China Technol. Sci. 61, 317–329.

Wicke, D., Tatis-Muvdi, R., Rouault, P., Zerball-van Baar, P., Dünnbier, U., Rohr, M., Burkhardt, M., 2022. Emissions from building materials—a threat to the environment? Water 14, 303.

Wittmer, I.K., Bader, H.-P., Scheidegger, R., Singer, H., Lück, A., Hanke, I., Carlsson, C., Stamm, C., 2010. Significance of urban and agricultural land use for biocide and pesticide dynamics in surface waters. Water Res. 44, 2850–2862.

Wittmer, I.K., Scheidegger, R., Bader, H.-P., Singer, H., Stamm, C., 2011. Loss rates of urban biocides can exceed those of agricultural pesticides. Sci. Total Environ. 409, 920–932.

Preface to chapter 7

In urban districts, leaching of urban biocides from facades (Chapter 5) and reactive transport through soil towards groundwater (Chapter 6) is strongly linked. Understanding this interplay involves a holistic framework, implementing results from previous studies, to predict biocide emissions and reactive transport for a whole district. Therefore, we proposed a framework based on a detailed field monitoring campaign in a 2.4 ha district in combination with a model to assess biocide mass fluxes from facades into various receiving compartments over time and to identify potential hot-spots of biocide infiltration towards groundwater. The field campaign was conducted in a field site, constructed according to typical sustainable storm water management practice with two local infiltration systems.

Combining an elaborated sampling campaign with detailed characterization of the field site and modeling of water infiltration on the district scale allows us to estimate biocide release and distribution in the catchment over eight years. Our model highlights, that a majority of biocides enter the subsurface close to facades and during transport before reaching sormwater infiltration systems. Therefore, the use of stormwater infiltration ponds to retain biocides might be limited as large fractions of biocides are bypassing infiltration facilities. However, measured concentrations of terbutryn and diuron in an infiltration pond and trench regularly exceeded predicted no effect concentrations, even eight years after construction of the district. Terbutryn was consistently detected in all sampled matrices (water, sediment, soil and plants). Altogether, this study provides important knowledge about the infiltration and distribution of urban biocides in urban districts.

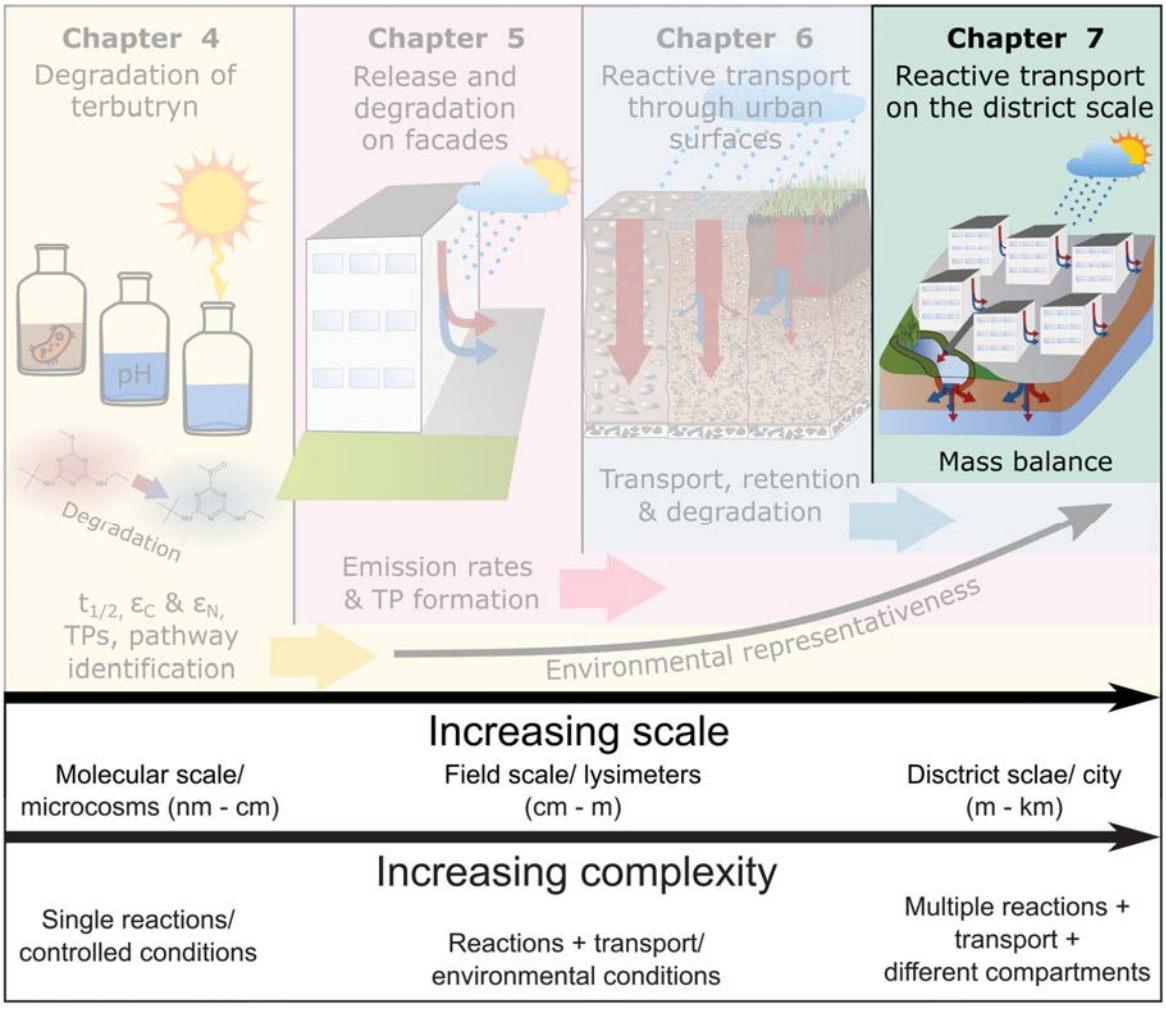
Chapter 4
Degradation of terbutryn
pH
Degradation
t1/2, εC & εN, TPs, pathway identification
Chapter 5
Release and degradation on facades
Emission rates & TP formation
Chapter 6
Reactive transport through urban surfaces
Transport, retention & degradation
Chapter 7
Reactive transport on the district scale
Mass balance
Environmental representativeness
Increasing scale
Molecular scale/ microcosms (nm - cm)
Field scale/ lysimeters (cm - m)
Disctrict sclae/ city (m - km)
Increasing complexity
Single reactions/ controlled conditions
Reactions + transport/ environmental conditions
Multiple reactions + transport + different compartments

Chapter 7
Urban biocide release from facades toward sustainable stormwater management systems: combining monitoring and modeling at the district scale

This chapter is an edited version of the article under preparation:

Sereni, L.‡, Junginger, T.‡, Imfeld, G., & Payraudeau, S. (2022). Urban biocide release from facades toward sustainable stormwater management systems: combining monitoring and modeling at the district scale

‡ These authors contributed equally to this work

Chapter 7

Abstract

Sustainable stormwater management in cities promotes the infiltration of water through ditches, trenches and swale systems towards groundwater to reduce surface water runoff but might result in leaching of contaminants. Although urban biocides such as terbutryn, used in construction materials (e.g., facade paint and render) to reduce algae growth, are released from construction materials with each rain event and have been detected in groundwater, knowledge of their distribution and infiltration on the district scale is missing. Here, we conducted a detailed field campaign including regular sampling of water, sediment, soil and plant material for biocide analysis, description of the water balance through hydroclimatic parameters and land use data and a modeling framework to identify distribution and hot spots of biocide infiltration in an eight-year-old district with sustainable stormwater management. Biocide monitoring indicated that predicted no effect concentrations were regularly exceeded for terbutryn and diuron in water while transformation product concentrations exceeded those of terbutryn. Measured concentrations in soil and sediment indicated accumulation, while plant uptake was confirmed with concentrations exceeding 1000 ng g^{-1} terbutryn in plant shoots and roots. Our modeling approach revealed high contribution of biocide infiltration towards groundwater close to facades (27 – 73%), while only a small biocide fraction (7-39%) reached stormwater management systems (infiltration trench and pond). Major biocide input towards groundwater occured prior to reaching infiltration systems, through permeable surfaces (e.g., pavement), bypassing infiltration systems. Overall, our model holds potential to improve implementation of measures to reduce biocide infiltration towards groundwater in sustainable stormwater management.

1 Introduction

Current urban planning strategies promote sustainable stormwater management (SSM) with the aim to reduce stormwater runoff by infiltration through ditches and swale systems, however, contaminants such as biocides might not be sufficiently retained, therefore enter groundwater (Barbosa et al., 2012; Goulden et al., 2018; Hensen et al., 2018; Linke et al., 2021; Vijayaraghavan et al., 2021). In the urban environment, biocides are used in building materials (e.g., facade paint and render) to prevent growth of algae, mosses, fungi and bacteria (Burkhardt et al., 2011; Paijens et al., 2021). Those biocides leach from facades with wind driven rain and emissions can continue for several years, while the release of transformation products (TPs) can exceed emissions of parent compounds (Bollmann et al., 2017b, 2016; Hensen et al., 2018; Linke et al., 2021). In contrast to agricultural pesticide application, urban biocides are discharged with each rain event, resulting in chronic exposure of the environment. Urban biocides and their TPs have been detected ubiquitously in rivers, soil and groundwater with concentrations regularly exceeding predicted no effect concentrations (PNEC) (Bollmann et al., 2017b, 2016; Burkhardt et al., 2011; Hensen et al., 2018; Linke et al., 2021; Paijens et al., 2021; Quednow and Püttmann, 2007; Schoknecht et al., 2016; Vega-Garcia et al., 2020; Wittmer et al., 2010). However, detailed distribution and infiltration mechanisms on the district scale have rarely been addressed.

Most studies focused on urban biocide percolation into groundwater through storm water infiltration and swale systems which may be accelerated by fast flow through macropores (Bork et al., 2021; Hensen et al., 2018; Pinasseau et al., 2020). In contrary, a large fraction of the biocides diuron (> 90%) and terbutryn (89%) remained on the release site rather than being transported towards surface water or stormwater drainage and infiltration systems (Linke et al., 2022; Wicke et al., 2022). This biocide fraction may thus enter groundwater through via leaching Biocide release was monitored mainly from freshly experimental painted facades (Vega-Garcia et al., 2020), direct release in drainage pipes (Linke et al., 2021) or as a function of weather characteristics (Bester et al., 2014; Burkhardt et al., 2012; Schoknecht et al., 2016). However, only scarce, and incomplete data about long term distribution and reactive transport of urban biocides and their TPs in urban compartments (e.g., surface runoff, infiltration, retention and transformation in urban surfaces receiving leachate from facades) is available. In addition, estimations of mass fluxes on the district scale and the identification of hotspots for biocide accumulation and infiltration towards groundwater are currently missing. However, this

knowledge is crucial for measures to prevent groundwater resources and reduce ecotoxicological risk through biocides in urban districts.

For extrapolation of long-term biocide emissions from facades, models such as COMLEAM (COnstruction Material LEAching Model), FReWaB-PLUS (FReiburger Regewasser-bewirtschaftung – Plus Strofftransport), and others might be used (Bork et al., 2022; Burkhardt et al., 2020; Coutu et al., 2012a; Wittmer et al., 2011). These models incorporate material properties (as emission functions) and weather data (precipitation, wind speed and wind direction) for calculations that infer wind-driven rain as the primary factor controlling leaching. The models also integrate runoff coefficients for various building materials as well as the building geometry of structures to estimate facade leaching. Although models differ in the spatial and temporal resolution, they may help for preliminary risk assessments. Those models rely on available field data, initial applied biocide mass, precipitation and wind data or the facade surface area, as well as sufficient data to calibrate the models for biocide release and distribution in different environmental compartments. Moreover, the model genericity is currently limited by the high heterogeneity of catchments and city in terms of land-use and impervious surfaces, the age and the orientation of buildings or the weather conditions (Gaylarde et al., 2003). Even though several surface runoff models exist to predict biocide discharge into surface waters, local infiltration into groundwater remains largely unknown and is not yet accounted for.

The purpose of this study was thus to estimate the fate of biocides at the district scale to assess potential hot spots of infiltration towards groundwater and assess associated environmental risk. Therefore, we developed a general framework to assess biocide leaching and infiltration in urban residential areas using terbutryn as a model urban biocide due to its ubiquitous use in facade paints, abundance in various environmental compartments (Bollmann et al., 2017a; Hensen et al., 2018; Quednow and Püttmann, 2007) and high toxicity (Burkhardt et al., 2009; Kresmann et al., 2018). Within this framework, we conducted a detailed monitoring campaign in a 2.4 ha district including detailed monitoring of water discharge, hydroclimatic variables and biocide and TP measurements in various environmental compartments (water, soil, sediment, plants) over 4 months to establish a site-specific hydrological and chemical mass balance. This allowed to develop a modeling framework, coupling biocide release from facades with transport in the district towards SSM infiltration systems. Finally, we assess the effects on water quality by comparing measured concentration in the different compartments (soils,

retention basins, vegetation sediments and groundwater) with predicted no effect concentrations (PNEC) (Wicke et al., 2022). Our approach, including a detailed field campaign with a modeling framework, may improve prediction of urban biocide distribution on the district scale to quantify biocide release toward urban surface-soil interfaces and groundwaters and its effect on non-targeted organisms.

2 Material and Methods

2.1 Description of the field site

Field monitoring was conducted at a study site north of Strasbourg, France (Schiltigheim, Adelshoffen district, 48°36'31.7"N 7°44'54.8"E), on an area of 2.4 ha constructed from 2014 to 2015 (Figure 7. 1). The field site includes two sub-catchments (Figure E 1-Figure E 3) with water draining either into a vegetated stormwater retention pond with an overflow area and infiltration wells (activated during high water levels) or an infiltration trench (Figure 7. 1). The district is composed of 10 buildings and a playground area. Positions of automatic samplers and devices are marked in Figure 7. 1. Field sampling and monitoring were conducted between May 5th (Day 0) and August 24th, 2021 (Day 112).

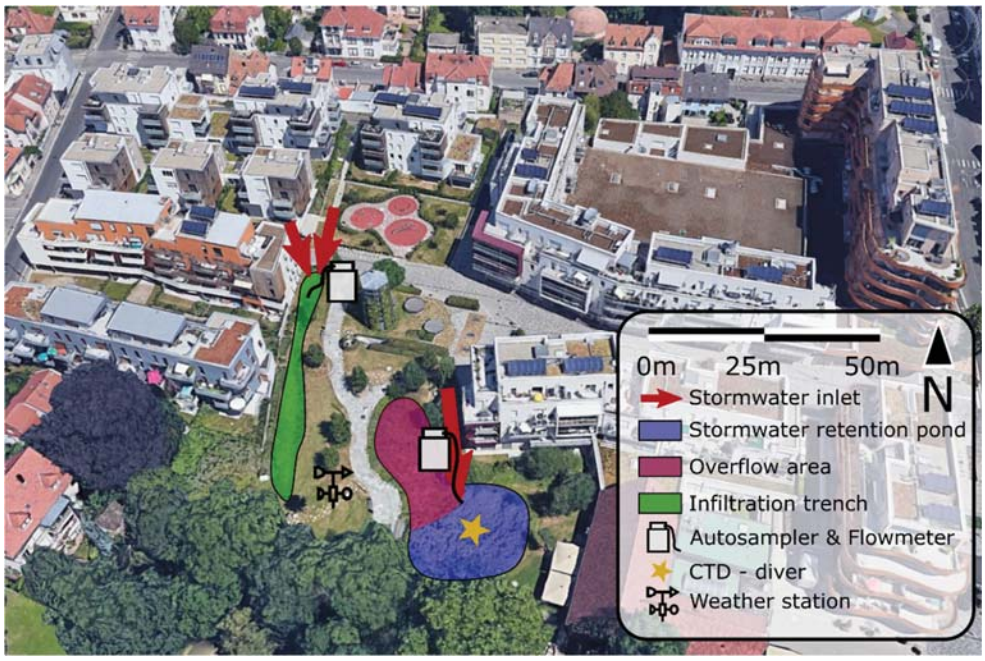

Figure 7. 1. Aerial overview of the field site, including two stormwater retention systems, and location of sampling devices and inlets of drainage pipes.

2.1.1 Land use characterization

The two main characteristics of the district surfaces were determined: i) delineation of the sub-catchments either discharging into pond or the trench system according to EMS LiDAR data (Figure E 3) ii) the land use type and therefore the runoff coefficient of the respective surfaces. The land use type was categorized into conventional, gravel, non-connected, sealed and vegetated roofs for buildings, and into wood chips, grass, permeable surface (e.g., gravel or pavement with joints), playground and sealed pavement (Figure E 3). The land use type was characterized by field surveys with an emphasis on the material in direct contact with the facades (e.g., first meter from facade), where direct infiltration of biocides into sub-surface occurs during rain events.

Each land use type was defined as polygon in GIS (Figure E 3). For each land use type, we assessed the runoff coefficient based on the biocide leaching model FreWAB-PLUS (Bork et al., 2022) and data from the technical information of the district engineers (e.g., for the playground surface). Table E 1 summarizes the area of each land use type and associated runoff coefficient for each catchment.

2.1.2 Facade characterization

Building characteristics such as height and area were extracted based on LIDAR data and analyzed in GIS (Figure E 4) to estimate facade areas. The proportion of windows (estimated through field photographs and field surveys) was calculated as it contributes to facade runoff but not to biocide leaching. Facades in direct connection with ground and in connection with intermediate roof were considered, assuming that terbutryn leached from facades in connection with intermediate roof reached ground through gutters.

2.1.3 Hydroclimatic data

Discharge and water level at each sub-catchment outlet (pond and trench inlet) were continuously measured by a flowmeter (ISMA DLK 102, 1 min resolution) connected to a venturi channel equipped with an ultrasonic sensor. Water level in the pond was measured using a CTD diver (DI 282, 5 min resolution) with barometric compensation (Baro-Diver DI 800). Elevation-storage curves were derived for the pond and the trench from LIDAR data.

2.2 Biocide monitoring

2.2.1 Automatic event-based sampling

Water was sampled using an automated sampler (ISCO Avalanche) coupled to a flowmeter for flow proportional sampling, consisting of two sampling schemes: (i) for the first 9 samples, 110 mL was taken after 1 m^3 of discharge, three times into the same sampling bottle. (ii) bottle 10 - 12 were filled by collecting 110 mL after 10 m^3 three times per sampling bottle. Due to flooding of the venturi channel for large discharge events, the automatic sampling was limited.

2.2.2 Grab sampling

Water. Grab samples of water were taken weekly or bi-weekly in the infiltration pond and trench if water was available (e.g., water level higher than 5 cm). Samples were taken using a cleaned

telescope sampling scoop from 5 random locations within the pond or trench, respectively. Samples consisted of around 10 L (pond) and 5 L (trench) and were successively filtered at 11 µm (Whatmann 1001-047) followed by 0.45 µm (CA Membrane filter) and stored for < 24 h at 4°C until further analysis.

Sediment, soil and plants. Soil and sediment samples were taken according to US EPA soil sampling procedure. Samples were taken four times from 04th May to 27th July (every four weeks). One sampling campaign included five individual sediment samples in pond (n=5), one trench soil sample (n=1), one plant sample from the pond (n=1) and one plant sample from the trench (n=1). For soil and sediment sampling, surface material, like grass, roots and debris (top 5 cm) was removed with a cleaned shovel. Each sample consisted of three subsamples of about 20 g from the top 5 cm of a 50 × 50 cm radius, collected in a prelabelled plastic bag and mixed to obtain homogeneity. In the trench, five subsamples of soil and plant material, respectively were collected each meter for 5 m from the main inlet. Plants of the Genus *Phragmatis* in the infiltration pond (covering 60-80% of the surface) were collected at five random locations. Plant material was separated into roots and aerial material directly in the field. All 5 respective plant samples were separated into aerial and root parts and respective aerial or root parts were pooled to one sample. All samples were transported to the laboratory within 2 h and prepared for extraction within 24 h. Samples were stored prior to extraction at 4°C.

Soil and sediment samples were sieved to 2 mm prior to extraction. The physicochemical characteristics of the sieved soil and sediment samples (Table E 2) were measured using standard analytical procedures (NF/ISO) (Droz et al., 2021). Plant material was washed prior to extraction (Gilevska et al., 2022). Briefly, roots and rhizosphere were shaken for 10 min in ultrapure water followed by replacement of water until no more turbidity change in water was observed. Roots were rinsed twice with 0.9% NaCl to remove rhizosphere and rhizoplane sediment. Samples were homogenized with a hand blender (Bosch MSM66110) and samples were frozen (-20°C) prior to extraction.

2.3 Extraction and analysis

2.3.1 Extraction

Biocides in sediment, soil and plant materials were extracted in triplicates using a modified ultrasonic-assisted solid-liquid extraction (MUSE), described and validated previously for terbutryn (Gilevska et al., 2022; Junginger et al., 2022, Chapter 6). Briefly, 5 g of soil or sediment (dry weight) and 3 g of plant material were placed in an amber glass centrifuge tube. Samples were extracted using 3 mL DCM:Pentance (3:1, V:V) followed by vortexing (5s) and ultrasonication (Branson 5510, 40 kHz) for 5 min. Solvent was separated from the sample by centrifugation (2400 rpm) for 20 min. Supernatants were transferred to amber glass vials and the procedure was repeated two more times. Solvent was evaporated under gentle N_2 stream and resuspended in 1 mL acetonitrile. All samples were cleaned prior to measurement using anhydrous magnesium sulfate ($MgSO_4$, 75 mg) and primary-secondary amine (PSA bond silica, 13 mg) (Anastassiades et al., 2003).

2.3.2 Analysis

Terbutryn, four of its TPs (terbutryn-sulfoxide (TerSO), terbutryn-2-hydroxy (TerOH), terbutryn-desethyl (TerDesE), terbutryn-desethyl-2-hydroxy (TerDesEOH)), diuron and octylisothiazolinone (OIT) were quantified using HPLC-MS/MS (Dionex/Thermo Scientific UltiMate Dionex 3000 coupled to Thermo Scientific TSQ Quantiva) as described previously (Chapter 6). LOQ, LOD, mass transitions and solvent gradients were reported previously (Chapter 6). Recoveries are provided in Table E 3.

2.4 Water balance

A water balance over the district was established by considering infiltration between buildings into soil, discharge into trench and pond, evapotranspiration in pond and trench and infiltration towards groundwater in the pond and trench. The amount of rainfall was calculated based on a local weather station in the field site recording amount of rainfall each 10 min as described in

(Chapter 5). Due to lack of data because of a power failure and flooding between June 1st and June 19th and after August 15th, we focused on 2 separated periods of study (May 5th to May 31st further named “May period” and June 20th to August 5th further named “summer period” (Figure E 5).

Considering discharge dynamics, independent rain-runoff events were extracted, separated by > 20 h without rainfall. Rain event intensity and volume were characterized using the IETD R package (Duque, 2020). The event rainfall volume in trench and pond sub-catchments was then calculated based on the respective catchment area. As the flooded surface of both trench and pond depend on their volume according to elevation-storage curves, the uncertainty in rainfall volume directly falling in them was taken into account considering a minimal and a maximal surface area.

For each rain event, we calculated cumulative discharge volume in the trench and pond systems. For the pond, flowmeter data was missing in a large part of the studied period due to flooding of the venturi channel. Therefore, we reconstructed the cumulative runoff volume per event based on CTD records rather than flowmeter discharge, using the elevation-storage curve. Event-based infiltration and runoff coefficients were derived from observed rainfall and water volume reaching the trench and the pond.

Evaporation on flooded pond and trench surfaces was calculated based on daily estimation of potential evapotranspiration (PET) provided by MeteoFrance (Entzheim station) assuming that PET was systematically effective on flooded areas. The dynamic of flooded areas was derived from elevation-storage curves both for trench and pond systems. Infiltration rates in trench and pond were estimated by fitting the decrease of volume using elevation-storage curves both for trench and pond using R lm and nls regression functions.

Based on the technical plan of the district and direct observation, we expected i) a connection from trench to pond above a defined water level ii) infiltration wells around the pond designed to enhance infiltration, activated above a defined water level. The observed dynamics of water level confirmed a faster decrease of water level, i.e., differing by one order of magnitude, in trench when the trench was connected to the pond (only for 7 rain event during the campaign) and when the infiltration wells around the pond were activated (associated to the 3 largest rain events).

2.5 Biocide mass balance

The concentration of biocides measured in the grab samples and reconstructed water volume for the investigated period were used to calculate the quantity of biocide in each retention system at each sample.Concentrations of terbutryn from event sampling with autosamplers were transferred to mass loads (M_{obs}) using discharge volume and used to inversely estimate initial terbutryn concentration in facades (C0) using COMLEAM (detailed in SI). The cumulative leaching from facades was discretized in weekly leaching amount from the 4th of May to the 28th of August.

The fraction of biocides reaching trench and pond (B_{outlet}) and the amount of biocides infiltrated ($IF_{biocide}$) over each sub-catchment (SC) was calculated based on the mean infiltration coefficient (IC) and biocide mass in runoff ($R_{biocide}$) for each event (i) as:

$$IF_{biocide}\,(SC, i) = IC \times R_{biocide}\,(i, SC) \quad \textbf{(7.6)}$$

$$B_{outlet}\,(SC, i) = (1 - IC_{SC}) \times R_{biocide}\,(i, SC) \quad \textbf{(7.7)}$$

2.6 Long-term biocide mass balance

Long term biocide release, i.e., from 2014 (district building) to the end of the 2021 campaign, was modelled with a three-step approach. First, biocide leaching for each facade orientation and land use connection of building's facade was model based on COMLEAM for highest and lowest estimated initial concentrations (Figure E 6) (Burkhardt et al., 2020). Additional hydro-climatic data was collected to cover the 8-year reactive transport estimation. Hourly precipitation was measured and provided by the EMS in Schiltigheim (5 km south-east of the studied district) and in Bischeim (5 km north-west of the studied district). Wind data was obtained from MeteoFrance weather station situated in Enzheim (48.55°N, 7.63°E), 10 km southeast of the studied district.

Chapter 7

3 Results

3.1 Water mass balance

The yearly rainfall measured 2021 by EMS was of 929 mm, indicating that the studied period, with 109 mm during the May period and 299 mm during the summer period, covered 44% of the yearly precipitation. During the field campaign, most rain events were associated with wind from south or southwest. Few rain events were associated with wind from east or southeast and no rain event was associated with rain from north (Figure E 7). Evaporation remained limited at the seasonal scale with volumes 20 to 50 times smaller than rainfall (Figure E 8).

Based on the two periods cumulative discharge into the trench was estimated to 444 m^3 for May (05/05 to 31/05) (Figure E 9a) and of 648 m^3 for June and August (19/06 to 09/08) (Figure E 9b), representing 30 – 40% of rainfall volume. For the pond, the cumulative discharge was 179 m^3 for May and 1106 m^3 for the summer period (40 – 90% of precipitation in sub-catchment). Based on water-level recordings, only 35 m^3 were transferred through the connection from trench towards pond (6.6 m^3 being in May and 20 m^3 in summer).

The event-based runoff coefficients (based on rain volume in sub-catchment vs. discharge) for the trench sub-catchment was 39 ± 7% across the study periods (Figure E 10). For the pond system, the event-based runoff coefficient for both periods was 36 ± 4%, except for three intense storm events in summer. Storm events with heavy rainfall during short time led to soil saturation and an increase of the runoff coefficients up to 90% (Ren et al., 2020; Xue and Gavin, 2008). Comparatively, the mean runoff coefficients for trench and pond sub-catchments based on the type of land use and the runoff coefficient from the FreWab-Plus model and literature were 53% and 58%, respectively. The computed runoff coefficients estimated eight years after construction of the district (30% less than in FreWaB-Plus) are in line with predictions as runoff is expected to reduce with soil aging and increasing pavement pore porosity (Díaz-Sanz et al., 2020; Shuster et al., 2014; Yang and Zhang, 2011).

Three different infiltration rates in the pond system were derived from the water elevation data. A slow infiltration rate of 0.008 (± 0.005) $m^3\ min^{-1}$ (8 E^{-6} m s^{-1}) was close to the 3.6 E^{-7} m s^{-1} reported for loess soil by the technical reports after infiltration tests. A median infiltration rate of 0.005 (± 0.003) $m^3\ min^{-1}$ can be explained by preferential flow in macropores, as previously

reported in aged stormwater retention ditches, which may result in biocide transport toward groundwater (Bork et al., 2021). The fast infiltration rate of 0.16 (±0.01) m^3 min^{-1} correspond to the activation of three infiltration wells (Figure E 11) with a designed infiltration capacity of 0.11 m^3 min^{-1}. The fast infiltration through infiltration wells poses an elevated risk for groundwater contamination as the organic rich sediments and 4-m loess soil layer is by-passed. Biocides may thus directly reach deeper gravel layers, and the water table 6-m below the ground level. The fast water level decrease rates in the trench indicated activation of the connection to the pond with an estimated discharge volumes of 6.6 m^3 in May and 20 m^3 in summer.

3.2 Biocide concentrations in the infiltration systems

Terbutryn was detected systematically in all investigated matrices (Figure 7. 2). Concentrations of weekly grab samples in water of the infiltration pond were lower than concentrations in the trench for terbutryn and its four TPs (Figure 7. 2a). Concentrations of TPs in the trench regularly exceed those of terbutryn. Regular detection of terbutryn and TPs is in line with previous studies, indicating chronic release of biocides and TPs from facades over several years (Hensen et al., 2018; Linke et al., 2021; Wicke et al., 2022). Concentrations were in agreement with previous field studies conducted in Germany, Switzerland and Denmark (Bollmann et al., 2014; Burkhardt et al., 2011; Hensen et al., 2018; Linke et al., 2021). High concentrations for terbutryn-sulfoxide, previously identified as a major TP during photodegradation and biodegradation (Junginger et al., 2022 and Chapter 5), was observed predominantly in the trench. Contrary to terbutryn, diuron concentrations in the pond were higher than in the trench system, and regularly exceeded 100 ng L^{-1} (Figure 7. 2b), whereas OIT was not detected. In both systems, measured concentrations regularly exceeded PNEC values for terbutryn (3 – 34 ng L^{-1}) and diuron (20 ng L^{-1}) (Burkhardt et al., 2009; Kresmann et al., 2018). Therefore, even eight years after constructions potential ecotoxicological risk might exist, especially considering the chronic exposure of soil and water biota. Concentrations of terbutryn and diuron suggest that different paints have been used in the sub-catchments, with different proportions of terbutryn and diuron. Additionally, the initial concentrations of terbutryn may differ among facades (e.g., through different used paints) or not all facades were coated with biocide containing materials. However, the detailed information of used paints was not available eight years after the district construction.

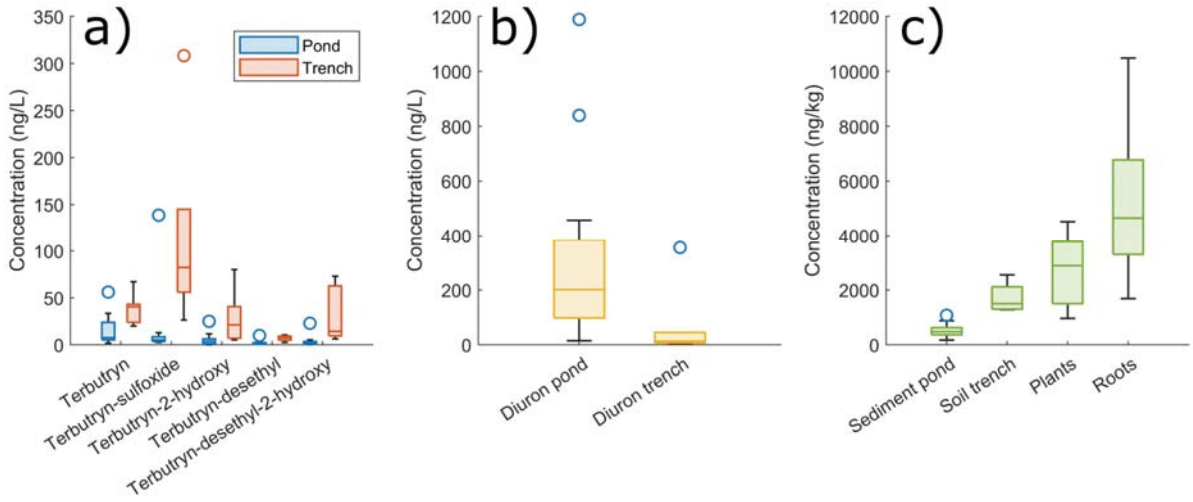

Figure 7. 2. a) Measured concentrations of terbutryn and transformation products in pond (n=13) and trench (n=6) water. b) Diuron concentrations in pond (n=13) and trench (n=6) water. c) Concentrations of terbutryn in sediment (n=20) and soil (n=4) and plant material (n=8) (ng/kg dry weight). Outliers are defined as data points located outside the whiskers.

The detailed screening of sediment, soil and plant material (Figure 7. 2c) indicated accumulation of terbutryn in the soil of the trench system with concentrations exceeding 1500 ng kg^{-1} as well as abundance of terbutryn in the sediment of the stormwater pond (500 ng kg^{-1}), while concentrations of diuron and OIT where below the detection limit**.** Higher concentrations of terbutryn in trench soil compared to sediment of the pond can be explained by higher emissions of terbutryn from the trench sub-catchment. In addition, higher organic carbon content, and thus higher potential sorption, in soil compared to sediment (Table E 2) may also contribute to terbutryn accumulation. Ecotoxicological data on soil microbioms remain scarce (Reiß et al., 2021), while ecotoxicological tests might be insensitive to specific mode of actions of biocides. E.g., microtox studies were conducted for terbutryn with the bacterium *Aliivibrio fischeri* indicated low effects of terbutryn, although terbutryn is a photosynthesis inhibitor, hence higher toxicity against algae than bacteria is expected (Bollmann et al., 2017a). Further, time-cumulative inhibition of bacterial growth was observed for terbutryn, indicating that effects of chronic exposure (e.g., through continuous facade runoff with each rain event) might be underestimated (Fernández-Calviño et al., 2021). Therefore, accumulation through constant input of biocides in soil and sediments and their ecotoxicological potential need to be investigated in further studies.

Overall, the results indicate terbutryn retention in soil and sediment during infiltration. Depending on the sorption and degradation rates, sediment and soil may thus reduce biocide emissions towards groundwater and accumulation in soil and sediment and therefore potential chronic ecotoxicological effects may occur onto soil and sediment ecosystems. Further, transformation products might contribute to ecotoxicology by additive or synergistic effects (Hensen et al., 2020).

Additionally, terbutryn was detected in plant and root material in both, trench, and pond system, in concentrations consistently exceeding 1 µg kg^{-1}, confirming plant uptake (Figure 7. 2c, Chapter 6). Uptake into plants was not reported previously in urban environments but might be an important sink for urban biocides (Figure 7. 2c). Plants might be able to metabolize and finally mineralize urban biocides and therefore reduce transport towards groundwater. Uptake of terbutryn in parrot feather (*Myriophyllum aquaticum*) was reported previously (Turgut, 2005) and aquatic plants were discussed for potential phytoremediation strategies of various pesticides (Gao et al., 2000; Turgut, 2005). However, detailed uptake rates are missing and the mass flux into plants on the district scale needs further consolidation.

3.3 Biocide masses in the infiltration systems

The terbutryn and TP masses in the pond and the trench during the sampling campaign were generally below 1 mg for each compound while one sampling associated to a heavy rain event resulted in 7.8 mg terbutryn and 42 mg TerSO, 8 mg TerOH, 3 mg TerDesE and 7 mg TerDesEOH in the pond, representing 1.9, 10.3, 1.9, 3 and 0.7 µg m^{-2} facade, respectively (13^{th} July, Figure E 12). Similar results were observed for diuron, with masses < 20 mg in all pond samples besides for the same heavy rain event leading to stored masses exceeding 250 mg, representing 61.4 µg m^{-2} facade in the catchment (Figure E 13).

Hence, while heavy rain events may not necessarily lead to high concentrations, they may carry large mass fluxes resulting from high mass release from facades, causing fast infiltration of high (> 100 mg) biocide loads towards groundwater (e.g., through macropores or infiltration wells).

Even though grab samples of water and solid samples allow to estimate potential entry paths and distribution of urban biocides in a field site, setting up mass balances based on observed data alone is not possible because reactive transport processes prior to sampling are not accounted for. As a result, biocides mass balances cannot be directly estimated. A modeling approach is thus needed to incorporate concentration measurements with the water mass balance to identify sinks, retention capacity and transport pathways towards groundwater.

3.4 Biocide mass balance and fluxes at the district scale

Estimated terbutryn C0 (in mg per m^2 facade) in facade leachate to predict the entering mass in the infiltration trench and pond systems varied weekly from 35 to 447 mg m^{-2} (median= 109 mg m^{-2}), based on the assumption that all buildings contain terbutryn and using default emission curves from COMLEAM (Burkhardt et al., 2020). Total terbutryn concentrations in paints ranging from 300 to 4000 mg m^{-2} have been reported (Burkhardt et al., 2011). Terbutryn concentrations ranged between 250 and 560 mg m^{-2} in paints in 2016 (Schoknecht et al., 2016), while previous reports in 2012 rather reported concentrations around 1200 mg m^{-2} (Coutu et al., 2012b). Either the initial concentrations in paints in the district were low, or some buildings were painted with terbutryn-free paint. Hence, the estimated C0 might corresponded to a dilution of facade runoff with paint containing and paint without terbutryn. According to the weekly calibrated values in 2021, two scenarios of C0 were considered for the initial concentration in 2014 with 79.55 “low” to 259.70 mg m^{-2} “high estimation” The cumulative emission curves are represented in Figure E 6. Estimated emissions of terbutryn over the eight years varied from 18.3 to 82.9 g (1.5 to 6.9 mg m^{-2}) using COMLEAM default release parameters.

The biocide mass balance is presented for the 2 initial C0 (“low” and “high” emission C0 scenario) in Table 7. 1. From the emitted terbutryn 27% and 73% for pond and trench sub-catchment, respectively, infiltrated directly in the soil. This represented a terbutryn mass from 11.0 to 49.7 g (0.9 and 4.0 mg m^{-2} catchment area, respectively) for the district over the eight years. For each sub-catchment and based on runoff coefficients calculated for water, the total biocide infiltration was estimated as the sum of the direct infiltration at the facade and the infiltration before the stormwater system. The total biocide infiltration varied between 34% and 65% of the leached mass of terbutryn for the pond sub-catchment, while it represented about

90% of the leached mass for trench sub-catchment (Table 7. 1). Between 13.5 and 71.3 g of terbutryn infiltrated over the whole district while 2.6 to 21.8 g reached the two basins. Overall, these results were in agreement with previous studies, indicating strong infiltration and retention prior to reaching infiltration systems (Linke et al., 2022; Wicke et al., 2022).

Table 7. 1. Summary of the quantity of terbutryn emitted and emissions normalized by catchment area, directly infiltrated close to facades, infiltrated over the whole district and reaching the infiltration facilities (pond and trench), calculated from Jan. 2014 to Dec. 2021 for 2 initial concentrations. Runoff coefficients of 0.3 and 0.4 were used for trench sub-catchment and of 0.4 to 0.9 were used for pond sub-catchment.

	"low" C0 = 79.55 mg m^{-2}				**"high" C0 = 259.70 mg m^{-2}**			
	Trench		**Pond**		**Trench**		**Pond**	
Emission (g) (mg m^{-2})	13.2 (1.7)		5.1 (1.3)		59.7 (7.4)		23.3 (5.7)	
Direct infiltration (g) (mg m^{-2})	9.6 (1.2)		1.4 (0.3)		43.3 (5.4)		6.4 (1.6)	
Runoff coefficient	0.3	0.4	0.4	0.9	0.3	0.4	0.4	0.9
Total infiltration (g) (mg m^{-2})	12.1 (1.5)	11.75 (1.5)	3.65 (0. 9)	1.78 (0.4)	54.75 (6.9)	53.12 (6.7)	16.51 (4.0)	8.05 (2.0)
Entering SSM system (g) (mg m^{-2})	1.08 (0.14)	1.45 (0.20)	1.50 (0.37)	3.37 (0.83)	4.90 (0.61)	6.53 (0.82)	6.77 (1.7)	15.23 (3.7)
Proportion infiltration (%)	92	89	71	35	92	89	71	35
Proportion to SSM (%)	8	11	29	65	8	11	29	65

	Total district			
	"low" C0 = 79.55 mg m^{-2}		**"high" C0 = 259.70 mg m^{-2}**	
Emission (g) (mg m^{-2})	18.34 (1.5)		82.94 (6.9)	
Direct infiltration (g) (mg m^{-2})	10.99 (0.9)		49.68 (4.0)	
Runoff coefficient	0.3	0.4	0.4	0.9
Infiltration total (g) (mg m^{-2})	15.76 (1.3)	13.53 (1.1)	71.27 (5.9)	61.17 (5.1)
To SSM system (g) (mg m^{-2})	2.58 (0.21)	4.82 (0.40)	11.67 (0.97)	21.77 (1.8)

Taking into account a K_{OC} for terbutryn of 663 and a typical soil organic content of 40 g.kg^{-1} (based on technical report of the construction site), it can be estimated that the mass of terbutryn accumulated in soil is 27 times larger than the terbutryn mass leached below the 4 m loess layer. A cumulative amount from 0.5 to 2.7 g of terbutryn leaching to groundwater and from 15.2 to 68.6 g of terbutryn sorbed in soil can thus be estimated over the eight years. Considering the long degradation half live times of terbutryn during biodegradation (80 - > 200 d) (Bollmann et al., 2017a; Junginger et al., 2022), leaching towards groundwater over long time periods can be expected, however, concentrations in groundwater might be low. A better

estimation of terbutryn reaching groundwater and incorporation of uncertainties could be provided in the future using a 1D reactive transport model, such as Hydrus (Šimůnek et al., 2013) or MACRO (Larsbo et al., 2005), explicitly accounting for retention processes (e.g., sorption, degradation and advection) of terbutryn into surface and deep soil layers with different physico-chemical characteristics.

For two events with heavy precipitation and strong runoff, activating the infiltration wells, the biocide amount bypassing the soil layers through the wells can be estimated. Based on concentrations and infiltrated volume (e.g., 48 m^3 and 90 m^3 on 18.05.2021 and 24.08.2021, respectively), 150 and 530 µg of terbutryn and 13 and 10 mg of diuron went through the infiltration wells.

Overall, these results highlight that, infiltration around buildings (in direct contact to facades) may be a major pathway of biocide entry towards groundwater in urban districts, accounting for up to 73% for the total biocide flux at the district scale. However, through organic rich materials (e.g., wood chips or vegetated soils), biocides with moderate to high Koc could be retained through sorption. In both sub-catchments, only a small proportion of the leached biocides reached the implemented SSM systems, whereas direct infiltration at facades or diffuse in the district prevailed (Figure 7. 3). In the SSM systems, biocides can bypass the retention systems through infiltration wells during heavy rain events.

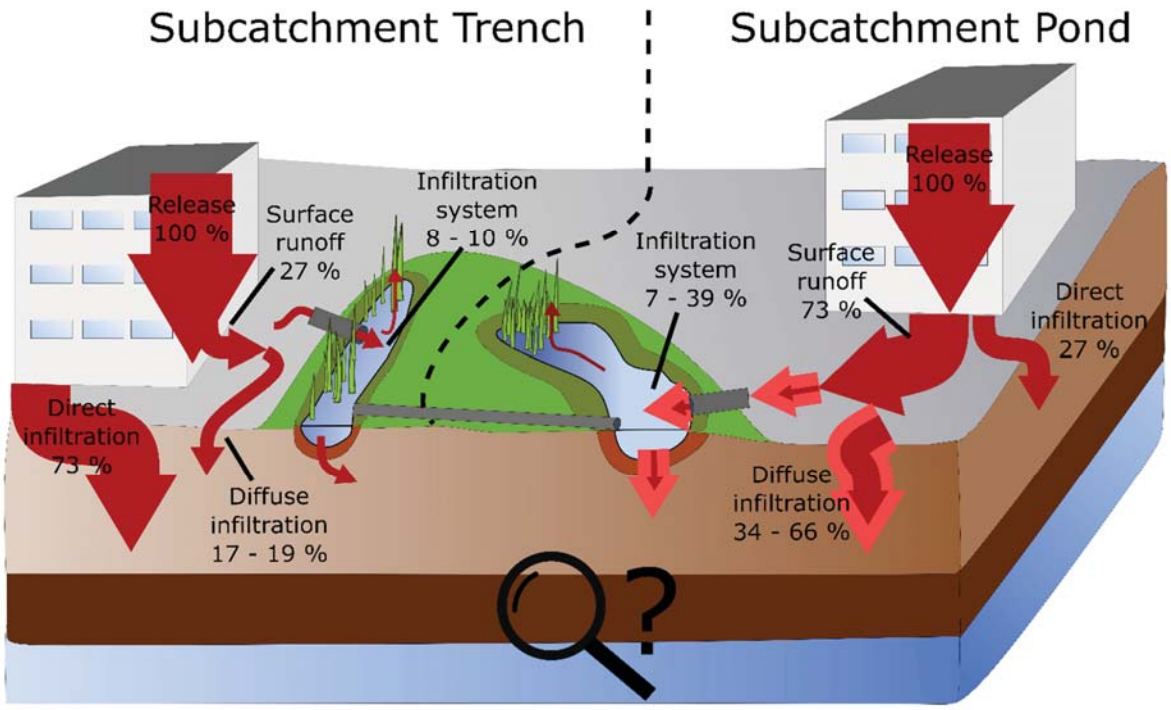

Figure 7. 3. Scheme of relative biocide transport and infiltration paths in the two investigated sub-catchments. Shaded arrows indicate uncertainties in estimations based on our model. Infiltration into deeper soil layers and groundwater are not considered within this study.

4 Conclusion and perspectives

Biocides are released from building facades during each rain event and chronically contaminate urban districts, posing potential ecotoxicological effects even eight years after the district construction. The ubiquitous occurrence of terbutryn in, water, soil, sediment and plant materials highlights the extent of contamination and the distribution among the district compartments. However, chronic ecotoxicological effects in soil, sediment and water are not well understood and should be addressed in future studies and incorporate TPs. Plant uptake in retention facilities might be an important sink of urban biocides

Our results emphasize that biocide mass balances on the district scale rely highly on the availability of data (e.g., characterization of facade areas and surface areas) of the district and

monitoring quality, including discharge measurements and biocide concentrations to identify potential entry points of biocides towards the sub-surface. We propose that in SSM systems infiltration of biocides into subsurface and successively groundwater might occur dominantly prior to reaching the retention systems. In contrast, vegetated infiltration systems may act as biocides sinks and hence their retention and degradation.

The proposed model framework enabled to identify mass fluxes e.g., infiltration and surface runoff, although reactive transport through soil towards groundwater is not considered yet and will be the next logical step. As discussed in Chapter 6, reactive transport through soil is highly influenced by soil properties and degradation rates. We thus suggest that in future studies, modeling approaches should be used that implement site-specific reactivity in soil layers to assess reactive transport towards groundwater, considering sorption and degradation. Thus, additional measures could be taken to reduce biocide reactive transport towards groundwater in identified hotspots of infiltration, e.g., through adding additional soil layers with high organic content to retain the biocides.

Finally, recent studies have emphasized that terbutryn and other biocides are already degraded on facades prior to leaching, mainly through photodegradation (Bollmann et al., 2017b, 2016, Chapter 5). The release models proposed here may thus integrate the release of TPs, as suggested in Chapter 5), using irradiation and precipitation as main hydroclimatic variables to predict the contribution of TPs in facade runoff.

References

Anastassiades, M., Lehotay, S.J., Štajnbaher, D., Schenck, F.J., 2003. Fast and Easy Multiresidue Method Employing Acetonitrile Extraction/Partitioning and "Dispersive Solid-Phase Extraction" for the Determination of Pesticide Residues in Produce. J. AOAC Int. 86, 412–431.

Barbosa, A.E., Fernandes, J.N., David, L.M., 2012. Key issues for sustainable urban stormwater management. Water Res., Special Issue on Stormwater in urban areas 46, 6787–6798.

Bollmann, U.E., Fernández-Calviño, D., Brandt, K.K., Storgaard, M.S., Sanderson, H., Bester, K., 2017a. Biocide runoff from building facades: degradation kinetics in soil. Environ. Sci. Technol. 51, 3694–3702.

Bollmann, U.E., Minelgaite, G., Schlüsener, M., Ternes, T., Vollertsen, J., Bester, K., 2016. Leaching of terbutryn and its photodegradation products from artificial walls under natural weather conditions. Environ. Sci. Technol. 50, 4289–4295.

Bollmann, U.E., Minelgaite, G., Schlüsener, M., Ternes, T.A., Vollertsen, J., Bester, K., 2017b. Photodegradation of octylisothiazolinone and semi-field emissions from facade coatings. Sci. Rep. 7, 41501.

Bollmann, U.E., Vollertsen, J., Carmeliet, J., Bester, K., 2014. Dynamics of biocide emissions from buildings in a suburban stormwater catchment – concentrations, mass loads and emission processes. Water Res. 56, 66–76.

Bork, M., Engel, Johannes, Krämer, Alexander, Lange, Jens, 2022. FReWaB-PLUS (Freiburger Regenwasserbewirtschaftung plus Stofftransport) [WWW Document]. FReWaB-PLUS: Mobilisierung von Bioziden in Stadtgebieten. URL https://www.biozidauswaschung.de (accessed 10.1.22).

Bork, M., Lange, J., Graf-Rosenfellner, M., Hensen, B., Olsson, O., Hartung, T., Fernández-Pascual, E., Lang, F., 2021. Urban storm water infiltration systems are not reliable sinks for biocides: evidence from column experiments. Sci. Rep. 11, 7242.

Burkhardt, M., Engelke, D., Gehrig, S., Hochstrasser, F., Rohr, M., Tietje, O., 2020. COMLEAM - Manual Version 3.0. HSR University of Applied Sciences Rapperswil, Switzerland.

Burkhardt, M., Junghans, M., Zuleeg, S., Boller, M., Schoknecht, U., Lamani, X., Bester, K., Vonbank, R., Simmler, H., 2009. Biozide in Gebäudefassaden – ökotoxikologische Effekte, Auswaschung und Belastungsabschätzung für Gewässer. Environ. Sci. Eur. 21, 36–47.

Burkhardt, M., Zuleeg, S., Vonbank, R., Schmid, P., Hean, S., Lamani, X., Bester, K., Boller, M., 2011. Leaching of additives from construction materials to urban storm water runoff. Water Sci. Technol. 63, 1974–1982.

Coutu, S., Del Giudice, D., Rossi, L., Barry, D.A., 2012a. Modeling of facade leaching in urban catchments. Water Resour. Res. 48.

Coutu, S., Rota, C., Rossi, L., Barry, D.A., 2012b. Modelling city-scale facade leaching of biocide by rainfall. Water Res. 46, 3525–3534.

Díaz-Sanz, J., Robert, S., Keller, C., 2020. Parameters influencing run-off on vegetated urban soils: A case study in Marseilles, France. Geoderma 376, 114455.

Droz, B., Drouin, G., Maurer, L., Villette, C., Payraudeau, S., Imfeld, G., 2021. Phase transfer and biodegradation of pesticides in water–sediment systems explored by compound-specific isotope analysis and conceptual modeling. Environ. Sci. Technol. 55, 4720–4728.

Duque, L.F., 2020. IETD: Inter-Event Time Definition.

Fernández-Calviño, D., Rousk, J., Bååth, E., Bollmann, U.E., Bester, K., Brandt, K.K., 2021. Short-term toxicity assessment of a triazine herbicide (terbutryn) underestimates the sensitivity of soil microorganisms. Soil Biol. Biochem. 154, 108130.

Gao, J., Garrison, A.W., Hoehamer, C., Mazur, C.S., Wolfe, N.L., 2000. Uptake and Phytotransformation of Organophosphorus Pesticides by Axenically Cultivated Aquatic Plants. J. Agric. Food Chem. 48, 6114–6120.

Gaylarde, C., Ribas Silva, M., Warscheid, Th., 2003. Microbial impact on building materials: an overview. Mat. Struct. 36, 342–352.

Gilevska, T., Wiegert, C., Droz, B., Junginger, T., Prieto-Espinoza, M., Borreca, A., Imfeld, G., 2022. Simple extraction methods for pesticide compound-specific isotope analysis from environmental samples. MethodsX 101880.

Goulden, S., Portman, M.E., Carmon, N., Alon-Mozes, T., 2018. From conventional drainage to sustainable stormwater management: Beyond the technical challenges. Journal of Environmental Management 219, 37–45.

Hensen, B., Lange, J., Jackisch, N., Zieger, F., Olsson, O., Kümmerer, K., 2018. Entry of biocides and their transformation products into groundwater via urban stormwater infiltration systems. Water Res. 144, 413–423.

Ivdra, N., Herrero-Martín, S., Fischer, A., 2014. Validation of user- and environmentally friendly extraction and clean-up methods for compound-specific stable carbon isotope analysis of organochlorine pesticides and their metabolites in soils. J. Chromatogr. A 1355, 36–45.

Junginger, T., Payraudeau, S., Imfeld, G., 2022. Transformation and stable isotope fractionation of the urban biocide terbutryn during biodegradation, photodegradation and abiotic hydrolysis. Chemosphere 305, 135329.

Kresmann, S., Arokia, A.H.R., Koch, C., Sures, B., 2018. Ecotoxicological potential of the biocides terbutryn, octhilinone and methylisothiazolinone: underestimated risk from biocidal pathways? Sci. Total Environ. 625, 900–908.

Larsbo, M., Roulier, S., Stenemo, F., Kasteel, R., Jarvis, N., 2005. An Improved Dual-Permeability Model of Water Flow and Solute Transport in the Vadose Zone. Vadose Zone J. 4, 398–406.

Linke, F., Olsson, O., Preusser, F., Kümmerer, K., Schnarr, L., Bork, M., Lange, J., 2021. Sources and pathways of biocides and their transformation products in urban storm water infrastructure of a 2 ha urban district. Hydrol. Earth Syst. Sci. 25, 4495–4512.

Linke, F., Olsson, O., Schnarr, L., Kümmerer, K., Preusser, F., Bork, M., Leistert, H., Lange, J., 2022. Discharge and fate of biocide residuals to ephemeral stormwater retention pond sediments. Hydrology Res. nh2022075.

Paijens, C., Bressy, A., Frère, B., Moilleron, R., 2020. Biocide emissions from building materials during wet weather: identification of substances, mechanism of release and transfer to the aquatic environment. Environ. Sci. Pollut. Res. 27, 3768–3791.

Paijens, C., Bressy, A., Frère, B., Tedoldi, D., Mailler, R., Rocher, V., Neveu, P., Moilleron, R., 2021. Urban pathways of biocides towards surface waters during dry and wet weathers: assessment at the Paris conurbation scale. J. Hazard. Mater. 402, 123765.

Pinasseau, L., Wiest, L., Volatier, L., Mermillod-Blondin, F., Vulliet, E., 2020. Emerging polar pollutants in groundwater: Potential impact of urban stormwater infiltration practices. Environ. Pollut. 266, 115387.

Quednow, K., Püttmann, W., 2007. Monitoring terbutryn pollution in small rivers of Hesse, Germany. J. Environ. Monit. 9, 1337–1343.

Reiß, F., Kiefer, N., Noll, M., Kalkhof, S., 2021. Application, release, ecotoxicological assessment of biocide in building materials and its soil microbial response. Ecotoxicol. Environ. Saf. 224, 112707.

Ren, X., Hong, N., Li, L., Kang, J., Li, J., 2020. Effect of infiltration rate changes in urban soils on stormwater runoff process. Geoderma 363, 114158.

Schoknecht, U., Mathies, H., Wegner, R., 2016. Biocide leaching during field experiments on treated articles. Environ. Sci. Eur. 28, 6.

Shuster, W.D., Dadio, S., Drohan, P., Losco, R., Shaffer, J., 2014. Residential demolition and its impact on vacant lot hydrology: Implications for the management of stormwater and sewer system overflows. Landsc. Urban Plan. 125, 48–56.

Šimůnek, J., Šejna, M., Saito, H., Sakai, M., van Genuchten, M. Th., 2013. The HYDRUS-1D Software Package for Simulating the Movement of Water, Heat, and Multiple Solutes in Variably Saturated Media, HYDRUS Software Series 3. Department of Environmental Sciences, University of California Riverside, Riverside, California, USA.

Turgut, C., 2005. Uptake and Modeling of Pesticides by Roots and Shoots of Parrotfeather (Myriophyllum aquaticum) (5 pp). Environ. Sci. Pollut. Res. Int. 12, 342–346.

Vega-Garcia, P., Schwerd, R., Scherer, C., Schwitalla, C., Johann, S., Rommel, S.H., Helmreich, B., 2020. Influence of façade orientation on the leaching of biocides from building façades covered with mortars and plasters. Sci. Total Environ. 734, 139465.

Vijayaraghavan, K., Biswal, B.K., Adam, M.G., Soh, S.H., Tsen-Tieng, D.L., Davis, A.P., Chew, S.H., Tan, P.Y., Babovic, V., Balasubramanian, R., 2021. Bioretention systems for stormwater management: Recent advances and future prospects. J. Environ. Manage. 292, 112766.

Wicke, D., Tatis-Muvdi, R., Rouault, P., Zerball-van Baar, P., Dünnbier, U., Rohr, M., Burkhardt, M., 2022. Emissions from building materials—a threat to the environment? Water 14, 303.

Wittmer, I.K., Bader, H.-P., Scheidegger, R., Singer, H., Lück, A., Hanke, I., Carlsson, C., Stamm, C., 2010. Significance of urban and agricultural land use for biocide and pesticide dynamics in surface waters. Water Res. 44, 2850–2862.

Wittmer, I.K., Scheidegger, R., Stamm, C., Gujer, W., Bader, H.-P., 2011. Modelling biocide leaching from facades. Water Res. 45, 3453–3460.

Xue, J., Gavin, K., 2008. Effect of Rainfall Intensity on Infiltration into Partly Saturated Slopes. Geotech. Geol. Eng. 26, 199–209.

Yang, J.-L., Zhang, G.-L., 2011. Water infiltration in urban soils and its effects on the quantity and quality of runoff. J Soils Sediments 11, 751–761.

Chapter 8
General conclusions

This thesis aimed to better understand the reactive transport of urban biocides from facades toward groundwater. It explored the degradation pathways of the urban biocide terbutryn, with emphasis on the hydrolysis, photodegradation and biodegradation (Chapter 4), the release of terbutryn from facades, highlighting the significant contribution of transformation products (TPs) to the overall biocide transport in leachates (Chapter 5), the infiltration and reactive transport of a mixture of urban biocides (terbutryn, diuron and OIT) through typical urban surfaces towards the subsurface and groundwater (Chapter 6), and quantified the release, distribution, and reactivity of urban biocides on the district scale (Chapter 7). Even though, biocides were previously detected in surface water, soil, and groundwater, the detailed reactive processes across the facade-runoff-soil-groundwater continuum remained largely unknown.

In particular, the contribution of different degradative processes constituted a major bottleneck concerning the fate of urban biocides in the environment. As each transformation process may lead to distinct TPs, it is crucial to understand the prevailing degradation mechanisms and their respective contribution to overall biocide degradation, because TPs might contribute significantly to the overall biocide emissions and ecotoxicology (Bollmann et al., 2016; Hensen et al., 2020). To distinguish between degradation pathways, compound specific isotope analysis (CSIA) was previously proven to be a useful tool for micropollutants (Elsner and Imfeld, 2016). However, to apply CSIA *in situ*, laboratory reference experiments under controlled conditions are needed to identify mechanism associated stable isotope fractionation and retrieve isotope fractionation value that may be reaction-specific (Fischer et al., 2016). Those

reference isotope fractionation values exist for urban contaminants, e.g., benzotraiazoles (Huntscha et al., 2014; Wu et al., 2021) but have not been established for urban facade biocides (e.g., terbutryn) before. Therefore, this thesis paves the road to examine urban biocide transformation on facades and receiving compartments based on ME-CSIA.

We further assessed the contribution of transformation processes on facades and the gaps existing between reference values retrieved from laboratory and field emission studies. While outdoor experiments are usually conducted for several months, laboratory immersion tests seek to simulate several years of rainfall. In contrary, immersion tests fail to reproduce degradation processes occurring in the environment, although they can reproduce diffusive release from facades, hampering the direct transfer to outdoor applications. Especially the relationship between hydro-climatic parameters and TP release from facades was not previously addressed. Even though urban biocides have been detected in groundwater (Hensen et al., 2018), their main entry points have not been identified and reactive transport, including advection, dispersion, sorption and degradation, from typical urban surfaces up to groundwater, has not been investigated systematically. In the context of current trends towards sustainable stormwater management (SSM), including infiltration of water in cities (e.g., through permeable paving or infiltration ponds), it was fundamental to set the basis to quantify the input of urban biocides towards groundwater. So far, data about potential of biocide accumulation (e.g., through chronic release in soil) or percolation through urban surfaces remained scarce and therefore addressed in thes thesis. Overall, a framework to assess the mass balance for urban biocides on the district and city scale is needed, including release, transport, retention and degradative processes, to investigate their fate from source to sink.

Here stems the motivation of this thesis to identify the main degradation pathways of urban biocides and to identify entry paths into the environment to guide future mitigation strategies for SSM and to reduce potential ecotoxicological effects, prevent accumulation of biocides and TPs in the environment and implement new monitoring strategies (e.g., CSIA and monitoring campaigns on the district scale). Generally, the thesis focused on one major research question: *What are the key processes and kinetics associated with the reactive transport of urban biocides and TPs from building facades up to groundwater?*

Based on our innovative approach, combining concentration with isotope fractionation measurements, small scale laboratory experiments with field studies and short-term assessments with modeling over several years, we were able to partly answer this question. In contrary, with conventional methods and approaches this question would have remained unanswered. Concentration measurements of parent compounds and TPs are not sufficient to quantify the contribution of respective processes in the environment (e.g., biodegradation vs. photodegradation vs. sorption vs. dilution), modeling of release of biocides from facades disregards the contribution of transformation products, with potential adverse effects on the ecosystem though mixture toxicity, and measurements on the district scale are only a snapshot in time of biocide release without being able to fully describe the complexity of the systems, identifying local sinks and entry paths into groundwater or set up mass balances. Therefore, novel approaches were needed to better understand and describe the complexity of various reactions occurring successively or simultaneously across the transport pathways.

The general approach of this thesis relied on analytical methods (e.g., concentration measurements and CSIA) field observations and modelling to advance the understanding of the reactive transport of urban biocides in cities, while integrating embedded scales (e.g., from the molecular to the district scale). A major result of this thesis is that terbutryn degradation in the environment may be very slow and lead to the formation of TPs that should be accounted for in the mass balance. High degradation half live times, together with continuous release of terbutryn and TPs from facades into the environment, leads to chronic input of biocides and TPs into groundwater with potential accumulation in the soil. Even though infiltration ponds and ditches are increasingly implemented to improve SSM, we expect significant percolation towards groundwater prior to reaching those systems (e.g., through cobblestones) as well as through those systems over long time periods. Additionally, in combined sewer systems, wastewater treatment facilities and combined sewer overflows will lead to significant contaminant loads into surface waters. Our results highlight the need to (i) reduce biocide emissions from existing buildings, (ii) account for the formation of TPs on facade and in receiving soil, and (iii) construct new buildings without biocides added as film preservatives. The way towards a “biocide free city” is discussed in Chapter 9.

Chapter 8

1 The importance of considering biocide degradation and transformation product formation in the environment

Our study highlighted the relevance to integrate transformation processes into assessments of biocide release and reactive transport towards groundwater. In Chapter 4, we showed, that transformation products depend on degradation pathways with significant differences between photodegradation, biodegradation and hydrolysis. Both acidic and alkaline hydrolysis resulted solely in terbutryn-2-hydroxy, while photodegradation lead to a variety of TPs. Based on TPs and isotope fractionation values, we were able to differentiate degradation pathways. This is of high importance since different TPs might have different ecotoxicological potential and physico-chemical properties, therefore potentially higher mobility towards groundwater or accumulation in the environment. The importance to consider TPs was confirmed in outdoor experiments, where TPs contributed to > 60% to terbutryn emissions from experimental facades (Chapter 5). Furthermore, we have confirmed that the contribution of TPs in facade leachate mainly depends on solar irradiation. We showed that, by implementing TPs into facade leaching models, emissions of urban biocide consisting of parent compound and TPs can be better assessed over long time periods (e.g., years).

These results represent a first step to include TPs into risk assessment of urban biocides. The reactive transport experiments through typical urban surfaces emphasized that TPs are formed during the soil passage (Chapter 6). However, the formation of TPs was largely dependent on the porous matrix intercepting the biocide runoff, controlling retention times, biological activity and thus degradation rates. The complexity of the reactive transport of TPs is driven by the wide range of physico-chemical properties (e.g., K_{OW} or water solubility) among TPs by several orders of magnitude. This may lead to the accumulation of some TPs and chronic exposure in soil and water ecosystem, while more hydrophilic TPs can be rapidly transported towards groundwater. Observations of stormwater infiltration in an urban district highlighted the relevance to consider TPs when assessing biocide transfer and risks (Chapter 7). While terbutryn exceeded regularly PNECs, terbutryn sulfoxide, as a major TP, exceeded terbutryn concentrations in a stormwater infiltration trench. This has strong implications in stormwater management since biocide and TP mixtures may cause yet unknown synergistic ecotoxicological effects (Hensen et al., 2020).

Overall, this thesis provided the basis of a framework to (i) understand transformation pathways leading to the formation of TPs, (ii) systematically integrate TPs in routine measurements in laboratory and outdoor experiments and field campaigns, and (iii) implement TPs in release and reactive transport models to improve assessment of ecotoxicological risks of biocides and TPs in the future.

2 Combining laboratory and field experiments with modelling to improve predictions of biocide reactive transport from source to sink

To assess the behaviour of contaminants in the environment, typically laboratory experiments are needed to evaluate the reactivity under controlled conditions. However, laboratory experiments often fail to reproduce the complexity of the environment, which is why validation of laboratory scale experiments under outdoor conditions are needed. Within this project, we consistently followed an approach in which we compared microcosm experiments to the real environmental conditions with discussing the limitations to describe environmental processes solely on laboratory experiments. Furthermore, we used models as tool to extrapolate over longer timeframes (e.g., several years), allowing to identify relevant reactive processes in the fate of urban biocides. Those models however rely on calibration and validation with experimental data. In Chapter 4, we retrieved reference degradation rates as well as carbon and nitrogen isotope fractionation values for the urban biocide terbutryn during direct photodegradation (UV light with λ = 254 nm and simulated sunlight), indirect photodegradation (simulated sunlight with nitrate) hydrolysis (pH = 1, 7 and 13) and aerobic biodegradation (stormwater pond sediment, soil and activated sludge). Those reference values, obtained under controlled conditions, were then used to interpret degradation processes occurring on facades (e.g., predominantly photodegradation) and during percolation towards groundwater under outdoor conditions. Strong limitations were observed when testing release and transformation processes based on laboratory experiments (Chapter 5). Photodegradation under laboratory conditions resulted only in little photodegradation while under environmental conditions the cumulated contribution of TPs in leachate exceeded 60%. The interplay between processes happening simultaneously or successively in the environment (e.g., diffusion of terbutryn to the facade surface followed by

photodegradation) was not observable based on laboratory experiments alone. Furthermore, we conducted immersion experiments that allowed to estimate the total amount of biocides leaching. The combination of field and laboratory studies allowed us to identify key hydro-climatic variables that are responsible for the contribution of TPs in facade leachate. The implementation of biocide transformation processes in dependence on hydro-climatic variables was implemented into a simple facade leaching model and therefore was able to estimate biocide emissions and the contribution of TPs for eight years. These models have the potential as powerful tool for better risk assessments and evaluation of emission scenarios for biocides and their TPs. Furthermore, results from laboratory degradation experiments (Chapter 4) were used to assess and validate terbutryn degradation half lives in typical urban surfaces (Chapter 6). Previously only scarce data was available to interpret biocide emissions towards groundwater and models were based solely on physico-chemical properties.

Therefore, our outdoor lysimeter experiments were used to calibrate a 1-D finite element reactive transport model for a more realistic assessment of biocides entering the subsurface based on observed data. Lysimeter reference experiments were based on one pulse injection, while under environmental conditions, biocides are released with each rain event. The reoccurring entry of biocides and the associated release towards groundwater over eight years was evaluate based on the model. Therefore, short-term lysimeter experiments coupled to 1-D modelling showed to be a great combination to identify potential entry points of biocides and therefore sources of groundwater contamination and quantify their respective contribution. Both models, based on experimental data, were able to help the prediction of biocide reactive transport from source to groundwater.

Overall, the combination of laboratory and field scale experiments with modelling approaches is meaningful to predict biocide reactive transport from sources to sink over time. The used combination of small-scale laboratory experiments (e.g., microcosms or immersion tests) with outdoor experiments provided insights that complemented each other and helped identifying prevailing processes. We demonstrated that laboratory experiments alone might fail to reproduce environmental processes and provided the necessary framework to allow for modelling and therefore evaluating biocide reactive transport with implementation of TPs. This framework is relevant for reliable assessment of urban contaminant pathways and conducted experiments are (with minor adaptions) applicable for other contaminants. In future, the

implementation of isotope fractionation values in reactive transport models might be helpful to get a complementary line of evidence of the contribution of degradation in the fate of urban biocides.

3 Towards a framework to quantify biocide release from facades and distribution on the district and city scale

With the aim of the thesis to understand biocide reactive transport from facades to sinks, a holistic framework was needed including the main reactive processes. The possibility to upscale biocide emissions to the district and city scale depends mainly on the data availability. First of all, hydro-climatic data is needed to describe the release processes (e.g., by using wind driven rain as main driver for urban biocide release and irradiation for the contribution of transformation products). This data is usually available through local meteorological weather stations. To assess the water balance, monitoring data is needed, including the type of discharge system (e.g., combined vs. separated vs. SSM) and urban surfaces to assess the contribution of infiltration and surface runoff.

Furthermore, facade areas need to be estimated to calculate the areas contributing to urban biocide emissions by considering that not all facades contain the same mix of biocides as well as may contain different initial concentrations. Depending on the availability and quality of this data, biocide emissions and distribution in various compartments can be quantified. In Chapter 7, we provided insights in how this framework can be applied on the district scale. Such framework might thus be helpful in urban planning to find complementary insights for SSM by considering biocide emissions and reactive transport towards groundwater.

4 Potential and limits of CSIA to evaluate reactive transport of urban biocides

Throughout our study, CSIA was used to investigate degradation mechanisms, degradation pathways, and quantify the extent of degradation of biocides, as a complementary tool to assess

the reactive transport of urban biocides. We first tested and evaluated extraction methods for a range of pesticides for CSIA, which is a crucial step prior to application of the methods to environmental samples. Methods were tested and selected with following prerequisites: (i) provide sufficient analyte mass for reliable isotope analysis, (ii) cause no stable isotope effect ($\Delta\delta^{H}E$), (iii) be applicable to a wide range of pesticides and matrices, and (iv) limit matrix co-enrichment to avoid co-elution during chromatographic separation (Gilevska et al., 2022b). SPE and the MUSE method provided fair results and their application was extended to plant material (e.g., aerial parts and roots) (Chapter 3).

Reference experiments suggested that photodegradation, hydrolysis and biodegradation of terbutryn can be distinguish based on isotope fractionation of carbon (i.e., values ranging from ε_C = -3.4 ± 0.3‰ (hydrolysis pH 1) to ε_C = +0.8 ± 0.1‰ (photodegradation under UV light), and nitrogen (i.e., values ranging from ε_N = -1.0 ± 0.4‰ (simulated sunlight photodegradation with nitrate) to ε_N = +3.4 ± 0.2‰ (hydrolysis at pH 1). Isotope fractionation during biodegradation was insignificant, likely because degradation through terbutryn-sulfoxide does not directly involve carbon and nitrogen bond cleavage. ME-CSIA enabled to differentiate degradation pathways and to identify possible mechanisms, together with TP analysis. This thesis thus provided reference isotope fractionation values for terbutryn and highlighted the potential of CSIA to follow degradation in situ and improve further remediation strategies.

In outdoor experiments with environmental concentrations, terbutryn emissions from facades were evaluated using concentration, TPs, and isotope measurements. Carbon isotope fractionation measurement for terbutryn were obtained from field samples, which was not done before for urban environments. Although the presence of > 60% TPs in leachate compared to the total leached biocide mass, no isotope fractionation of terbutryn was observed. Non-degraded terbutryn likely constantly diffuses to the outset layer of paint during rainfall events, thus confounding that isotope fractionation stems from photodegradation between rainfall events. If significant degradation occurs during photodegradation, rainfall events will release fresh terbutryn bearing the initial isotope signature, which may severely confound the signature hold by the degraded fraction of terbutryn at the paint surface. Nevertheless, a homogeneous isotopic source value of terbutryn could be attributed to facade paint through extraction of commercial paints. This underscores the opportunity to follow terbutryn degradation with CSIA in environmental compartments receiving facade runoffs.

In lysimeter experiments, peak concentrations of biocide emissions enabled to measure carbon isotope fractionation for both terbutryn and acetochlor. No significant isotope fractionation was observed for terbutryn, confirming a prevailing transformation to terbutryn-sulfoxide. In contrary, significant isotope fractionation of acetochor allowed (i) to estimate the extent of degradation of acetochlor and therefore estimate degradation kinetics during reactive transport in the subsurface, and (ii) to probe the reactivity of receiving surface, showing that transformation in the permeable pavement with sand was higher than that in the gravel lysimeter. Under environmental conditions with continuous input of non-degraded urban biocides from facades during rainfall-runoff events, isotope fractionation might be masked through constant mixing of degraded with fresh input of non-degraded terbutryn.

4.1 The next element for terbutryn stable isotope analysis: sulfur

GC-MC-ICPMS measurements of stable sulfur isotopes ($\delta^{34}S$) might provide additional insights into degradation pathways and estimation of the extent of degradation (Kümmel et al., 2020). Initial terbutryn transformation to terbutryn sulfoxide, e.g., during biodegradation, directly involves the S atom, while neither carbon nor nitrogen bonds are directly involved in bond cleavage or formation, therefore causing only secondary carbon and nitrogen isotope effects. Triple-element CSIA (3-D CSIA) may help to discriminate transformation pathways that are not distinguishable based on carbon and nitrogen isotope data alone (Torrentó et al., 2021).

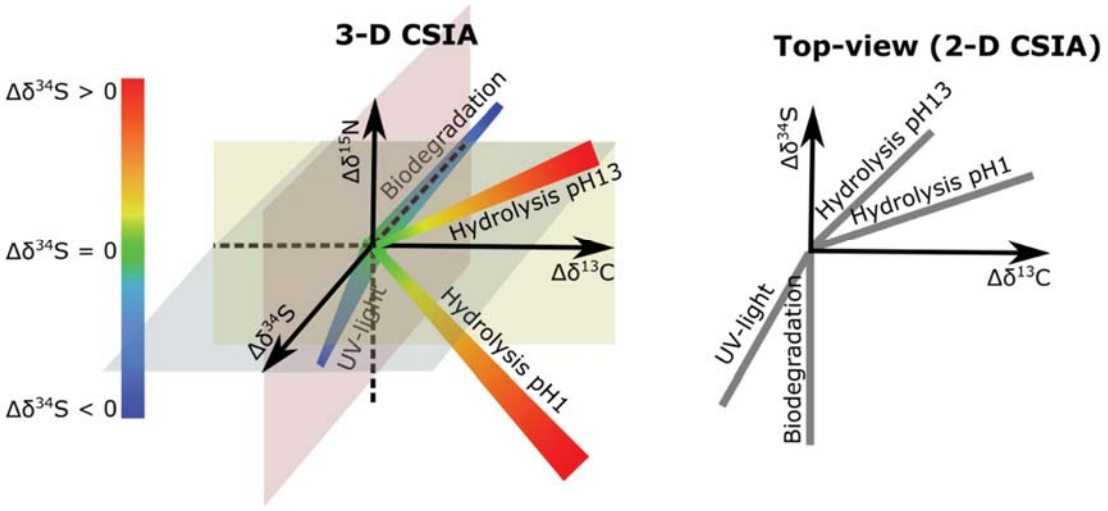

Figure 8. 1. Scheme of expected direction of sulfur stable isotope fractionation for terbutryn during biodegradation, photodegradation under UV-light and hydrolysis (pH 1 and pH 13) with known carbon and nitrogen isotope fractionation as 3-D plot and 2-D for sulfur and carbon stable isotopes.

Based on current knowledge we expect an inverse isotope effect for sulfur stable isotopes during biodegradation as well as during photodegradation under UV light: the heavy sulfur isotope (^{34}S) is more stable during the transition state of oxidation to terbutryn-sulfoxide than the light isotope, resulting of enrichment of isotopologues containing the light isotope (^{32}S) in the non-degraded fraction and therefore an inverse isotope effect (Figure 8. 1). In contrast, hydrolysis under pH 1 and pH 13 resulted solely in terbutryn-2-hydroxy through the cleavage of a carbon-sulfur bond. Therefore, in both cases, bond cleavage might occur preferentially for light isotopes, resulting in an enrichment of ^{34}S in the non-degraded fraction. A great advantage of sulfur-CSIA for terbutryn is that isotope effects are undiluted by the number of atoms of the same element, as there is only one sulfur atom in the molecule, in contrast to nitrogen (n=5) or carbon (n=10). With a higher number of atoms of a respective element in a molecule, the higher the probability that a heavy isotope is located at a non-reactive position within the molecule. Hence, for carbon and nitrogen, the isotope effect experienced by terbutryn molecules with a heavy isotope present at the reactive position becomes diluted by terbutryn molecules with a heavy isotope present at other positions, which is not the case for Sulphur isotopes (n=1), making sulphur more sensitive in terbutryn CSIA.

4.2 Perspective and developments of CSIA

Although CSIA is a promising tool for monitoring biocide degradation, it is currently limited by the low concentrations and the requirement of a large amount of molecule for reliable measurements (Elsner and Imfeld, 2016), e.g., 100 to 200 ng L^{-1} in water or 300 to 1000 ng g^{-1} in soil for carbon isotope measurements (Gilevska et al., 2022b). In addition, current preconcentration methods often lead to co-enrichment in dissolved organic species that may co-elute during CSIA, thereby hampering the analysis sensitivity. Reducing co-elution might be achieved through the addition of selective sorbents (e.g., PSA, florisil or graphitized black carbon) (Anastassiades et al., 2003; Ivdra et al., 2014; Muhammad et al., 2020; Wilkowska and Biziuk, 2011), cleanup by separation through a HPLC column (Schreglmann et al., 2013) or the application of molecular imprinted polymers (MIPs) (Bakkour et al., 2018). MIPs have the capability to selectively enrich analytes through molecular interactions and are typically coupled to SPE (Martín-Esteban, 2013; Sun et al., 2008). Even though MIPs are seen as one of the most promising cleanup methods for CSIA, they must be synthesized, tested and validated for each compound prior to usage. In water, polar organic integrated samplers (POCIS) may help to pre-concentrate organic contaminants directly in the field through integrative passive sampling over longer (e.g., 20-30 d) time periods (Dalton et al., 2014; Gallé et al., 2020; Miège et al., 2012, 2012; Vermeirssen et al., 2012). POCIS were recently combined for the first time for carbon CSIA in the ng L^{-1} range, confirming degradation of pesticides in an agricultural catchment (Gilevska et al., 2022a).

Chapter 8

References

Anastassiades, M., Lehotay, S.J., Štajnbaher, D., Schenck, F.J., 2003. Fast and Easy Multiresidue Method Employing Acetonitrile Extraction/Partitioning and "Dispersive Solid-Phase Extraction" for the Determination of Pesticide Residues in Produce. J. AOAC Int. 86, 412–431.

Bakkour, R., Bolotin, J., Sellergren, B., Hofstetter, T.B., 2018. Molecularly Imprinted Polymers for Compound-Specific Isotope Analysis of Polar Organic Micropollutants in Aquatic Environments. Anal. Chem. 90, 7292–7301.

Bollmann, U.E., Minelgaite, G., Schlüsener, M., Ternes, T., Vollertsen, J., Bester, K., 2016. Leaching of terbutryn and its photodegradation products from artificial walls under natural weather conditions. Environ. Sci. Technol. 50, 4289–4295.

Dalton, R.L., Pick, F.R., Boutin, C., Saleem, A., 2014. Atrazine contamination at the watershed scale and environmental factors affecting sampling rates of the polar organic chemical integrative sampler (POCIS). Environ. Pollut. 189, 134–142.

Elsner, M., Imfeld, G., 2016. Compound-specific isotope analysis (CSIA) of micropollutants in the environment — current developments and future challenges. Curr. Opin. Biotechnol., Analytical biotechnology 41, 60–72.

Fischer, A., Manefield, M., Bombach, P., 2016. Application of stable isotope tools for evaluating natural and stimulated biodegradation of organic pollutants in field studies. Curr. Opin. Biotechnol. 41, 99–107.

Gallé, T., Bayerle, M., Pittois, D., Huck, V., 2020. Allocating biocide sources and flow paths to surface waters using passive samplers and flood wave chemographs. Water Res. 173, 115533.

Gilevska, T., Masbou, J., Baumlin, B., Chaumet, B., Chaumont, C., Payraudeau, S., Tournebize, J., Probst, A., Probst, J.L., Imfeld, G., 2022a. Do pesticides degrade in surface water receiving runoff from agricultural catchments? Combining passive samplers (POCIS) and compound-specific isotope analysis. Sci. Total. Environ. 842, 156735.

Gilevska, T., Wiegert, C., Droz, B., Junginger, T., Prieto-Espinoza, M., Borreca, A., Imfeld, G., 2022b. Simple extraction methods for pesticide compound-specific isotope analysis from environmental samples. MethodsX 101880.

Hensen, B., Lange, J., Jackisch, N., Zieger, F., Olsson, O., Kümmerer, K., 2018. Entry of biocides and their transformation products into groundwater via urban stormwater infiltration systems. Water Res. 144, 413–423.

Hensen, B., Olsson, O., Kümmerer, K., 2020. A strategy for an initial assessment of the ecotoxicological effects of transformation products of pesticides in aquatic systems following a tiered approach. Environ. Int. 137, 105533.

Huntscha, S., Hofstetter, T.B., Schymanski, E.L., Spahr, S., Hollender, J., 2014. Biotransformation of benzotriazoles: insights from transformation product identification and compound-specific isotope analysis. Environ. Sci. Technol. 48, 4435–4443.

Ivdra, N., Herrero-Martín, S., Fischer, A., 2014. Validation of user- and environmentally friendly extraction and clean-up methods for compound-specific stable carbon isotope analysis of organochlorine pesticides and their metabolites in soils. J. Chromatogr. A 1355, 36–45.

Kümmel, S., Horst, A., Gelman, F., Strauss, H., Richnow, H.H., Gehre, M., 2020. Simultaneous compound-specific analysis of δ^{33} S and δ^{34}S in organic compounds by GC-MC-ICPMS using medium- and low-mass-resolution modes. Anal. Chem. 92, 14685–14692.

Martín-Esteban, A., 2013. Molecularly-imprinted polymers as a versatile, highly selective tool in sample preparation. TrAC Trend. Anal. Chem. 45, 169–181.

Miège, C., Budzinski, H., Jacquet, R., Soulier, C., Pelte, T., Coquery, M., 2012. Polar organic chemical integrative sampler (POCIS): application for monitoring organic micropollutants in wastewater effluent and surface water. J. Environ. Monit. 14, 626–635.

Muhammad, R., Ahad, K., Mehboob, F., 2020. Extraction techniques for pesticide residues analysis in edible oils and role of sorbents in cleanup. Ser. Sci. Plus 3, 51–62.

Schreglmann, K., Hoeche, M., Steinbeiss, S., Reinnicke, S., Elsner, M., 2013. Carbon and nitrogen isotope analysis of atrazine and desethylatrazine at sub-microgram per liter concentrations in groundwater. Anal. Bioanal. Chem. 405, 2857–2867.

Sun, Z., Schüssler, W., Sengl, M., Niessner, R., Knopp, D., 2008. Selective trace analysis of diclofenac in surface and wastewater samples using solid-phase extraction with a new molecularly imprinted polymer. Analytica Chimica Acta 620, 73–81.

Torrentó, C., Ponsin, V., Lihl, C., Hofstetter, T.B., Baran, N., Elsner, M., Hunkeler, D., 2021. Triple-element compound-specific stable isotope analysis (3D-CSIA): added value of Cl isotope ratios to assess herbicide degradation. Environ. Sci. Technol. 55, 13891–13901.

Vermeirssen, E.L.M., Dietschweiler, C., Escher, B.I., van der Voet, J., Hollender, J., 2012. Transfer Kinetics of Polar Organic Compounds over Polyethersulfone Membranes in the Passive Samplers Pocis and Chemcatcher. Environ. Sci. Technol. 46, 6759–6766.

Wilkowska, A., Biziuk, M., 2011. Determination of pesticide residues in food matrices using the QuEChERS methodology. Food Chem. 125, 803–812.

Wu, L., Suchana, S., Flick, R., Kümmel, S., Richnow, H., Passeport, E., 2021. Carbon, hydrogen and nitrogen stable isotope fractionation allow characterizing the reaction mechanisms of 1H-benzotriazole aqueous phototransformation. Water Res. 203, 117519.

Chapter 9
Perspective: towards a biocide-free city

1 Introduction

Biocide emissions from construction materials pose a risk for the environment through potential ecotoxicological effects of parent compounds and transformation products (TPs) that are released with each rain event (Chapter 5) by potential leaching into groundwater, accumulation in soil (Chapter 6 and Chapter 7) and fluxes into surface waters through combined and separated sewer systems. The ubiquitous detection of urban biocides in all environmental compartments highlights their potential to accumulate in the environment and exhibit ecotoxicological effects on water organisms, soil microorganisms or the ecosystem functions. Therefore, biocide emissions should be reduced, and measures must be taken, considering parent compounds and TPs. Measures might include the reduction of biocide emissions from facades as well as sustainable stormwater management (SSM) by considering reactive transport pathways on the district scale. Because biocides are added to facades to preserve the building aesthetics, alternative biocide-free materials must consider residents perception of facades as well as being economically feasible, maintain, and/or enhance living quality, and still fulfil the primary purposes of facades, including shelter, air exchange, light transition (windows) and separation of public and private areas (Herzog et al., 2012). Alternative biocide-free measures might need to involve the chain of stakeholders (e.g., manufacturers of facade coatings, painters, architects, urban planners, homeowners and municipalities).

In this chapter, we discuss how to move towards a biocide free city, through (i) reduction of biocide release from existing buildings through preventive measures during the transition period, (ii) improvement of groundwater and surface water quality through sustainable stormwater management and (iii) construction of new buildings without biocides. Solutions on how the use of biocides can be avoided are discussed, before setting perspectives on how to reach biocide free cities in the future.

2 Measures to reduce biocide emissions

Several of the measures mentioned below were already suggested by the "BaSaR" project of the German environmental protection agency (Wicke et al., 2021a). In a scenario of biocide free cities, the logical consequence is that upcoming buildings will have to be constructed without film preservatives in render and paint systems on facades. Even though there are several film-preservative free render and paint systems available, biocide-containing materials are sold in great quantities as they are guaranteed to have longevity (Burkhardt, 2015). Measures to reduce emissions from existing as well as to avoid biocides in new buildings are summarized in Figure 9. 1.

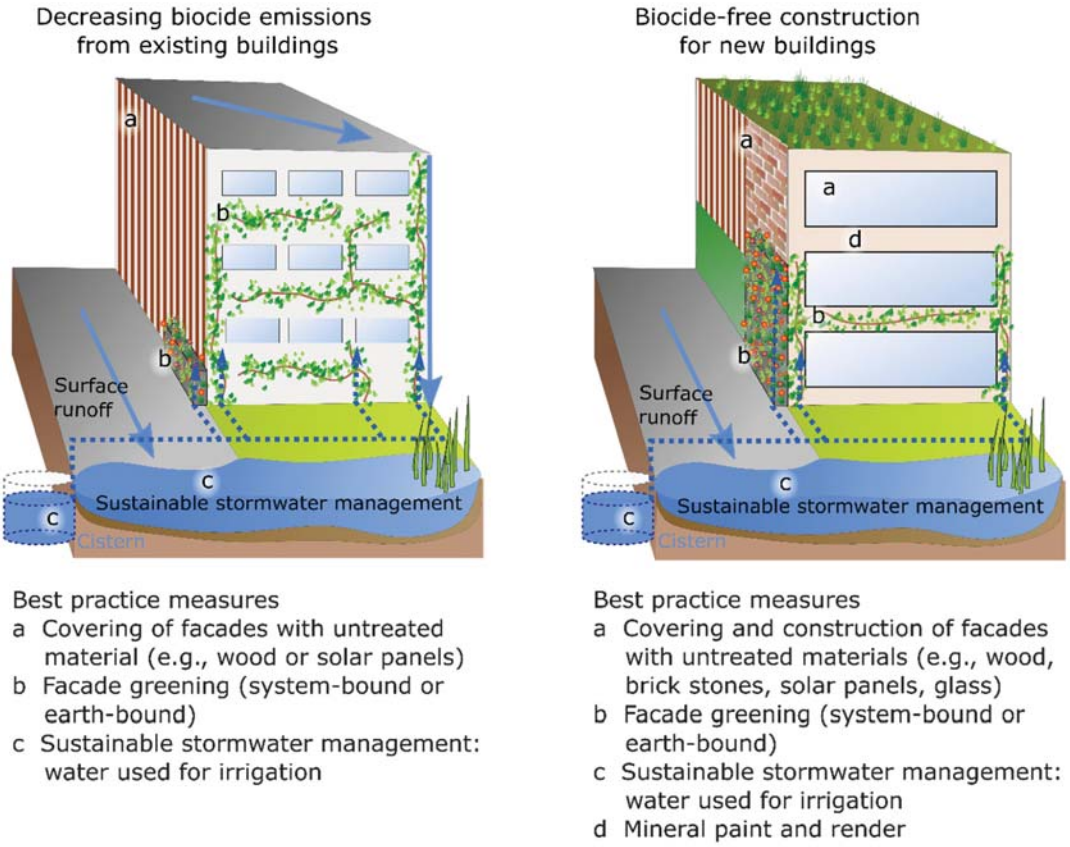

Figure 9. 1. Suggested measures for reducing biocide release from existing buildings (left) and facade without biocides in new buildings (right).

2.1 Prevention of biocide emissions

2.1.1 Physical protection of facades and innovative alternatives

As biocide emissions are mainly dependant on facade runoff (Chapter 5) and algae, fungi and microorganism growth is dependent on water availability (Johansson et al., 2010) systems to physically protect the facades from wind driven rain could be implemented. Physical measures might include balconies, drip edges and roof overhangs, planting of bushes and trees with adequate distance to the building and reduction of splashing water. Additionally, facades can be protected by adding wooden elements without biocidal preservatives onto the facades. Recently, photovoltaic panels and solar thermal collectors were added more often onto facade systems (Attoye et al., 2017; Freitas and Brito, 2019), which has supplementary socio-economic benefits

such as energy saving or generation (Frattolillo et al., 2020). Solar panels or wooden elements do not only protect the facades but can additionally hide aesthetic deterioration on existing facades.

Additionally, materials that are not accessible for microbial activity on facades or have no pollutant emissions can be used during construction of new buildings, including brick stones, glass or the already mentioned integration of photovoltaic systems within the facade. Sandak et al., 2019 proposes a variety of different bio-based building skins such as wood. If a fast deterioration of the facade material is expected and optical effects do not satisfy aesthetics, a double skin can be implemented on the facades to protect the aesthetics from exposures e.g., by glass (Figure 9. 2).

Figure 9. 2. Aesthetic covering of wood by a skin layer of glass at the Bayerische Vereinsbank Stuttgart (Picture: Sandak et al., 2019).

There are several alternative materials that do not contain biocides and have supplementary positive effects. Instead of removing algae from facades and see them as threat, current advancements started intentionally growing algae on facades for biomass generation (e.g., for biofuels), reduction of greenhouse gas emissions, energy savings and treatment of contaminated water in bioreactors (Elrayies, 2018). A first pilot project was installed in 2013 in Hamburg, Germany (Figure 9. 3). Glass panels are filled with microalgae to produce biomass from CO_2 and nutrients, while capturing thermal heat and light from the sun. Biomass can then be used for biofuel and electricity generation.

Figure 9. 3. The Bio-Intelligent Quotient house in Hamburg with algae bioreactors (Elrayies, 2018). Bioreactors are used for biomass generation.

2.1.2 Facade greening

Greened facades are an excellent example of green urban architecture (Figure 9. 4). Green facades (e.g., through system- or earth-bound systems) in urban areas are identified are part of SSM and as no-regret measures: measures can be justified economically and from environmental, social and health perspectives. The measures have benefits, whether certain events (e.g., extreme climate change or extreme precipitation events) take place or not.

Figure 9. 4. Vegetated facades (Lübeck, Germany) with an earth-bound system (left) and system-bound at the CMS building (Calwer-Passage, Stuttgart, Germany) (right) (Pictures: Tobias Junginger, Marie Hundhausen).

Greened facades can be implemented in new and old buildings and several different approaches are available on how plants can be integrated into facades (Figure 9. 4). Kozamernik et al., 2020 states that vertical greenery in the urban environment is generally perceived as more pleasant and that it contributes to the quality of urban living environment. Furthermore, green facades can have positive psychological effects, such as physical and psychological relaxation and an improved positive mood, which was tested by following the brain activity and other measurements (Elsadek et al., 2019). Additionally, vertical greening systems can also contribute to the biodiversity in cities (Mayrand et al., 2018).

Greened facades can also decrease temperatures in summer and increase temperatures in winter on facade surfaces (Vox et al., 2018), and were shown to be able to provide energy saving during cooling seasons (Coma et al., 2017; Susca et al., 2022). Therefore, green facades can also be economically sustainable through savings in air conditioning and higher real estate values, dependant on the local settings (Perini and Rosasco, 2013). Especially in densely populated urban areas, urban heat island effects can have negative impacts on energy demand and public health. This effect can be strongly mitigated through vertical green facades with maximum cooling effects of up to 8°C (Susca et al., 2022). Ottelé et al., 2014, 2011 conducted a live cycle analysis to assess the environmental burden of different green facade systems and states that several systems have the potential to be sustainable with positive impacts on the environment. Water supply can be integrated with intelligent systems combined with stormwater management, e.g., with underground cisterns (Figure 9. 1).

2.1.3 Mineral paint and render

Even though facade coatings that contain film-preservatives have a great contribution to the market of facade paints and render, there are several biocide-free alternatives. Mineral renders and paints are suitable with thermal insulation composite systems. However, the range of possible colors is limited, and thin layers of mineral render might still be exposed to microbial growth if water is not evaporating fast enough. Most major paint and render suppliers offer mineral paint and alternatives without biocides and complete systems for facades (e.g., *Sto* SE & Co. KGaA or *Brillux* GmbH & Co. KG).

2.2 Treatment of contaminated water and sustainable stormwater management

In sustainable stormwater management, water is retained and infiltrated on the district scale, which is in stark contrast to conventional stormwater systems (combined and separate sewer systems), that aim to remove stormwater as fast as possible from the district into the sewer systems.

2.2.1 Technical treatment systems

Technical treatment systems (e.g., underground facilities for retention and treatment of rainwater with adsorber materials, e.g., activated carbon) have the potential of filtering and treating heavily polluted stormwater. Those underground systems were tested in pilot systems (Burkhardt et al., 2017) and proved to have high removal rates of urban biocides. However, technical treatment systems need monitoring, are expensive and do not have other socio-economic benefits as surface infiltrations systems.

2.2.2 Permeable cities: the “sponge city” concept

Generally, sustainable stormwater management, as implemented in the sponge-city concept, aims to improve water quality, reduce surface runoff and flooding and increase infiltration for stormwater reuse, while the urban microclimate is improved (Nguyen et al., 2019). Measures include green roofs and facades (see above), permeable pavement and bioretention. Therefore, sustainable stormwater management can counteract sewer overflows, surface water pollution and has a contribution to local groundwater recharge through the retention of stormwater for infiltration, reuse or evaporation (Goulden et al., 2018). Permeable infrastructure reduces the peak water discharge towards wastewater treatment systems and consequently prevents direct emission of contaminated water into surface waters. Due to urban stormwater management through green infrastructure further cross-benefits for environment and ecosystems (e.g., reduced heat-island effects and increased urban biodiversity), that are beyond pollutant retention can be observed (Barbosa et al., 2012). However, in existing districts, the implementation of

stormwater treatment and infiltration systems is often difficult due to spatial requirements and should be addressed in the initial urban design.

Infiltration ditches, trenches and ponds. Infiltration ditches are typically implemented in urban environments with the primary goal to reduce surface water runoff and potentially sewer overflows by redirecting surface runoff into infiltration systems. As discussed in Chapter 7, an appropriate underground material (e.g., soil with high organic content and biocide retention potential) can prevent and significantly reduce leaching of urban biocides towards groundwater and favour degradation to mineralization. Therefore, the load of biocides in rainwater might be reduced by infiltration ditches with a high retention capacity, including a moderate permeability of the underlying soil. Swale and infiltration ponds with plant filters can be implemented. These systems are typically simple and cheap to maintain (Wicke et al., 2021b). However, macro pores, developed through biological activity, can still result in significant input of biocides towards deeper soil layers and the groundwater (Bork et al., 2021).

Reduction of stormwater surface-runoff. Rainwater retention offers the ability to reduce surface water runoff through evaporation and infiltration e.g., through permeable pavement. However, as shown in Chapter 7, those pavement systems are not suitable for sufficient biocide retention and can result in significant infiltration of urban biocides towards groundwater prior to reaching discharge or infiltration systems. Therefore, permeable surfaces retain water but act as source of biocides towards groundwater.

3 Evaluating measures to reduce biocide emissions on the path towards a biocide free city

In the following section, the above introduced measures are ranked on a scale from 0 to 3 based on their potential to reduce biocide emissions (0: no reduction in emissions, 1: minor reduction of biocide emissions, 2: major reduction of biocide emissions, 3: no biocide emission), and water quality improvement on a scale from 0 to 2 for surface waters (SW) and groundwater (GW) (0: no water quality improvement, 1: major water quality improvement, 2: no biocides entering water). Furthermore, advantages and disadvantages are discussed (Table 9. 1).

Table 9. 1 Evaluation of measures to reduce biocide emissions from buildings and evaluation of water quality in surface water (SW) and groundwater (GW).

Measure	Reduction of biocide emissions (0-3)	Advantages	Disadvantages	Applicability for…	
				existing buildings / districts	new buildings / districts
Measures on buildings					
Balconies, drip edges and roof overhang	1/3	Drip edges simple and cheap to implement	Roof overhang and balconies complicated to upgrade and expensive to implement on existing buildings, limited effect on biocide release	(✓)	✓
Biocide- free wooden elements on facades	2/3	Cheap and easy implementation, can improve aesthetics and cover whole facade	Aesthetic deterioration of wooden elements over time, frequent replacements and associated costs	✓	✓
Biocide-free paint and render	3/3	Not necessarily higher cost, no risk of aesthetic deterioration	Not all colours available, specific know-how for painters	(✓)	✓
Use of materials that are not susceptible for microbial spoilage (e.g., glass, brick stones)	3/3	Not necessarily higher cost, no risk of aesthetic deterioration	Different aesthetics, limited freedom in design	×	✓
Photovoltaic and solar thermal collectors	3/3	Improved aesthetics, electricity generation and decreasing energy consumption	Expensive for initial installation (cost amortisation over several years through decreasing energy consumption and electricity generation), Restricted to sun-oriented side	✓	✓
Greened facades	2-3/3	Improved aesthetics, reduced energy consumption, improvement of urban climate and	Dependant on system cost intensive for installation and maintenance	✓	✓

			psychological wellbeing			
Treatment of runoff water						
	Improvement of water quality in …					
	SW	GW				
Infiltration ponds/ ditches/ trenches	2/2	1/2	Cheap maintenance, green spaces for public	Potential of infiltration into groundwater, expensive installation, spatial requirements, potential accumulation of biocides in soil	✗	✓
Technical on-site treatment systems with filters	1/2	-	Low special requirements, reduced acute concentrations through stormwater retention in discharging streams	Capture only part of the runoff, expensive to install and high maintenance costs	✓	✓
Rainwater retention	1/2	0-1/2	Enhanced infiltration, reduced acute concentrations through stormwater retention in discharging streams, no spatial requirements for pavement infiltration	Higher risk of infiltration towards groundwater in pavement systems, high spatial need for retention ponds, capture only a part of the runoff	(✓)	✓

4 Knowledge transfer

4.1 Visualization of hazard potential

Current approaches in facade treatment aim to remove or limit the growth of microorganisms on facades (Romani et al., 2022). However, we suggest that a change in the paradigm is needed to see and accept algae and fungi growth on facades as part of the urban environment and rethink facade systems. This change needs to be communicated throughout different actors (Figure 9. 5) including authorities, architects, private homeowners as well as painters and paint manufacturers. A holistic concept in urban planning is needed that does not only incorporate urban biocide emissions but also urban climate mitigation and stormwater management (Figure

9. 1). The usage of facades can go beyond the traditional prerequisites (shelter, air exchange, light transmission, and separation of private and public space (Herzog et al., 2012)) and might be adapted for urban climate mitigation, ecosystem service, energy generation or biomass generation and therefore has unexplored potential.

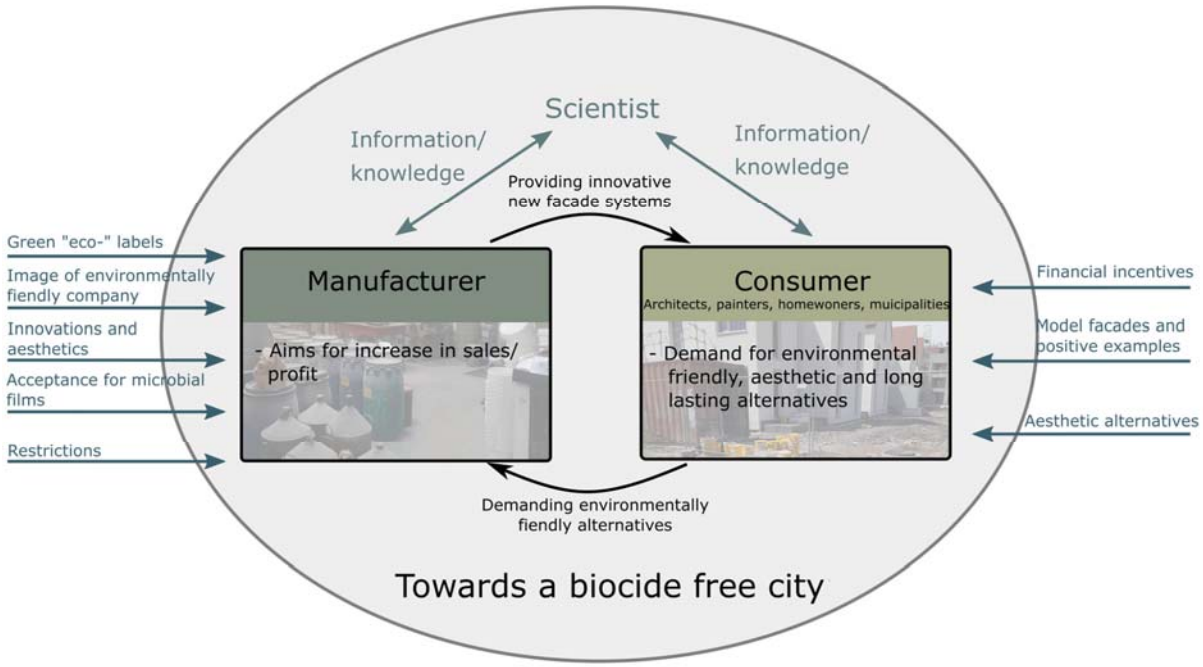

Figure 9. 5 Actors and factors towards a biocide free city.

In a first step, the risk of biocide emissions must be communicated. Various factors such as roof overhang, drip edge, shading and greening of a facade, the facade material, as well as the facade condition are risk indicators for biocide release that can be surveyed on buildings and mapped on a district level. This was done in the NAVEBGO project cities Freiburg, Landau, Lüneburg and Strasbourg in different city districts and visualized in the form of digital maps on the project homepage (Figure 9. 6). A comparison of different city districts is thus possible and the awareness in the public of risk of biocide leaching and infiltration towards groundwater can be increased.

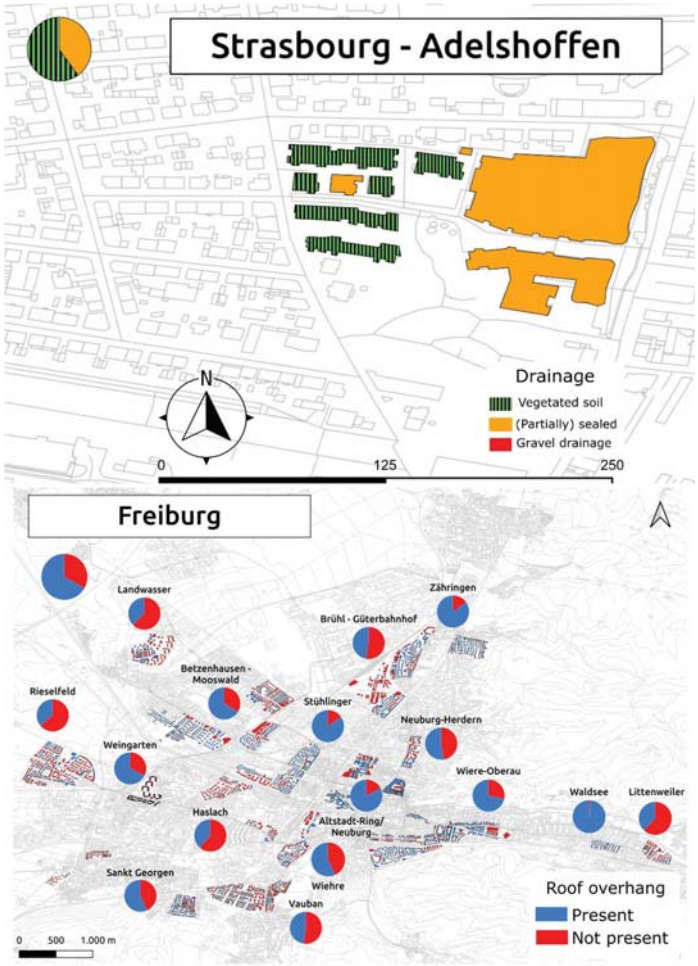

Figure 9. 6. Risk map for Strasbourg-Adelshoffen district with land use of receiving compartments as indicator for biocide leaching towards groundwater (top) and several districts of the city of Freiburg for the selected risk factor of drainage (top) and roof overhang (bottom) (modified from www.navebgo.uni-freiburg.de).

In recent years, several countries (e.g., Germany and France) implemented the pesticide free cities, in which pesticides e.g., for the application on sidewalks, green stripes and urban city gardening applications are prohibited and replaced by the communes by mechanical methods or different plants (Lehmphul, 2015a). Communication on the municipal level can improve citizens awareness of problems and has advertising effects for the municipalities. More than 550 cities in Germany participate, proving that pesticides do not have to be used in the urban environment. Various European countries have similar actions and projects implemented (e.g., Luxembourg "ouni pestiziden", Great Britain "Pesticide-Free-Towns" (Lehmphul, 2015b, 2015a). However,

urban biocides used in construction materials are not addressed yet within most of the projects and concrete plans of action for urban biocides are still lacking. Based on this concept, communes could increase the pressure on stakeholders and decision makers from manufacturers to increase the range of biocide-free alternatives (Figure 9. 5).

Another tool to communicate the risk of urban biocides might be through labels on the respective paint, render or other facade materials to communicate environmentally friendly and biocide free materials. In Germany, “Der Blaue Engel” is a label that is already applied for environmental friendly materials. In Switzerland, facade systems are branded in 7 categories from A to G, where the categories A and B need to be biocide free (Selter and Burkhardt, 2018). Based on labels, consumers (painters, architects, municipalities and private) can easily spot relevant materials and decide for environmentally friendly products. Labels might also be helpful for policy makers to identify relevant materials that might profit from financial incentives. By financial incentives, products could be supported, and the market of application of biocide-free alternatives might be increased.

In the long term, biocide containing materials should be prohibited and only authorized in exceptional situations. Products that can be applied in those situations should contain fast degradable and fully mineralizable film preservatives, only.

Existing information about biocides, risk and alternatives then needs to be transferred into a plan of action by addressing communes, manufacturers and consumers. Workshops for consumers, factsheets for manufacturers and publicly available information and knowledge transfer through media are possible tools for addressing respective parties. Consumers must be able to identify the problem and ask for alternative environmentally friendly products. Acceptance of these products can be achieved through financial incentives, improved aesthetics of the facades as well as restrictions in construction works. Based on the consumer demands for environmentally friendly products and restrictions on biocidal products (e.g., on the municipal level), manufacturers must adapt their portfolio and can use green labels to advertise alternative products. With a combination of suggested strategies, we might pave the way towards a biocide-free city.

Chapter 9

References

Attoye, D.E., Tabet Aoul, K.A., Hassan, A., 2017. A Review on Building Integrated Photovoltaic Façade Customization Potentials. Sustainability 9, 2287.

Barbosa, A.E., Fernandes, J.N., David, L.M., 2012. Key issues for sustainable urban stormwater management. Water Res., Special Issue on Stormwater in urban areas 46, 6787–6798.

Bork, M., Lange, J., Graf-Rosenfellner, M., Hensen, B., Olsson, O., Hartung, T., Fernández-Pascual, E., Lang, F., 2021. Urban storm water infiltration systems are not reliable sinks for biocides: evidence from column experiments. Sci. Rep. 11, 7242.

Burkhardt, M., 2015. Reduction of environmental risks from the use of biocides: Environmental sound use of disinfectants, masonry preservatives and rodenticides Annex IV 36.

Burkhardt, M., Schmidt, S., Gohl, M., Zenker, A., Schmocker, M., Zbinden, D., Loretz, A., Bigler, R., Boller, M., 2017. Behandlung von Regenwasser: Grosstechnische Erfharung mit unterirdischer Retention und nachgeschaltetem adsorptionsfilter. Aqua und Gas 4, 78–85.

Coma, J., Pérez, G., de Gracia, A., Burés, S., Urrestarazu, M., Cabeza, L.F., 2017. Vertical greenery systems for energy savings in buildings: A comparative study between green walls and green facades. Build. Environ. 111, 228–237.

Das deutsche Umweltzeichen [WWW Document], Blauer Engel. URL https://www.blauer-engel.de/de (accessed 8.8.22).

Elrayies, G.M., 2018. Microalgae: Prospects for greener future buildings. Renew. Sust. Energ. Rev. 81, 1175–1191.

Elsadek, M., Liu, B., Lian, Z., 2019. Green façades: Their contribution to stress recovery and well-being in high-density cities. Urban For. & Urban Green. 46, 126446.

Frattolillo, A., Canale, L., Ficco, G., Mastino, C.C., Dell'Isola, M., 2020. Potential for Building Façade-Integrated Solar Thermal Collectors in a Highly Urbanized Context. Energies 13, 5801.

Freitas, S., Brito, M.C., 2019. Solar façades for future cities. Renew. Energy Focus 31, 73–79.

Goulden, S., Portman, M.E., Carmon, N., Alon-Mozes, T., 2018. From conventional drainage to sustainable stormwater management: Beyond the technical challenges. J. Environ. Manage. 219, 37–45.

Herzog, T., Krippner, R., Lang, W., 2012. Facade Construction Manual. Walter de Gruyter.

Johansson, S., Wadsö, L., Sandin, K., 2010. Estimation of mould growth levels on rendered façades based on surface relative humidity and surface temperature measurements. Build. Environ. 45, 1153–1160.

Kozamernik, J., Rakuša, M., Nikšič, M., 2020. How green facades affect the perception of urban ambiences: Comparing Slovenia and the Netherlands. Urbani izziv 31, 88–100.

Lehmphul, K., 2015a. Pestizidfreie Kommune [WWW Document]. Umweltbundesamt. URL https://www.umweltbundesamt.de/themen/chemikalien/pflanzenschutzmittel/pestizidfreie-kommune (accessed 8.8.22).

Lehmphul, K., 2015b. Pestizidfreie Kommune Information [WWW Document]. Umweltbundesamt. URL https://www.umweltbundesamt.de/pestizidfreie-kommune-information (accessed 8.8.22).

Mayrand, F., Clergeau, P., Vergnes, A., Madre, F., 2018. Chapter 3.13 - Vertical Greening Systems as Habitat for Biodiversity, in: Pérez, G., Perini, K. (Eds.), Nature Based Strategies for Urban and Building Sustainability. Butterworth-Heinemann, pp. 227–237.

Nguyen, T.T., Ngo, H.H., Guo, W., Wang, X.C., Ren, N., Li, G., Ding, J., Liang, H., 2019. Implementation of a specific urban water management - Sponge City. Sci. Total Environ. 652, 147–162.

Ottelé, M., Perini, K., Fraaij, A.L.A., Haas, E.M., Raiteri, R., 2011. Comparative life cycle analysis for green façades and living wall systems. Energy Build. 43, 3419–3429.

Ottelé, M., Perini, K., Haas, E.M., 2014. 19 - Life cycle assessment (LCA) of green façades and living wall systems, in: Pacheco-Torgal, F., Cabeza, L.F., Labrincha, J., de Magalhães, A. (Eds.), Eco-Efficient Construction and Building Materials. Woodhead Publishing, pp. 457–483.

Perini, K., Rosasco, P., 2013. Cost–benefit analysis for green façades and living wall systems. Build. Environ. 70, 110–121.

Romani, M., Warscheid, T., Nicole, L., Marcon, L., Di Martino, P., Suzuki, M.T., Lebaron, P., Lami, R., 2022. Current and future chemical treatments to fight biodeterioration of outdoor building materials and associated biofilms: Moving away from ecotoxic and towards efficient, sustainable solutions. Sci. Total Environ. 802, 149846.

Sandak, A., Sandak, J., Marcin, B., Kutnar, A., 2019. Designing Building Skins with Biomaterials. pp. 65–97.

Selter, A., Burkhardt, M., 2018. Umwelt-Etikette auch für die Fassadenfarbe.

Susca, T., Zanghirella, F., Colasuonno, L., Del Fatto, V., 2022. Effect of green wall installation on urban heat island and building energy use: A climate-informed systematic literature review. Renew. Sust. Energ. Rev. 159, 112100.

Vox, G., Blanco, I., Schettini, E., 2018. Green façades to control wall surface temperature in buildings. Build. Environ. 129, 154–166.

Wicke, D., Rouault, P., Rohr, M., Burkhardt, M., 2021a. BaSaR Leitfaden - Steckbrief 2: Grundsätze für die Planung von Fassaden.

Wicke, D., Rouault, P., Rohr, M., Burkhardt, M., 2021b. BaSaR Leitfaden - Steckbrief 3: regenwasserbewirtschaftung auf dem Grundstück.

Chapter 9

Appendix A Supporting information of Chapter 3

1 Material and Methods

Table A 1. Ions used for the quantification of pesticides in the GC-MS system.

Compound	Ions used for quantification (GC-MS)
Atrazine	215/200
Terbutryn	226/185
Acetochlor	142/162
Alachlor	188/162
Butachlor	176/160
Metalaxyl	206/132
S-Metolachlor	215/200
Tebuconazole	249/173
Dimethomorph Z	301/165
Dimethomorph E	301/165

Table A 2. Compounds, precursor ions, mass transitions, collision energy, limit of detection (LOD), and limit of quantification (LOQ) of compounds for UHPLC-MS/MS measurements.

Compound	Retention time (min)	Precursor (m/z)	Transition 1 (m/z)	Collision Energy 1 (eV)	Transition 2 (m/z)	Collision Energy 2 (eV)	LOD (ng L^{-1})	LOQ (ng L^{-1})
Terbutryn	5.00	242	242 → 258.054	25.56	242 → 186.083	19.11	2.0	6.8
Diuron	5.23	233.6	233.6 → 72	20.00	233.6 → 73	20.00	1530	4635
OIT	6.56	214.8	214.8→ 102	17.00	214.8 → 103	17.00	309	937
Acetochlor	6.79	270	270 →148	20.00	270 → 224	12.00	184	559
TerOH	3.14	212	212 → 86.083	25.39	212 → 156.083	16.96	4.3	14.4
TerSO	4.12	258	258 → 256.083	20.29	258 → 258.054	25.56	1.7	5.8
TerDesE	4.09	214	214 → 110.155	26.57	214 → 157.982	18.18	2.4	8.0
TerDesEOH	0.57	184	184 → 86.083	24.84	184 → 128.083	15.7	8.3	27.7

Appendix A

2 Validation of extraction methods

2.1 Used chemicals

Extraction solvents: dichloromethane (DCM), acetonitrile (ACN), ethyl acetate (EtOAc), pentane, methanol (MeOH) were HPLC grade purity (> 99.9%) and purchased from Sigma–Aldrich (St. Louis, MO, USA). Analytical standards (purity > 98%) atrazine, atrazine-d5 terbutryn, acetochlor, alachlor, butachlor, *S*-metolachlor, *S*-metolachlor d-11, dimethomorph, tebuconazole, and metalaxyl were PESTANAL grade purchased from Sigma–Aldrich (St. Louis, MO, USA)

Table A 3. Chemical properties of studies compounds, [b] - *banned as pesticides but used as paint additives, NA – not applicable, - not measured.*

Name	Use	Approval in EU (revision date) http://sitem.herts.ac.uk/aeru/	Structure	Chemical family	Chemical formula	$t_{1/2,water-sediment}$ (d) http://sitem.herts.ac.uk/aeru/	Water solubility (20 ºC, mg L^{-1}) http://sitem.herts.ac.uk/aeru/	Log*Kow*; pH7, 20°C	pKa, 25°C	Sorption capacities, $logK_{oc}$	
										Experimental, Rouffach sediment (Droz et al., 2021)	Predicted from EPA CompTox (Williams et al., 2017)
atrazine	herbicides	banned (2004)	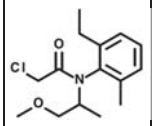	Triazine	$C_8H_{14}ClN_5$	80	35	2.7	1.7	1.5 – 2.6	2.1 – 2.2
terbutryn		banned (2002)[b]	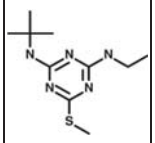		$C_{10}H_{19}N_5S$	60	25	3.7	4.3	2.8 – 3.1	2.8 – 2.9
acetochlor		banned (2013)	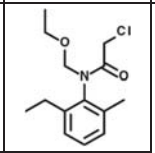	Chloroacetamide	$C_{14}H_{20}ClNO_2$	20	280	4.1	NA	2.2 – 2.5	2.3 – 2.5
alachlor		banned (2009)	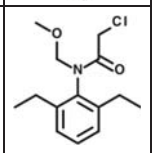		$C_{14}H_{20}ClNO_2$	2	240	3.1	NA	-	2.3 – 2.7
butachlor		banned (2009)	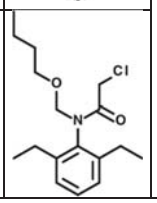		$C_{17}H_{26}ClNO_2$	200	20	4.5	NA	-	2.9

S-metolachlor		approved (2019)	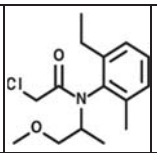		$C_{15}H_{22}ClNO_2$	47	480	3	NA	2.3 – 2.6	2.4 – 2.5
dimethomorph	fungicide	approved (2022)	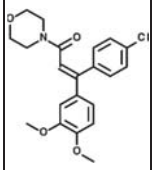	Morpholine	$C_{21}H_{22}ClNO_4$	38	29	2.7	-1.3	-	2.4 – 3.4
tebuconazole		approved (2022)	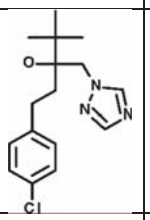		$C_{16}H_{22}ClN_3O$	365	36	3.7	5.0	-	2.6 – 3.0
metalaxyl		approved (2023)	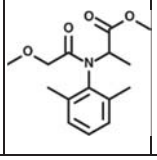	Phenylamide	$C_{15}H_{21}NO_4$	32	8400	1.8	1.4 (Arias et al., 2006)	1.1 – 1.7	1.6 – 1.7

2.2 Pesticide extraction from water samples

The extraction procedure was performed with an AutoTrace 280 SPE system (Dionex®, CA, USA) for the simultaneous extraction of 6 samples. Maximum volume of water that can be pumped this system is 4 L. SPE cartridges, SolEx C18 cartridges (1 g, Dionex®, CA, USA) were washed with 5 mL of EtOAc, followed by 5 mL of ACN. The cartridges were then sequentially conditioned by 10 mL of ultrapure water. Cartridges were loaded with the samples and dried under nitrogen flux for 10 min. Elution of pesticides was performed by 5 mL of EtOAc followed by 5 mL of ACN. The extract was subsequently concentrated under nitrogen flux to 1 droplet and suspended in 0.5 mL of ACN for quantification and isotope analyses. For the isotope analysis, lower concentration samples were further pre-concentrated up to 10 times, by placing 250 µL of the sample in the glass GC vial inserts, followed by evaporation under nitrogen flux the samples and subsequent reconstitution in 0.5 mL.

Appendix A

Table A 4. Hydrochemistry of the environmental waters. Analytical uncertainties were 5% for major ions, metals and carbon concentrations. Precision was ± 0.5% for conductivity and dissolved oxygen measurements, ± 0.01 unit for pH and ± 10 mV for redox potential. D.O. – dissolved oxygen, E.C. – electrical conductivity, TOC – total organic carbon, DOC – dissolved organic carbon.

		Vineyard runoff water, Rouffach, France	Crop runoff water, Alteckendorf, France	River water, Souffel, France
		47°57'43'' N, 7°17'26'' E	48°47'17"N, 7°35'25"E	48°38'20"N, 7°44'35"E
Compound	Unit	Range		
D.O.	mg L^{-1}	0.2 – 3.9	-	-
Redox	mV	- 44 – 47	-	123 – 128
pH	-	7.0 –7.3	6.0 –7.8	7.0 – 7.3
E.C.	µS cm^{-1}	448 – 925	-	900 – 1100
TOC	mg L^{-1}	7.6 – 12.4	0.4 – 1.9	4.12
DOC	mg L^{-1}	6.9 – 12.4	0.2 – 50	3.19
TSS	mg L^{-1}	2 – 172	3 – 65	-
Al^{3+}	mg L^{-1}	0.04 – 0.2	4 – 50	-
Na^{+}	mg L^{-1}	3.3 – 12.5	8.2	13.5 – 14.2
Mg^{2+}	mg L^{-1}	3.3 – 12.3	23.3	45.9 – 47.3
K^{+}	mg L^{-1}	3.4 – 7.1	0.8	6.4 – 14.0
Fe^{3+}	mg L^{-1}	0.2 – 2.8	-	13.5 – 14.2
Fe^{2+}	mg L^{-1}	0.8 – 3.3	-	-
Cu^{2+}	mg L^{-1}	3.8 – 37	-	-
SO_4^{2-}	mg L^{-1}	10.5 – 48.5	31.8	213.4
NO_2^{-}	mg L^{-1}	n.d. – 2.7	0.1 – 0.8	
NO_3^{-}	mg L^{-1}	n.d. – 2.7	27 – 114	62.8 – 63.9
NH_4^{+}	mg L^{-1}	n.d. – 3.2	1 – 12	n.d. – 0.3
PO_4^{3-}	mg L^{-1}	0.4 – 0.6	0.4 – 1.9	-
Cl^{-}	mg L^{-1}	5.0 – 22.4	41.7	34.4 – 50.9

Table A 5. Physicochemical properties of the selected soils.

		Forest soil, Strengbach, France	Vineyard soil, Rouffach, France	River sediment Alteckendorf, France	Storm water sediment Rouffach, France,
		48°12'58"N,7°11'53"E	47°57'44", 7°17'27"E	48°47'17"N, 7°35'25"E	47°57'43" N, 7°17'26" E
Texture	Clay (< 2µm) [%]	7 ± 0.3	23 ± 2	14 ± 0.4	24 ± 8
	Silt (2 - 50 µm) [%]	32 ± 1	68 ± 9	73 ± 2	45 ± 19
	Sand (50 - 2000 µm) [%]	62 ± 2	9 ± 7	13± 0.4	32 ± 22
	Organic carbon (O_C) [%]	4.5 ± 0.2	1.1 ± 0.2	2.0 ± 0.2	2.5± 0.4
	pH	3.4 ± 0.1	7.9 ± 0.1	7.8 ± 0.1	7.6± 0.1
	$CaCO_3$ [%]	-	27	15	19 ± 7
	Cation exchange capacity (CEC) [$cmol^+ kg^{-1}$]	14	18	15	14
	Bulk Density [$g\ cm^{-3}$]	1.0	1.5	-	1.7
	Water content [%]	47 ± 12	13 ± 7	39 ± 3	41 ± 6
Major elements [% dry soil] (ICP-AES analysis)	SiO_2	61.3	52.7	65	48
	Al_2O_3	14.9	7.7	8.5	11
	MgO	0.6	1.4	1.4	2.0
	CaO	0.0	15.1	6.7	13
	Fe_2O_3	2.6	3.2	3.	4.4
	MnO	0.0	0.1	0.1	0.1
	TiO_2	0.0	0.5	0.7	0.6
	Na_2O	0.6	0.8	1.0	0.5
	K_2O	4.3	1.8	1.9	2.3
	P_2O_5	0.2	0.4	0.2	0.3

Appendix A

Table A 6. Additional details of standards quantification and isotope analysis, mean value ± SD, n – number of samples, EA – elemental analyzer.

Compound	Ions used for quantification (GC-MS)	$\delta^{13}C$ (‰) (EA-IRMS) n = 3	$\delta^{15}N$ (‰) (EA-IRMS) n = 3	$\delta^{13}C$ (‰) (GC-IRMS) n = 30	$\delta^{15}N$ (‰) (GC-IRMS) n = 30
Atrazine	215/200	-25.7±0.2	-2.2±0.2	-25.7±0.4	-1.8±0.5
Terbutryn	226/185	-28.8±0.1	-2.9±0.2	-29.0±0.5	-3.0±0.3
Acetochlor	142/162	-29.1±0.1	-2.4±0.2	-29.5±0.4	-2.9±0.4
Alachlor	188/162	-29.4±0.1	-2.5±0.2	-29.5±0.5	-2.3±0.4
Butachlor	176/160	-26.6±0.1	0.6±0.2	-27.7±0.5	0.6±0.5
Metalaxyl	206/132	-31.5±0.1	0.3±0.2	-32.3±0.5	0.1±0.4
S-Metolachlor	215/200	-30.5±0.1	0.4 ±0.2	-31.0±0.5	0.3 ±0.3
Tebuconazole	249/173	-29.3±0.1	1.3±0.2	-29.9±0.4	1.3±0.4
Dimethomorph Z	301/165	-33.2±0.2	0.8±0.2	-34.2±0.5	-
Dimethomorph E	301/165	-33.2±0.2	0.8±0.2	-33.8±0.5	-

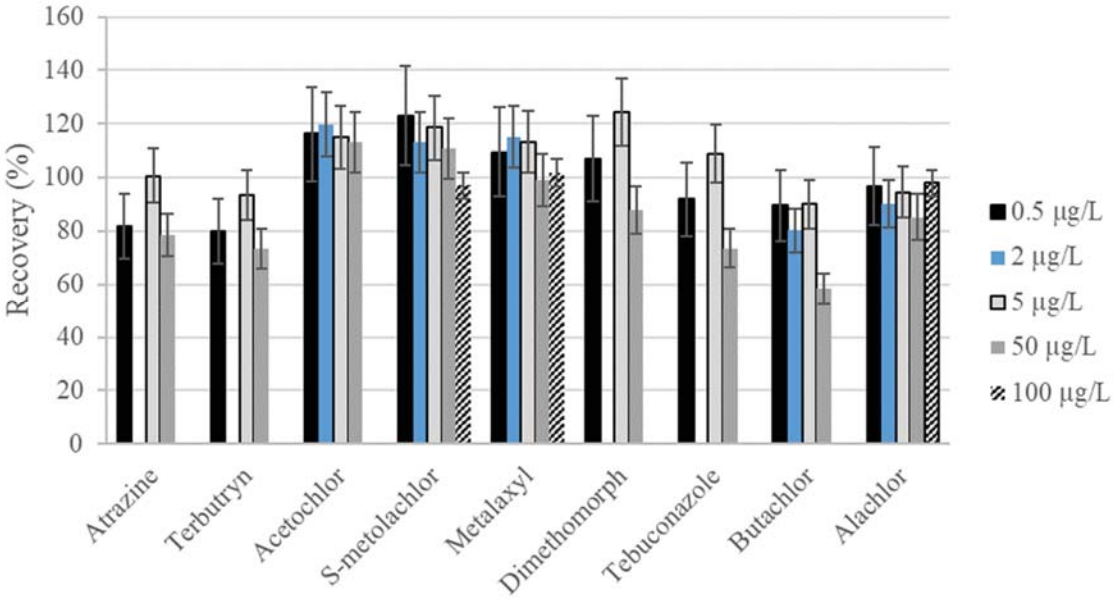

Figure A 1. Recovery for the studied pesticides for the volume of 1 L and varying concentrations.

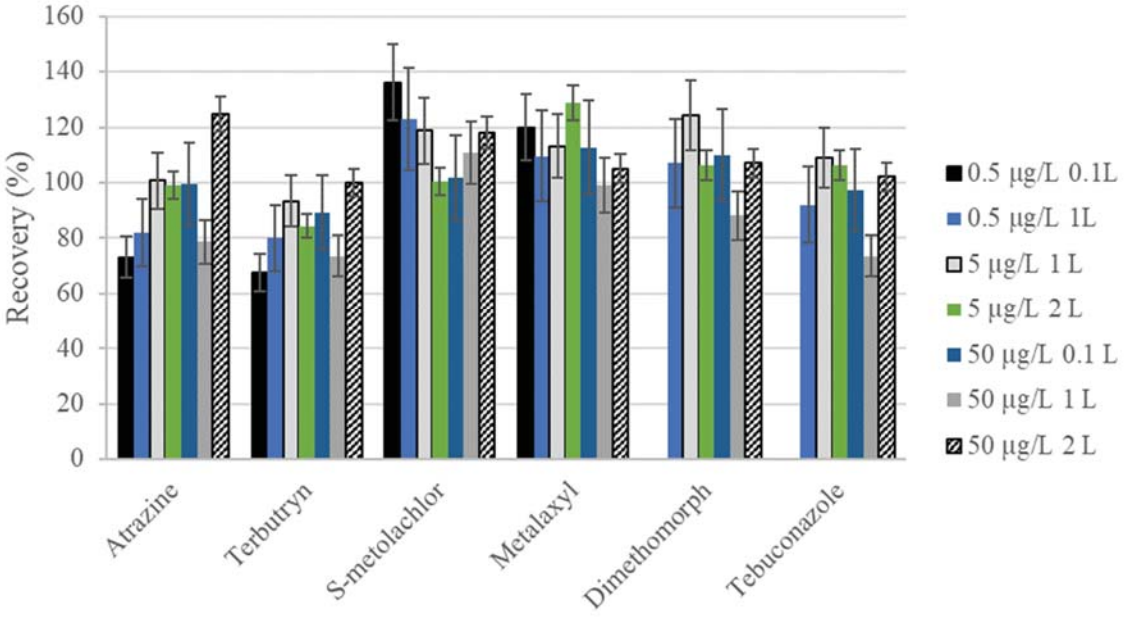

Figure A 2. Recovery for the studied pesticides for the different volumes and concentrations.

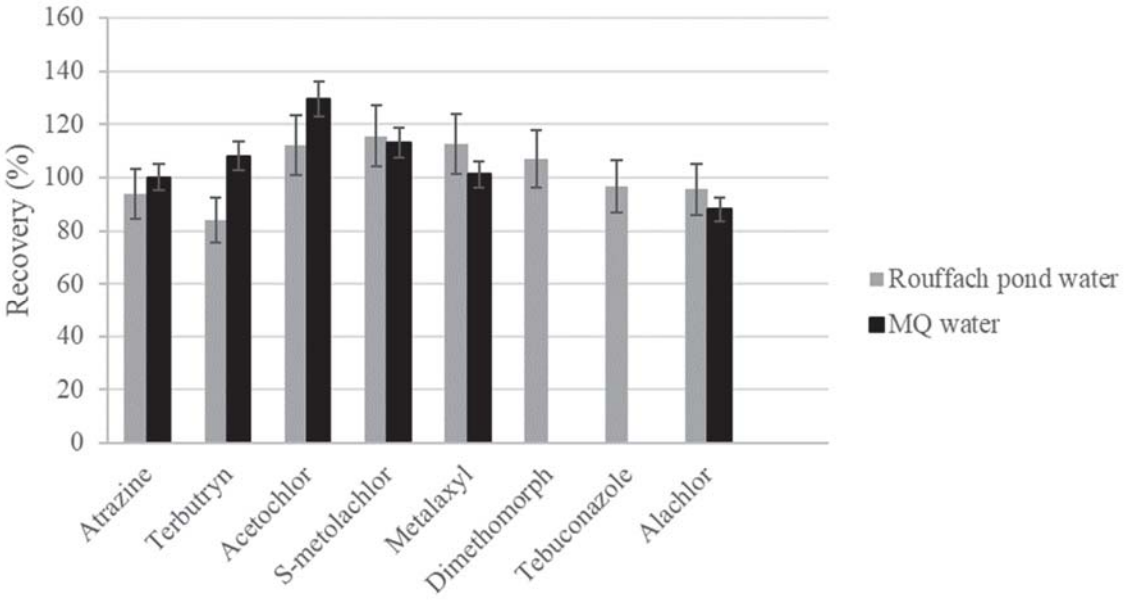

Figure A 3. Recovery for the studies pesticides for different matrix (volumes 0.1 L, 1 L, 2 L).

Appendix A

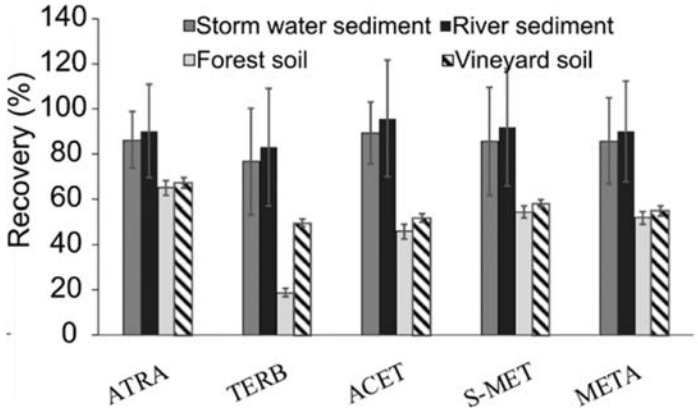

Figure A 4. Recoveries of pesticide extraction with DCM:Pentane for different types of soil and sediment. ACET – acetochlor, S-MET – S-metolachlor, META – metalaxyl, ALAC – alachlor, ATRA– atrazine, TERB –terbutryn. Error bars denote standard deviation (1 σ, n ≥ 12).

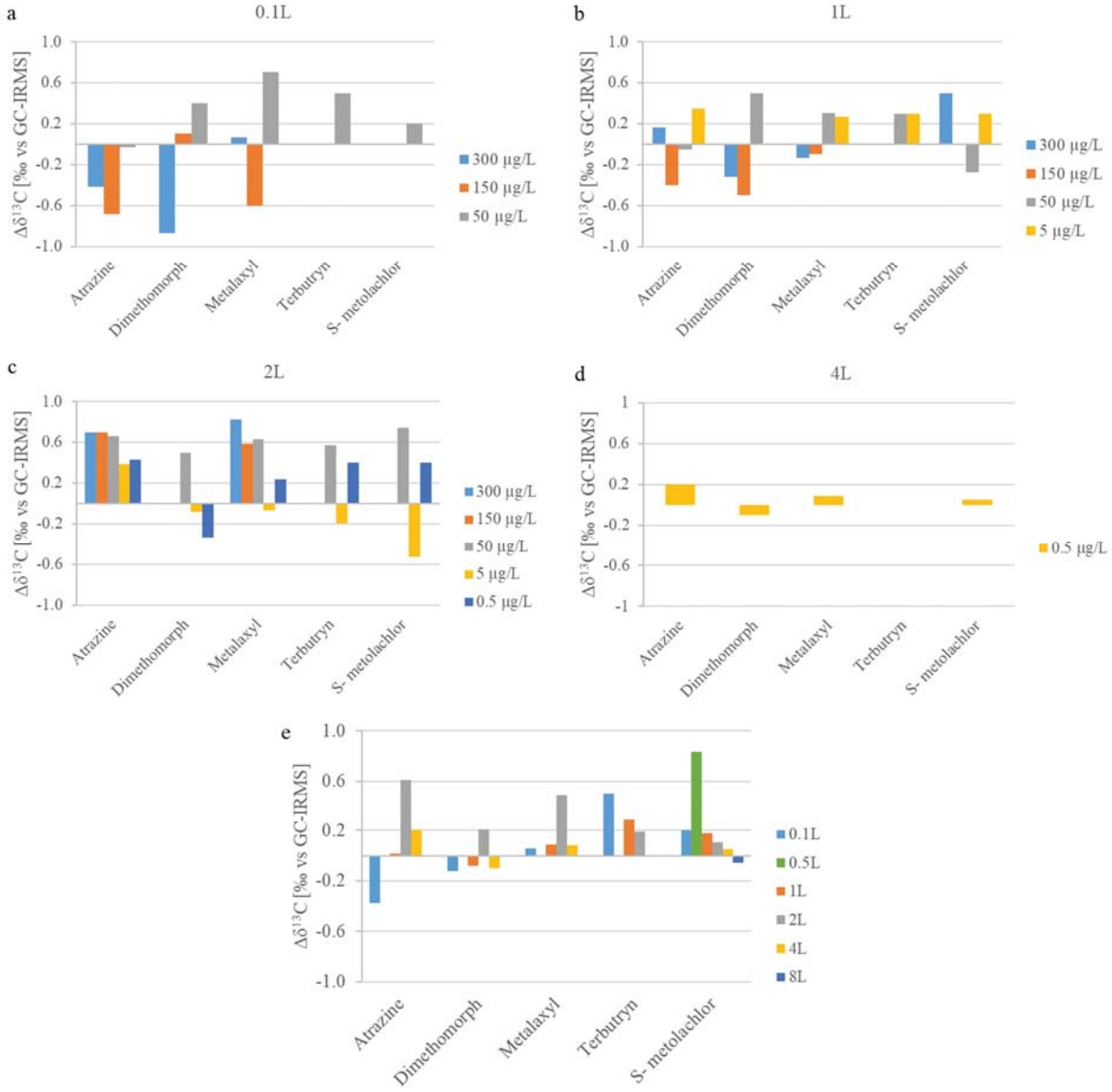

Figure A 5. Effect of extraction on carbon isotope values of standard ($\Delta\delta^{13}C$ [‰ vs GC-IRMS]) for different concentration and volume (a, b, c, d) and between volumes (all concentrations) (e).

Appendix A

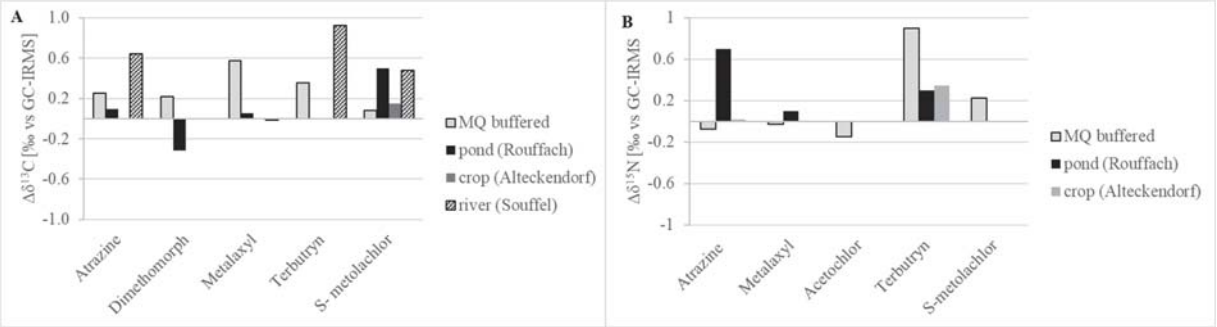

Figure A 6. Effect of SPE extraction method and different water matrices on A - $\Delta\delta^{13}C$, carbon isotope values and B - $\Delta\delta^{15}N$, nitrogen isotope values.

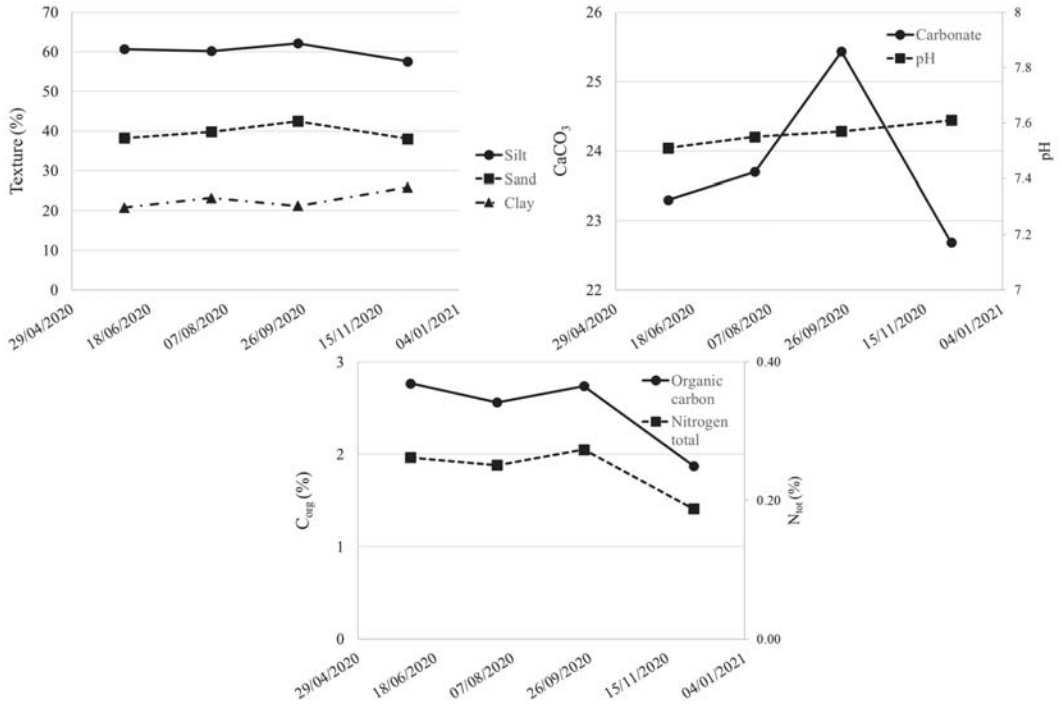

Figure A 7. Properties of the storm water Rouffach sediment across seasons.

2.3 Detailed discussion of extraction recoveries from soil and sediments

In this study, we tested different pesticides with amines or amides functional groups, which do not ionize at pH 7 (Table A 3). The sorption mechanism governing the action of nonionic pesticides includes physical interaction, e.g., the hydrophobic effect, when a nonpolar compound interacts with a nonpolar soil organic component, or chemical interactions, e.g., hydrogen bonding, interactions with humic substances and clay in the soil (Sigmund et al., 2022). Parameters of hydrophobicity (i.e., K_{ow}) and soil sorption properties (i.e., K_{oc}, adsorption coefficient of soil) are thus prevailing factors influencing the extraction recovery.

In addition, the physicochemical characteristics of the soil or the sediment affect the extraction efficiency. Figure 3. 5 shows the variation of extraction efficiencies among environmental samples. For all compounds, extraction recoveries were above 70% in sediment samples (Figure 3. 5 B). In contrast, the forest soil with the highest organic carbon (OC) content (Table A 5), displayed the lowest extraction recovery. Interestingly, the forest soil was characterized by a pH=3.4. The low soil pH may increase the amount of protonated functional groups in soil, such as carboxylic or thiol, thereby enhancing sorption of non-ionic pesticides (Arias et al., 2006; Gondar et al., 2013). The low soil pH may also enhance ionic interactions between soil components and pesticides, such as terbutryn, with a pKa value of 4.3, which may reduce extraction recovery (Figure 3. 5 B, Table A 5).

The vineyard soil (Rouffach, France) featured low initial water content (13 ± 7%) and lower extraction yields (Figure 3. 5 B), although the OC contents and pH of the vineyard soil, and both the river and wetland sediments (Rouffach and Alteckendorf) were similar (Table A 5). The fraction of non-extractable residues may increase with lower water content due to the more hydrophobic nature of soil organic matter controlling pesticide extraction (Barriuso et al., 2008; Mao et al., 2019; Mielnik et al., 2021; Rodríguez-Liébana and Peña, 2020). Therefore, together with changes in soil texture and structure, pH, soil OC content and the initial soil water content appears as fundamental parameters controlling pesticide aging in soil (Beulke et al., 2004) and thus extraction yields from soil and sediment samples.

Appendix A

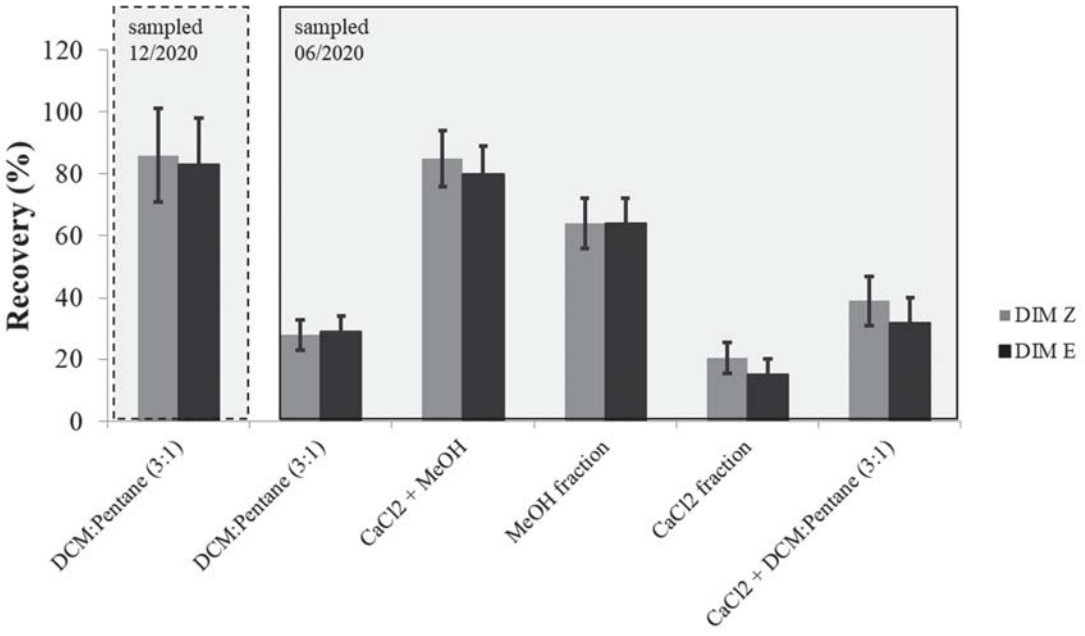

Figure A 8. Recovery of Z and E isomers of dimethomorph with DCM:Pentane extraction (3:1) and 2-step extraction with $CaCl_2$ and MeOH. Shading highlights sampled collected in winter period and in summer period.

Table A 7. Extraction recovery, isotope effect ($\Delta\delta^{13}C$, $\Delta\delta^{15}N$) for SPE, soil sediment, and plant extraction. (n) - the number of samples extracted, NA – not analysed.

			Atrazine	Terbutryn	Acetochlor	*S*-metolachlor	Metalaxyl	Dimethomorph	Tebuconazole	Butachlor	Alachlor
SPE	Recovery	% ± SD	87 ± 8 (41)	88 ± 10 (31)	102 ± 6 (44)	115 ± 12 (73)	95 ± 8 (61)	107 ± 24 (12)	92 ± 20 (16)	77 ± 6 (30)	98 ± 5 (39)
	$\Delta\delta^{13}C$, GC-IRMS	‰ ± SD	-0.01 ± 0.7 (87)	0.2 ± 0.7 (50)	-0.2 ± 0.3 (44)	0.03 ± 0.4 (94)	-0.04 ± 0.6 (106)	-0.3 ± 0.8 (39)	0.01 ± 0.6 (35)	0.5 ± 0.2 (30)	0.02 ± 0.2 (56)
	$\Delta\delta^{13}C$, EA-IRMS	‰ ± SD	-0.1 ± 0.7 (87)	0.6 ± 0.7 (50)	-0.6 ± 0.3 (44)	-0.1 ± 0.4 (94)	-0.3 ± 0.6 (106)	0.5 ± 0.8 (39)	-0.5 ± 0.6 (35)	-0.1 ± 0.3 (30)	-0.2 ± 0.1 (56)
	$\Delta\delta^{15}N$, GC-IRMS	‰ ± SD	0.3 ± 0.7 (21)	0.6 ± 0.6 (17)	0.6 ± 0.6 (17)	-0.2 ± 0.5 (8)	0.3 ± 0.8 (7)	NA	0.0 ± 0.6 (21)	0.1 ± 0.7 (10)	-0.1 ± 0.2 (4)
	$\Delta\delta^{15}N$, EA-IRMS	‰ ± SD	0.3 ± 0.7 (21)	0.9 ± 0.6 (21)	0.2 ± 0.6 (17)	0.6 ± 0.5 (8)	0.1 ± 0.8 (7)	NA	0.0 ± 0.6 (21)	0.3 ± 0.7 (10)	0.1 ± 0.2 (4)
Sediment/soil	Recovery	% ± SD	77 ± 12 (237)	57 ± 14 (216)	71 ± 10 (240)	72 ± 13 (240)	71 ± 11 (240)	82 ± 17 (25)	66 ± 14 (21)	35 ± 2 (24)	54 ± 9 (24)
	$\Delta\delta^{13}C$, GC-IRMS	‰ ± SD	0.04 ± 0.4 (202)	0.1 ± 0.3 (202)	-0.1 ± 0.2(218)	-0.5 ± 0.3 (218)	-0.1 ± 0.4 (218)	-0.2 ± 0.6 (12)	0.4 ± 0.2 (8)	-0.9 ± 0.1 (114)	0.1 ± 0.2 (114)
	$\Delta\delta^{13}C$, EA-IRMS	‰ ± SD	-0.5 ± 0.4 (202)	0.1 ± 0.2 (202)	0.3 ± 0.2 (218)	-0.5 ± 0.3 (218)	-0.4 ± 0.4 (218)	0.6 ± 0.6 (12)	0.4 ± 0.2 (8)	-1.7 ± 0.1 (114)	0.4 ± 0.2 (114)
	$\Delta\delta^{15}N$, GC-IRMS	‰ ± SD	-0.2 ± 0.5 (25)	0.3 ± 0.5 (25)	0.5 ± 0.1 (15)	-0.9 ± 0.3 (15)	-0.3 ± 0.6 (28)	NA	0.4 ± 1.0 (10)	NA	NA
	$\Delta\delta^{15}N$, EA-IRMS	‰ ± SD	-0.6 ± 0.5 (25)	0.2 ± 0.5 (25)	0.9 ± 0.1 (15)	-1.0 ± 0.3 (15)	-0.2 ± 0.6 (28)	NA	0.4 ± 1.0 (10)	NA	NA
Plant	Recovery	% ± SD	54 ± 7 (30)	49 ± 12 (30)	NA	59 ± 10 (30)	53 ± 11 (30)	40 ± 16 (30)	50 ± 14 (30)	NA	NA
	$\Delta\delta^{13}C$, GC-IRMS	‰ ± SD	-0.7 ± 0.6 (8)	-0.2 ± 0.5 (12)	NA	-0.3 ± 0.2 (12)	-0.2 ± 0.5 (12)	-0.4 ± 0.4 (12)	0.0 ± 0.2 (12)	NA	NA
	$\Delta\delta^{13}C$, EA-IRMS	‰ ± SD	-0.6 ± 0.6 (8)	0.2 ± 0.5 (12)	NA	-0.9 ± 0.2 (12)	-0.5 ± 0.5 (12)	1.8 ± 0.4 (12)	-0.3 ± 0.3 (12)	NA	NA
	$\Delta\delta^{15}N$, GC-IRMS	‰ ± SD	-0.7 ± 0.3 (8)	0.0 ± 0.5 (8)	NA	-0.4 ± 0.4 (8)	0.8 ± 0.3 (8)	NA	0.3 ± 0.3 (8)	NA	NA
	$\Delta\delta^{15}N$, EA-IRMS	‰ ± SD	0.7 ± 0.3 (8)	0.3± 0.5 (8)	NA	-0.3 ± 0.4 (8)	0.9 ± 0.3 (8)	NA	0.4 ± 0.3 (8)	NA	NA

Appendix A

Table A 8. Method detection limit (MDL) for SPE, soil sediment, and plant extraction. NA – not analysed.

			Atrazine	Terbutryn	Acetochlor	*S*-metolachlor	Metalaxyl	Dimethomorph	Tebuconazole	Butachlor	Alachlor
MDL $\delta^{13}C$	On column	ng of C	6	7	6	7	5	5	6	7	6
	In extract	mg L^{-1}	4	5	3	4	3	4	4	4	3
	In water 12L (3*4L)	µg L^{-1}	0.2	0.2	0.1	0.1	0.1	0.2	0.2	0.2	0.1
	In soil/sediment (10 g)	µg g^{-1}	0.5	0.7	0.4	0.4	0.3	0.4	0.5	1.1	0.6
	In plant (5 g)	µg g^{-1}	0.4	0.5	NA	0.3	0.3	0.4	0.4	NA	NA
MDL $\delta^{15}N$	On column	ng of N	37	87	17	17	18	NA	100	21	37
	In extract	mg L^{-1}	38	100	111	113	122	NA	100	157	38
	In water 12 L (3*4 L)	µg L^{-1}	2.0	3.9	4.5	3.7	5.6	NA	4.5	8.5	NA
	In soil/sediment (10 g)	µg L^{-1}	4.8	14.5	15.4	13.4	15.0	NA	13.9	44.9	NA
	In plant (5 g)	µg L^{-1}	14.2	40.8	NA	38.5	46.4	NA	40.4	NA	NA

References

Arias, M., Paradelo, M., López, E., Simal-Gándara, J., 2006. Influence of pH and soil copper on adsorption of metalaxyl and penconazole by the surface layer of vineyard soils. Journal of agricultural and food chemistry 54, 8155–8162.

Barriuso, E., Benoit, P., Dubus, I.G., 2008. Formation of pesticide nonextractable (bound) residues in soil: magnitude, controlling factors and reversibility. Environmental science & technology 42, 1845–1854.

Beulke, S., Brown, C.D., Fryer, C.J., van Beinum, W., 2004. Influence of kinetic sorption and diffusion on pesticide movement through aggregated soils. Chemosphere 57, 481–490.

Droz, B., Drouin, G., Maurer, L., Villette, C., Payraudeau, S., Imfeld, G., 2021. Phase Transfer and Biodegradation of Pesticides in Water–Sediment Systems Explored by Compound-Specific Isotope Analysis and Conceptual Modeling. Environmental Science & Technology 55, 4720–4728.

Gondar, D., López, R., Antelo, J., Fiol, S., Arce, F., 2013. Effect of organic matter and pH on the adsorption of metalaxyl and penconazole by soils. Journal of hazardous materials 260, 627–633.

Mao, J., Nierop, K.G.J., Dekker, S.C., Dekker, L.W., Chen, B., 2019. Understanding the mechanisms of soil water repellency from nanoscale to ecosystem scale: a review. Journal of Soils and Sediments 19, 171–185.

Mielnik, L., Hewelke, E., Weber, J., Oktaba, L., Jonczak, J., Podlasiński, M., 2021. Changes in the soil hydrophobicity and structure of humic substances in sandy soil taken out of cultivation. Agriculture, Ecosystems & Environment 319, 107554.

Rodríguez-Liébana, J.A., Peña, A., 2020. Differences in the sorption kinetics of various non-ionisable pesticides in a limited number of agricultural soils from the Mediterranean basin. Journal of Environmental Management 276, 111336.

Sigmund, G., Arp, H.P.H., Aumeier, B.M., Bucheli, T.D., Chefetz, B., Chen, W., Droge, S.T.J., Endo, S., Escher, B.I., Hale, S.E., 2022. Sorption and Mobility of Charged Organic Compounds: How to Confront and Overcome Limitations in Their Assessment. Environmental Science & Technology 56, 4702–4710.

Williams, A.J., Grulke, C.M., Edwards, J., McEachran, A.D., Mansouri, K., Baker, N.C., Patlewicz, G., Shah, I., Wambaugh, J.F., Judson, R.S., 2017. The CompTox Chemistry Dashboard: a community data resource for environmental chemistry. Journal of cheminformatics 9, 1–27.

Appendix B Supporting information of Chapter 4

1 Material and Methods

1.1 Sampling

Table B 1. Sampling times of hydrolysis, photolytic degradation and biodegradation experiments. ‡Extraction for concentration measurement of terbutryn and GC-IRMS measurement, †sampling for transformation products[q], * sampling of control and blanks.

Sampling time	pH1	pH7	pH13	UV_{Dir}	$Photo_{NO3}$	$Photo_{Dir}$	Soil	PondSed	Activated Sludge
t0	0 h*‡	0 h*‡	0 h*‡	0 min*‡†	0 h*‡†	0 h*‡	0 d*‡	0 d*‡	0 d*‡
t1	27 h‡	27 h‡	27 h‡	20 min‡†	1 h‡†	23 h‡†	7 d‡	8 d‡	1 d‡
t2	55 h‡	55 h‡	55 h‡	40 min‡†	2 h‡	48 h‡†	13 d‡	14 d‡	3 d‡
t3	70.5 h‡	70.5h‡	70.5h‡	60 min‡†	3 h‡	72 h‡†	27 d‡	28 d‡	6 d‡
t4	143 h‡	215 h‡	215 h‡	120 min‡†	7 h‡	159.5 h‡†	55 d‡	56 d‡	9 d‡
t5	215 h*‡	383 h*‡	383 h*‡	180 min*‡†	12 h*‡	232 h*‡†	116 d*‡	117 d*‡	14 d*‡
t6	-	551 h‡	551 h‡	240 min‡†	16 h‡	328 h‡	167 d‡	168 d‡†	38 d‡
t7	-	720.5 h‡	720.5 h‡	300 min†	36 h‡†	400 h‡†	263 d‡	264 d‡†	62 d‡†
t8	-	1175 h*‡	1175 h*‡	360 min	60 h‡†	500 h*‡	407 d‡	408 d‡†	80 d‡†
t9	-	-	-	420 min*†	100 h‡†	-	525 d*‡†	499 d*†	113 d‡†
t10	-	-	-	-	164 h‡†	-	-	-	209 d*‡†
t11	-	-	-	-	260 h‡†	-	-	-	-
t12	-	-	-	-	355 h*‡†	-	-	-	-

[q] Hydrolysis experiment for transformation products was sampled at different time points for pH1 (t0 = 0 h, t1 = 22.25 h, t2 = 46.4 h, t3 = 119.2 h, t4 = 144.4 h and t5 = 167 h) and pH13 (t0 = 0 h, t1 = 22.25 h, t2 = 46.4 h, t3 = 144.4 h and t4 = 167 h)

Appendix B

1.2 Hydrolysis experiment

Buffer solutions were prepared under sterile conditions. Water was filtered (0.22 µm cellulose membrane filters) and autoclaved. Buffer solutions were split into autoclaved shot bottles. Shot bottles were spiked from a 2.5 mg L^{-1} terbutryn stock solution in DCM to achieve a concentration of 10 mg L^{-1}. After spiking, samples were stirred open until full evaporation of DCM (at least 1h). The bottles were closed tightly, covered with aluminum foil and incubated at 60°C. During sampling, 30 mL of the solution were withdrawn and extracted as described in section 1.5. For the analysis of transformation products, an extra experiment was performed under the same conditions. 0.5 mL of the aqueous sample was withdrawn and neutralized with the corresponding inverse buffer solution to reach pH 7. Samples were stored at -20°C until analysis.

Table B 2. Buffer composition of hydrolysis experiments and measured pH during experiment.

	pH 1	pH 7	pH 13
Composition	0.2 M KCl 0.2 M HCl	0.1 M KH_2PO_4 0.1 M NaOH	0.2 M KCl 0.2 M NaOH
Initial measured pH	1.0	7.1	13.0
pH measured after 11 days	1.0	7.0	12.9
pH measured at end of experiment	1.0	7.0	12.9

1.3 Photodegradation

For direct photodegradation under UV light (UV_{Dir}), 3 L of autoclaved DI-water was prepared in autoclaved shott bottles and filtered with 0.22 µm cellulose membrane filters. 1.5 L of water was spiked with 10 ml of a 1.5 mg L^{-1} terbutryn stock solution from acetonitrile (ACN) to get to a final concentration of 10 mg L^{-1}. Solvent was evaporated in the dark under constant stirring at 1500 rpm for at least 1 h. Autoclaved beakers were filled with 100 mL of the solution. Additional dark controls (wrapped with 3 layers of aluminum foil) and process blanks (non-spiked DI water) were prepared. All samples were treated under the same conditions in the UV chamber. At each sampling time, 3 samples, each of 30 mL, were collected to extract terbutryn according to section 1.5. Additionally, triplicate samples of 1 mL were withdrawn at each sampling point for TP analysis and frozen until analysis (direct injection in LCMS).

For simulated sunlight, the QSun Xe-1-B test chamber, equipped with a Daylight-Q filter with a nominal cut-on of 295 nm was used. A detailed emission spectrum is presented in Figure B 4. Direct Photodegradation was conducted in autoclaved DI-water. For Photodegradation in presence of nitrate, 76.17 mg of calcium nitrate tetrahydrate ($Ca(NO_3)_2 \cdot 4\ H_2O$) were dissolved in 2 L of autoclaved DI water to reach a final concentration of 20 mg L^{-1}. The solution was filtered through 0.22 µm cellulose membrane filters. 1.5 L of each aqueous solution was spiked with 10 mL of 1.5 g L^{-1} terbutryn stock solution (in ACN) to reach a final concentration of 10 mg L^{-1}. The solution was stirred in the dark until complete evaporation of the solvent (> 60 min). 40 ml of the solution was transferred into sterilized 50 mL beakers. Dark controls (wrapped in three layers of aluminum foil) and process blanks without terbutryn were prepared. Samples (30 mL) were collected at each sampling time. The remaining water was frozen for further analysis of terbutryn transformation products.

1.4 Biodegradation

Sample collection: Water, soil and sediment for biodegradation experiments were sampled on 09/06/2020 in Aldelshoffen district, Schiltigheim, France (GPS: 48°36’33.8”N, 7°44’55.8”E). The samples included 2 kg of soil (composite sample from 5 locations alongside an infiltration ditch that receives façade runoff), 2 kg of sediment from an urban stormwater retention pond (composite sample from 5 locations in the retention pond) and 6 L of stagnant water from the retention pond. Water content of soil and pond sediment was 42.5% and 136%, respectively. Activated sewage sludge was sampled on 20/02/2020 in Strasbourg (La Wantzenau, treatment capacity of 1 M population equivalent (PE)).

Sample preparation: soil and sediment were sieved at 2 mm and shaken for 24 h on an overhead shaker for homogenization. Aliquots were dried at 105°C for determination of the water content. Further aliquots were sterilized three times in 24 h intervals and used for abiotic controls.

Aliquots of dried samples were analyzed for chemical composition. Samples were powdered by using an agate disk mill to < 250 µm followed by alkaline fusion (heating with $Li_2B_4O_5$) and dissolution in acid (HNO_3 with glycerol). Geochemical analyses were carried out

using an inductively coupled plasma mass spectrometer (ICP-AES, ICAP6500, Thermo Fisher Scientific) and an inductively coupled mass spectrometer (ICP-MS, X series II, Thermo Fisher Scientific). Geological standards were used as references for quality control, Including BE-N, GS-N and BR.

1.4.1 Microcosm preparation

Soil microcosms were prepared by adding 1.5 g soil into sterilized crimp vials. Soil microcosms were spiked with 50 µL of a 6 g L^{-1} terbutryn stock solution in pure ethanol. After full evaporation of solvent (at least 2h under a laminar flow fumehood), soil was added to achieve a 5 g (dry weight) soil per microcosms. A subsequent spiking of a small soil fraction, followed by subsequent adding of the remaining unspiked soil was done to prevent toxic effects on the microbial community (Brinch et al., 2002). Water content was not adjusted as it was already at 40% (of soil weight). For blank microcosms, only ethanol without terbutryn was spiked. Additionally, abiotic controls were prepared with the sterilized soil. Soil microcosms were shaken for 1h at 600 rpm for homogenization.

Activated sludge was diluted 1:10 in DI water (2.5 L total volume) and 1 L of the mix was autoclaved 3 times within 24 h for the abiotic controls. Nine process blanks were prepared by adding 30 mL diluted activated sludge under constant stirring at 1500 rpm of the solution into 50 ml crimp vials. 1.3 L of the biotic and 1.0 L of abiotic solutions were spiked by adding 13 µg and 10 µg respectively of terbutryn standard (as powder). The powder was added first into an aliquot of 100 ml of the respective aqueous solution under constant stirring and then recombined with the respective volume of abiotic and biotic solutions. The solutions were constantly stirred for 1 h to achieve complete dissolution and homogeneous distribution of terbutryn. Individual microcosms were prepared from the homogeneous solution under constant stirring at 1500 rpm by adding 30 mL into 50 mL crimp vials.

PondSed microcosms were prepared from 1 kg of pond sediment, sieved at 2 mm and homogenized with an overhead shaker for 24 h at 20 rpm. 100 g of sediment were filled up to 1 L with retention pond water and autoclaved 3 times in 24 h intervals. Biotic samples were

prepared by mixing 150 g of sediment with 1.5 L of stormwater retention pond water. Spiking and sample preparation was similar to activated sludge microcosms.

All microcosms were crimped with butyl/PTFE caps. A syringe with a 0.2 µm PTFE syringe filter is stuck through the caps to maintain oxic conditions and prevent water loss (Torabi et al., 2020). Samples were incubated in dark (covered by aluminum foil and closed incubator) at 21 ± 2°C under constant orbital shaking at 120 rpm.

1.4.2 Microcosm sampling

At each sampling, triplicate microcosms were retrieved. The whole microcosm content was transferred into a 50 ml brown glass tube. Microcosms were washed with 2 x 2 ml DI-water which was also transferred into the glass tube. At designated time points additional samples were retrieved for transformation product measurements. Sampling for TPs analysis from PondSed and activated sludge included shaking of the samples for 10 min at 600 rpm and ultracentrifugation for 5 min. Samples were filtered through 0.22 µm cellulose membrane filters (Rotilabo®, Carl Roth®, France) and directly frozen at -20°C. For soil TPs, 5 mL of water was added to the sample prior to vortexing, ultracentrifugation and filtration to transfer TPs into the liquid phase.

The organic carbon content of sediment and soil was estimated from independent triplicates by loss on ignition (LOI) according Hoogsteen et al., 2015 (550°C for 3 h). LOI was 5.4 ± 0.7% for sediment and 12.1 ± 0.5% for soil, resulting in an organic carbon content of 3.2 ± 0.4% and 7.0 ± 0.29%, respectively

Table B 3. Chemical composition of pond water and activated sludge from degradation experiments.

	pH	NH_4^+ mmol L^{-1}	Na^+ mmol L^{-1}	K^+ mmol L^{-1}	Mg^{2+} mmol L^{-1}	Ca^{2+} mmol L^{-1}	CL^- mmol L^{-1}	NO^{3-} mmol L^{-1}	SO_4^{2-} mmol L^{-1}	PO_4 mmol L^{-1}	DOC ppm
Pondwater	7.4	0.032	0.211	0.442	0.353	2.352	0.230	0.006	0.072	<l.d	11.46
Activated sludge	7.9	<l.d	2.761	1.001	0.894	1.958	2.466	0.139	0.289	1.372	41.950

Appendix B

Table B 4. Elemental analysis of major and trace elements for soil and sediment used in microcosm experiments.

	Element	Soil	Sediment
Major elements (% of weight per dry soil) from ICP-AES analysis	SiO_2	61.45	64.67
	Al_2O_3	8.00	7.87
	MgO	1.21	1.07
	CaO	5.47	3.37
	Fe_2O_3	2.88	2.68
	MnO	0.09	0.07
	TiO_2	0.47	0.45
	Na_2O	0.88	0.97
	K_2O	2.05	2.13
	P_2O_5	0.27	0.24
Trace elements (μg g^{-1} of dry weight) of dried sample from ICP-AES analysis	Sr	147	127
	Ba	332	356
	Sc	7	7
	Y	25	23
	Zr	270	240
Trace elements (ppm of dried samples) from ICP-MS analysis	V	59.3	52.0
	Cr	93.3	141.0
	Co	10.0	8.6
	Ni	25.8	23.0
	Cu	124.5	62.0
	Zn	874.3	1063.3
	Rb	93.8	87.0
	Nb	11.9	12.0
	Mo	0.7	0.5
	Sn	6.6	5.7
	Cs	6.3	5.5
	La	29.2	26.1
	Ce	60.4	54.0
	Pr	7.1	6.3
	Nd	27.1	24.3
	Sm	5.6	5.0
	Eu	1.0	0.9
	Gd	4.6	4.1
	Tb	1.0	0.7
	Dg	4.4	4.0
	Ho	0.9	0.9
	Er	2.5	2.3
	Tm	0.4	0.4
	Yb	2.6	2.4
	Lu	0.4	0.4
	Hf	7.9	6.9
	Ta	1.0	1.0
	Pb	49	40.3
	Th	10.1	8.9
	U	2.9	2.4

1.5 Recoveries of terbutryn from different matrixes and validation of absence of isotope fractionation during extraction

Recoveries of terbutryn with the extraction method described above were tested for water, pH 1, pH 13, activated sludge, pondwater with sediment and soil. Matrixes were spiked separately with three different concentrations for aqueous samples in duplicate (0.05 mg L^{-1}, 0.5 mg L^{-1} and 5 mg L^{-1}) from a terbutryn stock solution (2 g L^{-1} or 0.1 g L^{-1} respectively). Samples were vortexed for 1 h at 600 rpm. Soil, PondSed and activated sludge samples were incubated at 4°C (to limit bioactivity) for 3 days prior to extraction. Water, alkaline and acidic samples were extracted directly to limit the effects of degradation on the recovery rate by using the same extraction method as for microcosms. Samples were extracted and diluted for HPLC-MS measurements. Recoveries for terbutryn were: water: 85 ± 11%, pH 1: 78 ± 12%, pH12:89 ± 11%, diluted activated sludge: 65 ± 7%, and pond water with sediment: 64 ± 7%. The absence of isotope fractionation and influence of matrix effects caused by the terbutryn extraction was validated for concentrations between 1 mg L^{-1} and 100 mg L^{-1} (shown as peak amplitude at m/z 44) (Figure B 1).

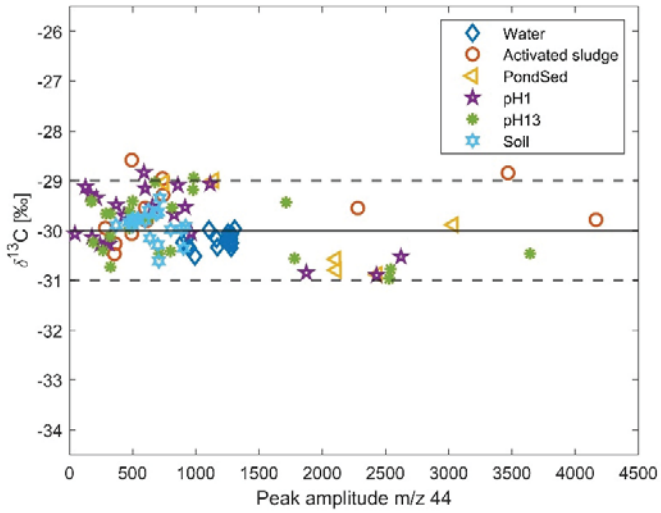

Figure B 1. Range of $\delta^{13}C$ for terbutryn where isotope values are independent of signal intensity with the used extraction method. Solid and dashed lines represent the EA value and the ±1‰ associated uncertainty, respectively.

Appendix B

Table B 5. Validation of the terbutryn extraction method for isotope fractionation free extraction for carbon and nitrogen. Photodegradation experiments refer to the matrix "water". The influence of pH on isotope fractionation free extraction was tested with the same buffer solutions as described above (Table B2). Values are given as difference to the measured EA values. Uncertainties denote the standard deviation from replicate measurements (n = 9).

	Water	Activated sludge	PondSed	pH1	pH13	Soil
$\Delta\delta^{13}C$	0.2 ± 0.1	0.5 ± 0.4	0.7 ± 0.1	0.5 ± 0.3	0.5 ± 0.3	0.2 ± 0.1
$\Delta\delta^{15}N$	0.4 ± 0.4	0.2 ± 0.3	0.1 ± 0.2	0.6 ± 0.6	0.3 ± 0.7	0.5 ± 0.5

1.6 Transformation products

Table B 6. Physico-chemical characteristics of terbutryn and its main transformation products.

Name	**Terbutryn**	**Terbutryn-Sulfoxide**	**2-Hydroxy-terbutryn**	**Desethyl-2-hydroxy-terbutryn**	**Desethyl-terbutryn**	**Desthiomethyl-terbutryn**[r]
Short name	Ter	TerSO	TerOH	TerDesEOH	TerDesE	TerDesS
Chemical formula	$C_{10}H_{19}N_5S$	$C_{10}H_{19}N_5OS$	$C_9H_{17}N_5O$	$C_7H_{13}N_5O$	$C_8H_{15}N_5S$	$C_9H_{17}N_5$
IUPAC Name	2-N-tert-butyl-4-N-ethyl-6-methylsulfanyl-1,3,5-triazine-2,4-diamine	2-N-tert-butyl-4-N-ethyl-6-methylsulfinyl-1,3,5-triazine-2,4-diamine	6-(tert-butylamino)-4-(ethylamino)-1H-1,3,5-triazin-2-one	6-amino-4-(tert-butylamino)-1H-1,3,5-triazin-2-one	2-N-tert-butyl-6-methylsulfanyl-1,3,5-triazine-2,4-diamine	2-N-tert-butyl-4-N-ethyl-1,3,5-triazine-2,4-diamine
WS (mg L^{-1})	17	7	906	8608	174	264
log K_{OW}	3.77	4.1	1.5	0.6	2.7	2.6
Molecular structure	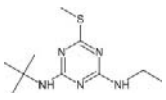	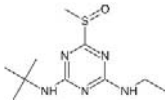	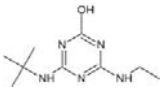	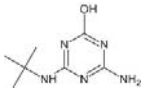	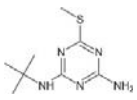	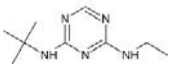
CAS	886-50-0	82985-33-9	66753-07-9	66753-06-8	30125-65-6	73956-51-1

[r] TerDesS is added for comparison but was not measured with our targeted approach

1.7 HPLC-MS/MS method

Compounds were separated on a C18 column (Accucore 100 x2.1, particle size 2.6 µm) and measured in positive ESI mode. Water (A) with 0.05% formic acid and Acetonitril (B) with 0.1% formic acid were used as mobile phase. In the first 8 minutes, solvent B was increased from 10% to 90% with a hold phase of 1 min at 90% solvent B, decrease of solvent B to 10 % within one minute, followed by 2 min at initial solvent composition (10% solvent B). Flow was 0.4 ml/min. A static spray voltage was used (1800 V). Sheath gas was 55 Arb, Aux gas 20 Arb and Sweep gas 2 Arb. The ion transfer tube was heated to 280°C. Vaporizer temperature was set to 300°C. The mass spectrometer was run in selected reaction monitoring (SRM) mode. The resolution in Q1 and Q3 was 0.7 full width at half maximum (FWHM).The CID gas was set to 1.5 mTorr. Compounds were identified and quantified based on their precursor and two fragment ions (Table B 7).

Table B 7. Compounds, precursor ion and mass transitions of the measured molecules. Analytical uncertainty was < 15 %.

Compound	Retention time (min)	Precursor (m/z)	Transition 1 (m/z)	Collision Energy 1 (eV)	Transition 2 (m/z)	Collision Energy 2 (eV)	LOD (ng L^{-1})	LOQ (ng L^{-1})
Terbutryn	5.00	242	242 → 258.054	25.56	242 → 186.083	19.11	2.0	6.8
TerOH	3.14	212	212 → 86.083	25.39	212 → 156.083	16.96	4.3	14.4
TerSO	4.12	258	258 → 256.083	20.29	258 → 258.054	25.56	1.7	5.8
TerDesE	4.09	214	214 → 110.155	26.57	214 → 157.982	18.18	2.4	8.0
TerDesEOH	0.57	184	184 → 86.083	24.84	184 → 128.083	15.7	8.3	27.7

1.8 CSIA method and quality control

The GC-IRMS temperature program for carbon and nitrogen started with a 2 min hold time at 50 C, heating to 150°C with 20°C min^{-1}, heating to 245°C with 5°C min^{-1} heating with 30°C min^{-1} to 320°C and holding the temperature for 0.5 min. For carbon, analytes were combusted

to CO_2, for nitrogen to N_2 respectively in a reactor oven (P/N 1255321, NiO tube and CuO-NiO-Pt wires, Thermo Fischer Scientific) at 1000°C. During nitrogen isotope measurements, liquid N_2 was used for cryogenic trapping of CO_2. Samples were bracketed with standards (after every 9 samples for C and every 3 samples for N). For C, the standard was BTEX with known isotopic signature (benzene, toluene, ethylbenzene and o-Xylene). For N measurements, Caffeine (international reference material AIEA600) was used at 100 mg L^{-1} in acetone. Additionally, terbutryn standards (100 mg L^{-1} in DCM) were injected after each standard. Terbutryn standards were previously characterized using an elemental analyzer to get the reference isotope signature (Flash EA IsoLinkTM CN IRMS, Thermo Fisher Scientific). Reference values were $\delta^{13}C_{Terbutryn}$= -30.0 ± 0.1 and $\delta^{15}N_{Terbutryn}$= -3.4 ± 0.2.

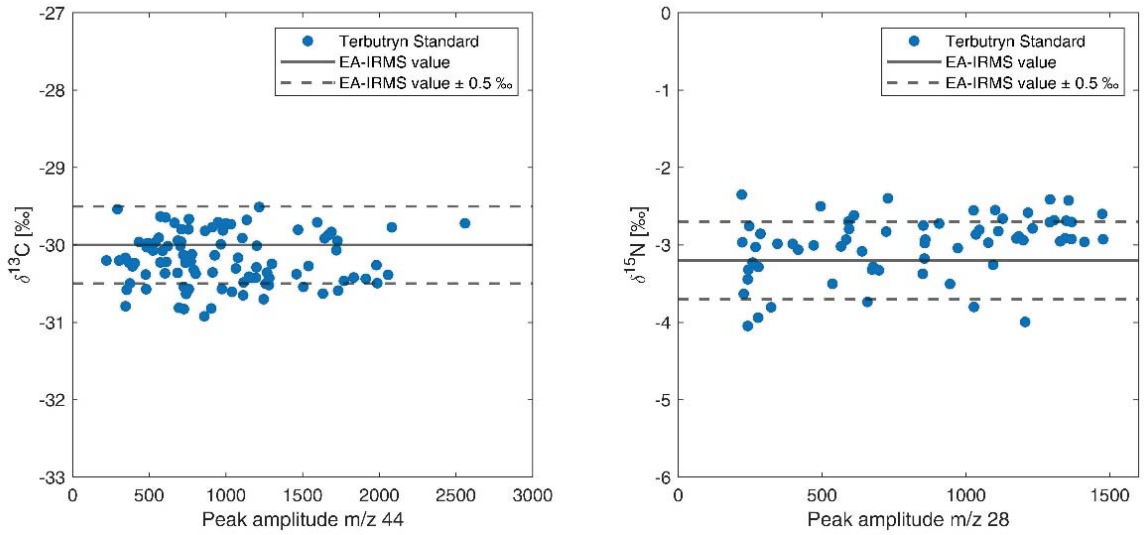

Figure B 2. Ranges where isotope values are independent of signal intensity for $\delta^{13}C$ as a function of the peak amplitude m/z 44 (left), and $\delta^{15}N$ as a function of the peak amplitude m/z 28 (right) for terbutryn. Solid line indicates EA-IRMS measurement, dashed lines show typical ±0.5‰ associated uncertainties.

2 Results

2.1 Degradation of terbutryn

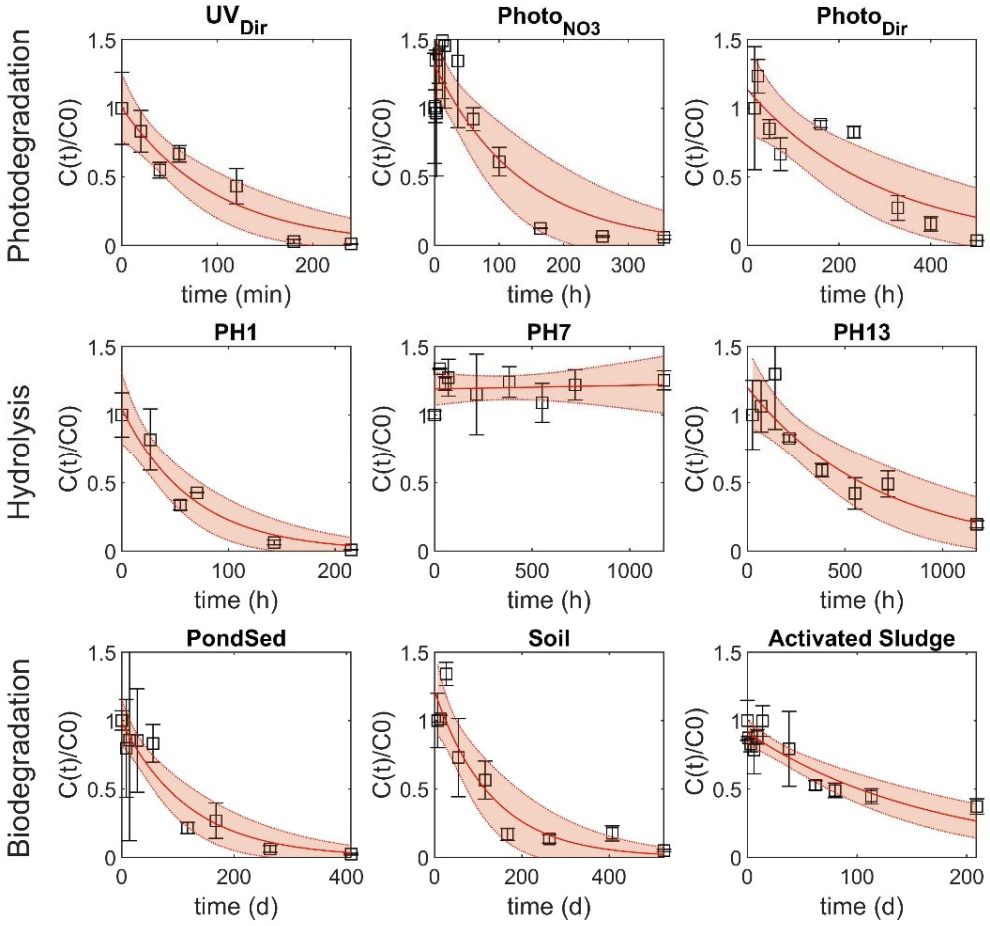

Figure B 3. Evolution of terbutryn concentration during photodegradation under UV irradiation (UVDir), photodegradation under simulated sunlight with NO_3^- (PhotoNO_3), photodegradation under simulated sunlight in pure water (PhotoDir), abiotic hydrolysis at pH 1 (pH1), pH 7 (pH7) and pH 13 (pH13), biodegradation at the pond water sediment interface (PondSed), soil (soil) and in diluted activated sludge (activated sludge). Error bars represent standard deviation between independent triplicate microcosms/replicates for each sampling, red dotted lines indicate 95% CI of degradation kinetics.

Appendix B

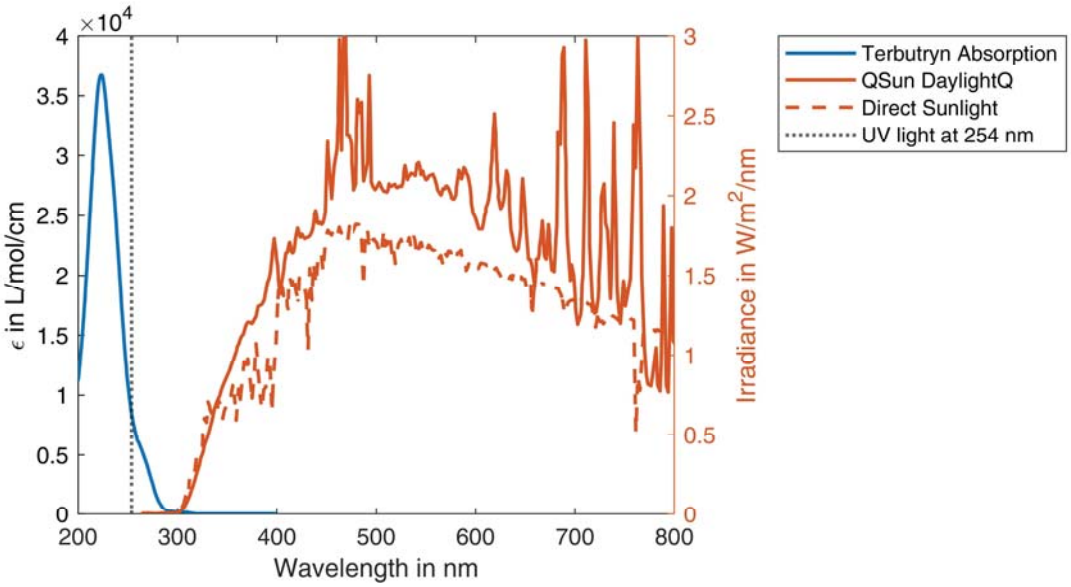

Figure B 4. Light absorption ε for terbutryn (blue, left y-axis), sunlight irradiation spectrum (dashed orange line, right y-axis) and reproduced sunlight spectrum of the QSUN test chamber with DaylightQ filter (orange line, right y-axis) (modified from Hensen et al., 2019; QSun/QLab, 2011).

During degradation, pH might change due to different composition of terbutryn and TPs. Major changes in pH might cause abiotic hydrolysis. Therefore, several solutions of terbutryn and transformation products with and without of calcium nitrate tetrahydrate ($Ca(NO_3)_2 \cdot 4\ H_2O$) were tested in the observed concentration range (1 - 10 mg L^{-1}). pH for all solutions was 7 ± 0.5. Because of the high hydrolytic stability of terbutryn, hydrolysis during photodegradation was assumed to be negligible. Additionally, a pre-experiment for terbutryn hydrolysis (T = 60°C, pH 2, pH 7 and pH 12) was launched prior to the photodegradation experiments with no significant degradation neither under neutral, nor under alkaline or acidic conditions within 30 d. This implied that hydrolysis is unlikely to occur in the tested timeframe (< 30 d) and conditions (pH =7) of the photodegradation experiments. As a result, no buffering of the solutions was applied. This has additionally the advantage to exclude possible interference of the buffer with photolysis.

2.2 Transformation product measurements

Transformation products for soil microcosms were only measured at one sampling point (Table B 1). The results show mainly a conversion to TerOH with a small contribution of TerSO with minor contributions of TerDesE and no detection of TerDesOH (Figure B 5).

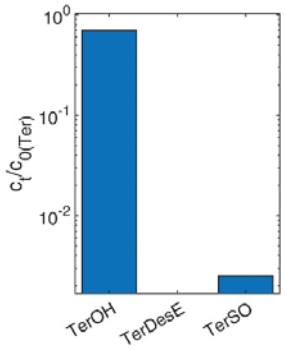

Figure B 5. Transformation product measurement for single soil microcosm after 525 days of incubation (Table B 1) as molar concentrations normalized to initial terbutryn concentrations (Ter). TerDesEOH was not detected, TerDesE contribution was very low.

2.3 Carbon and nitrogen isotope fractionation of terbutryn

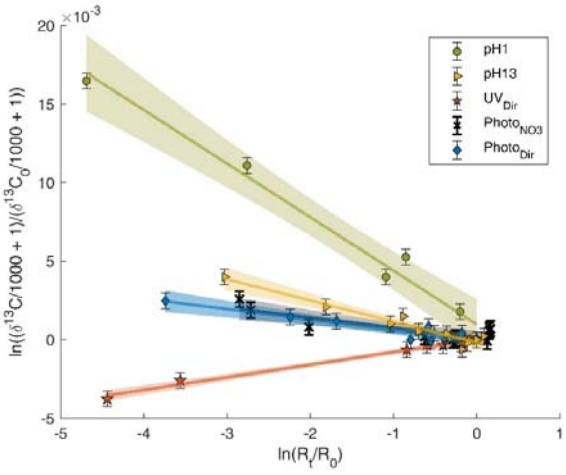

Figure B 6. Carbon isotope fractionation of terbutryn during abiotic hydrolysis at pH 1 (green circles) and pH 13 (yellow triangles), photodegradation under UV irradiation (orange stars), simulated sunlight with nitrates (black crosses) and in pure water (blue rectangles). Lines represent the linear regression of the log plot according to the Rayleigh equation; shaded areas indicate the 95% CI and error bars indicate associated uncertainty of ±0.5‰.

Appendix B

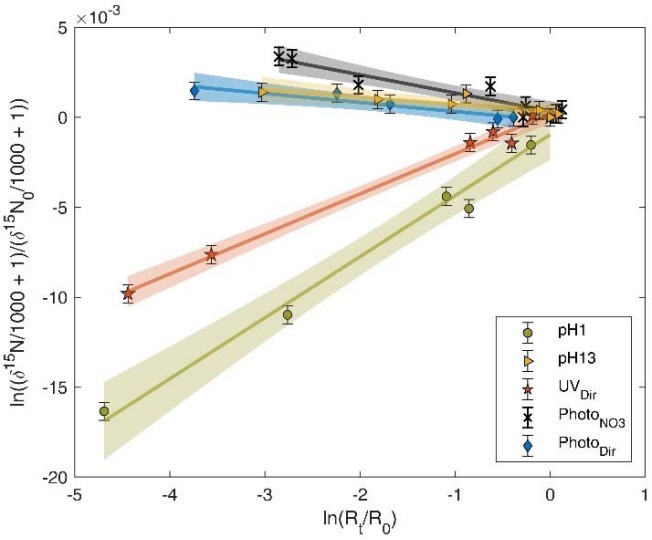

Figure B 7. Nitrogen isotope fractionation of terbutryn during abiotic hydrolysis at pH 1 (green circles) and pH 13 (yellow triangles), photodegradation under UV irradiation (orange stars), simulated sunlight with nitrates (black crosses) and in pure water (blue r rectangles). Lines represent the linear regression of the log plot according to the Rayleigh equation; shaded areas indicate the 95% CI and error bars indicate associated uncertainty of ±0.5‰.

References

Brinch, U.C., Ekelund, F., Jacobsen, C.S., 2002. Method for spiking soil samples with organic compounds. Appl. Environ. Microbiol. 68, 1808–1816.

Hensen, B., Olsson, O., Kümmerer, K., 2019. The role of irradiation source setups and indirect phototransformation: kinetic aspects and the formation of transformation products of weakly sunlight-absorbing pesticides. Sci. Total Environ. 695, 133808.

Hoogsteen, M.J.J., Lantinga, E.A., Bakker, E.J., Groot, J.C.J., Tittonell, P.A., 2015. Estimating soil organic carbon through loss on ignition: effects of ignition conditions and structural water loss. Eur. J. Soil Sci. 66, 320–328.

QSun/QLab, 2011. Q-Lab QSun Technical bulletin LU-0822: sunlight, weathering & light stability testing [WWW Document]. URL https://www.q-lab.com/documents/public/cd131122-c252-4142-86ce-5ba366a12759.pdf (accessed 2.9.22).

Torabi, E., Wiegert, C., Guyot, B., Vuilleumier, S., Imfeld, G., 2020. Dissipation of S-metolachlor and butachlor in agricultural soils and responses of bacterial communities: insights from compound-specific isotope and biomolecular analyses. J. Environ. Sci. 92, 163–175.

Appendix C Supporting information of Chapter 5

1 Material and Methods

Used chemicals. Solvents (dichloromethane (DCM) and *n*-Pentane) were HPLC-grade (> 99.9%) and purchased from Sigma-Aldrich (St. Louis, MO, USA). Analytical standards with purity > 98% (terbutryn and alachlor D-13) were purchased from PESTANAL (St. Louis, MO, USA). Standards of terbutryn TPs, including terbutryn-2-hydroxy (TerOH), terbutryn-desethyl (TerDesE) and terbutryn-desethyl-2-hydroxy (TerDesEOH) (purity > 98%), were purchased from HPC Standards GmbH (Borsdorf, Germany), terbutryn-sulfoxide (TerSO) (purity > 97%) was purchased from MicroCombiChem GmbH (Wiesbaden, Germany). Water, acetonitrile, and formic acid for analysis with HPLC-MS were LC/MS grade (Biosolve, France).

Table C 1. Characterization of major parameters of the used paints

	Paint A	Paint B
pH	8 - 10	9 - 10
Density at 20°C (g/cm^3)	1.3	1.5
Water solubility	completely soluble	completely soluble
Viscosity (mPa.s)	≈ 2000	≈ 2200
Supplier	Sto Se & Co. KGaA	Sto Se & Co. KGaA
Color	White	White

Table C 2. Sampling times and cumulated irradiation of photodegradation experiments on paint and pure terbutryn formulations (encapsulated and nonencapsulated).

	Paint A		Paint B		Encapsulated formulation		Non-encapsulated formulation	
	Irradiation (kJ m^{-2})	Δt (h)	Irradiation (kJ m^{-2})	Δt (h)	Irradiation (kJ m^{-2})	Δt (h)	Irradiation (kJ m^{-2})	Δt (h)
t0	0	0	0	0	0	0	0	0
t1	68	28	67	27:10	68	28	67	27:10
t2	174	71:13	715	291:56	350	143:02	715	291:56
t3	350	143:02	1526	623:35	1183	483:26	2116	864:26
t4	458	191:35	2116	864:26	2584	1056		
t5	771	315:17	2312	925:31				
t6	1183	483:26						
t7	1591	650:22						
t8	1994	815:14						
t9	2584	1056						

Figure C 1. Experimental setup of facade leaching experiment under environmental conditions.

Appendix C

Table C 3. Weather data from weather station next to facades over experimental time.

Mean temperature (°C)	15.6
Min. temperature (°C)	- 1.1
Max. temperature (°C)	30.9
Cumulative rainfall (L m^{-2})	611.1
Max. daily rainfall (L m^{-2})	52
Mean daily solar irradiation (Wh m^{-2})	1599
Min. daily solar irradiation (Wh m^{-2})	231
Max. daily solar irradiation (Wh m^{-2})	3071
Max. wind speed (m/s)	9.8
Mean humidity (%)	72.5

Immersion tests at lab-scale for long term release assessment: Pieces (10 × 10 cm) were cut from each 1 m² panel at the end of the experiment and from one replicate of each small facade panel that was collected throughout the experiment. The immersion test followed a European standard described previously (*DIN EN 16105*, n.d.; Vermeirssen et al., 2018). Individual facade pieces were placed in glass cases and plunged face down in deionized water (100 mL). The experiment was carried out for 18 days and consisted of 9 immersion days. Each immersion day comprised two 1 h immersion cycles separated by a drying period of 4 h. During immersion, slow horizontal shaking (30 rpm) enabled uniform leaching conditions. 10 L m^{-2} of water was used with each immersion cycle instead of 25 L m^{-2} to better fit the experimental setup and getting closer to real environmental conditions. Considering western oriented facades and estimates of wind driven rain, 9 immersion days (10 L m^{-2} per cycle) correspond to a total facade runoff representing 10 – 25 years of rainfall (Wicke et al., 2022).

Water (100 mL) was collected after the initial immersion and replaced by fresh deionized water after the drying phase. The two water samples representing one immersion day were combined and frozen. An aliquot of each sample was filtered through 0.45 µm (PTFE, 25 mm ∅, VWR chemicals) and prepared for LC/MSMS measurements.

Detailed description of extraction methods. Extraction of terbutryn from paint samples: Filters with dried paint were cut into approximately 0.5 cm² pieces and transferred into 40 ml amber glass vials. Terbutryn was extracted using 3 ml Pentane:DCM (3:1, V:V). samples were shaken for 5 min (600 rpm), ultrasonicated for 15 min, shaken again for 5 min and centrifuged at 1500 rpm for 5 min. Solvent was recovered and the whole procedure was repeated

three times. Respective solvent was pooled and evaporated under gentle N_2 stream. Samples were resuspended in 1 ml acetonitrile and frozen until analysis at -20°C.

Extraction of terbutryn and transformation products using SPE: Façade runoff samples were vacuum filtered to 0.45 µm (PTFE, 25 mm ∅, VWR chemicals). Samples were extracted using an automated solid phase extraction (SPE), using Chromabond HR-X cartridges (6 mL, 500 mg, particle size 85 µm). Cartridges were conditioned with 10 ml of methanol, followed by 10 ml of H_2O. The full volume of the sample was loaded onto the cartridge followed by drying of cartridges for 15 min with N_2. Cartridges were soaked with chloroform:methanol (1:1, V:V) and 10 ml solvent was collected. Solvent was evaporated under gentle N_2 flux and resuspended in 1 mL acetonitrile followed by a purification procedure using 75 mg of anhydrous $MgSO_4$ and 13 mg PSA. Vials were vortexed for 30 s, centrifuged at 2400 RCF before transferring the solvent in 1.5 mL GC vials. The samples were frozen until analysis at -20°C.

Table C 4. Compounds, precursor ions, mass transitions, collision energy, recovery through SPE, limit of detection (LOD) and limit of quantification (LOQ). LOD and LOQ are given for water after considering enrichment through SPE extraction of a volume of 500 mL (≈ mean extracted volume from facade runoff).

Compound	Retention time (min)	Precursor (m/z)	Transition 1 (m/z)	Collision Energy 1 (eV)	Transition 2 (m/z)	Collision Energy 2 (eV)	Recovery (%)	LOD (ng L^{-1})	LOQ (ng L^{-1})
Terbutryn	5.00	242	242 → 258.054	25.56	242 → 186.083	19.11	103.9	0.3	1.0
TerOH	3.14	212	212 → 86.083	25.39	212 → 156.083	16.96	117.7	0.9	2.7
TerSO	4.12	258	258 → 256.083	20.29	258 → 258.054	25.56	85.4	0.2	0.6
TerDesE	4.09	214	214 → 110.155	26.57	214 → 157.982	18.18	98.6	0.4	1.1
TerDesEOH	0.57	184	184 → 86.083	24.84	184 → 128.083	15.7	125.0	1.5	4.4

Appendix C

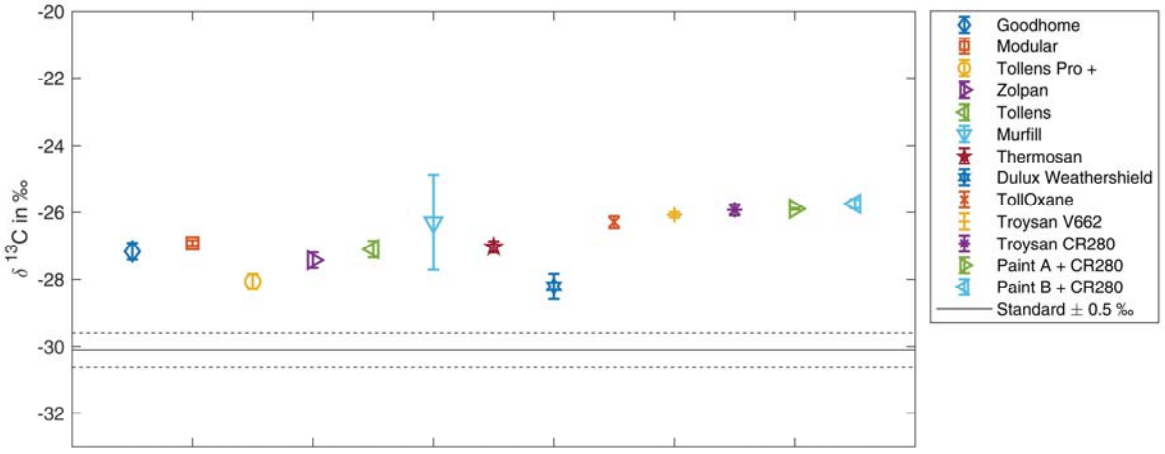

Figure C 2. $\delta^{13}C$ of various paints and pure encapsulated and non-encapsulated terbutryn formulation. Extraction was performed with the same method as described above.

Table C 5. Characteristics of the used geometry input file for COMLEAM of model facade runoff.

Facade orientation	Facade area (m²)	slope to ground (°)	height (m)	length (m)	runoff coefficient (-)
North	18.75	90	2.5	7.5	0.9
East	43.75	90	2.5	17.5	0.9
South	18.75	90	2.5	7.5	0.9
West	43.75	90	2.5	17.5	0.9
Roof	145	5	2.5	17.5	1.0

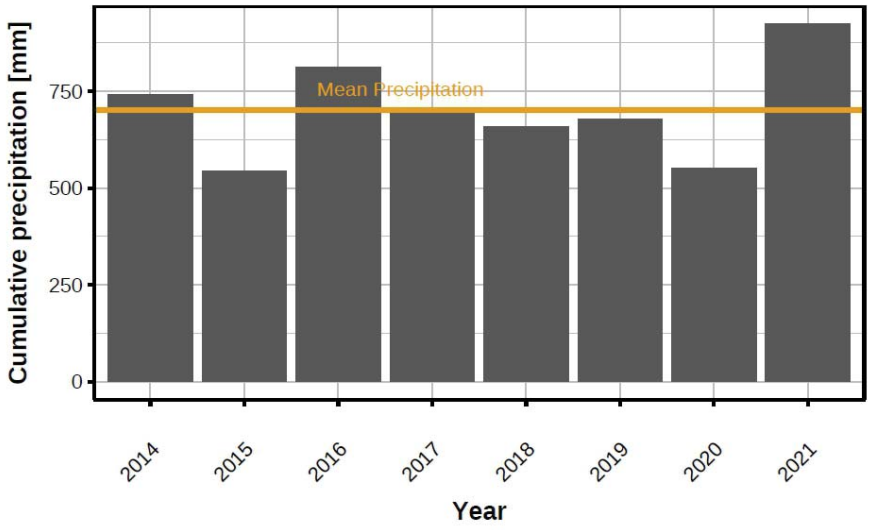

Figure C 3. Grouped cumulative rain amount in mm per year from COMLEAM input data.

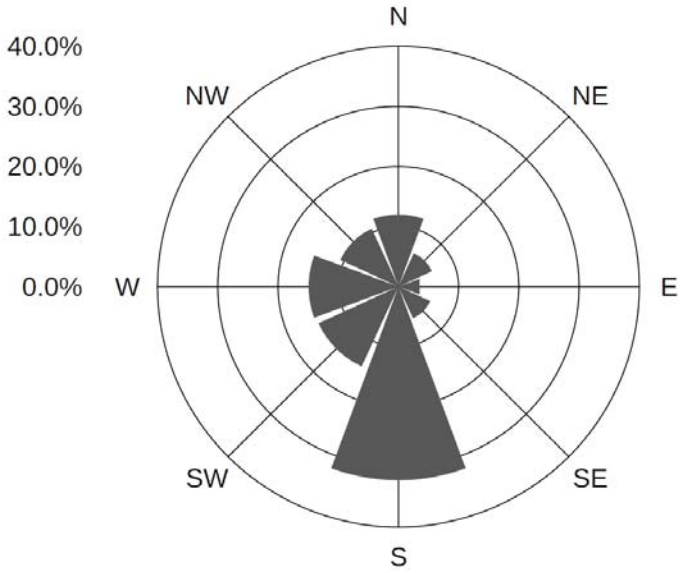

Figure C 4. Relative rain amount in dependence of wind direction.

Appendix C

2 Results

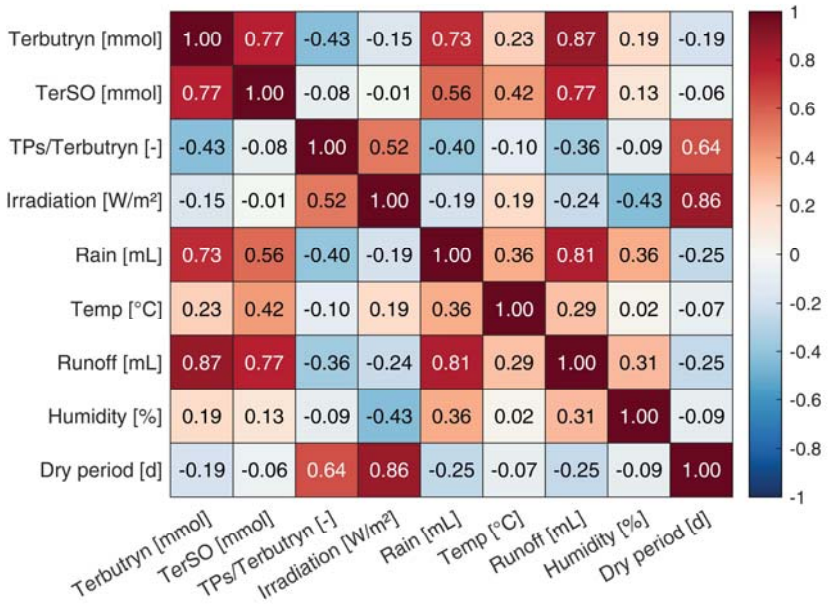

Figure C 5. Pearson correlation coefficient (ρ) between emissions of Terbutryn (Ter), Terbutryn-Sulfoxide (TerSO), the ratio of transformation products to terbutryn (TPs/Ter) and hydro-climatic variables (cumulated Irradiation, cumulated rain volume, mean temperature, cumulated runoff volume, mean humidity, and length of dry period prior to the rain event).

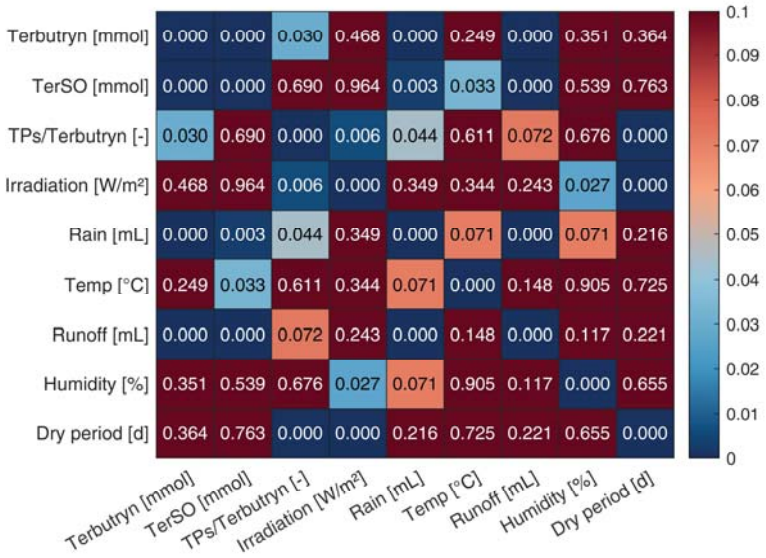

Figure C 6. P-value (p) of Pearson correlation between emissions of Terbutryn (Ter), Terbutryn-Sulfoxide (TerSO), the ratio of transformation products to terbutryn (TPs/Ter) and hydro-climatic variables (cumulated Irradiation, cumulated rain volume, mean temperature, cumulated runoff volume, mean humidity, and length of dry period prior to the rain event).

Table C 6. Fitting parameters for terbutryn emission in the field experiments and laboratory immersion tests from newly painted facades (Δt = 0 d) and exposed facades in the field collected over time (Δt = 33 d, 160 d and 194 d). The volume and mass of already leached terbutryn (and transformation products) was added to the measured immersion test. Parameters were calculated for terbutyn leaching (Ter) and terbutryn and all measured TPs (Ter+TPs).

			a_{char}	q_{char} (L m^{-2})	q (L m^{-2}) for leaching 1 % of Ter	q (L m^{-2}) for leaching 10 % of Ter
Field		Ter	0.02	24.3	73.8	1.25×10^{9}
		Ter+TPs	0.88	622.1	15.2	184.3
Immersion	Δt = 0 d	Ter	0.74	365.8	10.6	133.4
		Ter+TPs	0.86	414.6	10.4	127.2
	Δt = 33 d	Ter	0.83	566.6	14.2	179.6
		Ter+TPs	0.99	598.2	12.7	153.5
	Δt = 160 d	Ter	0.57	471.3	15.1	246.4
		Ter+TPs	1.06	656.6	13.1	155.2
	Δt = 194 d	Ter	0.32	188.8	10.2	231.2
		Ter+TPs	0.45	174.3	7.6	123.6

Appendix C

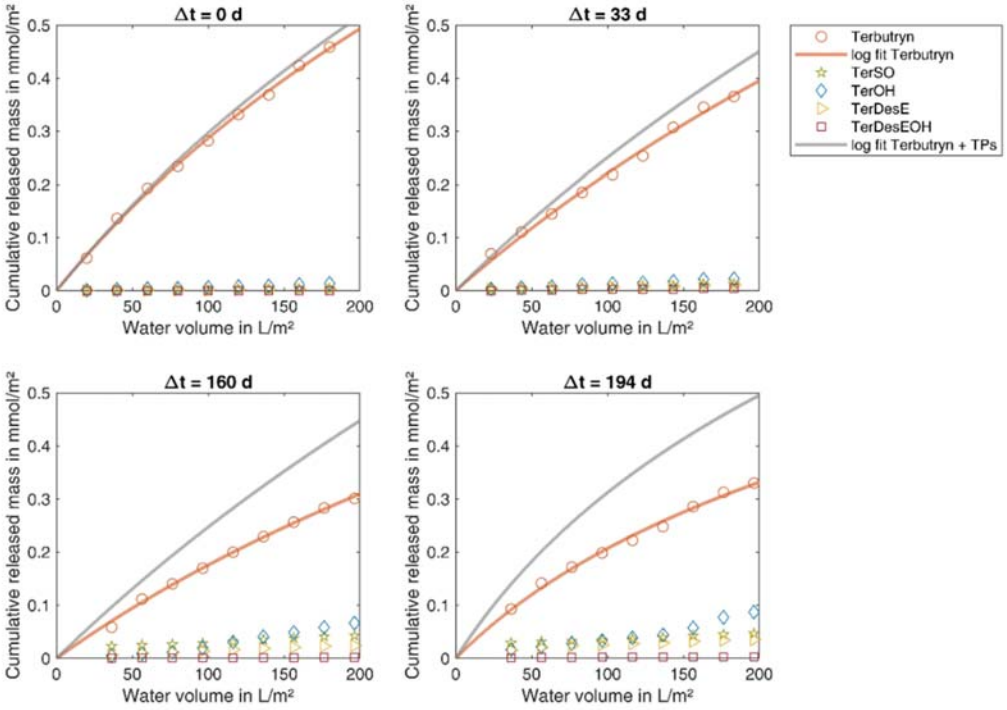

Figure C 7. Cumulative released mass of terbutryn and transformation products over water volume in immersion experiment. Results are normalized to 1 m² facades. Immersion of facade panels, retrieved from natural weather after t = 0, 33, 160 and 194 d. Solid lines indicate logarithmic emission functions for terbutryn only (orange) and for terbutryn plus released transformation products.

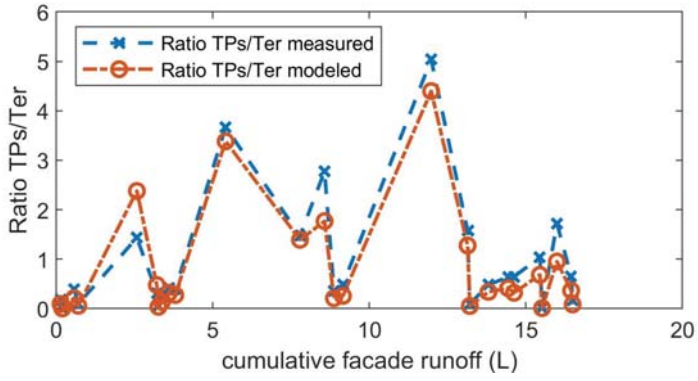

Figure C 8. Comparison between measured and modeled ratios of TPs/Terbutryn over cumulative facade runoff from scenario B, considering irradiation and facade runoff as driving parameters for the contribution of transformation products to leaching.

References

DIN EN 16105:2011-12 Beschichtungsstoffe - Laborverfahren zur Bestimmung der Freisetzung von Substanzen aus Beschichtungen in intermittierendem Kontakt mit Wasser; Deutsche Fassung EN_16105:2011, n.d. . Beuth Verlag GmbH.

Vermeirssen, E.L.M., Campiche, S., Dietschweiler, C., Werner, I., Burkhardt, M., 2018. Ecotoxicological assessment of immersion samples from facade render containing free or encapsulated biocides. Environ. Toxicol. Chem. 37, 2246–2256.

Wicke, D., Tatis-Muvdi, R., Rouault, P., Zerball-van Baar, P., Dünnbier, U., Rohr, M., Burkhardt, M., 2022. Bauen und Sanieren als Schadstoffquelle in der urbanen Umwelt. Umweltbundesamt 108.

Appendix D : Supporting information of Chapter 6

1 Material and Methods

1.1 Used chemicals and suppliers

Solvents (dichloromethane (DCM) and *n*-Pentane) were HPLC-grade (> 99.9%) and purchased from Sigma-Aldrich (St. Louis, MO, USA). Analytical standards with purity > 98% (terbutryn, diuron, acetochlor and alachlor D-13) were purchased from PESTANAL (St. Louis, MO, USA). Standards of terbutryn TPs, including terbutryn-2-hydroxy (TerOH), terbutryn-desethyl (TerDesE) and terbutryn-desethyl-2-hydroxy (TerDesEOH) (purity > 98%), were purchased from HPC Standards GmbH (Borsdorf, Germany), terbutryn-sulfoxide (TerSO) (purity > 97%) was purchased from MicroCombiChem GmbH (Wiesbaden, Germany). Water, acetonitrile and formic acid for analysis with HPLC-MS were LC/MS grade (Biosolve, France). Dichloromethane and n-Pentane were HPLC-grade (> 99.99%) and purchased from Siga-Aldrich (St.Louis, MO, USA).

Table D 1. Molecules, molecular weight (MW), chemical structure, water solubility (WS) and octanol-water partitioning coefficient (K_{OW}) of used compounds and transformation products (‡).

Class of molecule	Name and MW (g/mol)	Chemical structure	WS (mg L^{-1})	Log K_{OW}
Triazine	Terbutryn (241.36)	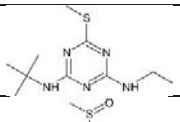	42	3.65
	Terbutryn-Sulfoxide (257.13) ‡	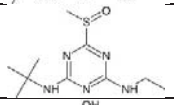	7	4.1
	Terbutryn-2-Hydroxy (211.14) ‡	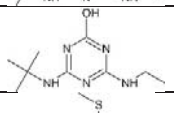	906	1.5
	Terbutryn-Desethyl (213.11) ‡	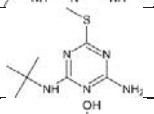	174	2.7
	Terbutryn-Desethyl-2-Hydroxy (183.11) ‡	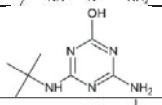	8608	0.6
Phenylurea	Diuron (233.09)	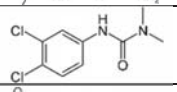	35	2.71
Isothiazolinones	Octylisothiazolinone (OIT) (213.34)		480	2.45
Chloroacetanilide	Acetochlor (269.77)	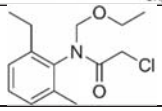	223	4.14

Appendix D

1.2 Experimental setting

Figure D 1. Picture of lysimeters during the experiment.

1.3 Characterization of lysimeters

Gravel lysimeter was filled with coarse gravel (1.6 – 6.4 cm grain size). The top layer of the pavement lysimeter consisted of pavement stones (8 cm × 22.5 cm × 11.25 cm; h × l ×w) with joints (0.5 cm) in between stones. Further characteristics of layers are described in Table D 2.

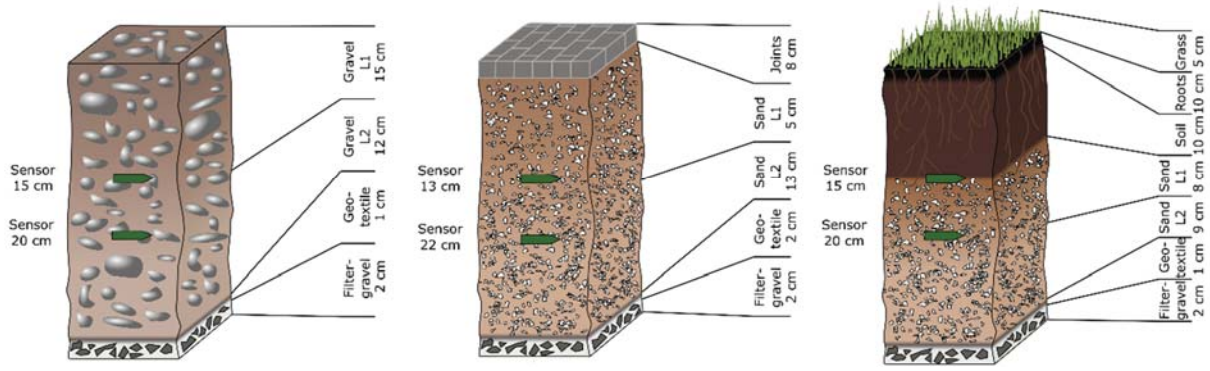

Figure D 2. Composition and depth of lysimeter layers for gravel (left), pavement (middle) and vegetated soil (right).

Table D 2. Soil and sand characterization.

		% clay < 2µm	% silt 2µm to 50µm	% sand 50µm to 2000 µm	pH in water fraction < 2 mm	% carbonates fraction < 2 mm	% organic carbon fraction < 2mm
Pavement	Joints	3.0	9.4	87.6	8.7	17.3	0.27
	Sand_L1	7.1	20.9	72.0	9.2	25.3	0.17
	Sand_L2	9.3	27.2	63.5	9.1	26.3	0.05
Vegetated soil	Soil	5.6	26.5	68.0	7.1	7.9	7.27
	Sand_L1	8.9	29.3	61.9	8.8	26.5	0.28
	Sand_L2	8.3	24.3	67.4	9.0	26.3	0.28

Due to size of gravel and to achieve homogeneous samples, the extraction procedure was slightly varied: 100 g of gravel was weighted in a brown glass bottle and extracted 2 times with 20 mL of DCM:Pentane (1:3, V:V).

1.4 Weather during the experiment

Table D 3. Summary of weather data in the studied period.

Mean temperature (°C)	14.4
Min. temperature (°C)	- 1.1
Max. temperature (°C)	30.9
Cumulative rainfall (L m^{-2})	653.7
Max. daily rainfall (L m^{-2})	52
Mean daily solar irradiation (Wh m^{-2})	1599
Min. daily solar irradiation (Wh m^{-2})	231
Max. daily solar irradiation (Wh m^{-2})	3071
Max. wind speed (m/s)	9.8
Mean humidity (%)	72.5

Appendix D

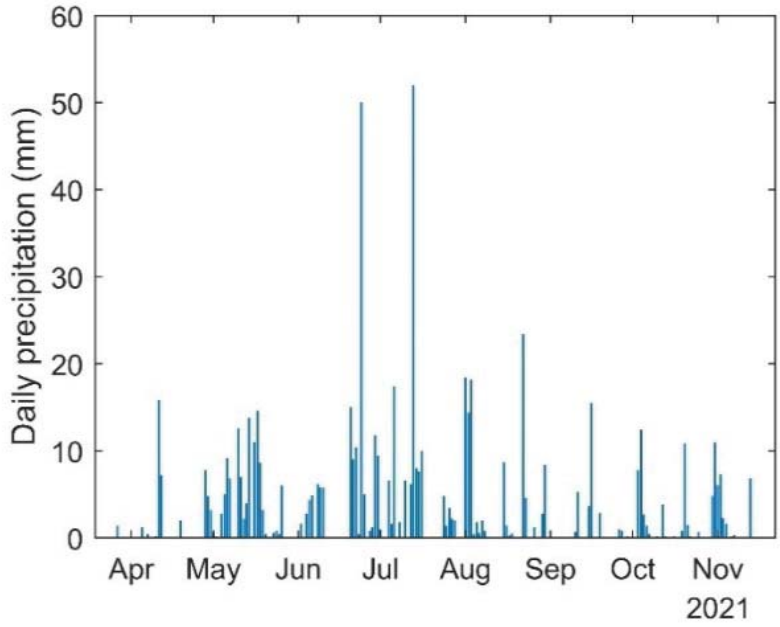

Figure D 3. Daily precipitation during the studied period.

1.5 Recoveries of extraction methods

Table D 4. Recovery, limit of detection (LOD and limit of quantification (LOQ) for extractions from water using SPE and soil. LOD and LOQ for water consider extraction of 100 mL of leachate or 5 g of soil.

	SPE				Solvent extraction			
	Recovery (%)	Stdev. Recovery (%)	LOD (ng/L)	LOQ (ng/L)	Recovery (%)	Stdv Recovery (%)	LOD (ng/g)	LOQ (ng/g)
Terbutryn	103,9	15,3	1,7	5,0	68,4	14,8	0,03	0,08
Acetochlor	79,2	9,0	2,3	7,1	37,3	9,7	0,05	0,15
OIT	84,8	6,8	3,6	11,0	13,3	1,5	0,23	0,70
Diuron	95,3	8,6	16,1	48,7	49,1	13,9	0,31	0,94
TerSO	85,4	12,2	1,2	3,6	22,5	5,4	0,05	0,14
TerDesE	98,6	7,1	1,8	5,4	60,1	17,5	0,03	0,09
TerOH	117,7	19,6	3,8	11,4	9,5	3,8	0,47	1,42
TrDesEOH	125,0	24,3	5,9	17,7	8,6	2,7	0,85	2,58

1.6 Compound-specific isotope analysis

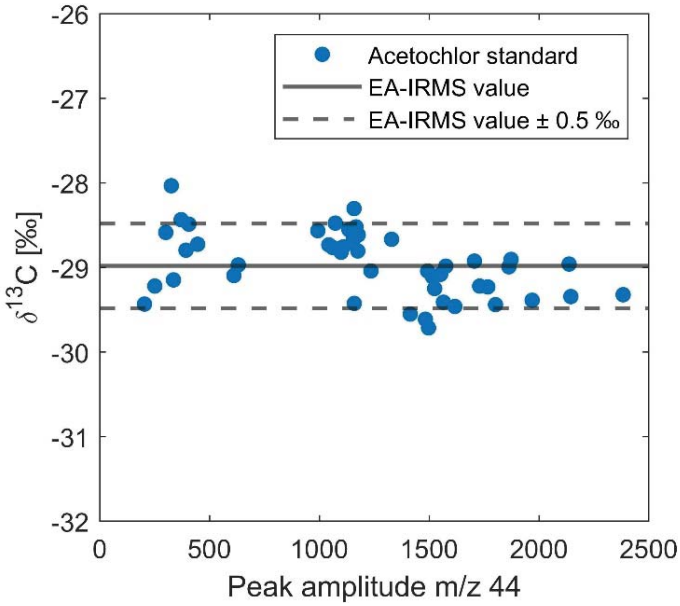

Figure D 4. Ranges where isotope values are independent of signal intensity for δ13C as a function of the peak amplitude m/z 44 for acetochlor. Solid line indicates EA-IRMS measurement, dashed lines show typical ±0.5‰ associated uncertainties.

1.7 Parametrization of Hydrus 1-D

Parameters such as the residual and saturated soil water content θ_r and θ_r, parameters of the soil water retention function α and n, saturated hydraulic conductivity K_s were optimized using Hydrus-1D. Breakthrough curves of terbutryn and TerSO were used to estimate degradation half-lives

Table D 5. Initial estimates of van Genuchten soil hydraulic parameters.

		θ_r	θs	α	n	Ks
		cm^3/cm^3	**cm^3/cm^3**	**1/cm**	-	cm/d
Pavement	**Joints**	0.0438	0.3840	0.0393	2.3176	243.47
	Sand_L1	0.0378	0.3872	0.0385	1.4637	57.31
	Sand_L2	0.0400	0.3873	0.0289	1.4045	40.79
Vegetated soil	**Soil**	0.0336	0.3914	0.0363	1.4298	58.42
	Sand_L1	0.0391	0.3883	0.0270	1.4061	40.96
	Sand_L2	0.0386	0.3872	0.0337	1.4177	47.16

Appendix D

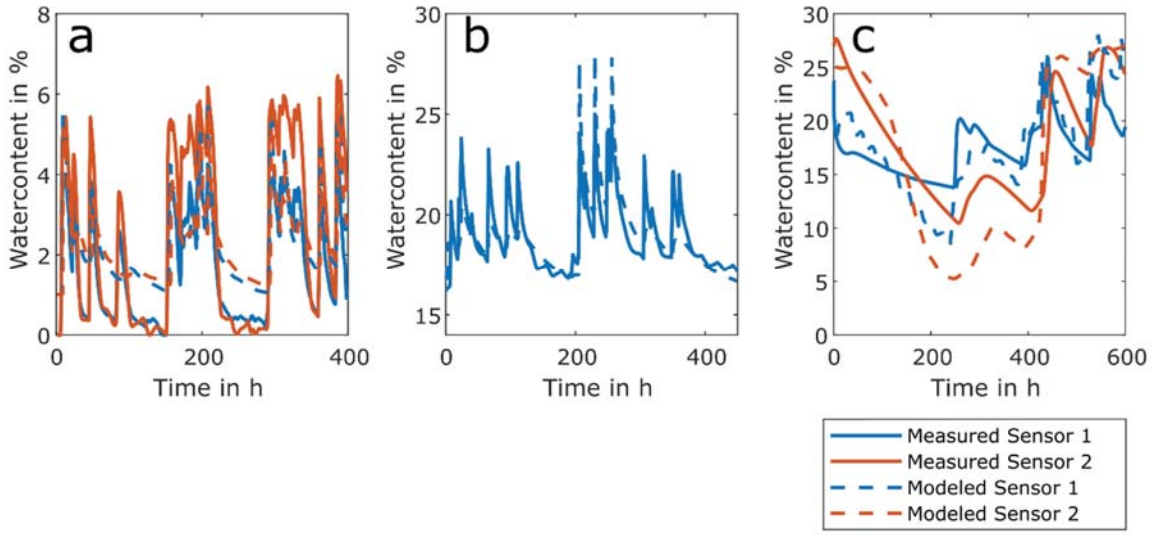

Figure D 5. Modelled water contend with optimized van Genuchten's water retention parameters for selected time periods for gravel (a), pavement (b) and vegetated soil (c).

Table D 6. Optimized van Genuchten's parameters.

		θ_r	θs	α	n	Ks
		cm^3/cm^3	**cm^3/cm^3**	**1/cm**	-	cm/h
Gravel		0.0001	0.45	4.93	2.19	1500
Pavement	**Joints**	0.0003	0.30	0.14	1.71	449.96
	Sand	0.064	0.43	0.14	1.63	112.95
Vegetated soil	**Soil**	0.057	0.40	0.17	1.76	0.55
	Sand	0.003	0.47	0.013	1.60	7.80

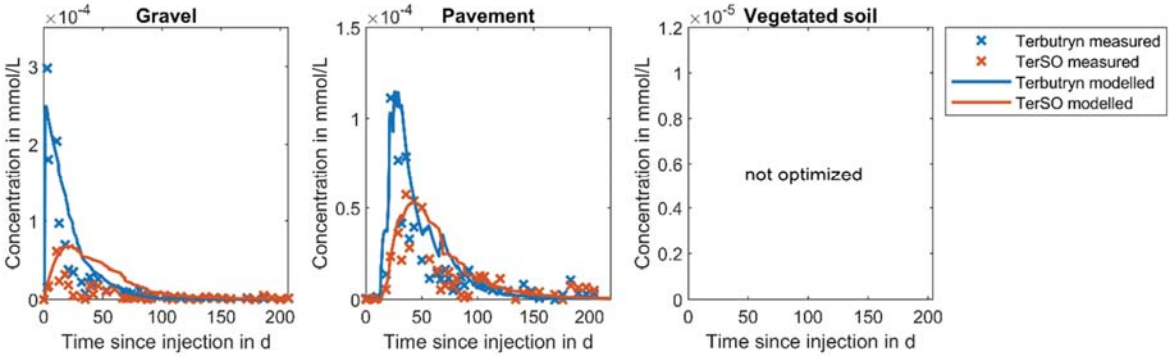

Figure D 6. Measured breakthrough curves of terbutryn and main TP TerSO as well as modelled data.

1.8 COMLEAM model results as input for Hydrus-1D

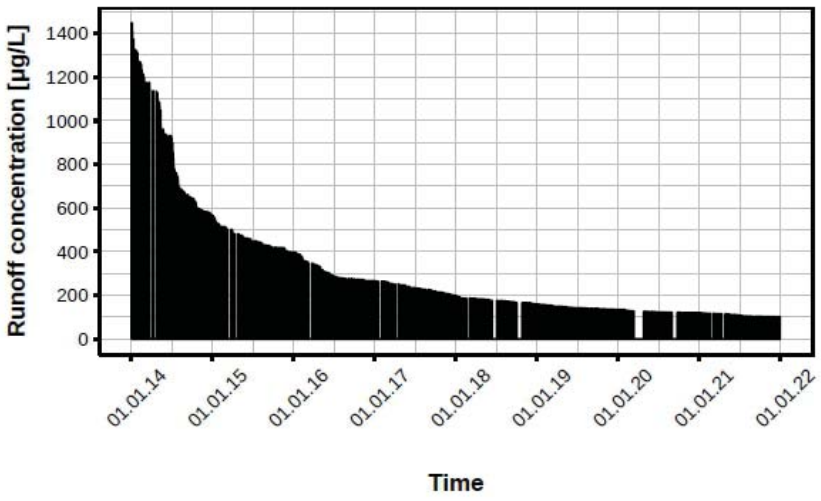

Figure D 7. COMLEAM output for Terbutryn concentrations at a 10 m² facade oriented towards the west.

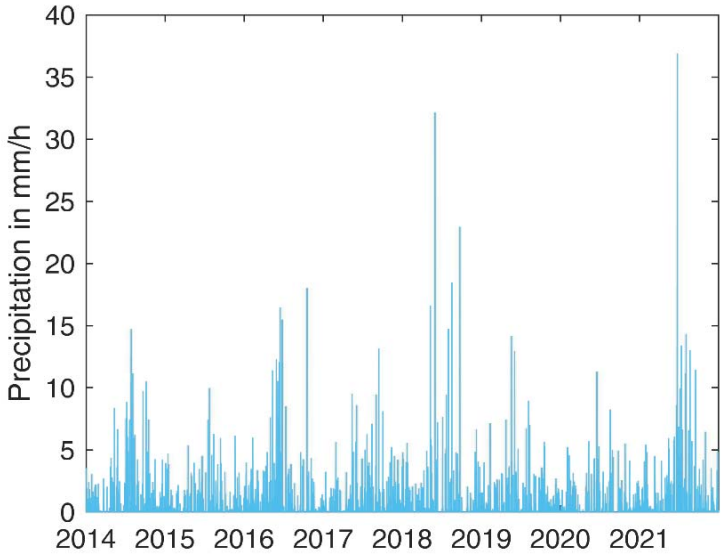

Figure D 8. Precipitation for modeled period as input data for COMLEAM.

Appendix D

2 Results

2.1 Water balance

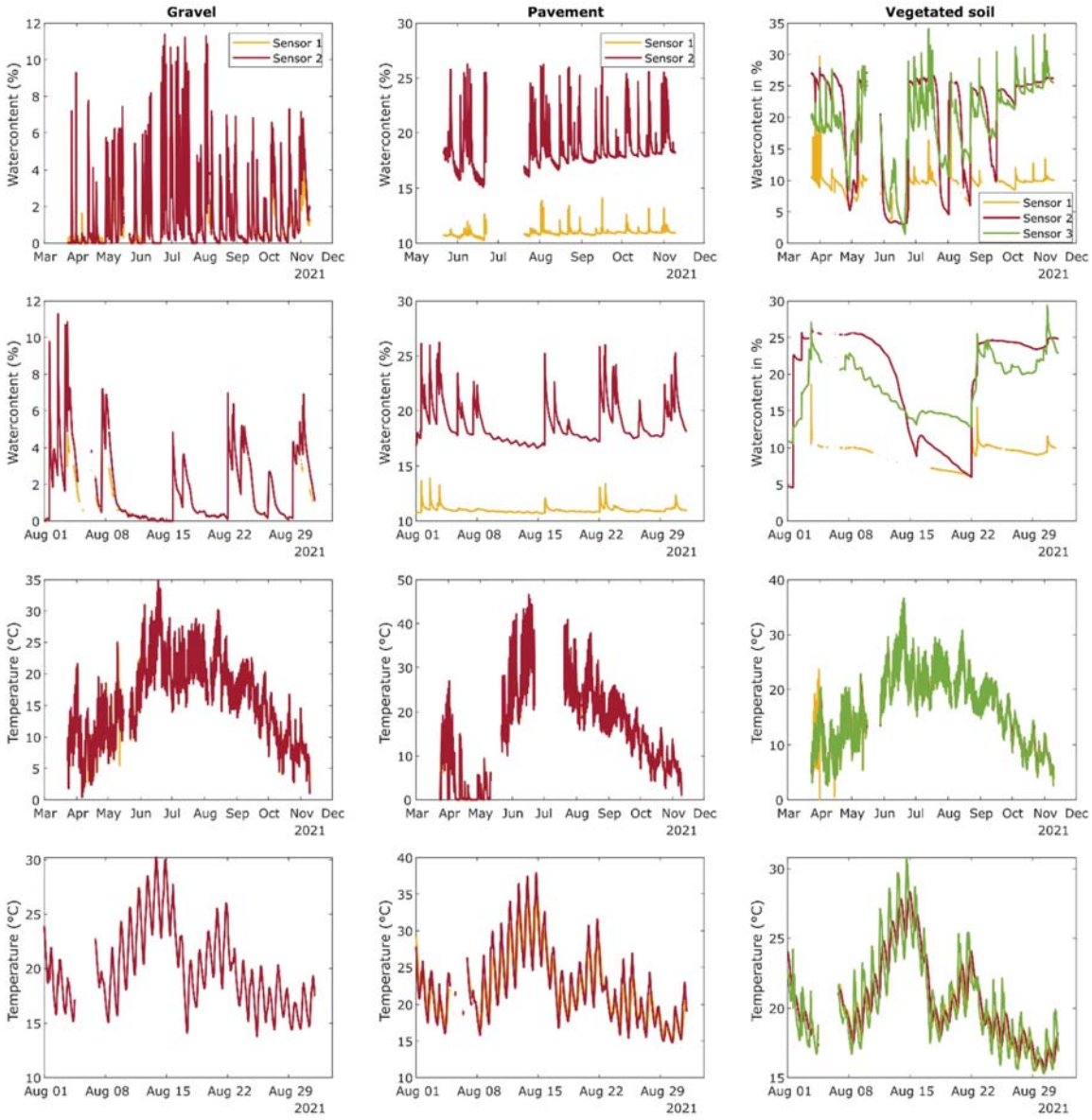

Figure D 9. Water content (top two rows) and temperature (two bottom rows) measured in the lysimeters for gravel (left), pavement (middle) and vegetated soil (right) during the experiment and enlarged for the month August. Depth of the sensors were 15 cm and 20 cm (sensor 1 and sensor 2 and 3, respectively).

2.2 Breakthrough curves and transport parameters of tracers and reactive compounds

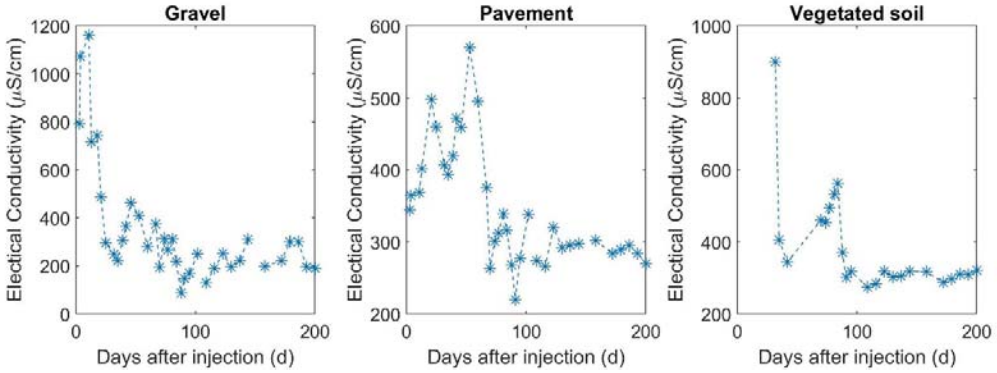

Figure D 10. Electrical conductivity as indicator for the conservative tracer (NaCl).

Table D 7. Observed breakthrough parameters for NaCl, terbutryn, transformation product terbutryn-sulfoxide (TerSO), acetochlor and diuron.

		Time of first arrival (d)	Time peak concentration (d)	Max concentration (µg L^{-1})	Cumulative drainage at peak concentration (L)
Gravel	NaCl	3	11	3.6E+5	1.0
	Terbutryn	3	3	72	0.4
	TerSO	3	11	16	1.0
	Acetochlor	3	3	249	0.4
	Diuron	3	3	207	0.4
Pavement	NaCl	3	21/53	6.2E+4 /9.9E+4	24.2/ 99.8
	Terbutryn	3	25	27	36.7
	TerSO	3	39	15	84.6
	Acetochlor	3	25	137	36.7
	Diuron	3	32	6	76.7
Vegetated soil	NaCl	42	84	7.8E+4	88.9
	Terbutryn	21	42	14	36.1
	TerSO	21	123	2	152.5
	Acetochlor	21	70	0.1	62.1
	Diuron	81	116	0.006	152.4

Appendix D

Table D 8. Recoveries of compounds in leachate and remaining in material.

		Gravel	Pavement	Vegetated soil
NaCl	NaCl released (%)	83		
Terbutryn	Leached (%)	9.5	16.8	0.1
	TPs leached (%)	4.9	13.5	0.4
	In material (%)	8.8	8.5	9.4
	TPs in material (%)	4.9	5.0	4.2
	Total (%)	28.1	43.8	14.1
Acetochlor	Leached (%)	47.2	39.5	0.0
	In material (%)	0.1	1.2	0.5
	Total (%)	47.3	40.7	0.5
Diuron	Leached (%)	40.2	5.0	0.0
	In material (%)	0.4	7.7	0.7
	Total (%)	40.6	12.7	0.7
OIT	OIT (%)	0	0	0

2.3 Suspect screening for non-targeted transformation products

Table D 9. Suspect screening: compounds and mass spectrometric parameters.

ID	Name	Precursor (m/z)	Product (m/z)
MEBT/ Terbumeton	2-N-Tertbutyl-4-N-ethyl-6- methoxy-1,3,5-triazine-2,4- diamine	226,17	114
			170
TBOHDesB	2-Hydroxy-4-N-ethyl-1,3,5- triazine-4,6-diamine	156	114
			128
TerDesS	2-N-Tertbutyl-4-N-ethyl 1,3,5-triazine-2,4-diamine	196	140
			70
TerDesSDesE	2-N-Tertbutyl-1,3,5-triazine2,4-diamine	168	112
			70
TerDesSDesB	2-N-Ethyl-1,3,5-triazine-2,4-diamine	140	70
			98

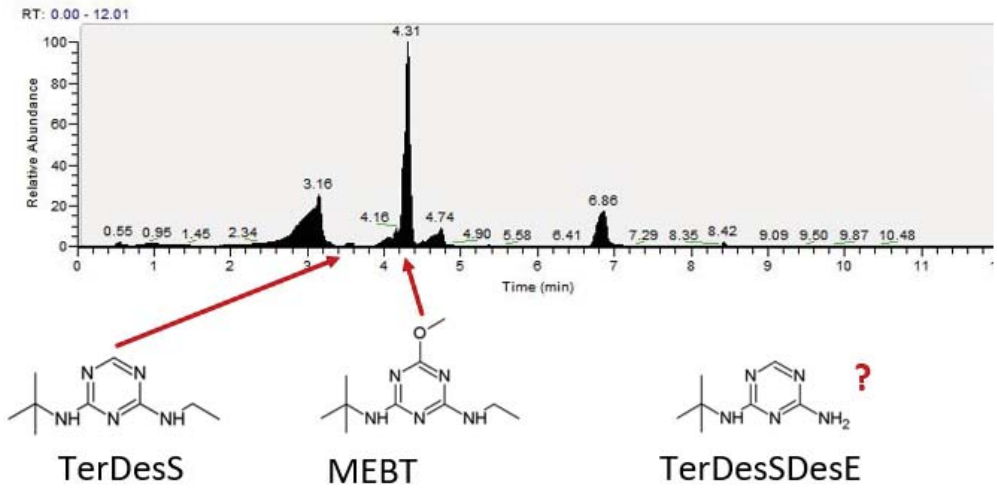

Figure D 11. Chromatogram of suspect screening with identification of TerDesS and MEBT.

2.4 Concentrations retained in lysimeter material

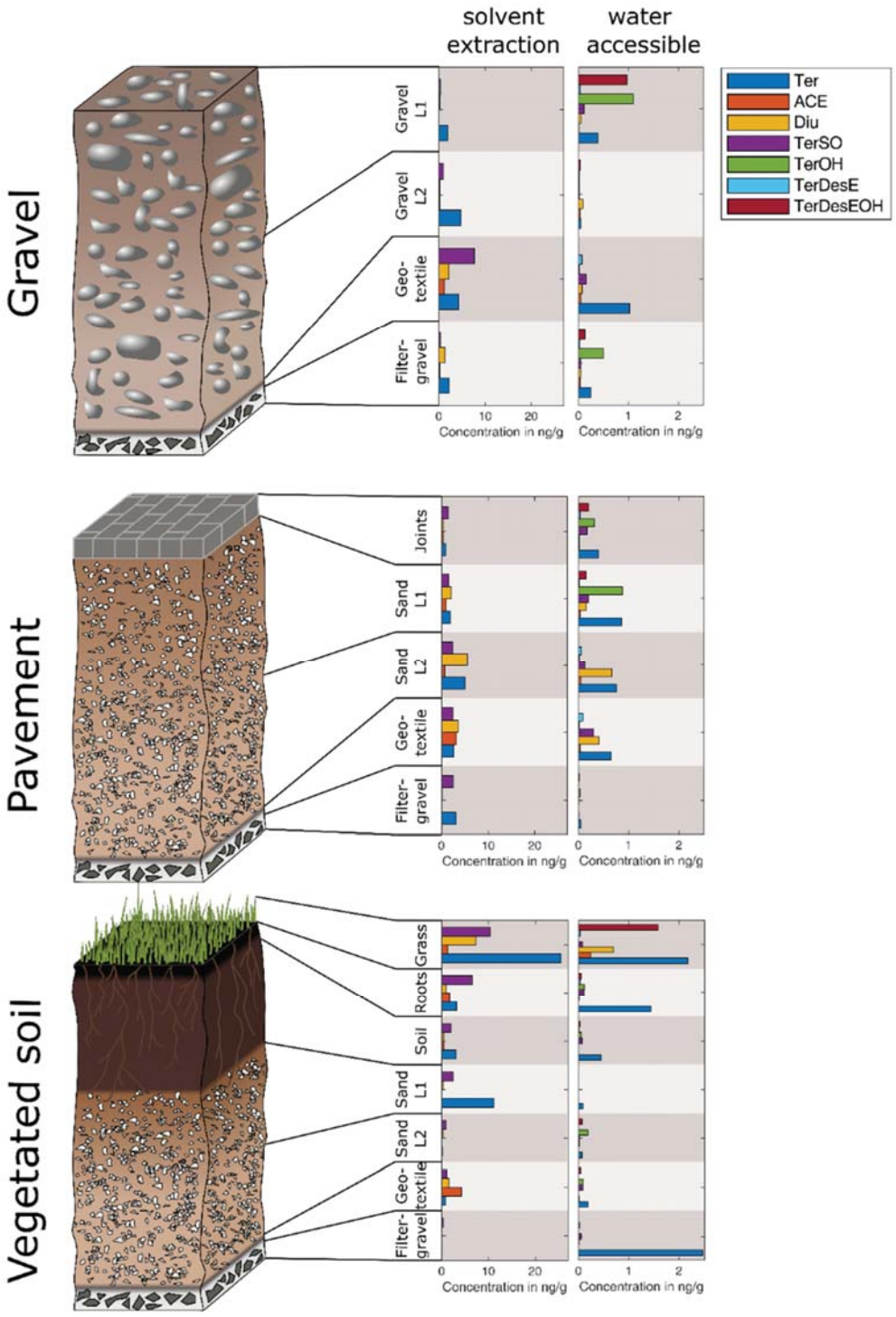

Figure D 12. Concentrations of biocides extracted with solvent and water (i.e., water accessible fraction) from material of the different lysimeter layers.

2.5 Estimation of degradation kinetics

Table D 10. Kd-values estimated using EPI Suite based on K_{OW} and half-live times ($t_{1/2}$) optimized in Hydrus-1D and used for long term estimation of biocide leaching.

		Kd	$t_{1/2,water}$ (d)	$t_{1/2,solid}$(d)
Gravel	Ter	0.5	2.9	28.9
	TerSO	0.7	28.9	28.9
Pavement	Ter	1.7	2.9	338.6
	Ter	0.3	3.3	34.1
	TerSO	3.3	38.5	17.0
	TerSO	0.6	38.5	17.0
Vegetated soil	Ter	45.8	84.9	84.9
	Ter	1.8	84.9	84.9
	TerSO	86.9	84.9	84.9
	TerSO	3.4	84.9	84.9

Based on the remaining fraction of respective biocide in the lysimeter at the end of the experiment, half-live times can be calculated solving for k with $t_{1/2} = \ln(2)/k$:

$$m_i = m_{i-1} \cdot e^{-k \cdot (t_i - t_{i-1})} - c_i^{leached} V_i^{leached} \quad \textbf{(D1)}$$

where m_i is the mass of biocides at sampling i, k is the degradation rate constant, t is the time, and $c_i^{leached} V_i^{leached}$ is the released mass. Results and estimated half-life times are shown below.

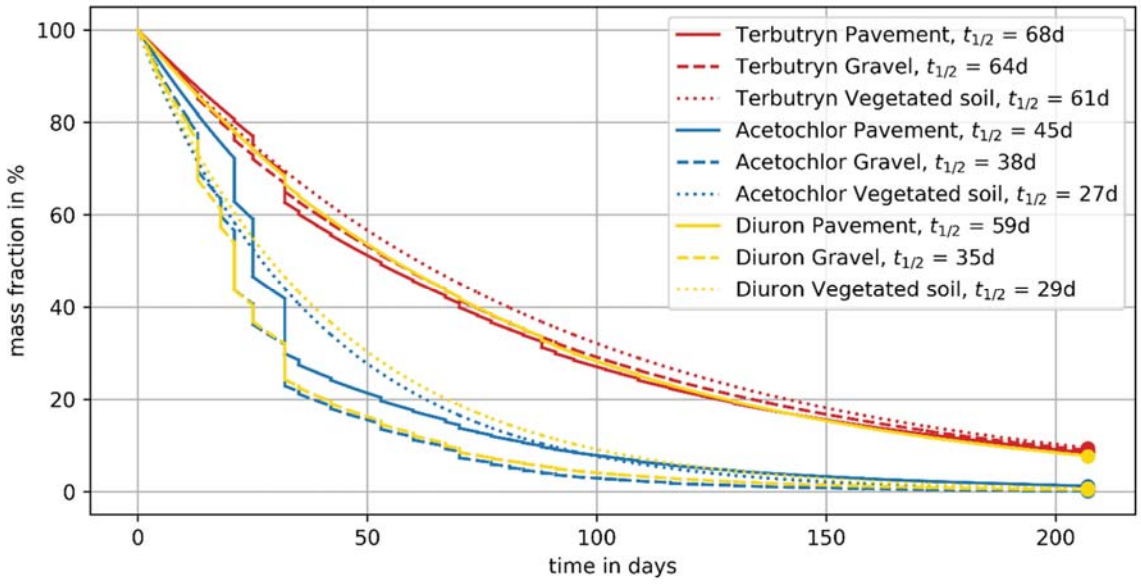

Figure D 13. Estimation of degradation half-live times based on Equation D1.

2.6 Hydrus-1D model results

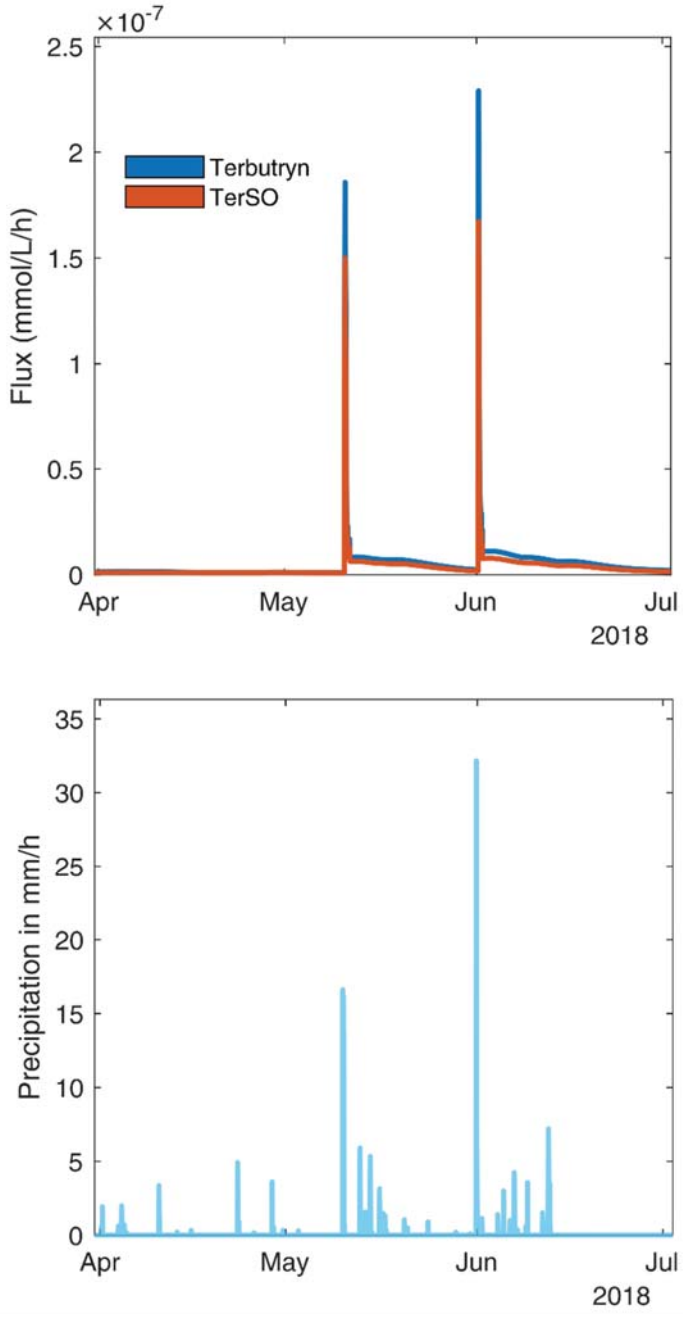

Figure D 14. Biocide emissions (as flux in 30 cm depth) from vegetated soil during heavy rain events.

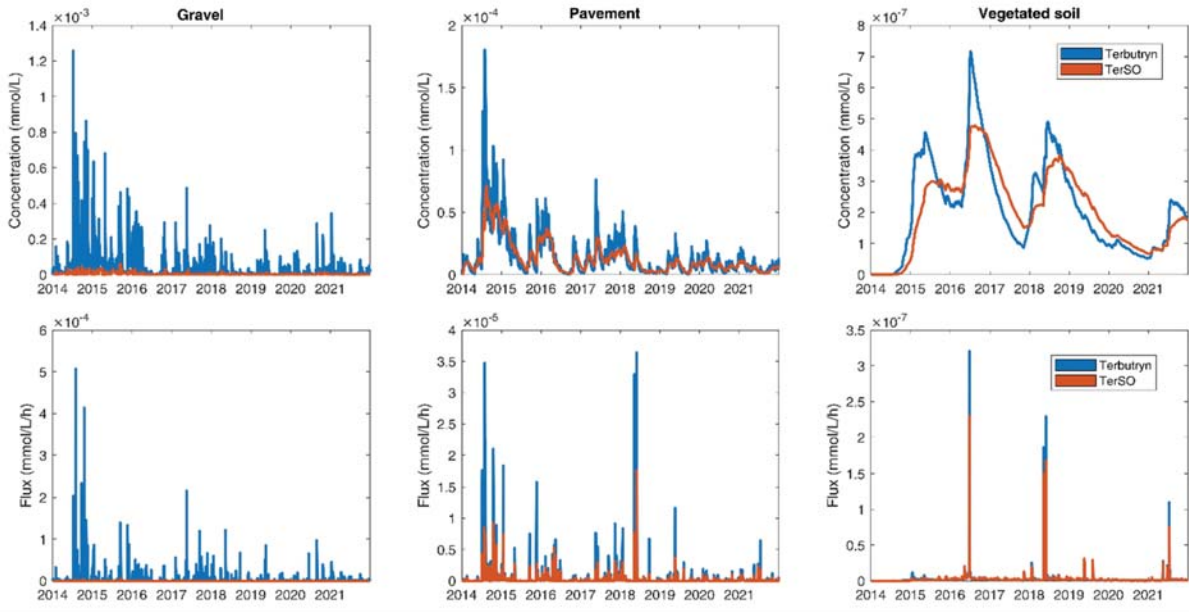

Figure D 15. Concentration in leachate (30cm depth, top) and mass fluxes (bottom).

Appendix E : Supporting information of Chapter 7

1 Material and Methods

Figure E 1. Infiltration pond in spring 2021.

Figure E 2. Infiltration trench in summer 2021.

Figure E 3. Categorization of buildings and surface materials and delineation of sub-catchments (sub-catchment trench in red, sub-catchment pond in blue).

Table E 1. Area and soil type for the two sub-catchments.

		Trench sub-catchment	Pond Sub-catchment
	Numbers of buildings	8	4
	Sub-catchment area, excluding buidlings [m²]	5330.7	3945.5
	Building area [roof m²]	2637.3	127.5
	Facades surface [m²]	7968	4073
Soil type in contact with surface [m^2 of facade] and runoff coefficient	Grass (0.1)	578	108
	Sealed pavement (1)	156	220
	Permable surface (0.2)	4.89	-
	Sealed Road (1)	27.6	-
	Wood Chips (0.1)	231	-
Area of soil type in the sub catchment [m^2]	Grass (0.1)	2986.6	108
	Pavement with vegetation (0.4)	91.3	265.9
	Permable surface (0.2)	148.7	-
	Playground (0.28)	155.3	-
	Sealed Road (1)	480.7	-
	Sealed pavement (1))	1034.9	915.5
	Wood Chips (0.1)	433	42.3

Appendix E

Figure E 4. Building heights in the district.

Table E 2. Sediment and soil characterization.

	% clay < 2 µm	% silt 2 µm to 50 µm	% sand 50 µm to 2000 µm	pH in water fraction < 2 mm	% carbonates fraction < 2 mm	% organic carbon fraction < 2 mm
Sediment 04.05.2021	7.5	35.2	57.3	7.6	5.9	1.9
Soil 04.05.2021	12.2	48.9	38.9	7.5	9.7	2.3
Sediment 27.07.2021	8.0	36.2	55.8	7.4	6.8	2.5
Soil 27.07.2021	9.2	39.9	50.9	7.6	9.7	3.2

Table E 3. Recoveries and standard deviation (n=9) of targeted compounds in soil and sediment and for SPE for terbutryn, octylisothiazolinone (OIT), diuron, terbutryn-sulfoxide (TerSO), terbutryn-desethyl (TerDesE), terbutryn-2-hydroxy (TerOH) and terbutryn-desethyl-2-hydroxy (TerDesEOH).

	Soil/sediment		SPE	
	Recovery (%)	Stdev. Recovery (%)	Recovery (%)	Stdev. Recovery (%)
Terbutryn	68.4	14.8	103.9	15.3
OIT	13.3	1.5	84.8	6.8
Diuron	49.1	13.9	74.1	7.8
TerSO	22.5	5.4	85.4	12.2
TerDesE	60.1	17.5	98.6	7.2
TerOH	9.5	3.8	117.7	19.6
TerDesEOH	8.6	2.7	125.0	24.3

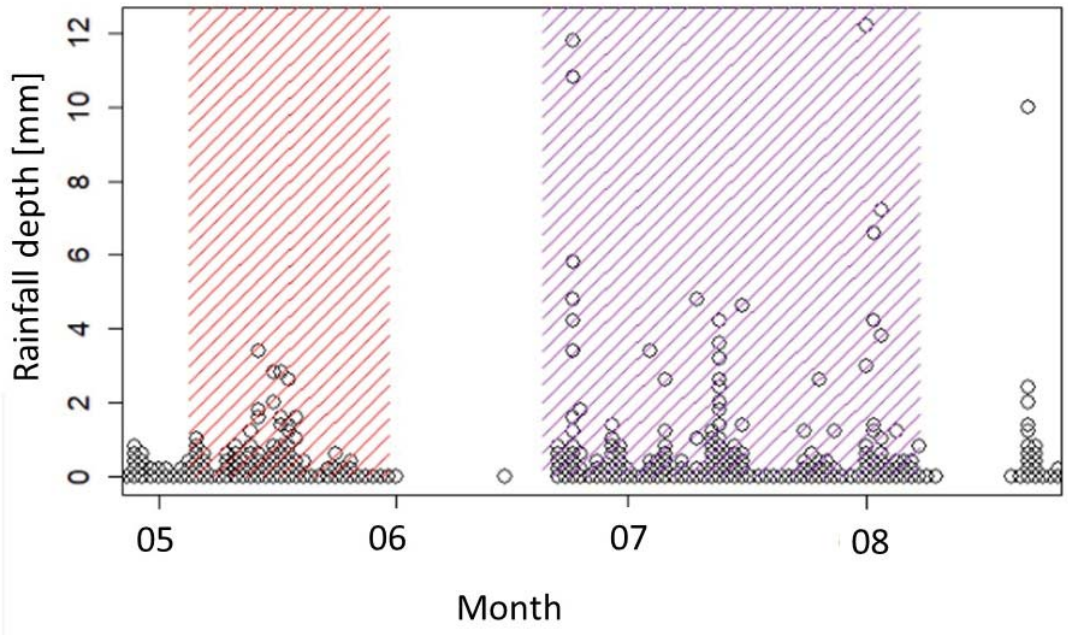

Figure E 5. Precipitation per 10 min in the studied catchment in 2021. Two time periods were investigated ("May" in red and "summer" in purple).

Appendix E

1.1 Biocide reactive transport and estimation of initial terbutryn concentrations on facades

Biocide leaching was modeled based on equations and approaches used in COMLEAM.

Hourly wind driven rain (wdr) was calculated according to ISO as Eq. E1:

$$wdr = C_r \times C_t \times O \times W \times cos\left(d_{wind} - d_{building}\right) \times v_{wind} \times p^{0.88} \quad \textbf{(E1)}$$

With C_r the terrain roughness factor (C_r= 0.67), C_t the topography factor (C_t=1), O the obstruction factor (O=0.4), W the wall factor (W=0.2 for building higher than 10m, W= 0.3 for buildings between 5 and 10 m, W=0.4 for building of height between 2 and 5 m and W= 0.55 for building smaller than 2 m), wind direction d_{wind} and building exposition $d_{building}$ the angle between north and hourly wind direction or building exposition rounded to one of the 8 major angles (0°, 45°, 90°, 135°, 180°, 225°, 270°, 315°), v_{wind} the hourly wind speed in m s^{-1}, and p the hourly precipitation in mm.

We computed runoff for each material and its respective contribution to the overall facade $f_{material}$ of building's facade as Eq.3:

$$runoff = wdr \times \sum_{materials} RC_{F,material} \times f_{material} \quad \textbf{(E2)}$$

In the studied district, facade surfaces contained 2 materials: glass for windows and coated concrete for walls with respective runoff coefficients RC_F of 1 and 0.9.

We calculated cumulative runoff from district construction (2014) to 2022. Cumulative biocide emission (E_{cum}) was modeled using a logarithmic emission function:

$$E_{cum} = C0 \times a_{char} \times log\left(1 + 1.72\frac{q_{cum}}{q_{char}}\right) \times A_{facade} \times f_{painted} \quad \textbf{(E3)}$$

In our case, the fraction of material painted ($f_{painted}$) is the proportion of material without glass, with a_{char} and q_{char} from [3] as a_{char}= 0.0062 and q_{char} = 12.1 were used.

The cumulative leaching was discretized in weekly leaching amount for the field campaign period. At each time step and for each building portion we calculated the proportion of biocides directly infiltrated at the bottom of the facade as

$$DI_{biocide}(i, A_{facade}) = DI_{soiltype} \times M_{mod}(i, A_{facade}) \quad \textbf{(E4)}$$

And $R_{biocide}$ in the surface runoff as

$$R_{biocide}\,(i, A_{facade}) = (1 - DI_{soiltype}) \times M_{mod}(i, A_{facade}) \quad \textbf{(E5)}$$

with direct infiltrated biocide at timestep i for facade portion A_{facade} and biocide in surface runoff $R_{biocide}$ (i, A_{facade}) the amount of biocide infiltrated at the bottom of facades and in the surface runoff in district in the time step for the considered portion of facade, M_{mod} (i, A_{facade}) the modeled amount of biocide leached in the time step for the considered portion of facade and $DI_{soiltype}$ the coefficient of direct infiltration of the soil type at the bottom of the portion of facade.

The amount of biocides reaching trench and pond and the amount of biocides infiltrated over each sub-catchment (SC) was then calculated based on the infiltration coefficient (IC) calculated with the water mass balance as:

$$IF_{biocide}(SC, i) = IC \times R_{biocide}\,(SC, i) \quad \textbf{(E6)}$$

$$B_{outlet}\,(, i) = (1 - IC_{SC}) \times R_{biocide}\,(SC, i) \quad \textbf{(E7)}$$

Based on biocide concentrations measured with the auto sampler, transferred to mass loads with discharge volume (M_{obs}) we can estimate initial concentration of biocides in facades (C0) as:

$$M_{obs}(i) = (1 - DI_{soiltype})(1 - IC_{SC})M_{mod}(i) \quad \textbf{(E8)}$$

$$M_{mod}(i) = E_{cum}(i + 1) - E_{cum}(i) \quad \textbf{(E9)}$$

Appendix E

$$M_{mod}(i) = C0 \times a_{char} \times A_{facade} \times f_{painted} \times \left(log\left(1 + 1.72\frac{q_{cum}(i+1)}{q_{char}}\right) - log\left(1 + 1.72\frac{q_{cum}(i)}{q_{char}}\right)\right) \quad \textbf{(E10)}$$

With M_{obs} the mass of biocides measured in the trench and M_{mod} the modeled mass of biocides leached. Therefore, C0 can be estimated in two ways:

$$C0 = \frac{M_{mod}(i)}{E_{cum,rel}(i+1) - E_{cum,rel}(i)} \quad \textbf{(E118)}$$

$$C0 = \frac{\frac{M_{obs}(i)}{(1-DI)(1-IC)}}{E_{cum,rel}(i+1) - E_{cum,rel}(i)} \quad \textbf{(E12)}$$

With the initial concentration, the facade leaching model is set up and discretized at the daily time step and used in the infiltration module.

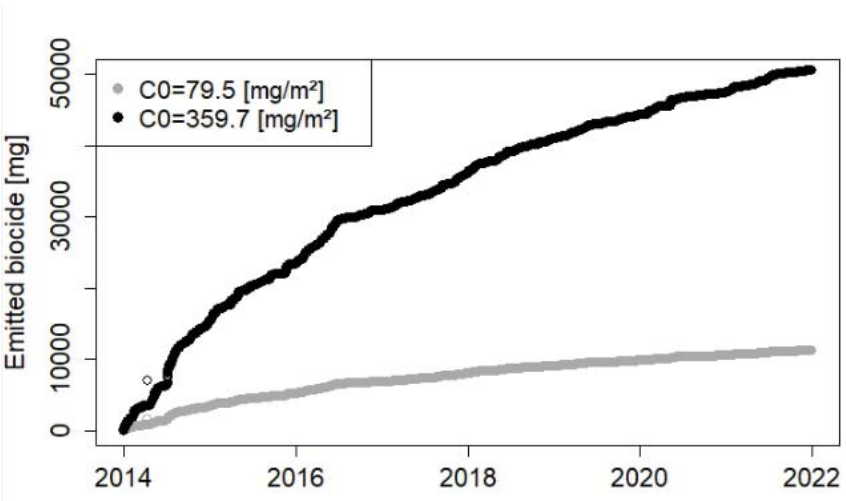

Figure E 6. Cumulative emission curves of terbutryn from 2014 to 2022 over the studied district. Emissions were modeled for gradients of initial concentrations spanning median minimal range and maximal range of estimated C0.

2 Results

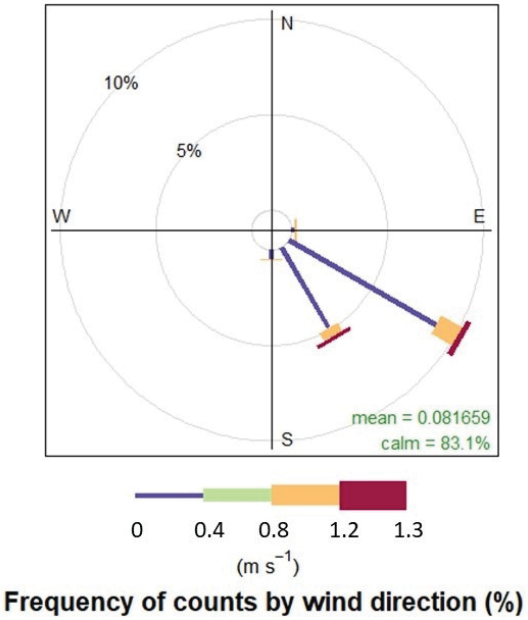

Figure E 7. Frequency of the main wind direction in Entzheim EMS station during the rainfall events occurring during the field campaign (May to August 2021).

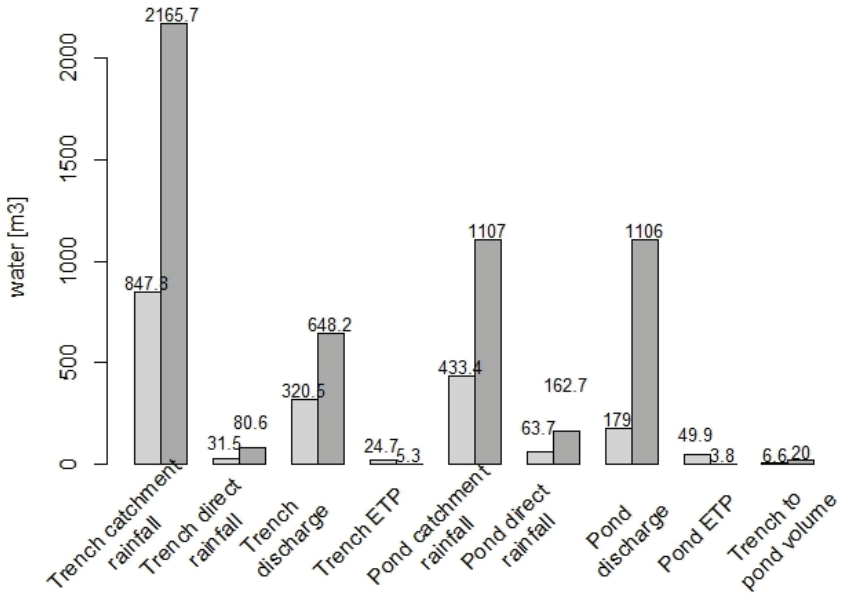

Figure E 8. Water volume in each compartment of the two sub-catchments for the two periods of the study.

Appendix E

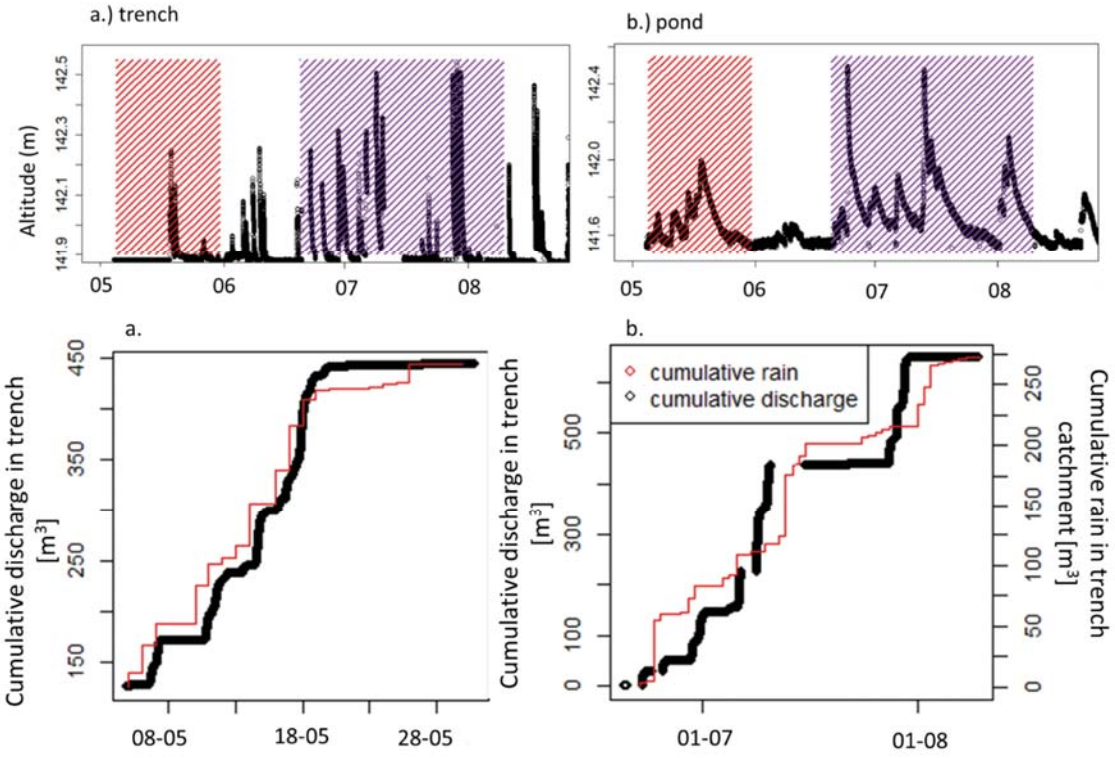

Figure E 9. Volumetric content of trench cumulative discharge and cumulative rainfall depth over the catchment over the two studied period: a. in May, b. in June/August.

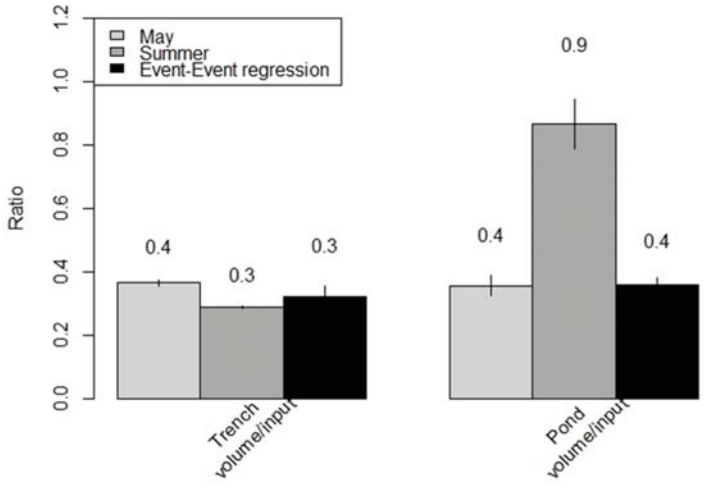

Figure E 10. Aggregated water mass balance allowing the estimations of runoff and infiltration coefficients over the two catchments for the 2 periods of study (May in light grey, June/August in dark grey).

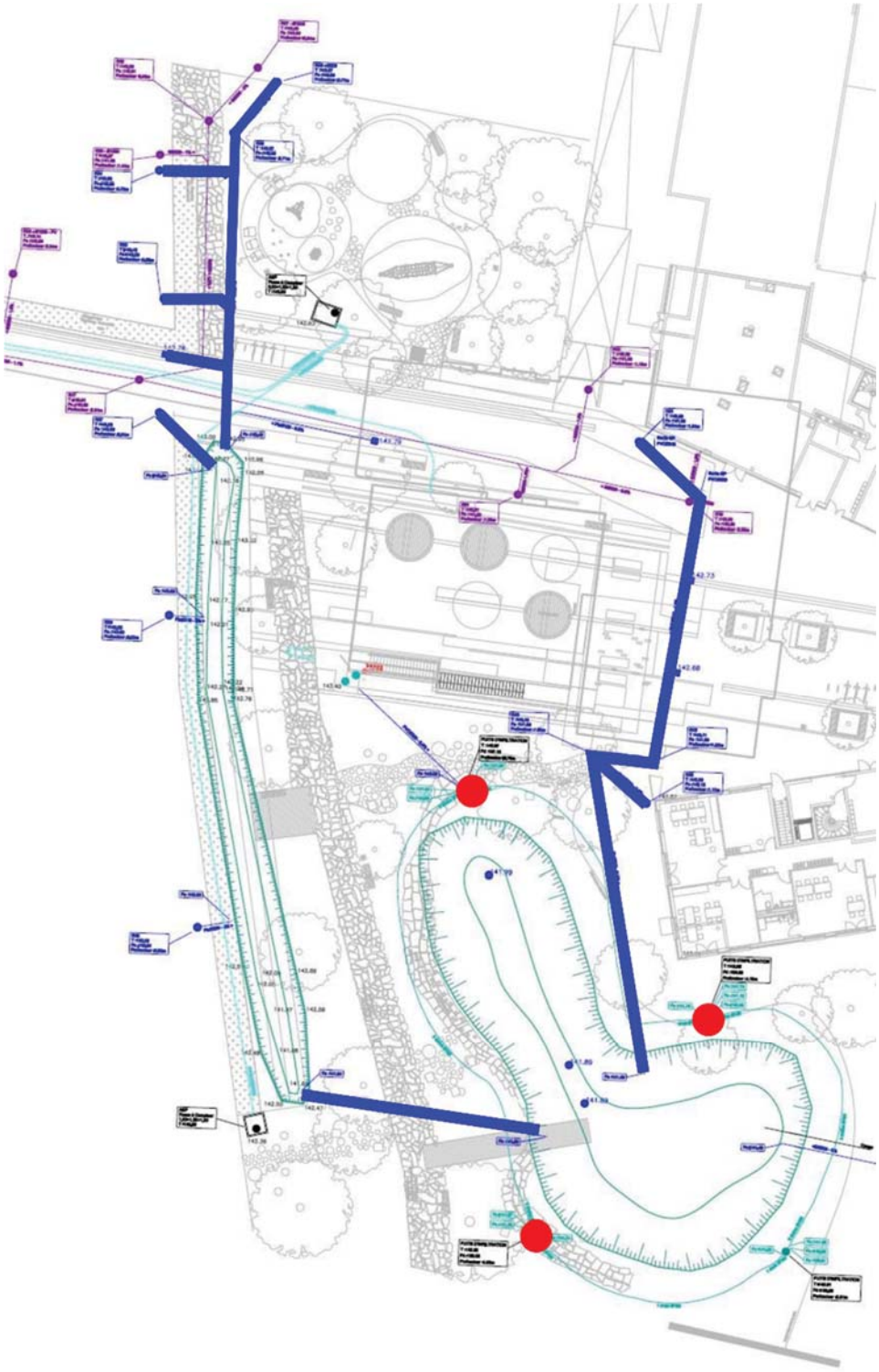

Figure E 11. Technical drawing of the infiltration systems. Blue lines indicate drainage system, red points indicate locations of infiltration wells.

Appendix E

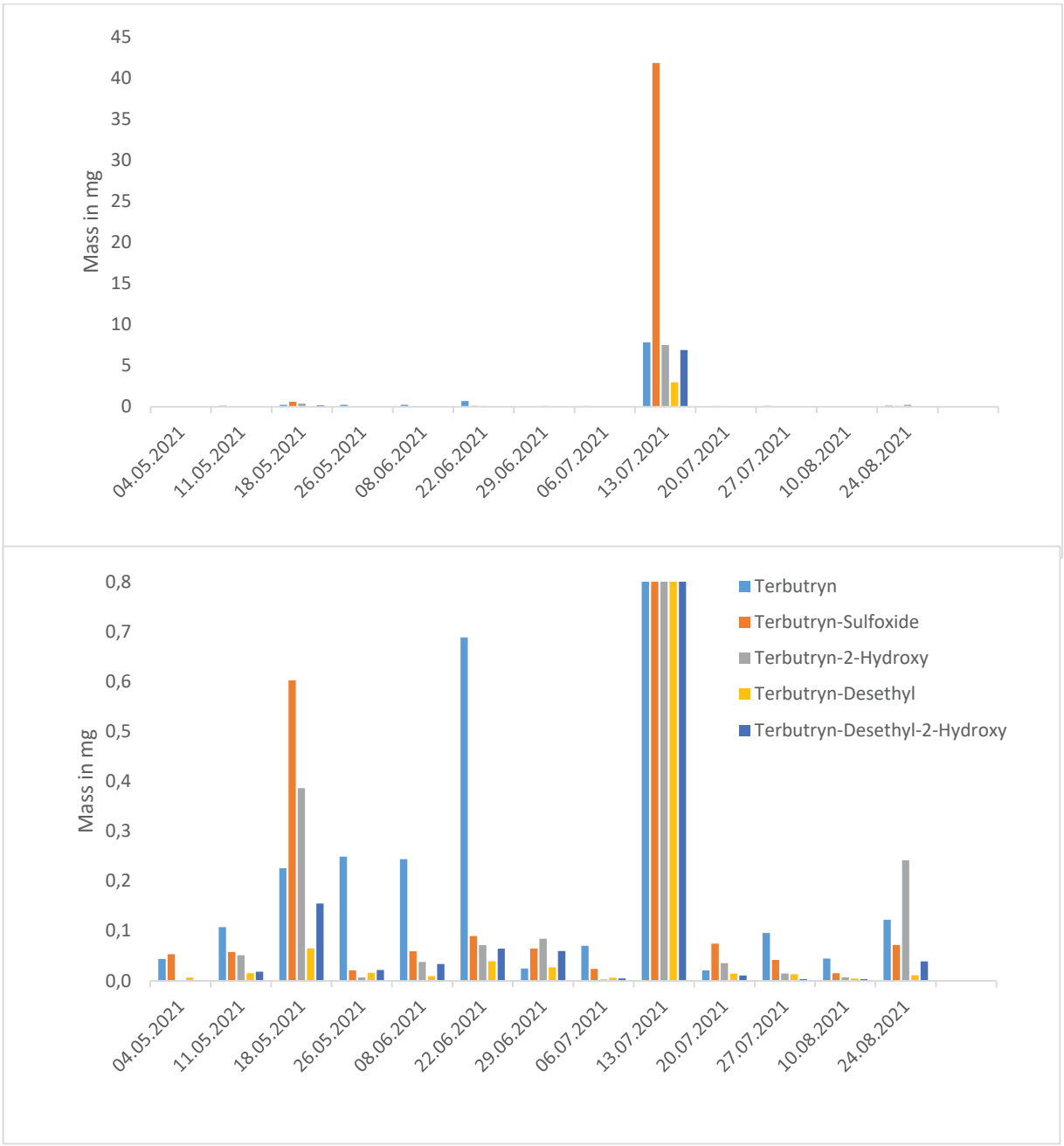

Figure E 12. Stored masses of terbutryn and transformation products in the pond. Y-axis scale is changed in the bottom graph to visualize smaller stored masses during most events.

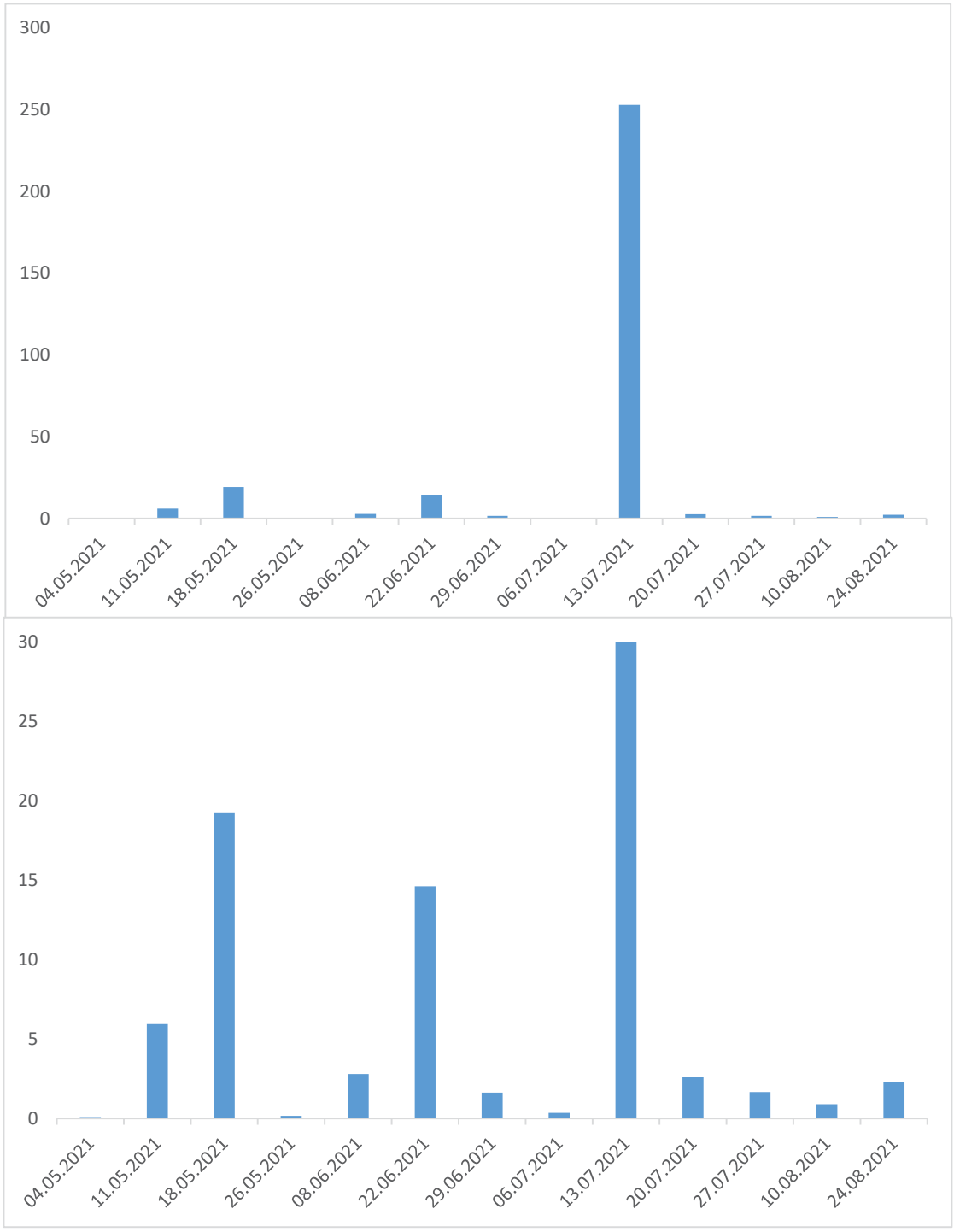

Figure E 13. Stored masses of diuron in the pond. Y-axis scale is changed in the bottom graph to visualize smaller stored masses during most events

Université de Strasbourg

JUNGINGER Tobias

Institut Terre & Environnement de Strasbourg | ITES | UMR 7063 de l'Université de Strasbourg & CNRS & ENGEES

Transport and degradation of urban biocides from facades to groundwater

Résumé

Les biocides urbains, utilisés dans les peintures des façades pour empêcher la croissance des algues et des champignons, sont libérés par la pluie qui ruissellent sur ces façades, contaminantes les eaux de surface, le sol et les eaux souterraines avec des effets écotoxicologiques potentiels pour l'écosystème. L'objectif général de cette thèse était d'améliorer la compréhension du transport réactif des biocides urbains depuis leurs sources (i.e., matériaux de construction/façades) jusqu'aux compartiments environnementaux récepteurs (i.e., eaux de surface, sol et eaux souterraines). Nous avons d'abord examiné les voies et les mécanismes de dégradation du biocide terbutryne au cours de la photodégradation, de l'hydrolyse et de la biodégradation dans des conditions de laboratoire, en utilisant l'analyse isotopique multi-éléments composé-spécifique et la quantification des produits de transformation. Nous avons également appliqué l'analyse isotopique composé-spécifique aux biocides urbains dans des conditions environnementales, en discutant de son potentiel et de ses limites. Nous avons montré que le rayonnement solaire est la principale variable hydro-climatique provoquant la transformation de la terbutryne en produits de transformation au sein des façades et nous avons fourni des estimations de leur contribution dans les lixiviats de façade sur plusieurs années. En outre, nous avons montré que les revêtements perméables et les graviers drainant au pieds des façades sont des " points chauds " potentiels pour l'entrée des biocides dans les eaux souterraines, tandis que les surfaces végétalisées agissent largement comme un puits pour les biocides. Dans l'ensemble, cette thèse souligne les risques environnementaux associés à la libération de biocides urbains et de leurs produits de transformation, mais discute également d'approches alternatives avec des matériaux sans biocides, ouvrant ainsi la voie à une ville sans biocides.

Mots clés : biocides, analyse isotopique composé-spécifique, transport réactif, dégradation.

Abstract

Urban biocides, used in facade materials like paint and render to prevent growth of algae and fungi, are released with wind driven rain and contaminate surface water, soil and groundwater with potential ecotoxicological effects to the ecosystem. The general goal of this thesis was to improve the understanding of reactive transport of urban biocides from their sources (i.e., construction materials/facades) to receiving compartments (i.e., surface water, soil, and groundwater). We first examined the degradation pathways and mechanisms of the biocide terbutryn during photodegradation, hydrolysis and biodegradation under laboratory conditions, using multi-element compound specific isotope analysis and transformation product measurements. We further applied compound-specific isotope analysis for urban biocides under environmental conditions, discussing its potential and limitations. We showed that solar irradiation is the main hydroclimatic variable causing release of transformation products of terbutryn from facades and provide estimates of their contribution in facade leachate over several years. Additionally, we showed that permeable pavements and gravel drainage close to facades are potential 'hot spots' for biocide entry towards groundwater, while vegetated surfaces acted largely as a sink for biocides. Altogether, this thesis underscores environmental risks associated with the release of urban biocides and their transformation products but also discusses alternative approaches with biocide-free materials, thus paving the way towards a biocide-free city.

Keywords: biocides, compound-specific isotope analysis, reactive transport, degradation